POLYSILOXANE-POLYARYLESTER BLOCK COPOLYMERS: SYNTHESIS AND CHARACTERIZATION

by

Patricia J. Andolino Brandt

Dissertation submitted to the Faculty of the
Virginia Polytechnic Institute and State University
in partial fulfillment of the requirements for the degree of
DOCTOR OF PHILOSOPHY
in
Chemistry

APPROVED:

J. E. McGrath, Chairman

T. C. Ward

J. P. Wightman

M. A. Ogliaruso

H. M. Bell

February, 1986
Blacksburg, Virginia

POLYSILOXANE-POLYARYLESTER BLOCK COPOLYMERS: SYNTHESIS AND CHARACTERIZATION

by

Patricia J. Andolino Brandt

Committee Chairman: James E. McGrath

Department of Chemistry

(ABSTRACT)

Passive damping has been defined as a key element in vibration control. It is believed that the approach to passive damping could be addressed through the use of carefully designed viscoelastic polymeric materials. This dissertation describes the synthesis and characterization of multiphase, transparent block copolymers that are potential candidates for passive damping applications in large space structures.

Relatively high molecular weight polysiloxane-polyarylester block copolymers were prepared by two different synthetic routes. A solution technique was used to synthesize well-defined, perfectly alternating block copolymers by reacting a difunctional silylamine-terminated siloxane oligomer with a difunctional hydroxyl-terminated polyarylester oligomer. A second approach involved the preparation of a segmented (or random) block copolymer by an interfacial, phase-transfer technique in which various polyarylester

block lengths are formed during the copolymerization by reacting bisphenol-A, terephthaloyl chloride, and isophthaloyl chloride with a difunctional aminopropyl-terminated siloxane oligomer. To vary the miscibility of the siloxane and ester phases, and in turn the physical properties of the block copolymers, the block molecular weights and the siloxane block compositions (dimethyl, dimethyl-diphenyl, or dimethyl-trifluoropropylmethyl) were controlled.

Structure analysis by NMR (proton and silicon) and FTIR verified that the desired starting oligomers and block copolymers were successfully prepared. Intrinsic viscosity measurements, size exclusion chromatography, and the fact that tough transparent films could be solution cast and compression molded indicated that relatively high molecular weight materials were prepared.

Due to the high degree of incompatibility of the "soft" siloxane segments and the "hard" ester segments in the block polymers, a two-phase microstructure developed at relatively low block molecular weights. In addition to microphase separation, partial phase mixing was apparent from thermal, mechanical, and microscopic characterization techniques. Compared to a polyarylester homopolymer, the siloxane modified polyarylester block polymers displayed improved resistance to atomic oxygen degradation as seen from x-ray pho-

toelectron spectroscopy and scanning electron microscopy. All physical properties were found to be dependent upon siloxane block composition and copolymer block molecular weights.

In conclusion, new siloxane-ester block copolymers were prepared and characterized. They are believed to be potentially useful materials for passive damping applications in the space environment.

ACKNOWLEDGEMENTS

My sincere thanks and appreciation are extended to Dr. James E. McGrath for his guidance throughout the fulfillment of my degree requirements and the writing of this dissertation. I also wish to thank the other members of my advisory committee, Dr. Thomas C. Ward, Dr. James P. Wightman, Dr. Michael A. Ogliaruso, and Dr. Harold M. Bell.

Grateful acknowledgement goes to several technicians and undergraduate research chemists who assisted in obtaining the data and results discussed herein. They include

, and . I would also like to thank my graduate colleagues, especially and her husband , for their friendship during my graduate work. Special thanks goes to for her dedication and time spent on typing this dissertation.

My deepest thanks goes to my family, in particular my parents, and my husband, , for years of understanding, encouragement, and support throughout fulfillment of the requirements for this degree.

TABLE OF CONTENTS

APPENDICES

LIST OF TABLES

LIST OF FIGURES

Figure

Chapter I

INTRODUCTION

1.1 OBJECTIVES

The use of large precision space structures (LPSS) for navigation, weather forecasting, and communications is significantly increasing. A new domain in spacecraft configuration brought on by the Space Shuttle has dictated a transition in vibration control strategy. Traditional methods of active control do not effectively accommodate the excess of very low frequency, closely spaced vibration modes inherent in LPSS.

Passive damping has recently been identified as a key element in vibration control. Though it is believed that the approach to passive damping could be addressed through the use of carefully designed viscoelastic polymeric materials, little work has been done in this area [106]. The research reported in this dissertation is multidisciplinary in nature and includes the synthesis and characterization of ductile, multiphase, transparent block copolymers that are potential materials for passive damping applications in large space structures.

1.2 MATERIAL CRITERIA

In general, there are several properties that must be addressed in a material to be used for vibration control in large space structures. These include low creep, relatively low density, low outgassing characteristics, and adequate mechanical properties. Since these space structures should have lifetimes greater than five years, it is also important that damping materials be able to survive long term exposure in the space environment. Therefore, potential damping materials should be resistant to ultraviolet and high energy radiation, as well as atomic oxygen degradation [109].

One material that is suggested by the above requirements is siloxane modified polyarylesters. The aromatic polyesters are a relatively new class of engineering thermoplastic that shows good mechanical behavior. The Fries rearrangement of polyarylesters may possibly be utilized to dissipate absorbed ultraviolet energy from polymeric structures since it does not result in chain scission. Rather, it leads to the formation of an ortho-hydroxybenzophenone structure that may further stabilize the polymer against photolytic degradation [52,53].

The incorporation of polysiloxane blocks in these types of polyarylesters offers an opportunity for many improvements such as lower temperatures for the ductile-to-brittle

transitions and improved impact strength. The polysiloxanes display a unique combination of properties such as low glass transition temperature, hydrophobicity, thermal stability, high gas permeability, a wide temperature use range, and good ultraviolet resistance [1,12]. In addition, polysiloxanes have a lower surface energy than most other materials and, therefore, tend to predominate on the surface of materials, even if it is a component of a microphase separated copolymer system [64,135-137]. Thus, siloxanes can be used for surface modification of engineering thermoplastics while retaining much of their bulk properties. Such surface modification may lead to improved lubricity and better resistance to atomic oxygen [133].

In the literature review that follows, Chapter 2, a more detailed discussion of the synthesis, structure-property relationships, and applications of polysiloxanes, polyesters, and block copolymers is presented. Chapter 2 also provides a brief overview of passive damping and atomic oxygen degradation, two areas of importance to this work. Chapter 3 discusses the experimental methods, both synthetic and analytical, used in this research. A discussion of the experimental results are presented in Chapter 4, followed by conclusions, future work, and references.

Chapter II

LITERATURE REVIEW

2.1 POLYORGANOSILOXANES

2.1.1 Overview

Polyorganosiloxanes are unique among the commercially important polymers, both in basic chemistry and in variety of industrial applications. Elastomers based on polyorganosiloxanes are considered to be in the family of specialty elastomers because of their ability to perform in extreme environment situations. This would include service at relatively high temperatures or at very low temperatures, where the conventional organic elastomers are either oxidatively degraded or too stiff to be usable.

Polyorganosiloxanes are characterized by a repeating silicon-oxygen backbone with two organic substituents attached to the silicon atoms by silicon-carbon bonds. The generalized structure of the polyorganosiloxane chain can be represented as:

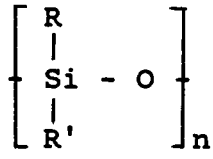

where R and R' can be alkyl, haloalkyl, vinyl or phenyl. The properties of silicone products depend to a considerable extent on the type of organic substituents on the silicon atoms and on the molecular structure of the polymer chains. The properties listed in Table 1 are characteristic and have determined the field of application for polydimethylsiloxane and polymethylphenylsiloxane, which have become the "classical" products of silicone chemistry and make up the bulk of technical products. In order to appreciate the unique properties of polyorganosiloxanes, a knowledge of their molecular structure, bond strengths, and physiochemical behavior is necessary. A brief and rather general discussion of the molecular properties which determine the bulk characteristics of the polyorganosiloxanes is addressed in the following section. More detailed discussions are available in various books [1-6] and reviews [7-10].

2.1.2 Structure-Property Relationships

2.1.2.1 Bond Angles and Rotational Barriers

The most common organosilicon materials are those composed of dimethyl substituted polysiloxanes. The polydimethylsiloxane chain is represented in Figure 1. These materials exhibit a very low glass transition temperature (Tg) of -123°C which is attributable to the weak intermo-

TABLE 1

Physical Characteristics of Siloxanes

Low surface energy
High compressibility
Biological inertness
Atomic oxygen resistance
Low temperature flexibility
Low polarity (hydrophobicity)
Thermal and oxidative stability
Ultraviolet radiation resistance
High permeability to small molecules
Low viscosity for a given molecular weight
Minimum change in viscosity with temperature
Broad service temperature range due to low Tg

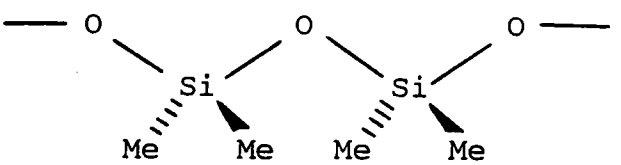

Figure 1: Polydimethylsiloxane segments [7].

lecular attractions between the polymer chains. This is related to the large degree of freedom of motion possible in the polysiloxane chains because of free rotation about the Si-O and Si-C axes. The Si-O-Si bond angle has a reported value of 144°, while the C-Si-C bond angle has a value of 111° [7]. The rotational barriers of the bonds in polydimethylsiloxane chains are compared to those of organic polymers in Table 2 [7]. It is evident that the rotational barriers are much lower in polysiloxanes than in organic polymers which leads to larger intermolecular distances and weaker intermolecular forces between siloxane chains. This not only implies a low Tg, but also relatively high gas permeability.

2.1.2.2 Bond Types and Strength

The polysiloxanes are well-known for their high thermal and oxidative stability. This property is derived from the high Si-O bond strength which is 23 kcal higher than that of the C-C bond as is shown in Table 3 [10]. The unique bonding nature of the Si-O bond is responsible for the high bond energy. Two types of bonding form the Si-O bond: (1) a σ type of bonding occurs between the hybridized s and p electrons of the silicon atom with the p electrons of the oxygen and (2) a π type of bonding which results from the combina-

TABLE 2

Silicon and Carbon Bond Rotational Barriers [7]

Bond	Energy (kJ/mole)
Si - O	< 0.8
C - O	11.3
Si - CH_3	6.7
C - CH_3	15.1

TABLE 3

Silicon and Carbon Bond Energies [10]

Bond	Energy (kcal)
Si-O	106
C-H	99
C-O	86
C-C	83
Si-C	76
Si-H	76

tion of the oxygen unshared p electrons and the unfilled 3d orbitals [2]. In addition to strengthening the Si-O bond, this unusual $p\pi$-$d\pi$ interaction shortens the Si-O bond length which has a reported value of 1.63Å. This value is substantially smaller than the 1.83Å sum of the atomic radii (1.17Å for silicon and 0.66Å for oxygen) [2].

2.1.2.3 Ionic Character

The polar nature of the Si-O bond also contributes to the shortness of the bond. The ionic character of this bond has been estimated to be 50% ionic [2], with silicon being the positive member. The siloxane bond also has a high heat of formation (108 kcal/mole) and is very resistant to homolytic cleavage. This, along with the fact that these molecules do not contain double bonds, renders them generally resistant to oxidative degradation. However, siloxanes are susceptible to heterolytic cleavage (attack by acids and bases) due to the highly ionic character of the siloxane bond.

The Si-C bond is slightly ionic (12%), again with silicon being the positive member. The heat of formation is about 80 kcal/mole and depending upon the substituents on the carbon, the Si-C bond may or may not be susceptible to heterolytic cleavage. For example, chloromethyl, cyano-

methyl or even phenyl groups are more easily cleaved from silicon by water, acids, or bases than are methyl groups [2]. For comparative purposes, the bond lengths and ionic character of various silicon and carbon bonds are listed in Table 4 [8].

2.1.2.4 Molecular Structure

Many physical properties of the polyorganosiloxanes are explained on the basis of a flexible helical structure for linear polysiloxane molecules. The twisting of the siloxane molecule into a spiral is explained by the tendency of the Si-O dipoles to undergo intramolecular compensation due to the fact that a dipole with a different O-Si orientation corresponds to each Si-O dipole. The intramolecular compensation of the individual dipoles is confirmed by the small change in the dipole moment with an increase in the molecular weight of the polyorganosiloxanes. The helical structure consists of a coil of Si-O bonds (6 to 7 per turn) which forms the polymer backbone around which the organic substituents protrude outwards [2]. If the polar Si-O backbone was not surrounded by the hydrophobic organic substituents, polysiloxanes would be expected to be more polar and exhibit higher intermolecular forces. However, the shielding effect of the organic substituents renders the polyorga-

TABLE 4

Silicon and Carbon Bond Lengths and Polar Character [8]

Bond	Length (Å)	Calculated Ionic Character (%)
Si-O	1.63	50
Si-C	1.88	12
Si-H	1.47	2
C-O	1.42	22
C-C	1.52	--
C-H	1.07	4

nosiloxanes hydrophobic. Physical properties such as compressibility, hydrophobicity, and weak intermolecular forces are explained by the helical structure of these molecules [7].

The relatively small change in viscosity with temperature is also explained on the basis of a flexible helical structure for linear molecules. When the temperature rises the helix tends to relax, resulting in an increasing molecular size which compensates for the normal increase in molecular mobility. Therefore, the viscosity of a simple methyl silicone fluid changes relatively little with temperature.

2.1.2.5 Surface Activity

The surface activity of the polysiloxanes can be attributed to their highly non-polar nature and weak intermolecular forces. Surface tensions range from 15 dyne/cm for hexamethyldisiloxane to 22 dyne/cm for high molecular weight silicone oils [7]. Due to its low surface energy and non-polar character, the siloxane component of a phase separated copolymer or blend generally tends to migrate to the air-polymer interface of a solution cast film and provides a siloxane-rich surface to the polymer film. The tendency for surface migration depends upon the polarity at the interface. For example, if the surface of a siloxane-containing

polymer is exposed to a polar atmosphere (e.g., high relative humidity), the non-polar polysiloxanes will tend to reside in the bulk of the polymer instead of migrating to the polymer surface.

2.1.2.6 Effect of Substitution

Alkyl Substituents

As previously mentioned, the properties of silicone products depend to a considerable extent on the type of substituents on the silicon atoms of a polysiloxane backbone. Polydimethylsiloxane has found important commercial applications, and groups other than methyl are generally substituted for particular property enhancements [9]. For example, substitution of the methyl groups by higher alkyls generally results in a material with improved lubricity and better compatibility with organic compounds. However, higher alkyl substitution also leads to reduced thermal and oxidative stability due to the lower stability of the C-C bonds.

Phenyl Substituents

Due to the inherent stability of aromatic rings, the thermal and oxidative stability of diphenyl substituted polysiloxanes (1) is significantly improved relative to other substituents. The phenyl groups bring about a

strengthening of the siloxane bond by increasing dπ-pπ bond contributions.

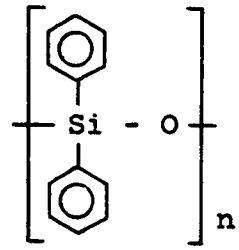

(1)

Typically, a few diphenyl units are incorporated into a polydimethylsiloxane chain to enhance low temperature flexibility by disrupting the symmetry and the crystallinity of the methyl sequences. An increase in the glass transition temperature and viscosity are observed since molecular motions are restricted by the large, bulky phenyl groups. It should be noted that incorporation of too many phenyl groups may cause some adverse effects due to the crystallinity of long phenyl sequences.

The polarity of the Si-C bond is increased by phenyl substituents due to the drain-off of the electronic charge through resonance. This increases the susceptibility of heterolytic cleavage of the Si-C bond by acids and bases. The increase in polarity also enhances intermolecular attractions which in turn leads to a higher solubility parameter. For dimethyl, methyl-phenyl and diphenyl substi-

tuted siloxanes, the solubility parameters are 7.5, 9.0 and 9.5 $(cal/cm^3)^{1/2}$, respectively [7,11]. With increasing solubility parameter, the miscibility of polysiloxanes with polar organic polymers is improved.

Trifluoropropylmethyl Substituents

One of the outstanding properties of trifluoropropylmethyl substituted polysiloxanes (2) is their excellent resistance to degradation at elevated temperatures in hydrocarbon fuels, oils and hydraulic fluids [13,14].

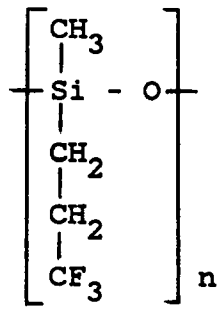

(2)

An increase in the glass transition temperature, solubility parameter, and viscosity are due to the presence of the bulky trifluoropropyl substituents. The high polarity of these groups creates a dipole moment across the C-Si-C bonds. This increases the intermolecular forces between polymer chains and, hence, results in a higher solubility parameter relative to polydimethylsiloxane. From swelling

experiments, the solubility parameters of poly-(trifluoropropylmethyl)siloxane and polydimethylsiloxane have been determined to be 9.6 and 7.5 $(cal/cm^3)^{1/2}$, respectively [9,12]. Due to an increase in the solubility parameter and intermolecular forces between polymer chains, the activation energy for viscous flow also increases. This leads to a larger dependence of viscosity on temperature for trifluoropropylmethyl substituents relative to dimethyl substituents [11].

The thermal and oxidative stability of trifluoropropylmethyl substituted polysiloxanes is lower than polydimethylsiloxane. This is likely due to the fact that the polar Si-C bond of the trifluoropropyl group is more easily cleaved than the Si-C bond of the methyl substituent. Thermal degradation in an inert atmosphere involves the intermolecular reaction shown below:

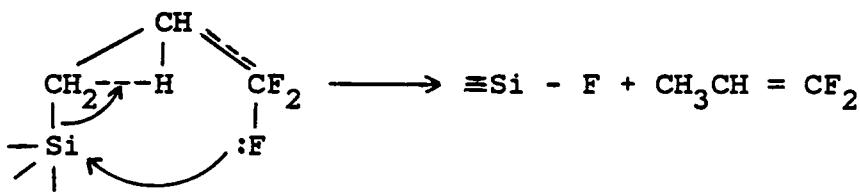

The intramolecular transfer of a fluorine atom from the CF_3 group to the Si atom is accompanied by elimination of 1,1-difluoropropylene, a gaseous product [15].

2.1.2.7 Applications of Polysiloxanes

The diverse applications of the silicones can easily be understood when their unique properties, as briefly discussed above, are considered. Various branches of industry have shown quite an interest in silicone fluids, elastomers, and resins because of their heat resistance, low temperature stability, low variation of physical properties with temperature, good electrical behavior, weather resistance, surface activity, and physiological inertness. A broad overview of the general applications of the technical silicone products is discussed below. More extensive reviews are found in various references [1,7-9,32-34].

The silicone fluids are linear, relatively low molecular weight materials which exhibit very low mechanical strength at room temperature due to their subambient glass transition temperature. Products derived from silicone fluids include greases, lubricants, hydraulic fluids, surfactants, and antifoam agents.

To enhance their mechanical strength for engineering applications, the silicones are generally crosslinked and often reinforced with fillers. Silicone elastomers are used in such applications as adhesives, sealants, gaskets, encapsulants, and protective coatings. The more highly crosslinked systems, the silicone resins, are typically used in surface coatings and glass fiber laminates.

2.1.3 Synthesis of Polyorganosiloxanes

There are a variety of routes available for the synthesis of linear, high molecular weight polyorganosiloxanes [1,7]. These synthetic routes include: (1) hydrolytic processes based on the hydrolysis of organohalosilanes or organoalkoxysilanes, (2) redistribution reactions involving the anionic or cationic polymerization of cyclic monomers or low molecular weight species, (3) non-hydrolytic processes based on reaction of organohalosilanes or organoalkoxysilanes with alcohols or acids, (4) Anionic polymerization of the cyclic siloxane trimer (D_3) using organolithium initiators, and (5) thermal polymerizations. Of these processes, the first two are commercially important. Only the second process, redistribution, was used to prepare the linear, functionally-terminated polyorganosiloxanes used in this research. Consequently, a discussion of this process will be reviewed herein. A brief overview of monomer synthesis will be presented next and is followed by a discussion of redistribution processes.

2.1.3.1 Monomer Synthesis

Organohalosilanes

In the 1930's, E. G. Rochow at General Electric and R. Muller in Germany independently discovered what is known as

the "direct process" [16,17] which pioneered an industry via the economical manufacture of the family of organohalosilanes necessary for siloxane production. Controlled hydrolysis of organohalosilanes then provided the cyclic trimers and tetramers used for polymerization.

The "direct process" involves the reaction of organic halides, such as methyl chloride or chlorobenzene, with silicon or silicon alloys in a gas-solid reaction. Scheme 1 illustrates the various types of reactions that occur during this process. A complex mixture of products is obtained and include various organohalosilanes, tetraalkylsilanes, organo-H-halosilanes, silicon tetrachloride, and small amounts of hydrocarbons. The composition of the product mixture can be modified by such parameters as the choice of suitable catalysts, controlling the temperature, or the use of diluent gases. Generally, the silane monomers can be separated by vacuum distillation with the organohalosilane being the predominant product of the reaction.

Different mechanisms have been proposed for this process. One involves a free radical process [18] and the second involves the adsorption of methyl chloride on a polar Si-Cu alloy active surface area [1]. General reaction schemes for the synthesis of dimethyldichlorosilane and diphenyldichlorosilane are shown in Schemes 2 and 3, respectively.

Scheme 1

Reactions Involved in the Direct Process

$$2\ RX + Si \longrightarrow R_2SiX_2$$

$$3\ RX + Si \longrightarrow RSiX_3 + 2\ R$$

$$3\ RX + Si \longrightarrow R_3SiX + X_2$$

$$2\ X_2 + Si \longrightarrow SiX_4$$

Generally, X = Cl and R = CH_3 or 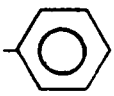

Scheme 2

Synthesis of Dimethyldichlorosilane

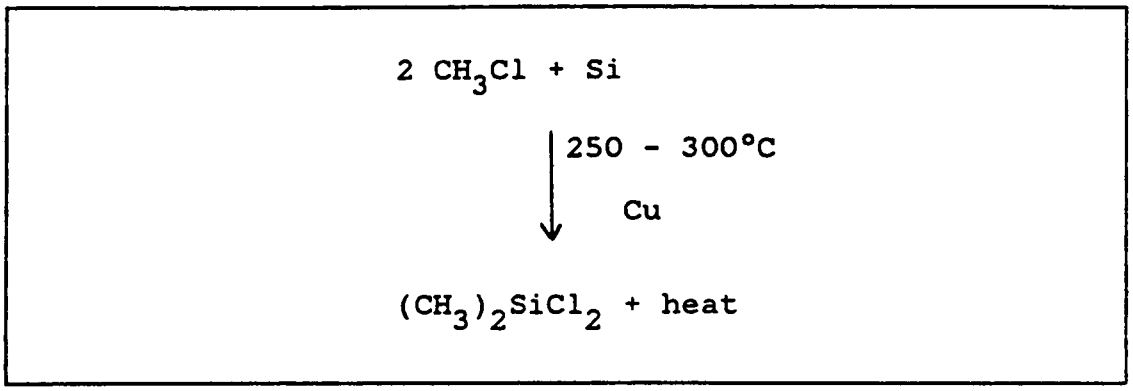

Scheme 3

Synthesis of Diphenyldichlorosilane

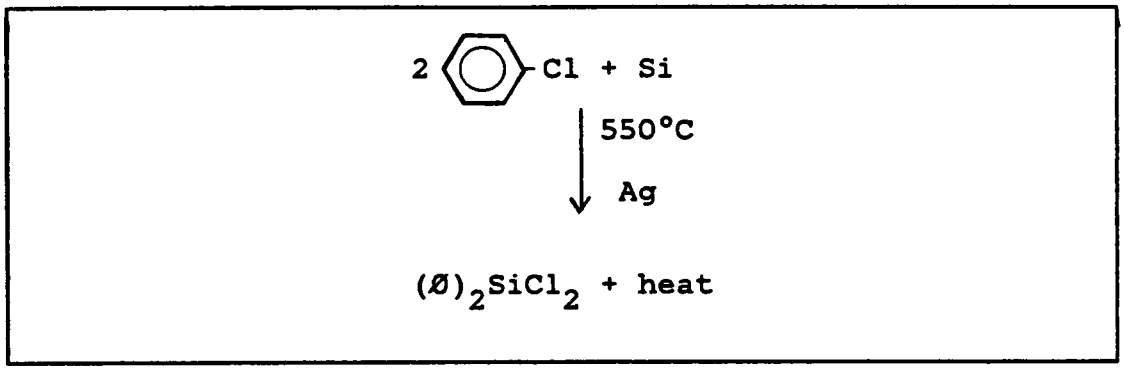

Trifluoropropylmethyldichlorosilane cannot be prepared by the "direct process." The trifluoropropyl groups tend to undergo extensive degradation under the experimental conditions of the "direct process." Therefore, trifluoropropylmethyldichlorosilane is generally prepared via the hydrosilation method as shown in Scheme 4 [7].

Cyclosiloxanes

Cyclosiloxanes are the starting materials for the synthesis of linear, high molecular weight polyorganosiloxanes. Generally, cyclosiloxanes are prepared by the hydrolysis of organochlorosilanes [1]. The hydrolysis of dimethydichlorosilane and the various chemical reactions involved are shown in Schemes 5 and 6, respectively. By varying the reaction conditions, the ratio of cyclic to linear structures can be controlled. For example, if the hydrolysis is carried out in the presence of sulfuric acid, the product mixture is predominantly high molecular weight, linear polysiloxanes. On the other hand, if the hydrolysis is carried out in the presence of an organic solvent that is slightly miscible or immiscible with water, up to 90 percent of the cyclic dimethyl siloxane tetramer (D_4) is obtained. This is explained by the fact that the organohalosilanes and the polyorganosiloxanes are soluble in the organic phase

Scheme 4

Synthesis of Trifluoropropylmethyldichlorosilane

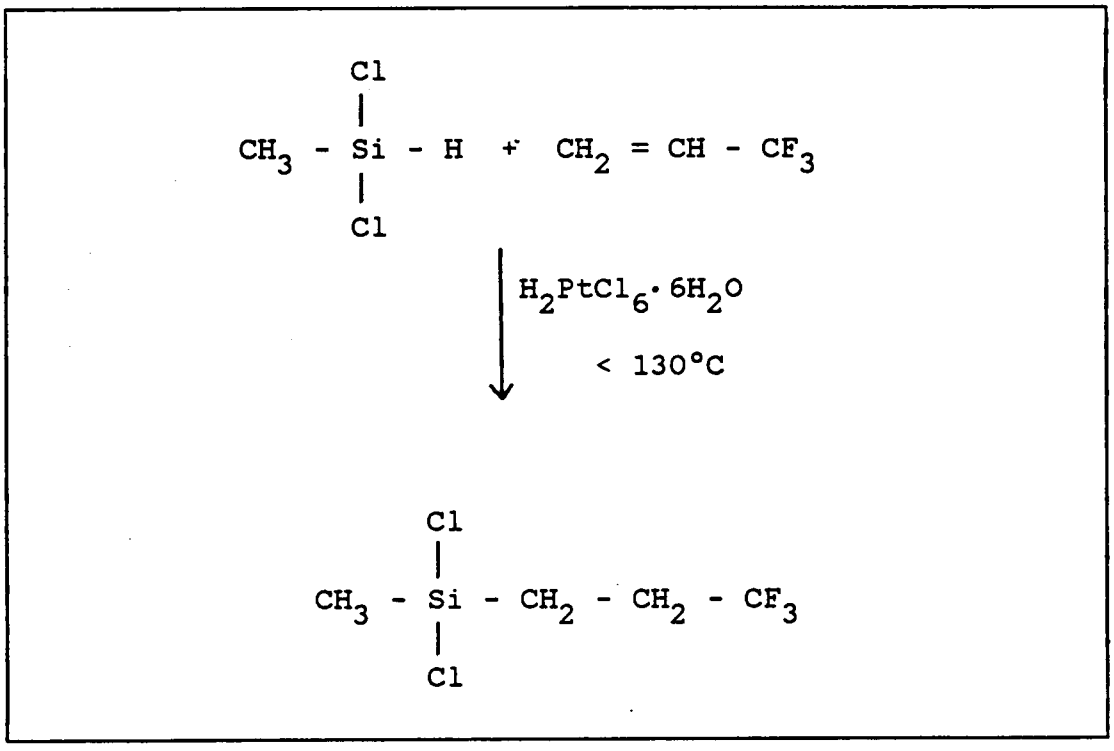

Scheme 5

Hydrolysis of Dimethyldichlorosilane

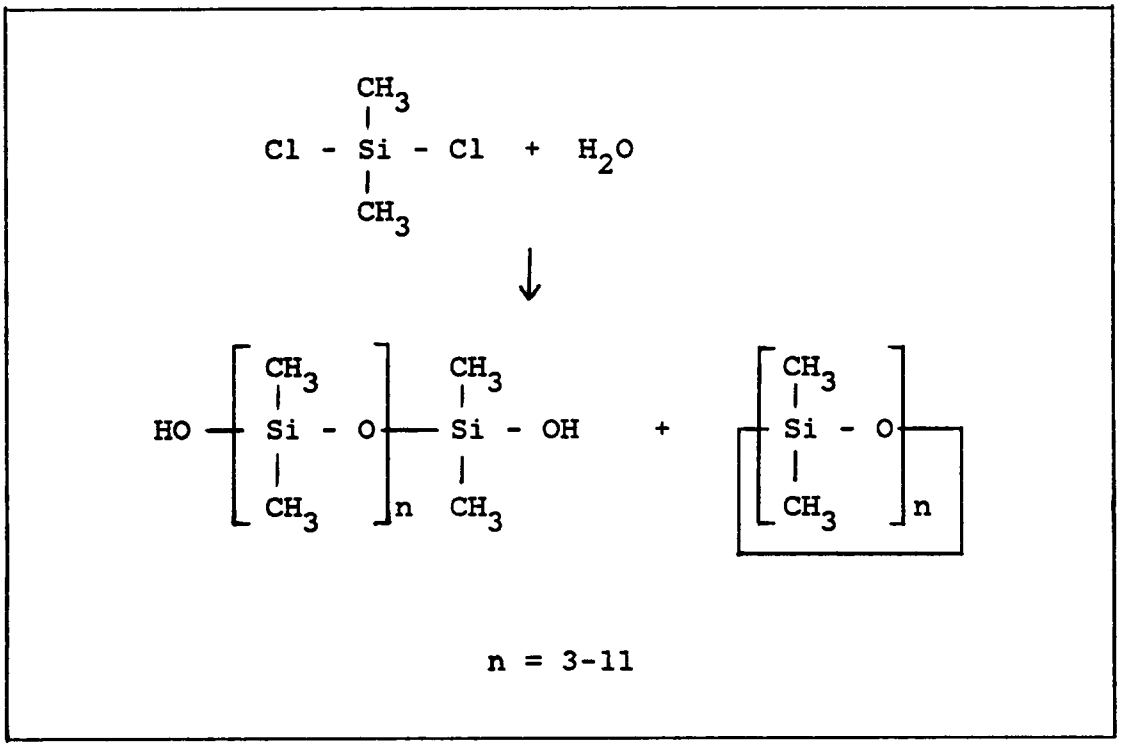

Scheme 6

Reactions Involved in the Hydrolysis of Organohalosilanes

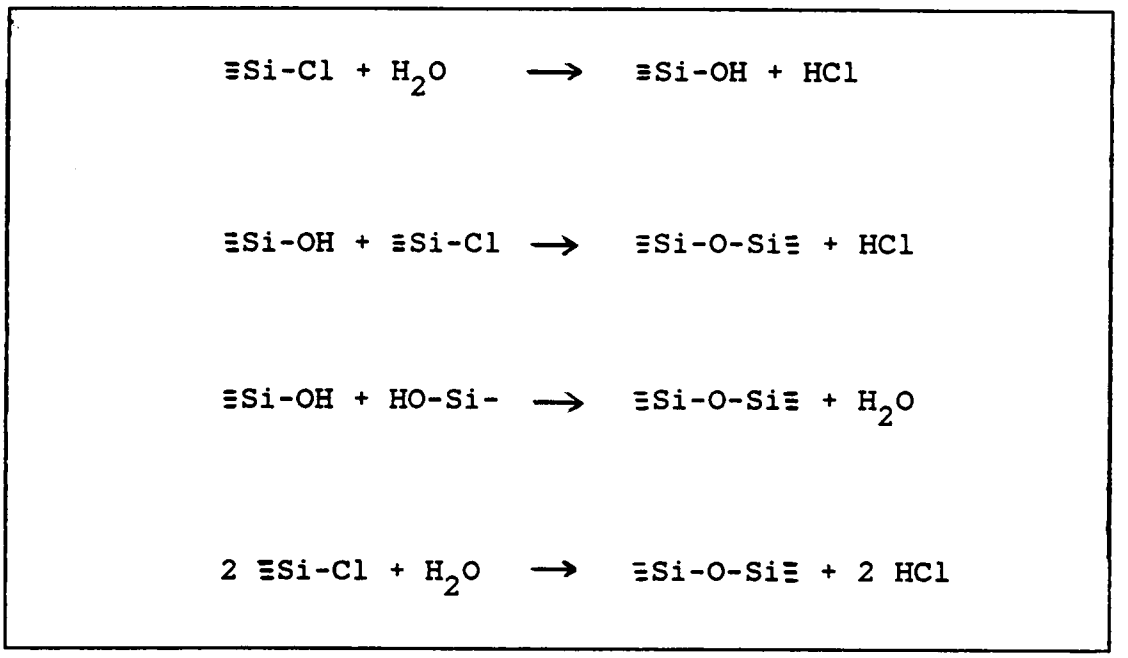

which reduces the concentration of chlorosilanes in the aqueous phase. Therefore, upon hydrolysis, the chlorosilanes have a greater tendency to undergo intramolecular, rather than intermolecular, condensation.

The cyclic diphenyl tetramer (D_4") and the cyclic trifluoropropylmethyl trimer (F_3) are synthesized by similar processes. The hydrolysis of diphenyldichlorosilane and trifluoropropylmethyldichlorosilane are illustrated in Schemes 7 and 8, respectively.

2.1.3.2 Polymerization of Cyclosiloxanes

General Overview

Cycloorganosiloxanes are the principal intermediate for the formation of high molecular weight polyorganosiloxanes. The ring-opening reaction can be initiated through the use of suitable basic or acidic catalysts. The transformation of cyclosiloxanes into linear polymer chains is an equilibrium process characterized by a very low heat of polymerization. At equilibrium conversions one produces 12-15% of cyclic oligomers, which are predominately, but not exclusively, the cyclic tetramer.

To prepare controlled molecular weight, difunctional polyorganosiloxanes, specified amounts of an endblocker (MM) are incorporated into the system [1,7]. A general reaction

Scheme 7

Hydrolysis of Diphenyldichlorosilane

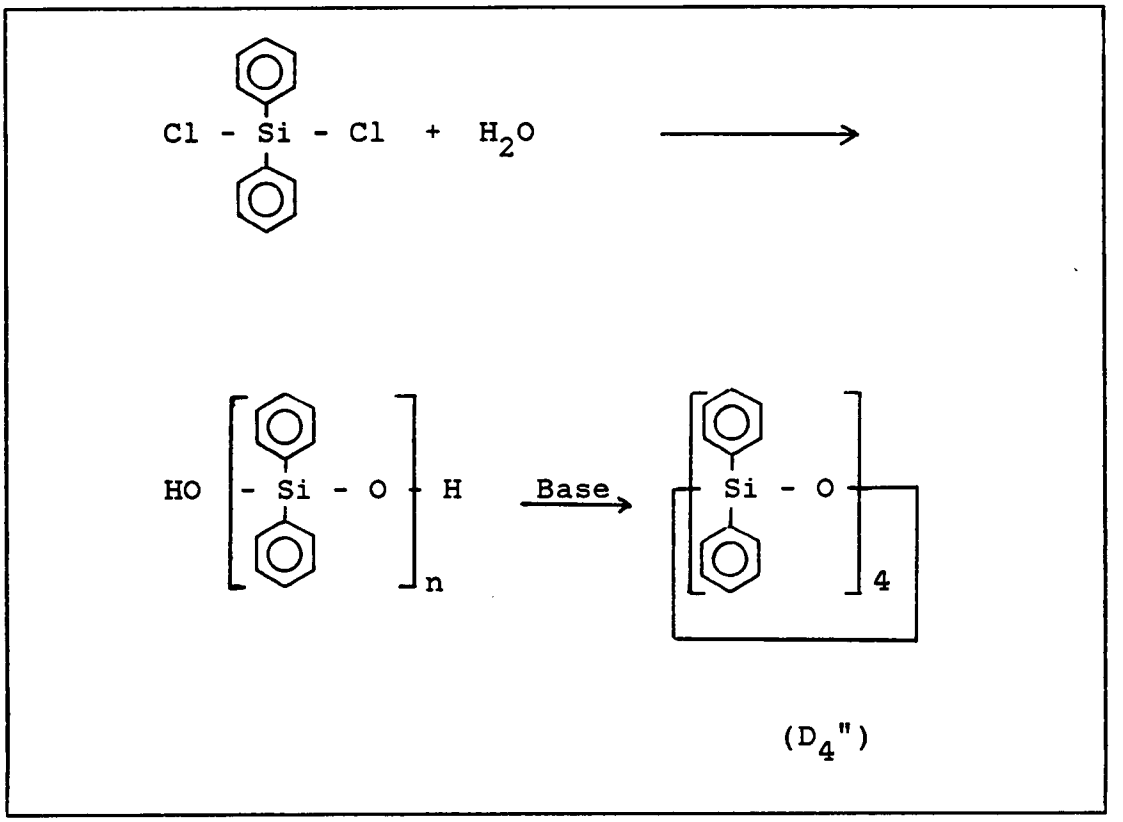

Scheme 8

Hydrolysis of Trifluoropropylmethyldichlorosilane

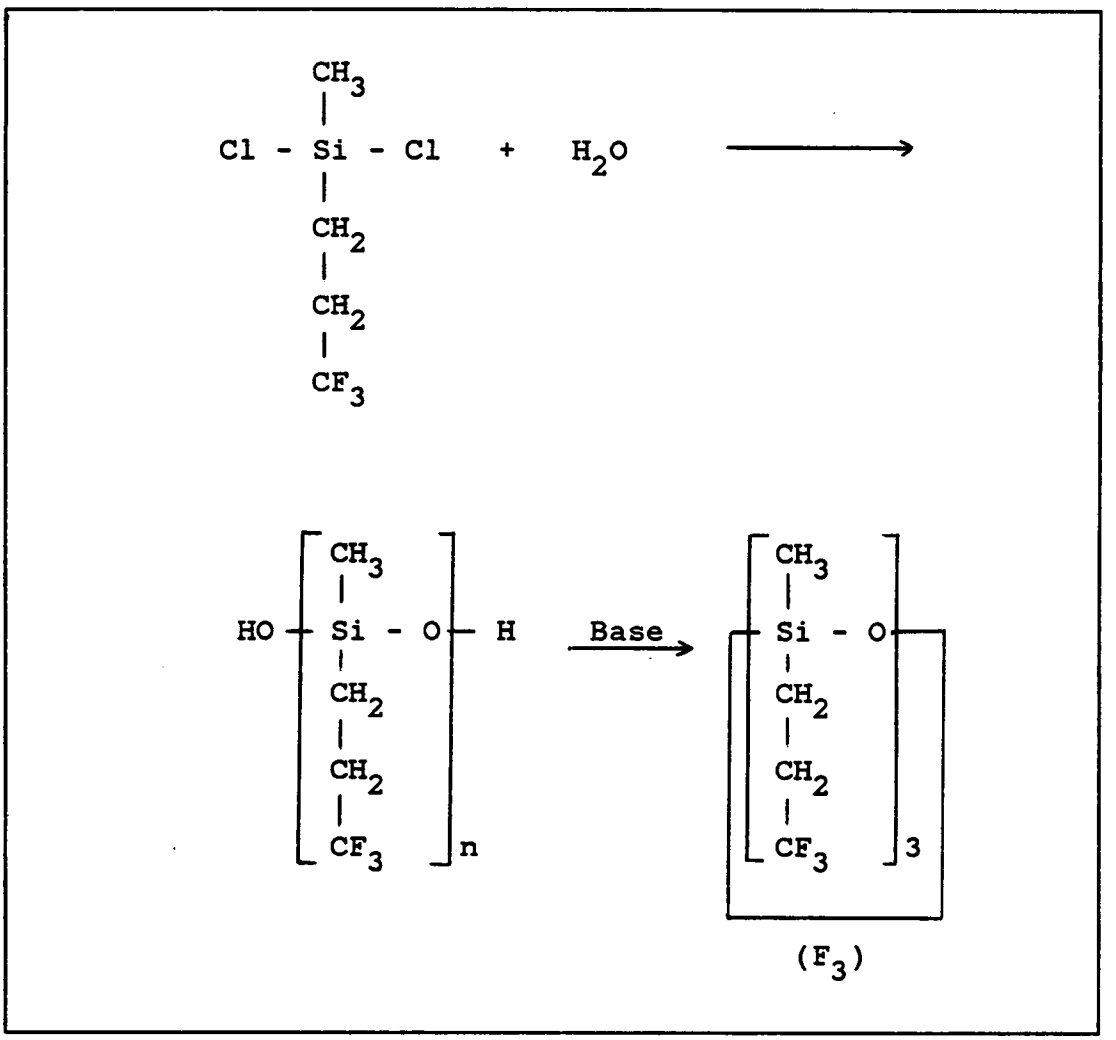

scheme for the polymerization of octamethylcyclotetrasiloxane (D_4) in the presence of an endblocker (MM) is shown in Scheme 9. The various reactions involved in the equilibration process are listed in Scheme 10 [20] and illustrated in Scheme 11 [35]. The theory of molecular weight distributions in such ring-chain equilibrated polymer systems has been described by Jacobson and Stockmayer [19] and reviewed elsewhere [20,21].

Due to the ionic character of the siloxane bond, the polymerization of cyclosiloxanes proceeds via an ionic mechanism under the influence of acid or base catalysis. The nature of the end groups on the endblocker and the types of organic substituents on the silicon atom dictate the choice of an acid or base catalyst [20]. An acid catalyst should be used when the end groups of the endblocker are acidic, and for basic end groups a basic catalyst is required. It is interesting to note that polymerization of cyclosiloxanes does not proceed via a radical process due to the high bond energy of the siloxane bond which is resistant to homolytic cleavage.

Base-Catalyzed Equilibration

Bases that catalyze the polymerization of cyclic siloxanes include: (1) hydroxides, alcoholates, phenolates, and

Scheme 9

Synthesis of Endblocked Polydimethylsiloxane

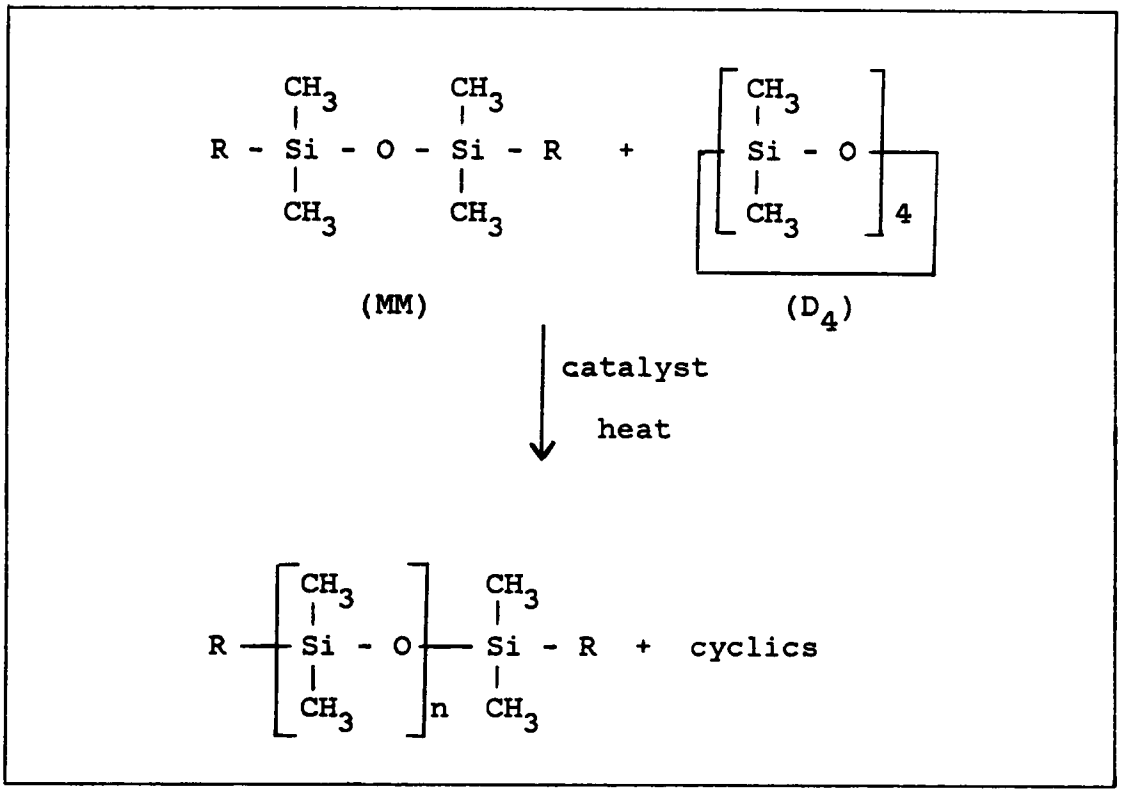

Scheme 10

Reactions Involved in the Equilibration Process

$$-D_x- + D_4 \longrightarrow -D_{(x+4)}-$$

$$-D_x- + MM \longrightarrow MD_xM$$

$$MD_xM + MM \longrightarrow MD_{(x-y)}M + MD_yM$$

$$MD_xM + MD_yM \longrightarrow MD_{(x+w)}M + MD_{(y-w)}M$$

Scheme 11

Reactions Occurring During Siloxane Equilibration

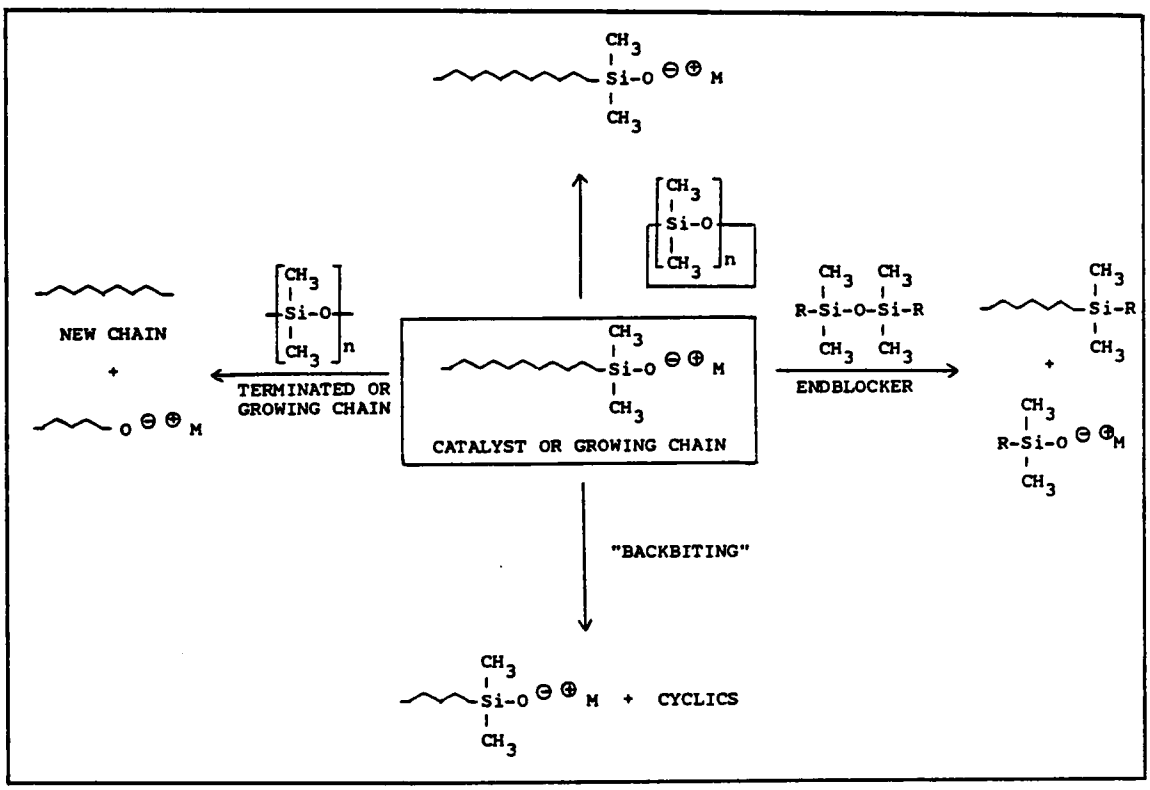

siloxanolates of the alkali metals, (2) quarternary ammonium and phosphonium bases, their siloxanolates and fluorides, and (3) organoalkali metal compounds [7,8]. If the catalyst is not completely removed after polymerization, the product may degrade slowly at room temperature and much more rapidly at elevated temperatures. To avoid this, the catalyst must be completely removed. Generally, this is done by neutralization or thorough washing. However, in siloxane chemistry transient catalysts are often employed. Transient catalysts are effective at polymerization temperatures, but subsequently can be completely destroyed by heating for a short time at somewhat higher temperatures [22,23]. Tetramethylammonium hydroxide, tetrabutylphosphonium hydroxide, and their siloxanolates are often used as transient catalysts for the preparation of silicone polymers with improved resistance to hydrolytic degradation at elevated temperatures. In the case of tetramethylammonium hydroxide and its siloxanolate, the catalyst is active at a polymerization temperature of 80°C, but can be readily decomposed at temperatures above 130°C to give products such as methanol, methoxysiloxane and trimethylamine which are volatile or easily stripped off after equilibration.

The base-catalyzed polymerization of cyclosiloxanes involves the attack of the siloxanolate anion on the

electropositive silicon atom of the cyclic or linear species as is illustrated in Scheme 12 [24,25]. The rate of reaction is proportional to the square root of the catalyst concentration and has been attributed to both the electronegativity of the substituents on the silicon atoms and the tendency of the active centers to form ion pairs [1,20]. For example, phenyl and trifluoropropyl groups cause faster rates of anionic polymerization than methyl groups. This observation is due to the electron-withdrawing effects of the phenyl and trifluoropropyl groups which increase the effective positive charge on the silicon atom which, in turn, facilitates nucleophilic attack [7,8].

The activity of siloxanes towards equilibration by base catalysis decreases in the order [7,21]

$$D_3 > D_4 > MD_2M > MDM > MM,$$

where M denotes endblocker groups and D refers to cyclic or linear $-Si(CH_3)_2O-$ groups. Polymerization of cyclic siloxanes in the presence of an endblocker and under base catalysis generally proceeds through a transient viscosity maximum after which the slower reacting endblocker equilibrates into the siloxane chains and begins to control the molecular weight [7,24,190]. The weight fraction of equilibrium cyclics remaining in a base-catalyzed polymerization has been

Scheme 12

Base-Catalyzed Equilibration

Initiation

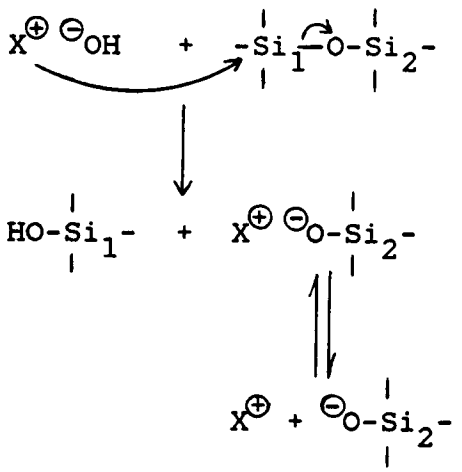

Propagation

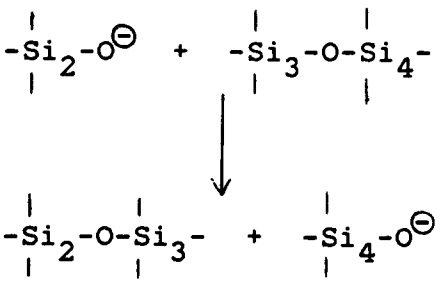

shown to increase with polarity and bulkiness of the silicon substituents: CH_3 < $-CH_2CH_3$ < $-CH_2CH_2CH_3$ < C_6H_5 < $-CH_2CH_2CF_3$ [26].

Acid-Catalyzed Equilibration

The cationic polymerization of cyclosiloxanes by acid catalysis is less studied than the anionic process and, therefore, is not yet well understood. Various Bronsted and Lewis acids have been studied, with sulfuric acid being the most widely used [26,27]. A generalized mechanism for the acid-catalyzed polymerization of cyclosiloxanes is shown in Scheme 13 [20,24]. Under acid catalysis it has been observed that the rate of polymerization increases when electron-donating groups are attached to the silicon atoms.

In the acid-catalyzed equilibration of cyclosiloxanes and an endblocker, there is no apparent viscosity maximum. This is due to the fact that the acid catalyst attacks the more basic endblocker (MM) before attacking the cyclic siloxane tetramer (D_4). Therefore, the order for activity of siloxanes toward acid catalysis is [7,21]:

$$D_3 > MM > MDM > MD_2M > D_4.$$

Scheme 13

Acid-Catalyzed Equilibration

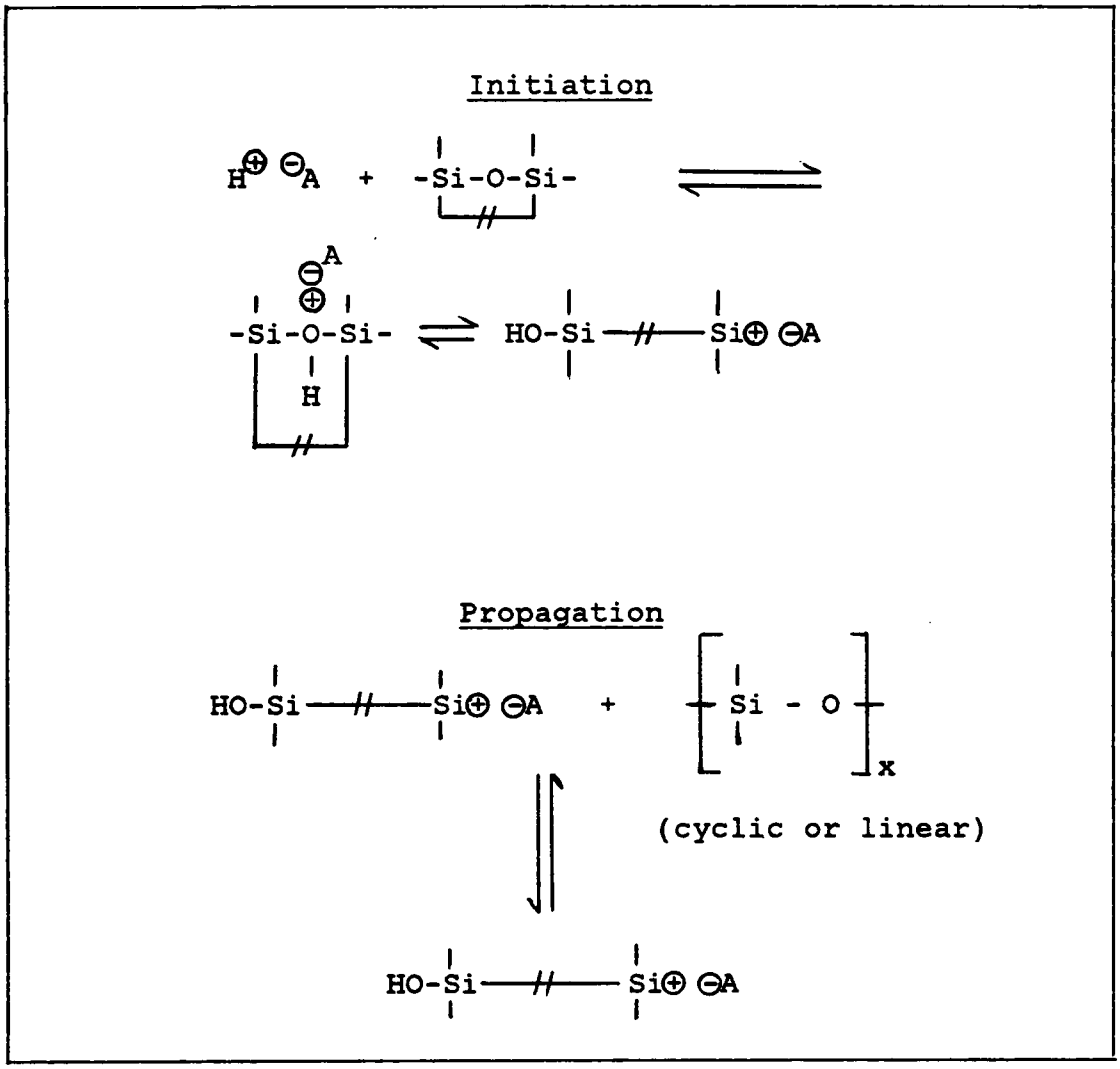

Siloxane Copolymerizations

Siloxane copolymerization extends even further the possibility of modifying these already versatile materials to provide specific properties for particular applications. The simplest copolymerization technique relies upon mixing different cyclic siloxanes with an endblocker and an appropriate catalyst, and allowing random copolymerization to occur.

The copolymerization of octamethylcyclotetrasiloxane (D_4) and octaphenylcyclotetrasiloxane (D_4") is a controversial subject of limited investigation. It should be noted that equilibration of D_4 and D_4" occurs only via base catalysis. The resonance and steric effects of the phenyl substituents render the silicon atoms electropositive which, in turn, make the oxygen atoms less basic and, therefore, less likely to be attacked by an acid catalyst.

In an extensive study of the kinetics of D_4 and D_4" copolymerizations over a wide range of D_4/D_4" ratios, it was reported that D_4 polymerizes earlier than D_4" [29]. It was noted that as the initial concentration of D_4" in the reaction mixture increased, the rate of copolymer formation and the equilibrium yield decreased. The equilibrium cyclics were generally identified as mixed dimethyl-diphenyl cyclics.

These findings contradicted the results of an earlier study [28] where it was observed that D_4" polymerizes first, and D_4 starts to polymerize only after the disappearance of D_4". The initiation of D_4 polymerization was slow because of the stability of the diphenylsiloxanolate anion. The resonance and steric effects of the phenyl rings make the siloxanolate anion less basic and, therefore, less reactive.

The copolymerization of trifluoropropylmethylcyclotrisiloxane (F_3) and D_4 is best accomplished by base catalysis. Due to its high degree of ring strain, the cyclic trimer, F_3, polymerizes much faster than the cyclic dimethylsiloxane tetramer, D_4. Also, F_3 is more susceptible to nucleophilic attack than D_4 since the electronegative and inductive effects of the trifluoropropyl groups increase the electropositive character of the silicon atoms relative to dimethyl substituted silicon atoms [7].

In copolymerizations of D_4 and F_3 where the concentration of F_3 is relatively high, and in polymerizations of F_3 only, it has been observed that F_3 is rapidly converted to linear polymers, but subsequently undergoes depolymerization at long reaction times to yield the thermodynamically stable cyclic tetramer, F_4 [2,28].

2.2 POLYESTERS

2.2.1 Overview

Polyesters are among the more versatile synthetic polymers in that they find wide commercial use as fibers, plastics, and coatings [36-39,41,42]. They may be classed as heterochain macromolecules that possess carboxylate ester groups (3) as integral components of their polymer backbones.

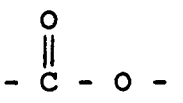

(3)

By this definition, polyesters are distinguished from other ester-containing polymers such as polyacrylates, poly(vinyl esters), and cellulose esters in which the ester groups form part of substituent groups pendant from the polymer backbone. These distinctions are relevant to the formation and structural integrity of the linear polyesters as well as to their properties and uses.

Polyesters were the first linear polymers of high molecular weight to be prepared by a controlled step-growth polymerization reaction in the pioneering work of Carothers [43]. His research in the polyester field was mainly concerned with the aliphatic, fiber-forming members which were

too low melting and solvent sensitive to be used directly as textile materials. The underlying structural concepts were later extended to crystalline ring-containing polyesters by Whinfield [44] who discovered the fiber- and film-forming material, poly(ethylene terephthalate) (4), which is one of the most important members of the polyester group.

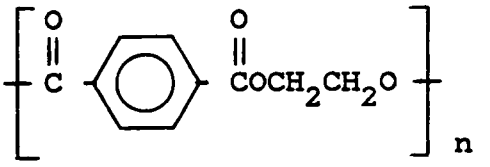

(4)

The aliphatic polyesters subsequently found uses in a variety of applications which include plasticizers and intermediates for polyurethane elastomers, foams, and spandex fibers.

Unsaturated polyesters are the most common polymers used in conjunction with glass fiber reinforcing. They are prepared from difunctional monomers, one of which contains a double bond that is capable of undergoing addition polymerization in a subsequent crosslinking reaction. Typically, the linear unsaturated polyester is processed to a relatively low molecular weight; then it is dissolved in a monomer such as styrene to form a viscous solution. Crosslinking, usually initiated by free radical initiators, is

thus a vinyl copolymerization between the unsaturated polyester and the solvent monomer. Further details concerning unsaturated polyesters will not be included in this discussion. The interested reader is referred to other reviews [45,46].

The following sections will briefly review the synthesis of polyesters and their various properties and applications. An emphasis will be placed on polyarylesters (or polyarylates) since they are pertinent to this research.

2.2.2 Synthesis of Polyesters

The common methods of synthesizing simple esters are used in the preparation of polyesters [32,39-40]. These include direct esterification, transesterification (ester exchange or ester interchange), and the reaction of alcohols with acyl chlorides or anhydrides. Scheme 14 illustrates the general reactions involved in polyester formation. Each of these reactions are mechanistically well understood and involve nucleophilic addition to the carbonyl group, an addition that is facilitated by the polar nature of the carbon-oxygen double bond and the ability of the carbonyl oxygen atom to assume a formal negative charge. A general mechanism may be written as shown in Scheme 15. Each step is reversible, although it should be recognized that in the

Scheme 14

General Reactions Involved in Ester Formation

Direct esterification

$$RCO_2H + R'OH \longrightarrow RCO_2R' + H_2O$$

Transesterification

$$RCO_2R'' + R'OH \longrightarrow RCO_2R' + R''OH$$

Reaction of alcohols with

1. Acyl Chlorides

$$RCOCl + R'OH \longrightarrow RCO_2R' + HCl$$

2. Anhydrides

$$(RCO)_2O + R'OH \longrightarrow RCO_2R' + RCO_2H$$

Scheme 15

Ester Formation Via Nucleophilic Addition

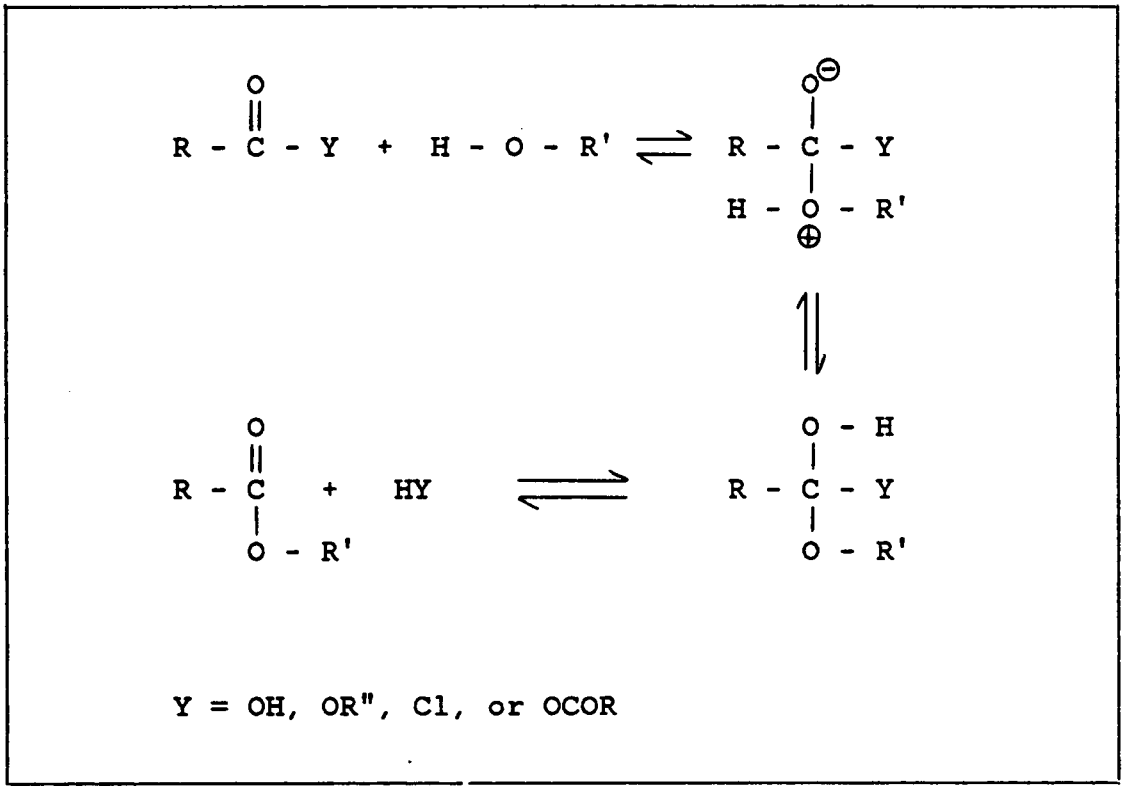

case of acid chlorides and anhydrides, the overall process is irreversible.

Direct esterification and transesterification are relatively slow, reversible reactions. Reaction rates are normally increased by using acid catalysts that coordinate with the carbonyl oxygen, and thus enhances the electrophilic character of the carbonyl carbon atom as shown below.

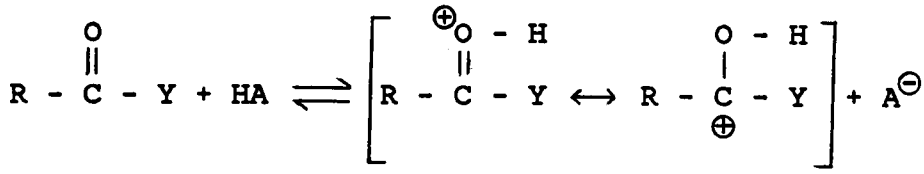

Weakly basic catalysts are also used in transesterification, presumably to increase the nucleophilicity of the alcohol by formation of alkoxide ion:

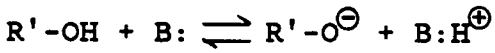

Reaction rates may also be increased by using an excess of one reactant, usually alcohol, and the reaction may be driven to completion by removal of by-product water or alcohol. Acyl halides and anhydrides react rapidly with alcohols in the absence of catalysts. These reactions are virtually irreversible because the by-products (HCl and carboxylic acid, respectively) are of much lower nucleophilicity than the alcohol. The extension of these reactions to

macromolecular synthesis represents a significant and commercially important application of step-growth polymerization.

Polyester chemistry is not limited to the above reactions. For example, ring-opening polymerization of lactones produces polyesters of commercial importance [47,48].

2.2.2.1 Direct Esterification

The simplest method of polyester synthesis is the reaction of a glycol with a dicarboxylic acid or the self-condensation of a hydroxycarboxylic acid. These two types of direct esterification are illustrated in Scheme 16. Both reactions are equilibrium processes and their progress, and hence their molecular weight, is determined by the efficiency with which by-product water is removed from the reaction [36-40].

Polymerization to high conversions require that an equal number of reacting groups be present at all stages of the reaction. This condition is satisfied in the self-polycondensation of hydroxycarboxylic acids. However, in the reaction of dicarboxylic acids with glycols, the latter are often relatively volatile and some portion of the initial charge may be lost by distillation with liberated water or in the carrier gas. It is therefore usual to employ an

Scheme 16

Direct Esterification Reactions

Glycol-Carboxylic Acid Condensation

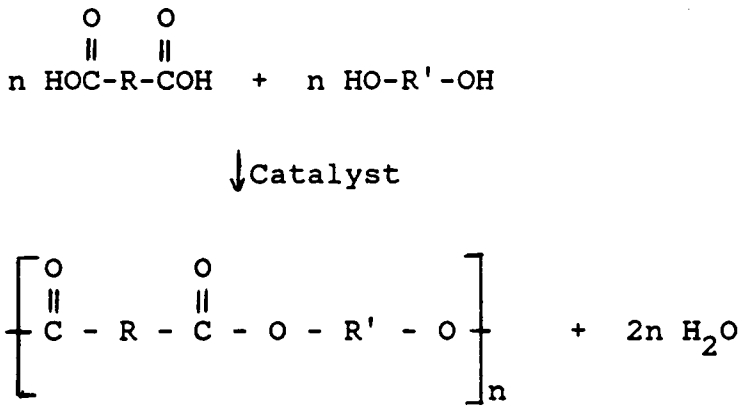

Hydroxycarboxylic Acid Self-Condensation

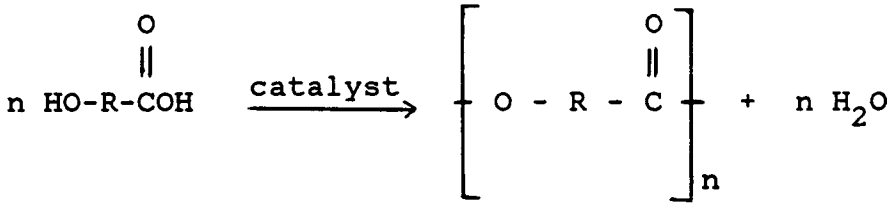

excess of glycol (about 10-20 mole %) to compensate for physical losses.

A calculated stoichiometric imbalance may be used to regulate the molecular weight as well as the nature of the endgroups. This is particularly important when a difunctional, controlled molecular weight oligomer is required for subsequent copolymerization.

As previously discussed, direct esterification reactions are relatively slow. Either the carboxylic acid functional groups provide protons to catalyze the esterification reaction, or small amounts of a protonic acid or a Lewis acid are required for catalysis.

2.2.2.2 Transesterification

This category of reactions, also known as ester exchange or ester interchange, includes the synthesis of polyesters by exchange reactions of alcoholysis or acidolysis between paired reactants comprising diols with dicarboxylic acid diesters, and diol-diesters with dicarboxylic acids, respectively [36-40]. Of lesser practical value, double ester exchange reactions of diol-esters with dicarboxylic acid diesters also yield polyesters. The reactions are expressed stoichiometrically in Scheme 17, and each procedure can also be adapted to self-condensation reactions by using the corresponding hydroxycarboxylic acid derivatives.

Scheme 17

Transesterification Reactions

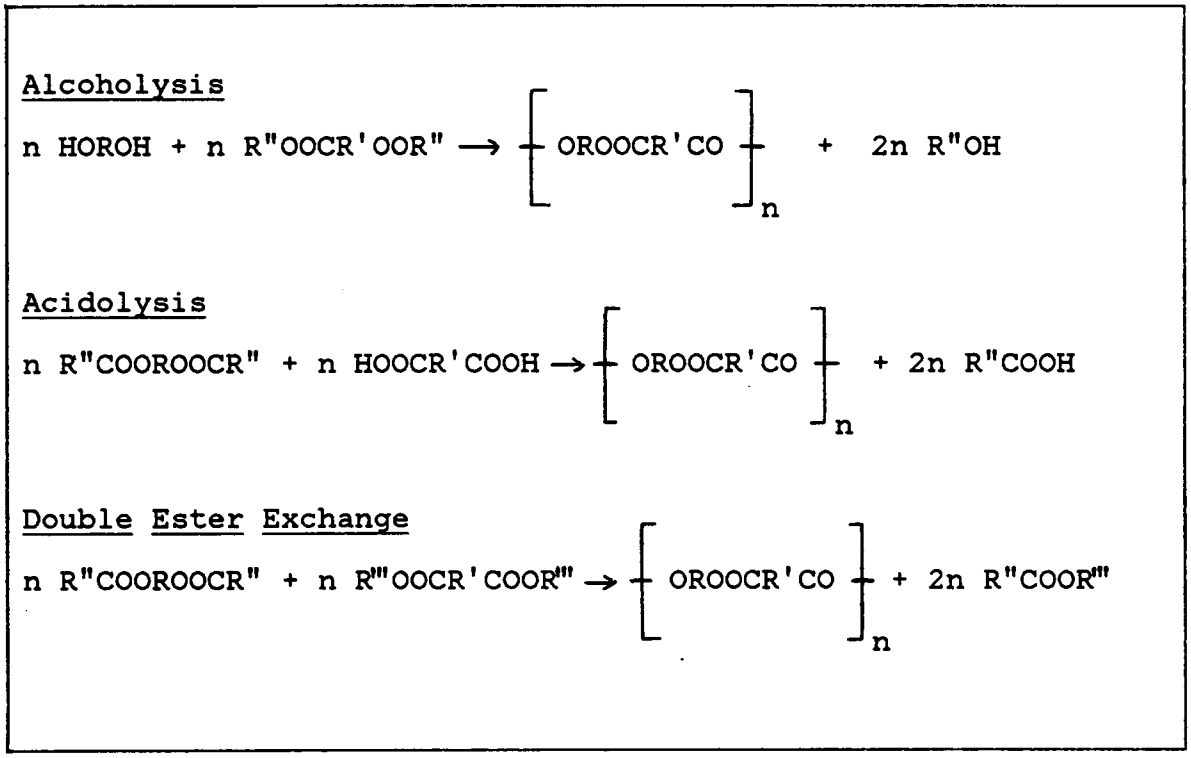

Transesterification reactions are generally carried out in the presence of a proton-donating or weak base catalyst. These processes are readily reversible, but the equilibrium may be continually displaced to the right by removal of the more volatile by-products.

2.2.2.3 Methods Involving Diacid Chlorides

An important commercial method of preparing polyesters is the reaction of diacid chlorides with dihydroxy compounds as shown below [36-40]:

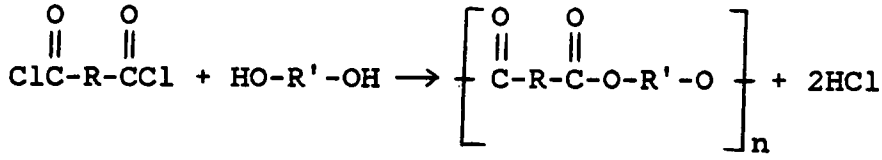

The reaction proceeds rapidly and requires no catalyst. When carried out in the presence of a base such as sodium hydroxide or pyridine, this is known as the Schotten-Baumann reaction. The base apparently catalyzes the reaction by increasing the nucleophilicity of the dihydroxy compound as well as neutralizing the HCl formed.

There are three general methods of preparing polyesters from diacid chlorides: (1) fusion of the two reactants in bulk and removal of HCl as it forms, (2) condensation in solution with HCl being removed by distillation or by salt

formation with added base, and (3) interfacial polymerization where solutions of a dihydroxy compound in aqueous base and a diacid chloride in an inert solvent are rapidly stirred together, allowing polymer formation at the interface.

The technique of interfacial polymerization [39] makes use of the virtually instantaneous reaction of phenolate anions with acid chlorides. The condensation, which is diffusion-controlled, takes place at the boundary between the two immiscible liquid phases (constantly renewed by mechanical agitation) and the liberated chloride ions are neutralized by the alkali in the aqueous phase. It is also useful to employ a phase-transfer catalyst, usually a tetraalkylammonium salt, which is believed to provide its corresponding phenolate which is more soluble at the organic phase boundary than the phenolate formed from the acid acceptor (such as NaOH or KOH). The esterification reaction liberates the tetraalkylammonium ion which returns to the aqueous phase and assists further reaction.

Very high molecular weights are obtainable by interfacial methods and do not depend on an exact stoichiometric balance since the reaction is diffusion-controlled. However, in solution polycondensation methods, purity and stoichiometric balance is critical for high molecular weight conversion. Often a calculated stoichiometric imbalance

(Carothers equation) is used to obtain a desired molecular weight oligomer with functional endgroups. Well-defined, difunctional oligomers are then used in subsequent copolymerization reactions.

2.2.2.4 Lactone Polymerization

Cyclic esters, lactones (5), undergo anionic and cationic polymerization to form polyesters [47,48].

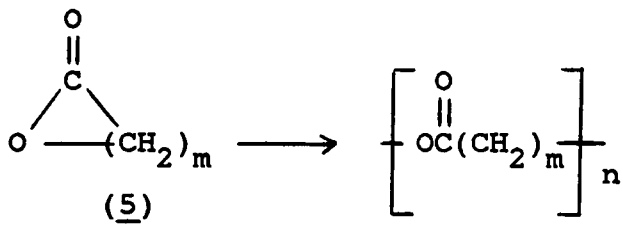

(5)

Anionic polymerization proceeds via acyl-oxygen cleavage for most lactones. Alkyl-oxygen cleavage appears to be the polymerization route for highly strained, sterically hindered cyclic monomers in the presence of a weakly nucleophilic initiator. Acyl- versus alkyl-oxygen cleavage is illustrated in Scheme 18.

Cationic polymerization proceeds via attack by monomer on a propagating center which is either the oxonium ion (6) or the acylium ion (7) formed by unimolecular ring opening of the oxonium ion.

Scheme 18

Acyl- Versus Alkyl-Oxygen Cleavage

Acyl-Oxygen Cleavage

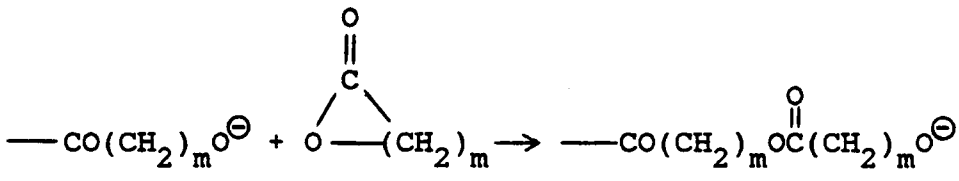

Alkyl-Oxygen Cleavage

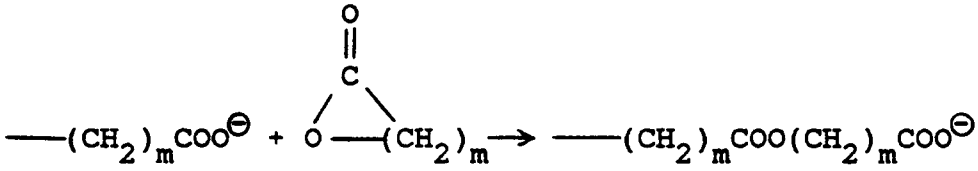

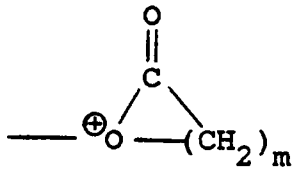

(6)

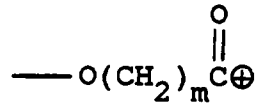

(7)

Products from the ring-opening polymerization of lactones have not gained the commercial significance of polyesters prepared by polycondensation. However, polycaprolactone (8)

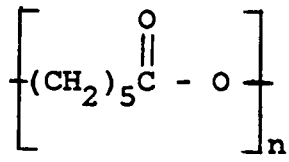

(8)

has been marketed and is recommended in applications where biodegradability is desirable.

2.2.3 Structure-Property Relationships

As with polymers in general, the properties of polyesters are determined by the geometry, symmetry, polarity, and segmental mobility of their chain structures. Their intermolecular interactions are relatively weak and the properties of polyesters are, therefore, more sensitive to changes in molecular geometry than are those of more strongly interacting polymers such as polyamides or polyurethanes.

2.2.3.1 Linear Acyclic Polyesters

In general, the oxidative, thermal, and chemical resistance of linear acyclic polyesters are satisfactory. However, they are rapidly degraded by warm alkalies and primary or secondary amines. Polyester degradation involves cleavage of the ester linkages, which liberates hydroxyl groups and yields salts or amide derivatives of the carboxylic function. The hydrophobic character of aliphatic polyesters assists in providing reasonable long-term stability to attack by water, except at high temperatures or in contact with steam, in which case hydrolysis occurs [38,39].

The effect of structural regularity on the melting point of polyesters has been studied [49]. Repeating units with an even number of carbon atoms along the backbone of the polymer chain generally exhibit disproportionately higher melting points than those with odd-numbered units, possibly because the former tend to form more fully extended linear chains than the latter. An example of this effect for a homologous series of polyesters is shown in Figure 2 [40].

At sufficiently high molecular weights, the linear polyesters are fiber-forming. However, because of the combination of low melting points, sensitivity to organic solvents, and limited hydrolytic stability, a majority of the

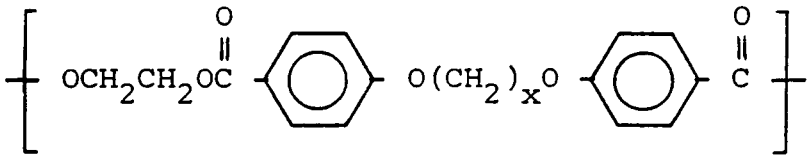

x	M.P., ^{o}C
2	240
3	190
4	215
5	150
6	170

Figure 2: Variation in melting point for polyesters [40].

acyclic polyesters are precluded from use as structural materials. Various applications do take advantage of their low glass transition temperatures. Two examples are the use of these materials as plasticizers and as components of polyurethanes. Both uses require materials having freely flexible molecules with little or no tendency to crystallize under the conditions of use. Therefore, asymmetric repeating units or copolyesters are employed.

More extensive discussions of the properties and applications of linear acyclic polyesters are found in various books and reviews [36-38].

2.2.3.2 Linear Polyarylesters

The characteristics of polyarylesters (or polyarylates) vary widely with structure, being particularly dependent upon symmetry and the ratio of cyclic to acyclic atoms in the repeating units. In 1959, Conix [54] and Eareckson [55] independently synthesized a number of aromatic polyesters with a wide range of softening temperatures, solubilities, and morphologies from various bisphenols and acid chlorides. For example, a highly crystalline polyester (9) may be prepared from bisphenol-A and terephthaloyl chloride.

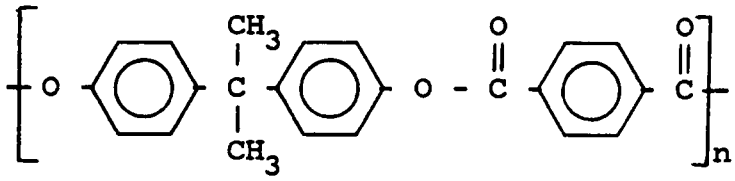

(9)

However, the polyester (10) synthesized from bisphenol-A and isophthaloyl chloride may be either crystalline or amorphous depending on the solvent casting conditions.

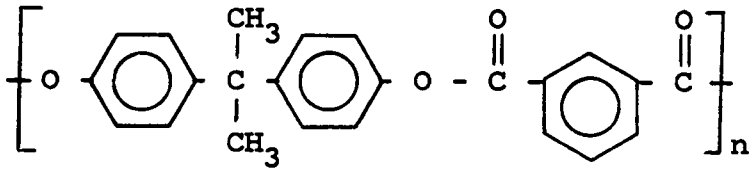

(10)

A completely amorphous polyarylester is obtained when as little as ten mole percent of one isomeric acid chloride is incorporated into a polymer containing the other acid chloride.

The ability to crystallize is also affected by (1) replacing the methyl substituents of bisphenol-A with bulkier groups such as ethyl or phenyl, and (2) restricting ring rotation by adding substituents to the aromatic rings of the bisphenol [56].

In general, polyarylester properties include ductility, UV and thermal stability, good electrical behavior, high

modulus, and relatively high glass transition temperature [50]. The chemical and environmental stability of the polyarylates is structure dependent. For example, poly(alkylene terephthalates) derived from hydroxyl compounds of the alcohol type are considerably more stable to hydrolysis than the acyclic polyesters. They are very resistant to water except at elevated temperatures, but are readily attacked by alkalies or organic bases. Polyesters derived from phenolic precursors are inherently less stable towards hydrolysis and aminolysis, but are somewhat protected by their hydrophobic nature which hinders penetration of aqueous reagents.

The thermal, oxidative, and photochemical stabilities of aromatic polyesters are typically of a high order, but the high melting and softening points of many of these materials necessitate the use of correspondingly high preparation or fabrication temperatures. In some cases this results in degradation by pyrolytic scission of ester groups, particularly those derived from secondary alcohols [36-38].

Generally, aliphatic or cycloaliphatic structures are chosen for applications where UV resistance is desired since aromatic structures absorb strongly in the UV region. Chain scission and degradation results from the release of the absorbed energy [51]. The resistance of the aromatic

polyesters to UV radiation is, therefore, an interesting and important aspect of these materials. The photo-initiated reaction, known as the photo-Fries rearrangement, is responsible for the UV stability of polyarylesters and is shown in Scheme 19. The reaction is thought to involve free radical intermediates and transforms aromatic ester linkages into ortho-hydroxybenzophenone structures which are believed to be more resistant to UV radiation [52,53,57].

Aromatic polyesters with an unsubstituted position ortho to the ester group undergo the Fries rearrangement. The rearranged ortho-hydroxybenzophenone structure is present in the topmost layer of a film where it protects the bulk of the sample. Upon prolonged exposure, the surface layer totally degrades and a protective layer is regenerated by more of the exposed polyarylester rearranging.

Various books and reviews [36-38,50,52-58] discuss the synthesis, properties and applications of aromatic polyesters in more detail.

2.3 BLOCK COPOLYMERS

2.3.1 Overview

The need for new cost effective materials for specific applications has generated wide interest in polymer "hybrids," i.e., block and graft copolymers, random/alter-

Scheme 19

The Photo-Fries Rearrangement of Polyarylesters

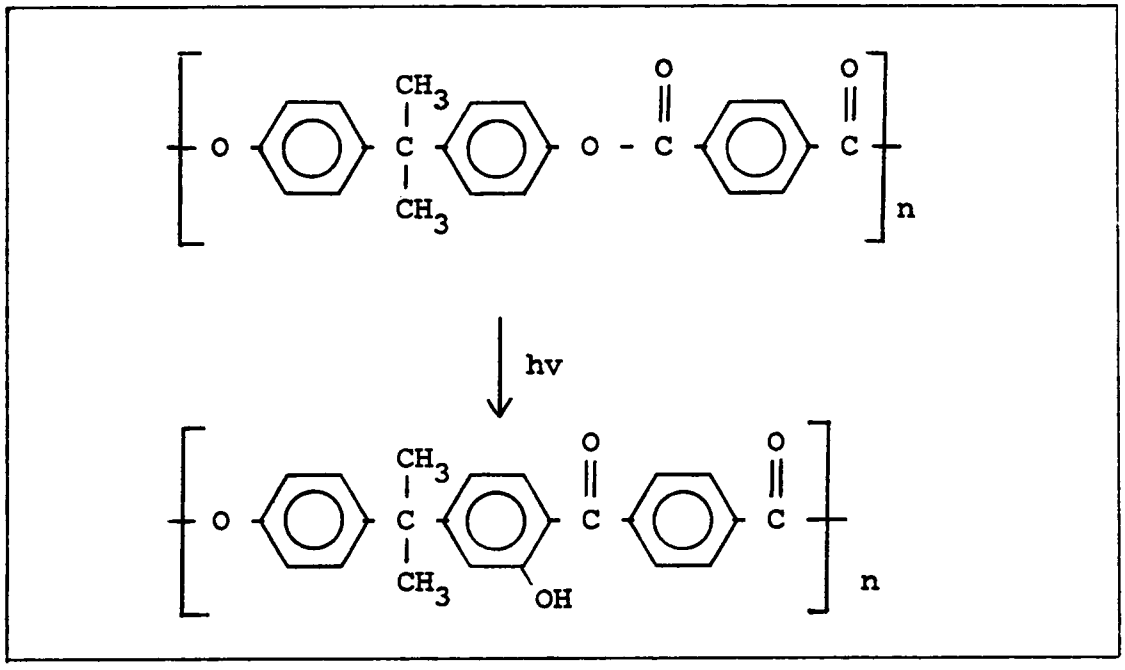

nating copolymers, and blends [63,64]. From an economical and preparative point of view, the most direct method of producing polymer hybrids is the physical blending of two or more polymers. The properties and utility of physical blends are strongly dependent upon the degree of compatibility of the components. Unfortunately, most amorphous physical blends of homopolymers are immiscible and give rise to low strength materials due to the lack of interfacial adhesion between the separate phases [68,69].

The most versatile, economical, and easily synthesized copolymers are the random/alternating copolymers. Most commercial random copolymers are derived from vinyl monomers and/or conjugated dieners. These materials are characterized by a statistical or random coupling of the monomer units which is dependent on the relative reaction rates of the two components. The properties of random copolymers are intermediate to those of the corresponding homopolymers and depend upon the weight fraction of each species [70].

Alternating copolymers are characterized by the alternate, rather than statistical, placement of the comonomer repeat units [71]. This type of copolymer is relatively rare since pairs of monomers with highly specific copolymerization reactivity ratios are required. Like random copolymers, the properties can usually be represented by a weighted average of the individual homopolymer properties.

Graft copolymers combine some of the features of physical blends and random copolymers since they are chemically linked pairs of homopolymers as shown below.

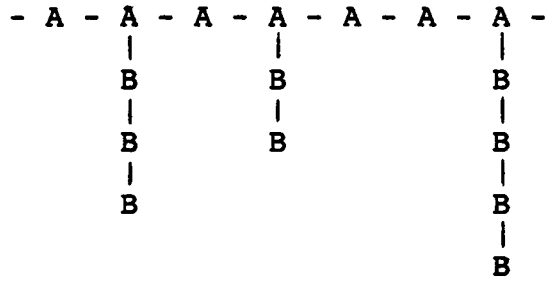

The presence of the chemical linkage (A-B) is responsible for the physical properties of these systems which are characteristic of each of the components, rather than an averaging of their properties [72,73].

Block copolymers are comprised of chemically dissimilar segments as are graft copolymers, however, the segments are terminally connected. Their sequential arrangement can vary from A-B structures containing two segments only, to A-B-A block copolymers with three segments, to multiblock $(A\text{-}B)_n$ systems possessing many segments. Another, but less common, variation is the radial block copolymer. Schematic representations of the various block copolymer types are shown in Figure 3.

Block and graft copolymers have several advantages over blends and include: (1) the covalently bonded segments elim-

A-B Block Copolymer

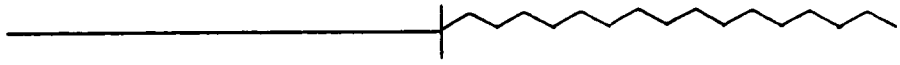

A-B-A Block Copolymer

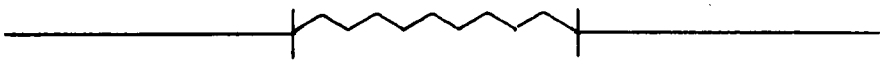

$(A\text{-}B)_n$ Block Copolymer

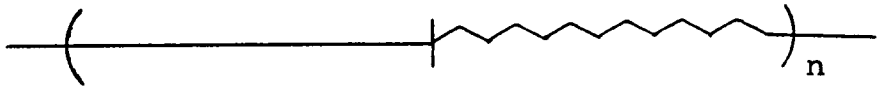

Radial Block Copolymer

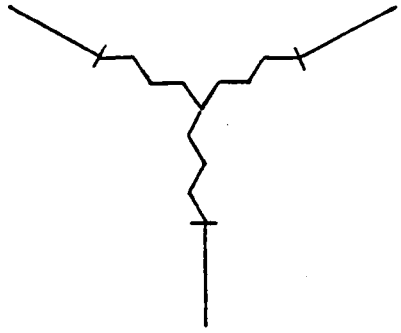

Figure 3: Block copolymer architectures.

inates the interface problem between dissimilar segments, (2) novel materials can be prepared by accurately controlling the molecular architecture, and (3) block and graft copolymers can be used to strengthen immiscible blends by serving as compatibilizers which improve the interfacial adhesion and load transferring capability of the components [67]. Most of the properties of block and graft copolymers can be attributed to microphase separation which has been exploited commercially in the form of impact modified thermoplastics and thermoplastic elastomers.

The following sections of this review will focus on block copolymers and microphase separation, since these topics are significant to this study.

2.3.2 Synthesis

Sophisticated synthetic techniques are necessary to prepare the well-defined structures of block copolymers. Step-growth, living addition polymerization and, to some extent, free radical methods have been used to prepare block copolymers [74-78]. A-B diblock and A-B-A triblock architectures are primarily synthesized by living anionic polymerization techniques. By contrast, $(A\text{-}B)_n$ copolymer structures are most often prepared via step-growth methods. Due to the statistical nature of the stoichiometrically control-

led step-growth reactions, it is not possible to synthesize A-B and A-B-A structures by this technique. On the other hand, it is inconvenient to prepare the well-defined $(A-B)_n$ architecture via living addition techniques because of the high probability of premature chain termination encountered during repeated sequential monomer addition cycles.

Blocks of predictable molecular weights and narrow molecular weight distributions are obtainable via living anionic polymerization. Long block lengths are also possible since the block molecular weight is governed only by the ratio of monomer to initiator. These features are not easily achieved with step-growth processes, however, the latter offers a wider selection of chemical structures, including many high performance materials.

From the brief discussion above it can be concluded that the available synthetic techniques are often restricted to a considerable extent by the block copolymer architecture desired. A wide range of chemical structures, encompassing all the architectural forms of block copolymers, can be prepared by selecting one, or a combination, of the available synthetic techniques.

2.3.3 Properties

Architecture exerts a major influence on some of the properties of block copolymers, while other properties are essentially independent of sequential arrangement. The properties that are dramatically effected by architecture are elastomeric behavior, melt rheology, and toughness in rigid materials. The architecture-independent properties include those derived from the chemical nature of the segments and include thermal transition behavior, electrical and transport properties, stability, and chemical resistance.

2.3.3.1 Morphology

Block copolymers may exist in a single-phase or a multiphase morphology. Both of these can offer unique property advantages. Single-phase block copolymers are desirable when the properties of a random copolymer are sought from pairs of monomers that cannot be combined via traditional random copolymerization techniques. However, block copolymer structures are more commonly chosen because of their unique properties possible with two-phase morphological systems. Domain size and shape are critical since these parameters ultimately govern the macroscopic bulk properties of the material. Five general morphological arrangements are

illustrated in Figure 4 [140] based on the volume fractions of the components. Both the domain arrangement and the sharpness of the domain interface are subject to variations in fabrication conditions [83].

2.3.3.2 Thermal Properties

Above certain critical block molecular weights, most block copolymers exhibit microphase separation, however, exceptions can occur for blocks with similar polar and dispersive forces and/or specific interactions. The modulus-temperature behavior of single-phase versus two-phase block and graft copolymers is contrasted in Figure 5 [141].

The existence of a single Tg intermediate between the constituents indicates a single amorphous phase block copolymer. In these types of systems, compositional changes cause horizontal temperature shifts.

In the two-phase systems, the identity of both segments is retained, as evidenced by the presence of two distinct glass transition temperatures. A constant temperature plateau exists between the two Tg values of a phase separated system. The flatness of the plateau is dependent upon the degree of phase separation; the more complete the phase separation, the more temperature insensitive the modulus becomes. For two-phase block copolymers in which the block

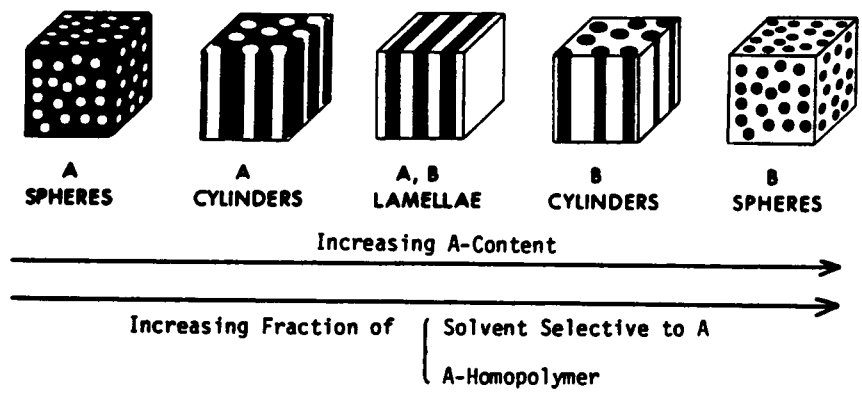

Figure 4: Block copolymer morphology [140].

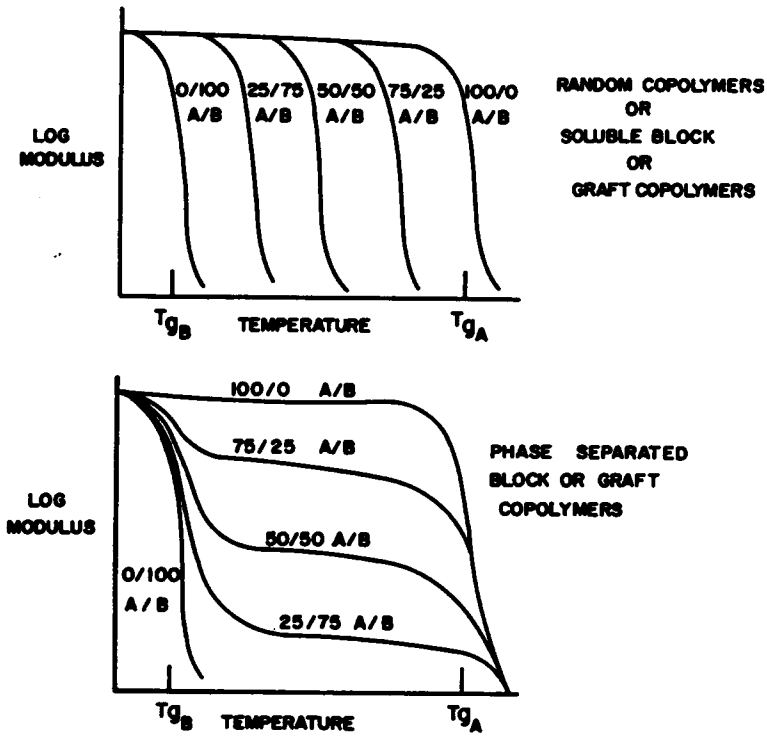

Figure 5: Generalized modulus-temperature behavior of homogeneous and microheterogeneous block copolymers [141].

lengths are beyond the level at which the number-average molecular weight ($\bar{M}n$) affects Tg, compositional changes cause vertical modulus shifts.

The determination of phase behavior is commonly accomplished via modulus-temperature measurements, mechanical loss data, and/or thermal analysis (i.e., differential scanning calorimetry). The most sensitive technique for determining minor, as well as major transitions in multiphase systems, is the measurement of dynamic mechanical loss characteristics.

2.3.3.3 Mechanical Properties

An important characteristic of elastomeric block copolymers is their ability to display rubbery properties while retaining thermoplastic processability. The materials exhibiting this type of behavior are generally comprised of a major portion of a soft segment (Tg below room temperature) and a minor portion of a hard segment (Tg above room temperature). The soft block affords a flexible elastomeric nature, while the hard bloc provides both physical crosslink sites and filler reinforcement characteristics. Due to microphase separation, the hard blocks associate with each other to produce small (100-300Å) dispersed domains that are chemically attached to the rubber matrix. The glassy or

crystalline hard domains provide high strength via reinforcement of the rubbery matrix. This is possibly due to (1) the discrete nature of the hard domains, (2) the ideally small size and uniformity of the domains, and (3) the perfect interphase adhesion insured by the chemical intersegment linkage [64].

The properties of thermoplastic elastomers are dependent upon the molecular weight and volume fraction of hard and soft segments present. Block length must be great enough to develop the two-phase system, yet not so excessive as to obviate thermoplasticity. Modulus, recovery characteristics, and ultimate properties are affected by the variation of the hard block/soft block ratio. The volume fraction of the hard block must be sufficiently high to provide an adequate level of physical crosslinking if good recovery properties and high tensile strengths are to be obtained. On the other hand, excessively high hard block concentrations can cause the hard domains to change from a discrete spherical shape to a co-continuous lamellar form, which in turn causes deterioration in recovery properties.

Architecture is extremely important in determining the mechanical properties of elastomeric block copolymers. To develop good ultimate properties, systems comprised of an A-B architecture are generally vulcanized or chemically

crosslinked. Elastomeric block copolymers having A-B-A (linear or radial) or $(A-B)_n$ architectures display unique properties without crosslinking. These latter systems combine the mechanical properties of a crosslinked rubber with the processing behavior characteristic of a linear thermoplastic polymer.

Block copolymers exhibit a marked dependence of mechanical properties on the method of sample preparation. Variations in casting solvent (from an A block preferred solvent to a B block preferred solvent) bring about significant changes in the stress-strain and dynamic mechanical behavior. The effect is most prominent in the initial stage of the stress-strain curve, i.e., the tensile modulus. The behavior can be rationalized by considering the phase separation process and the resultant morphological changes [84].

2.3.3.4 Processability

The capability of a material to be transformed into useful shapes via solution casting or melt fabrication techniques is termed processability. Solution fabrication of block copolymers presents no unusual problems, however, two-phase amorphous block copolymers are generally more difficult to melt fabricate than single-phase block copolymers of similar molecular weight. This is due to the unusual

rheological characteristics of these materials which results from the partial retention of their two-phase morphology in the melt. High processing temperatures and pressures are often necessitated by the high melt viscosity and elastic character of these materials. Shear rate sensitivity can also be a limitation in these systems.

Melt processability is greatly influenced by block copolymer architecture. Typically, A-B diblock copolymers process much more readily than A-B-A or $(A-B)_n$ copolymers. This is due to the network structures formed by the latter two architectures, which persist in the molten state.

In amorphous block copolymers, phase separation and melt processability are dependent upon the molecular weight and the differential solubility parameter (Δ) of the two segments. Processing ease increases as either the Δ value or the block lengths become smaller. Control of the Δ parameter is often preferable, since the alternative approach of shortening block length is invariably accompanied by a decrease in the Tg of the segment [64].

2.3.3.5 Optical Properties

Both rigid and elastomeric block copolymers offer significant advantages over homopolymer blends in optical clarity. Incompatible polymer blends are typically opaque due

to the refractive index differences and the large domain sizes of their constituent macrophases. However, block copolymers appear transparent even though their segments may differ significantly in refractive index. This is due to the entropy restrictions imposed by the insegment linkages which result in microphase separation. The domains are much smaller (< 1000Å) than the wavelength of light and, therefore, give rise to transparency. As domain sizes increase predictably with molecular weight, opacity does not occur except a very high block molecular weights.

2.3.4 Applications

Commercial acceptance of block copolymers has centered upon their utility as thermoplastic elastomers. The applications of block copolymers can be divided into three groups - elastomers, toughened thermoplastic resins, and surfactants.

The two-phase block copolymer elastomers that have been commercialized are of three structural types: (1) A-B-A or radial styrene-diene block copolymers and their hydrogenated derivatives (Kraton by Shell), (2) $(A\text{-}B)_n$ ester-ether block copolymers (Hytrel by DuPont), and (3) $(A\text{-}B)_n$ urethane-ester block copolymers (Estane by B. F. Goodrich). The thermoplastic elastomeric behavior of these materials make them

uniquely useful in a variety of application areas such as automotive, mechanical goods, electrical and electronic, sealants, caulks and adhesives, and footwear. The block copolymer properties most important in these applications are dimensional stability, recovery, compression set, utility at high and low temperatures, and, in some cases, oil, chemical, and abrasion resistance. Low dielectric constant and dissipation factor levels, along with weatherability, are of importance for electrical and electronic applications.

In contrast to chemically crosslinked thermoset rubbers, elastomeric block copolymers can be economically fabricated into final products by processes similar to those used for thermoplastics. These processes include injection or blow molding, extrusion, vacuum forming, and solution casting. Reprocessing is possible since these materials are not vulcanized.

Toughened thermoplastic resins include block copolymers containing a high volume fraction of a hard block and a minor concentration of a soft block. A commercially available example is an amorphous radial styrene-butadiene block copolymer containing approximately 75 weight percent polystyrene (Phillips K resins). These materials are used in transparent packaging applications since they are tough and optically clear.

Two types of block copolymer surfactants are in commercial use. One type contains both hydrophobic segments and hydrophilic segments. One example of such a material is the class of polypropylene oxide - polyethylene oxide A-B and A-B-A block copolymers. These nonionic surfactants are especially useful in applications that cannot tolerate the more commonly used anionic and cationic surfactants. The properties of the nonionic surfactants make them useful in applications requiring the emulsification of aqueous and nonaqueous components and/or the wetting of substrate surfaces.

The second commercially useful block copolymer surfactant is represented by the silicone-alkylene oxide copolymers which are used as polyurethane foam stabilizers. In such applications, the highly incompatible siloxane segment resides at the gas-urethane interface while the alkylene oxide segment is soluble in the urethane matrix. A more uniform foam structure results since the block copolymer controls bubble nucleation and cellular growth.

2.3.5 Siloxane-Containing Block Copolymers

Siloxane-containing block copolymers include diblock, triblock, and multiblock systems. The hard blocks that have been copolymerized with soft polysiloxane blocks include:

polystyrene, poly(α-methylstyrene), poly(methyl methacrylate), poly(alkylene ether), poly(arylene ether) (e.g., polysulfone), polyisoprene, polyacrylonitrile, polyester, polycarbonate, polyamide, polyimide, polyurethane, and polyurea. The subsequent discussion briefly summarizes the synthesis, properties, and applications of siloxane-ester block copolymers which are of interest to the research discussed herein. A detailed review of siloxane-containing copolymers can be found in reference [64].

The polyester blocks that have been copolymerized with poly(dimethylsiloxane) are of three types - bisphenol-A carbonate, tetramethyl cyclobutylene carbonate, and arylene (or alkylene) phthalates.

Preparation of bisphenol-A carbonate-dimethylsiloxane block copolymers (11) was first reported by Vaughn [86].

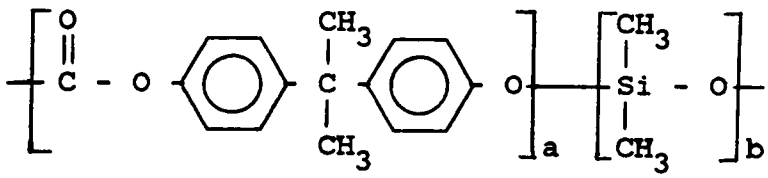

(11)

The synthetic technique involved phosgenation of a mixture of bisphenol-A and a bis(dichloro)-terminated dimethylsiloxane oligomer in the presence of pyridine. The resulting copolymer is an alternating random block copolymer in which

the blocks are polydisperse and of fairly low degree of polymerization.

A second synthetic approach involves the condensation reaction of dihydroxyl-terminated polycarbonate oligomers with bis(dimethylamine)-terminated dimethylsiloxane oligomers [21,172-174]. This technique produces a well-defined, perfectly alternating block copolymer since both blocks are synthesized and well-characterized prior to copolymerization.

High molecular weight block copolymers with varying carbonate/siloxane ratios have been prepared. The morphology and mechanical properties are dependent upon copolymer composition and block molecular weights [87]. Due to the large difference between the solubility parameters of the two blocks (10.0 for polycarbonate and 7.5 for polydimethylsiloxane), microphase separation has been observed in these systems [88]. The copolymers exhibit two glass transition temperatures - one at -110°C due to the siloxane block and another between 60 and 140°C due to the carbonate block. The range of observed Tg values for the carbonate block is explained by block molecular weight. As the block molecular weight was increased, a corresponding increase in the Tg was noted [89]. However, the low temperature transition displayed little dependence on siloxane block length.

Carbonate-siloxane block copolymers have shown useful electrical properties, corona resistance, and permeability properties [90]. Oxygen-rich air has been prepared using solution cast films of these copolymers as membranes [91]. These copolymers are also claimed to be useful in coating and adhesive applications [92].

The properties of bisphenol-A carbonate homopolymer can be modified by blending it with a low concentration (< 5%) of the carbonate-siloxane copolymer [93,94]. Such blends have reduced wettability and functional properties. This is due to concentration of the copolymer at the surface of the molded or solution cast blend as a result of the low surface energy and incompatibility of the siloxane component of the block copolymer.

Block copolymers containing segments of 2,2,4,4-tetramethyl-1,3-cyclobutylene carbonate and dimethylsiloxane (12) were synthesized by Matzner, et al. [95-97].

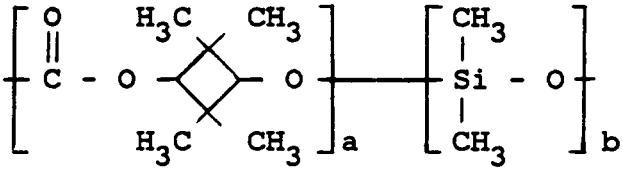

(12)

The preparation of these materials involves the reaction of preformed, well-characterized carbonate oligomers with bis(dimethylamine)-terminated dimethylsiloxane oligomers.

Copolymers with various carbonate/siloxane ratios were prepared. Those containing low siloxane content (< 10%) had high modulus, high tensile strength, and low elongation values. On the other hand, low modulus, moderate tensile strength, and high elongation values were observed for materials with high siloxane content (> 60%). The copolymers also displayed good thermal, hydrolytic, and ultraviolet stability. The excellent processability of these systems was attributed to the similarity of the solubility parameters of the two components. Thermal analysis indicated a low Tg of -120°C and a high Tg of 40-80°C due to the siloxane and carbonate blocks, respectively. A crystalline melting point (Tm) at 200-230°C due to the carbonate block was also observed.

Block copolymers containing dimethylsiloxane segments and segments of alkyl or aryl phthalates were also reported by Matzner, et al. [95-97]. Well-defined, perfectly alternating block copolymers were synthesized by the oligomer condensation technique involving the reaction of hydroxyl-terminated polyester oligomers with bis(dimethylamine)-terminated dimethylsiloxane oligomers. The types of polyester oligomer used include bisphenol-A isophthalate (or terephthalate) (13) and hexamethylene terephthalate (14).

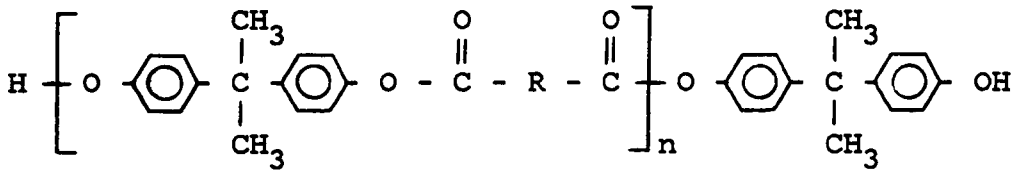

R = 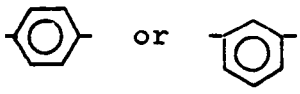

(13)

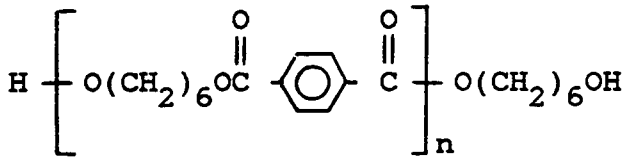

(14)

The elastomeric block copolymers obtained from the bisphenol-A phthalate oligomers show good mechanical properties. They displayed Tg values at -125°C due to the siloxane blocks and at 120-135°C for the polyester blocks. Polyester block melting transitions were observed at 260°C and 295°C for the isophthalate and terephthalate compositions, respectively. Due to the more flexible nature of the hexamethylene terephthalate-siloxane block copolymer, the mechanical properties and the Tm are lower than those of the more rigid aromatic polyesters discussed above.

The ester and siloxane segments of the block copolymers prepared by the silylamine-hydroxyl condensation route are linked by Si-O-C bonds. Under certain conditions, practi-

cally all compounds that contain the Si-O-C grouping can be hydrolyzed, although, depending on their structure, their ability to hydrolyze varies greatly [2]. In contrast to low molecular weight compounds, organic-siloxane block copolymers have shown superior hydrolytic stability [64,96,97,168]. This observation has been attributed to three factors: (1) hydrophobicity due to the presence of long siloxane segments, (2) steric shielding of the Si-O-C linkages by the long adjacent segments, and (3) low concentration of Si-O-C linkages in the polymer backbone. It should also be noted that hydrolysis is not of major concern if the material is to be used in the outerspace environment.

Segmented (or "random") ester-siloxane block copolymers have been prepared by interfacial techniques [98,99]. This method involves the reaction of an aminopropyl-terminated dimethylsiloxane oligomer with bisphenol-A and a mixture of isophthaloyl and terephthaloyl chlorides. The ester and siloxane segments are linked by the hydrolytically stable Si-C bond. The random nature of these materials is derived from the fact that the polyester block is formed in situ during the copolymerization.

2.4 AEROSPACE CONSIDERATIONS

2.4.1 Overview

The study of polymeric materials suitable for space applications is an active area of research. The thrust of such research is to gain a fundamental understanding of the performance of advanced composites, coatings, and polymer films in the space environment. To guide new materials development, the emphasis of current investigations has been placed on identification of damage mechanisms [101].

Long-term stability within the space environment is a major materials concern. The key elements of the space environment that are known to affect organic materials include high vacuum, ultraviolet radiation, ionizing radiation (electrons and protons), and thermal cycling. These major elements and the principal concerns associated with each are given in Table 5 [102]. The effects of these elements can be significant on polymeric materials. The constant low pressure for example, may cause dimensional changes due to outgassing and microcracking. Ultraviolet radiation and ionizing radiation may affect both the surface and bulk properties of an organic polymeric material. The combination of these environmental elements acting together on the structural element may also cause combined or synergistic effects. The combination of high vacuum, ionizing

TABLE 5

Space Environmental Parameters [102].

Environmental Parameter	Nominal Range	Effects on Materials
Vacuum	Pressure 10^{-5}-10^{-13} mPa	Vacuum outgassing, dimensional changes
Ultraviolet	Wavelength 0.1-0.4μm Intensity 1.4 Kw/m^2	Degradation of coatings
Protons	Energy 0.1-4 MeV Flux $10^8 p^+/cm^2$ sec	Degradation of coatings
Electrons	Energy 0.1-4 MeV Flux $10^8 e^-/cm^2$ sec	Surface and bulk damage, spacecraft charging
Temperature Cycling	Material temperature 80K to 420K	Microcracking, thermal warping, surface distortions

radiation, and thermal cycling can be a severe test of the material's ability to perform [102].

In addition to space environmental effects, the structural and dynamic characteristics that influence the control of large precision space structures (LPSS) are of major concern. Various interdisciplinary LPSS control technology programs bring together the structures technology that involves the strength and elasticity of the structure with structural dynamics technology that defines the dynamic response of the structure to both operational and environmental loads. Examples of the physical factors that are interdisciplinary and influence control include: (1) rigidity of both structural elements and joints, (2) damping inherent in both the material as well as discrete dampers located throughout the structure, and (3) the bandwidths of both sensors and actuators used to sense motion and control it. This interdisciplinary approach is essential in successfully controlling LPSS because structure strength, flexibility, and control are inseparable [103].

From the brief discussion above, it is apparent that there are several properties that a material must possess in order to be useful in space applications. The two properties of major consideration in the research reported in this dissertation, passive damping and atomic oxygen degradation,

will be briefly reviewed in the following sections of this literature review.

2.4.2 Passive Damping

The Space Shuttle has recently brought a new dimension to spacecraft configuration. LPSS encompass erectable structures, which free spacecraft configurations of the constraints imposed by the launch environment. With spacecraft assembled in orbit and supported by multiple shuttle launches, configurations are free to follow the dictates of the zero-gravity environment alone. Spacecraft models no longer retain the central rigid body, but now require distributed structural flexibility, which has a major and fundamental impact on performance for many missions [104,105].

In LPSS it is common for dimensional tolerances for high energy, electro-optical, and electromagnetic systems to approach small fractions (e.g., 1/50) of the operative wavelength. The precise tolerances must be maintained (or rapidly regained) during the system orbital operation and, therefore, necessitates vibration control. For LPSS, the control must accommodate very low frequency, closely spaced vibration modes whose properties continually change because the system has variable geometry, diminishing consumables, and temperature variation [106].

Presently, most of the materials used in aerospace structures (composites and metals) have damping factors of less than 0.001 so that the mechanism for energy dissipation must be sought elsewhere. The introduction of damping through the use of viscoelastic materials (passive damping) has been identified as a key element in meeting the vibration control requirements inherent in LPSS. This type of damping is particularly critical in the low frequency range where active control is no longer effective. Therefore, a successful vibration control approach must combine the best isolation of vibration excitation sources and active modal control systems with passive damping [106-108].

The qualitative relationship of the damping loss factor and modulus to temperature for polymeric materials is shown in Figure 6 [106]. It can be seen that the loss factor is greatest in the transition temperature range, decreasing rapidly as the temperature falls into the glassy region or the rubbery region. Material creep may become a problem as the damping material moves into the rubbery region and the modulus of the material decreases. Additionally, for low earth orbit structures, temperature cyclics of -80° to 70°C may make it difficult to provide stable passive damping. The use of polymer mixtures or block copolymers to produce damping materials having reduced temperature sensitivity may be the answer to the creep and thermal cycling problems.

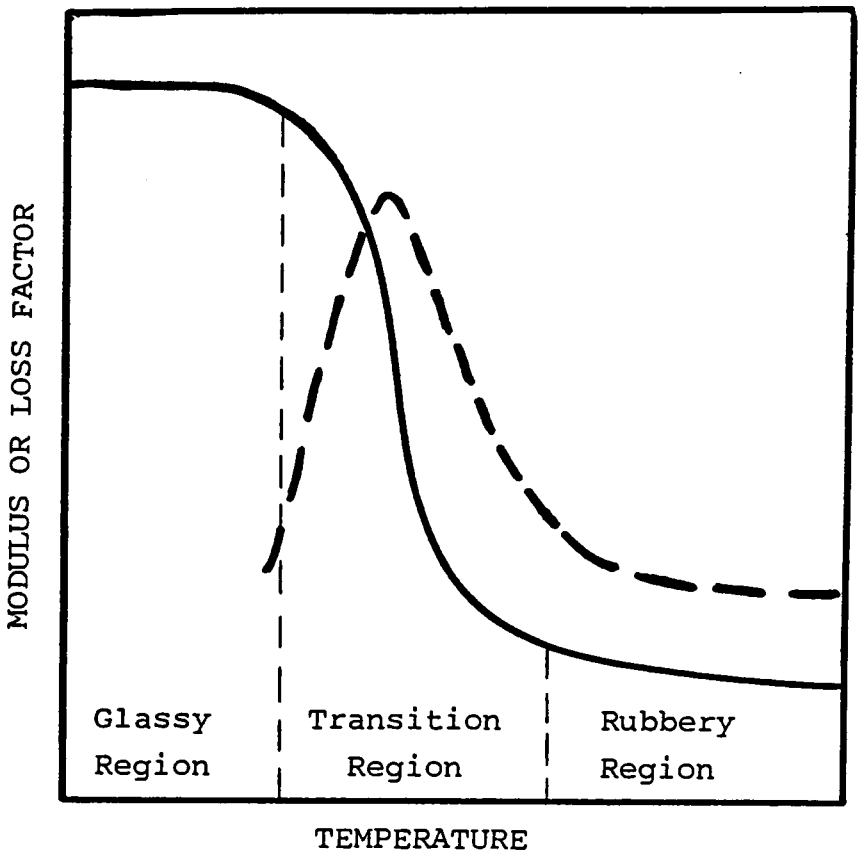

Figure 6: Temperature dependence of damping factor [106].

To accurately study passive damping, it is important to know the magnitude of this damping for various materials and its dependence on frequency. Both the magnitude and frequency dependence are a consequence of the physics of the damping mechanism and the type of vibration mode. Several damping mechanisms are affected by air pressure and gravity; as a result, research efforts must simulate high-vacuum, zero-gravity conditions to accurately measure the damping of typical space structures. It is obvious that this area of research is both costly and time-consuming.

For effective damping it is important that the structure transmits appreciably less energy to the support structure than it dissipates internally. In terrestrial laboratories this is usually accomplished by fastening the specimen to a rigid support or by supporting it with very flexible supports near points of small vibratory motion. Many space structures of interest are so flexible that they would require many more points of support in the presence of gravity relative to the free-floating condition of zero-gravity [108].

The above discussion establishes that (1) a technology need exists for vibration control in LPSS and (2) passive damping is critical to the solution of the problem. While viscoelastic damping technology is rapidly emerging, appli-

cations to LPSS pose a unique set of challenges and requirements which will not be addressed without a specifically focused program. Passive damping must be assessed in terms of the interaction of damping materials with the space environment, their effect on the local environment surrounding the space structure, and how passive damping may best be introduced into LPSS.

2.4.3 Atomic Oxygen Degradation

Data obtained from recent Space Shuttle flights indicate that surface erosion of common spacecraft materials, such as Kapton and Mylar, can be significant. As a result, the effects of the low earth orbit (LEO) atmosphere (200-600 km) on spacecraft materials is an emerging area of concern [109-125].

The LEO atmosphere interacts with polymeric materials in a variety of ways to effect degrading surface and bulk property changes. The degradation consists of changes in material weight (i.e., loss), surface morphology, strength, and thermal/optical properties. From simulated studies of the effect an oxygen and ultraviolet environment has on Kapton films, it was concluded that atomic oxygen was mainly responsible for the observed effects in LEO; the effect of ultraviolet radiation was negligible. The results of this study are illustrated in Figure 7 [109].

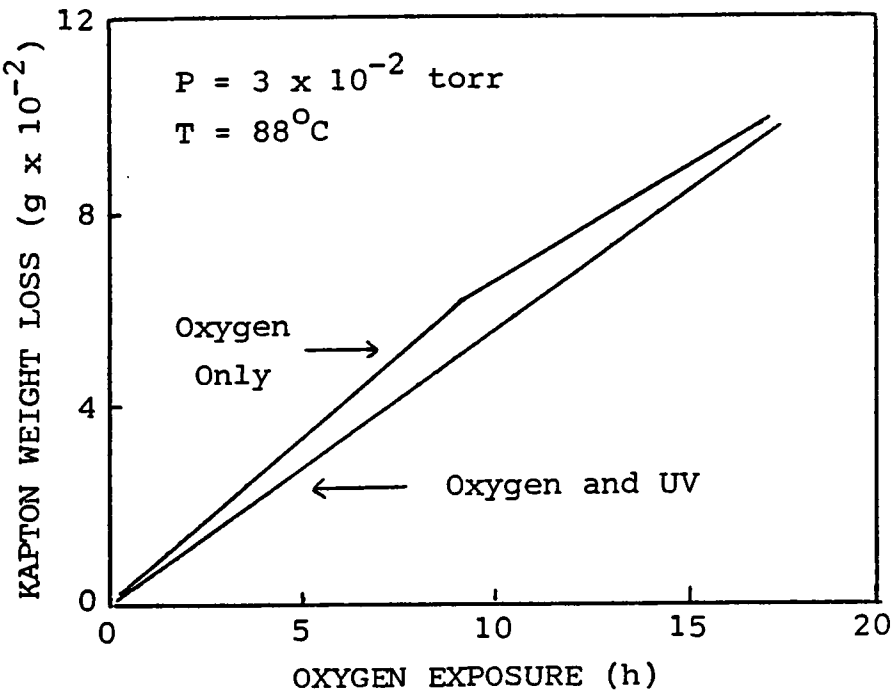

Figure 7: Weight loss as a function of exposure time for Kapton [109].

Ground-state, neutral atomic oxygen is the predominant species a spacecraft in LEO is bombarded by (see Figure 8) [113,114]. Due to the orbital velocity (8 km/sec) of the spacecraft, oxygen atoms strike the satellite's surfaces with an average collision energy of 5eV. These conditions, along with high-vacuum, present a regime of gas-surface chemistry which has been the subject of very little laboratory investigation because of the difficulties inherent in reproducing the impact velocity and the relatively high flux (10^{15}-10^{16} O-atoms/cm^2-sec) of oxygen atoms need to simulate the spacecraft environment of the LEO. An understanding of the chemical and physical processes that occur during atomic oxygen degradation is required in order to provide quantitative predictions of the useful lifetimes of materials subjected to the LEO [109,112].

Atomic oxygen in the space environment occurs as a result of ultraviolet dissociation of molecular oxygen:

$$O_2 \longrightarrow 2O$$

The rate of dissociation is relatively fast and depends on solar activity. Recombination is slow since conservation of both energy and momentum requires a third body, i.e.:

$$O + O \longrightarrow O_2 + M$$

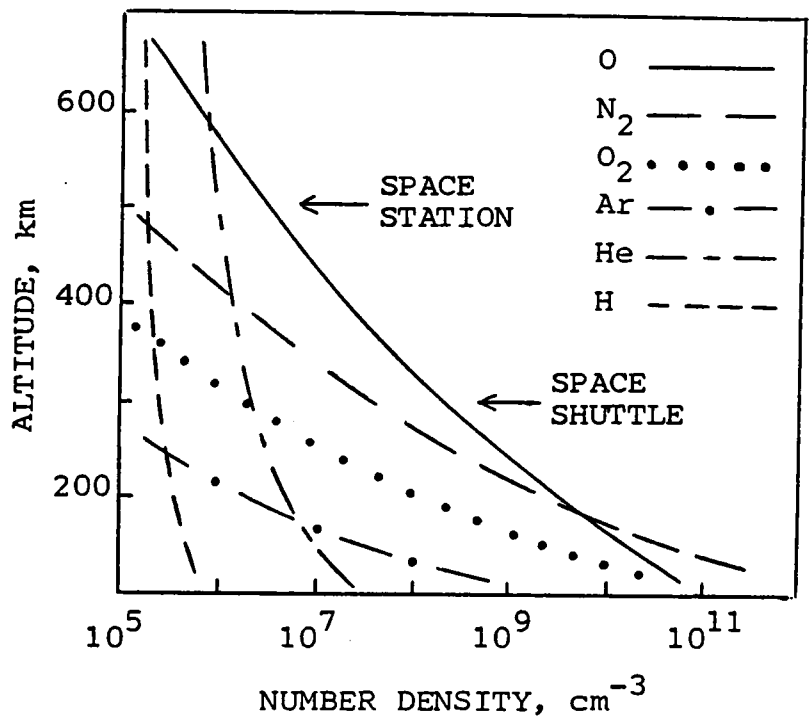

Figure 8: Atmospheric composition of the low earth orbital atmosphere [113,114].

where M is a third particle or body capable of accepting some of the reaction energy and momentum [112].

From fundamental studies, oxidation occurs due to the rupture of primary bonds, which leads to loss of functional properties and, ultimately, failure of the material. Hydrogen abstraction and hydroperoxide formation has been defined as the oxidation rate controlling step [111,117]. Therefore, oxidation depends on the types of carbon-hydrogen bonds present in the polymer. When elements other than carbon and hydrogen are present in a polymeric material, dissociation energy of the additive bonds becomes a contributing factor in the stability of the polymer in an oxidative environment. Teflon, for example, is significantly more resistant to oxidation than its hydrocarbon counterpart since it contains carbon-fluorine bonds rather than carbon-hydrogen bonds. Factors such as the degree of crystallinity, amorphous regions, and permeability to oxygen can also affect polymer stability.

Several laboratory and flight experiments concerning the atomic oxygen degradation of Kapton films (a polyimide) have shown rapid surface oxidation accompanied by weight loss and changes in surface morphology, while bulk properties remain virtually unchanged. Kapton degradation is thought to be due to a chain reaction involving hydroperoxide formation and free-radical initiation [111].

Laboratory and flight data also verify the stability of fluorocarbon and silicone coated substrates that are typically reactive in the LEO oxygen atmosphere. In some cases, however, poor adhesion between the protective coating and the substrate posed a problem in long-term stability. Increased surface roughness was accompanied by microcracking and crazing [111]. A novel polyimide-siloxane copolymer has been identified as a suitable material for long-term stability against atomic oxygen in the LEO environment [110,133]. The oxidation reaction efficiency was approximately an order of magnitude lower than the currently used polyimide (Kapton) thermal blanket material. These results have sparked an interest in a new class of materials that may be suitable for applications in the space environment.

The following chapters of this dissertation describe the work involved in the synthesis and characterization of polysiloxane-ester block copolymers that are potential materials for passive damping applications in the space environment.

Chapter III

EXPERIMENTAL METHODS

3.1 MATERIALS AND THEIR PURIFICATION

3.1.1 Siloxane Intermediates

Octamethylcyclotetrasiloxane (D_4) (15), octaphenylcyclotetrasiloxane (D_4") (16) and trifluoropropylmethylcyclotrisiloxane (F_3) (17) were obtained from the Silicone Products Division of the General Electric Company.

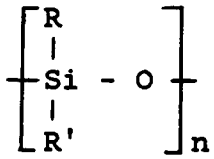

(15) D_4:R = R'= CH_3, n = 4

(16) D_4":R = R'=  , n = 4

(17) F_3:R = CH_3 and R'= $CH_2CH_2CF_3$, n = 3

The bis(α-aminopropyl)tetramethyldisiloxane (18) was purchased from either Petrarch Systems, Inc. or Silar Laboratories.

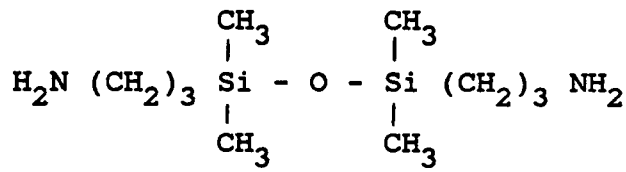

(18)

The low molecular weight bis(dimethylamino)polydimethylsiloxane oligomer (19) was obtained from Petrarch Systems, Inc. and used as a starting material for the synthesis of higher molecular weight terminally reactive polyorganosiloxanes.

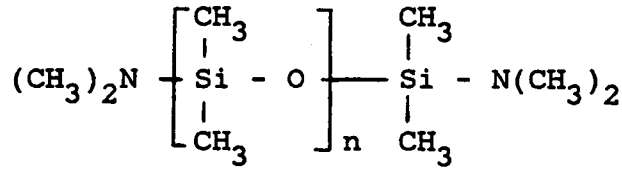

(19)

The above silicon-containing starting materials were of high quality and used without further purification.

3.1.2 Polyarylester Monomers

High purity polymer grade bisphenol-A (20) was obtained from the Dow Chemical Company and used without further purification.

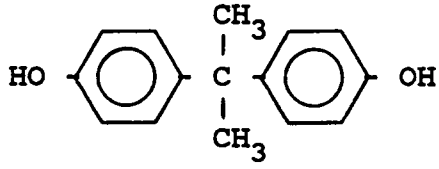

(20)

Reagent grade terephthaloyl chloride (21) and isophthaloyl chloride (22) were purchased from either Aldrich Chemical Company or Eastman Chemical Company.

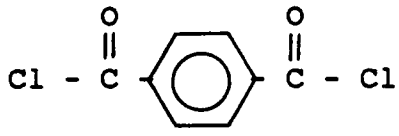

(21)

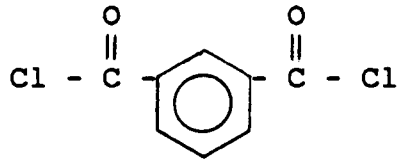

(22)

Purification of the acid chlorides was accomplished by recrystallization. This was typically done by dissolving 500 grams of the crude acid chloride in two liters of refluxing hexanes, with stirring. The hydrolyzed acidic impurities are insoluble and appear as a fine white precipitate in the hot hexanes solution. The solution was filtered through a paper filter into another Erlenmeyer flask which contained a small amount of refluxing hexanes. This procedure prevents the acid chloride from crystallizing during filtration. The filtered solution was concentrated, filtered through paper into a beaker, and cooled with an ice bath. The crystals were isolated by filtration and dried under vacuum. The purified acid chlorides were stored in a desiccator to prevent hydrolysis.

3.1.3 General Solvents and Reagents

General solvents and reagents were obtained from Fisher Scientific and typically distilled from calcium hydride and/or dried over molecular sieves.

3.2 SYNTHESIS OF OLIGOMERS AND POLYMERS

3.2.1 Synthesis of Oligomers

3.2.1.1 Siloxanolate Catalyst

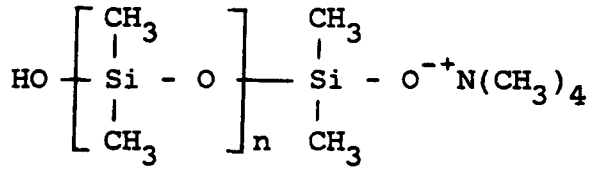

(23)

The siloxanolate catalyst (23) (or N-catalyst) used in the polysiloxane equilibration reactions was prepared from the reaction of one mole of tetramethylammonium hydroxide pentahydrate (24) with 4.5 moles of D_4.

$$(CH_3)_4NOH \cdot 5H_2O$$

(24)

The reaction was carried out in a 100ml, one-necked round bottom flask equipped with a magnetic stirrer, drying tube and an inert gas inlet that goes below the level of the

reactants. A schematic representation of the apparatus used for catalyst preparation is shown in Figure 9.

In a typical preparation of catalyst, 7.50g (0.0414 mole) of tetramethylammonium hydroxide pentahydrate was dispersed in 54.50g (0.1837 mole) of D_4 and the reaction was conducted under a rapid argon stream for 24 hours at 80°C. The rapid argon flow was sufficient to dehydrate the system. Generally, after about 5 hours the system appears rather opaque and the viscosity has increased significantly. As a function of time, the viscosity begins to decrease and the material increases in translucency. However, it may never become perfectly transparent. The final product is a viscous liquid and is stored in a desiccator. The catalyst produced in this manner is sufficiently active for the synthesis of all the polysiloxane oligomers discussed in this work [22,126]. Alternative methods of preparing suitable catalysts have also been reported [35].

3.2.1.2 Amine Terminated Polysiloxane Oligomers

The difunctional polysiloxane oligomers, shown in Figure 10, were synthesized in bulk by the anionic equilibration of a difunctional end-blocker with either D_4, D_4 and D_4'', or D_4 and F_3 [7,20,127-129]. The composition and molecular weight of the oligomers were varied by controlling

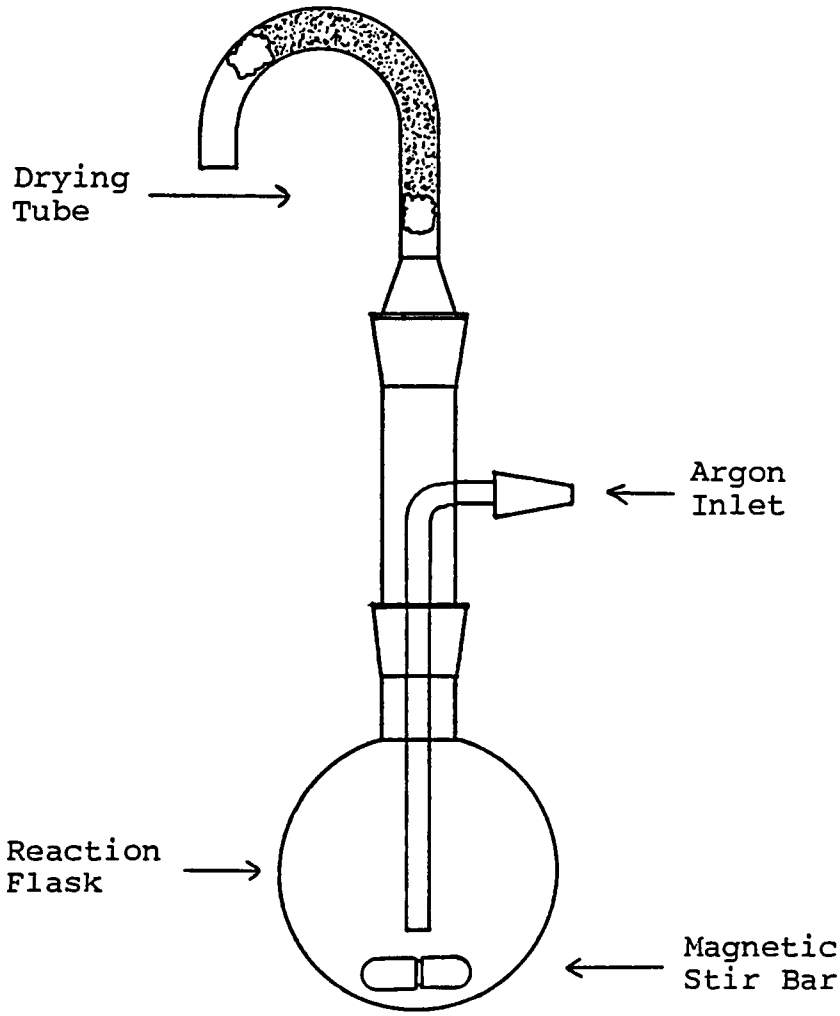

Figure 9: Apparatus used in the preparation of siloxanolate catalyst.

Dimethylsiloxane Oligomer

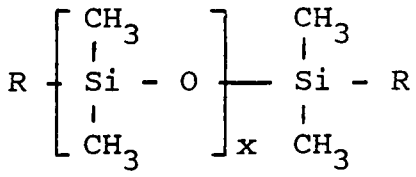

(Dimethyl-diphenyl)siloxane Oligomer

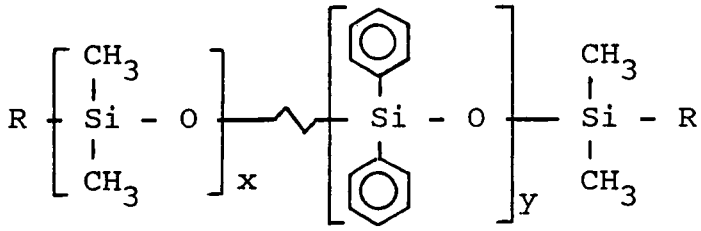

(Dimethyl-trifluoropropylmethyl)siloxane Oligomer

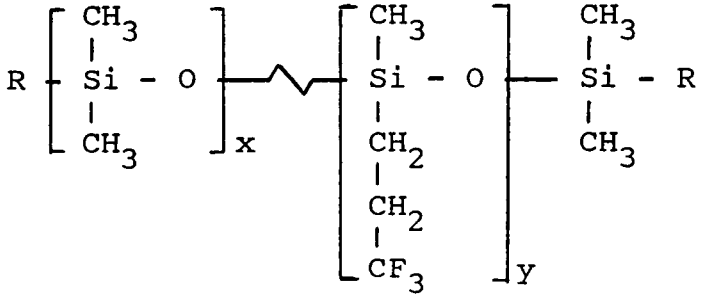

Silylamine-terminated : R = $-N(CH_3)_2$

Aminopropyl-terminated: R = $-(CH_2)_3NH_2$

Figure 10: Difunctional organosiloxane oligomers.

the ratio of the cyclic monomers to each other and to the end-blocker. Sample calculations are presented in Appendix A.

The equilibration reactions were carried out in a 250ml, two-necked round bottom flask equipped with a condenser, drying tube, inert gas inlet, thermometer and magnetic stirrer. In the cases where the oligomers were unusually viscous due to a high phenyl content (75 weight percent), a mechanical stirrer was used.

In a typical reaction to produce a 5,000g/mole aminopropyl terminated co-oligomer containing 50 weight percent methyl and 50 weight percent phenyl, 6.00g (0.0241 mole) of bis(α-aminopropyl)disiloxane along with 54.36g (0.1836 mole) of D_4 and 60.36g (0.0762 mole) of D_4'' were charged to the reaction flask. The mixture was heated, with stirring and inert gas flow, to 80°C and 0.48g (0.4 weight percent) of the siloxanolate catalyst was added. The reaction was maintained at 80°C for 48 hours to ensure complete equilibration. The reaction temperature was then increased to 150°C for 3 hours to decompose the catalyst into inert, volatile by-products. After cooling, the viscous liquid product was vacuum distilled (0.5 torr and 100°C) to remove the equilibrium cyclics.

The difunctional silylamine terminated polysiloxane oligomers were synthesized in bulk by the anionic equilibration of the low molecular weight bis(dimethylamino) polydimethylsiloxane oligomer with either D_4, D_4 and D_4", or D_4 and F_3. The procedure followed was as described above for the aminopropyl terminated oligomers. However, the silylamine terminated oligomers were stored in a desiccator due to the labile silicon-nitrogen bond of the functional endgroups.

3.2.1.3 Hydroxyl Terminated Polyarylester Oligomers

Controlled molecular weight, amorphous polyarylesters (25) were synthesized in solution by reacting bisphenol-A with a 50:50 mixture of terephthaloyl chloride:isophthaloyl chloride in the presence of triethylamine which acts as both an acid acceptor and a catalyst. The desired molecular weight was obtained through the use of a stoichiometric imbalance of reactants according to Carothers equation [130]. Sample calculations are presented in Appendix B.

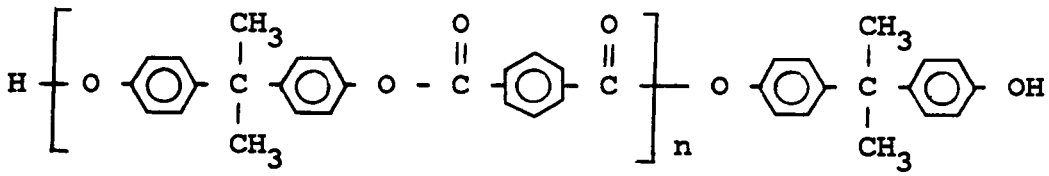

(25)

The reactions were carried out in a one liter, four-necked round bottom flask equipped with a mechanical stirrer, condenser, drying tube, inert gas inlet, addition funnel and thermometer. In a typical reaction to produce a 5,000g/mole hydroxyl terminated polyarylester, 30.00g (0.1316 mole) of bisphenol-A were charged to the reaction flask and dissolved in 550ml of dry methylene chloride and 40.28ml (0.2895 mole) of distilled triethylamine. With stirring and inert gas flow, a solution of 12.43g (0.0613 mole) of terephthaloyl chloride and 12.43g (0.0613 mole) of isophthaloyl chloride in 50ml of dry methylene chloride was placed in an addition funnel and added dropwise to the bisphenol-A solution over a period of one hour during which a slight exotherm above room temperature was noted. The reaction was allowed to run for 3 hours at room temperature. The reaction mixture was then filtered to remove the fine white precipitate of triethylamine-hydrochloride (salt complex) formed during the reaction. The filtrate was extracted with a 10 percent (weight to volume) aqueous solution of sodium bicarbonate until slightly basic or neutral. This extraction procedure removes the residual precipitate from the filtrate since it is slightly soluble in the reaction solvent, methylene chloride. The final product (white, powdery solid) was precipitated in excess methanol, fil-

tered, and dried under vacuum at 80°C overnight. The yield of the reaction after work-up was 75 percent and the number-average molecular weight, $\bar{M}n$, determined by end-group titration [131] was 4,900g/mole.

3.2.1.4 Capping Hydroxyl Terminated Polyarylester Oligomers

To confirm the titrated $\bar{M}n$ of the functionally terminated polyarylester oligomers, the hydroxyl end-groups were capped with trimethylsiloxy groups so they could be easily detected by proton NMR. The capping reactions were carried out in a 25ml, three-necked round bottom flask equipped with a condenser, drying tube, magnetic stirrer, thermometer and inert gas inlet. In a typical capping reaction, 1.00g (0.0002 mole) of a 5,000g/mole polyarylester was placed in the reaction flask with 10ml of distilled chlorobenzene. With stirring and inert gas flow, the temperature was raised to 100°C. Then, 0.10ml (0.0005 mole) of hexamethyldisilazane (26) was added and the progress of the reaction was continually monitored by running an FTIR spectrum every few hours.

$$(CH_3)_3Si - NH - Si(CH_3)_3$$

(26)

During the reaction, evolution of ammonia may be detected by using pH paper. The reaction was allowed to run until the hydroxyl band in the FTIR spectrum was no longer apparent (approximately 48 hours). The reaction mixture was cooled and the excess hexamethyldisilazane, along with the reaction solvent, was removed by a rotary vacuum distillation apparatus to afford a white solid product which was dried under vacuum at 80°C overnight. The reaction yield was 92 percent, and from the proton NMR spectrum of the capped polyarylester oligomer (27), the $\bar{M}n$ was 5,100g/mole.

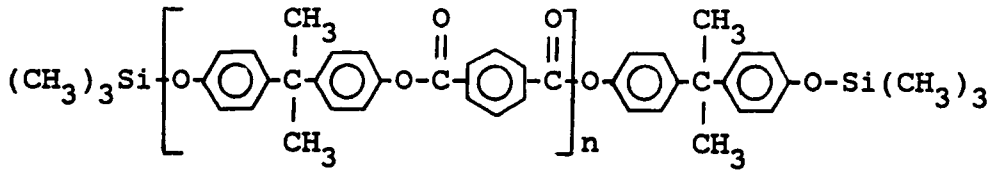

(27)

3.2.2 Synthesis of High Molecular Weight Polymers

3.2.2.1 Perfectly Alternating Polyarylester-Polysiloxane Block Copolymers

The silyamine-hydroxyl condensation reaction was used to synthesize perfectly alternating block copolymers in solution [96,97]. The reactions were carried out in a one liter, four-necked round bottom flask equipped with a mechanical stirrer, Dean Stark trap, condenser, drying tube,

thermometer, inert gas inlet, and an addition funnel as is shown in Figure 11.

In a typical reaction to produce a high molecular weight polyarylesterpolysiloxane block copolymer, 6.00g (0.0012 mole) of a 5,000g/mole hydroxyl terminated polyarylester was placed in the reaction flask with 200ml of distilled chlorobenzene. With stirring and inert gas flow, the temperature was raised to chlorobenzene reflux (132°C). Approximately, 80ml of solvent was removed through the trap to dehydrate the system. Then, 6.48g (0.0012 mole) of a 5,400g/mole silylamine terminated polysiloxane oligomer was placed in an addition funnel and added dropwise to the polyarylester solution over a period of two hours. As the stoichiometric point was approached, a noticeable increase in the viscosity of the reaction mixture was observed. During the reaction, evolution of dimethylamine may be detected by using pH paper. Once the amine by-product was no longer observed (generally 3-5 hours after complete siloxane addition), the reaction mixture was cooled and the product was precipitated in excess methanol/isopropanol. Note that this copolymer purification should further eliminate any residual minor amounts of siloxane cyclics. The white, fibrous product was filtered, then dried under vacuum at 80°C overnight. The recovered yield was 95 percent.

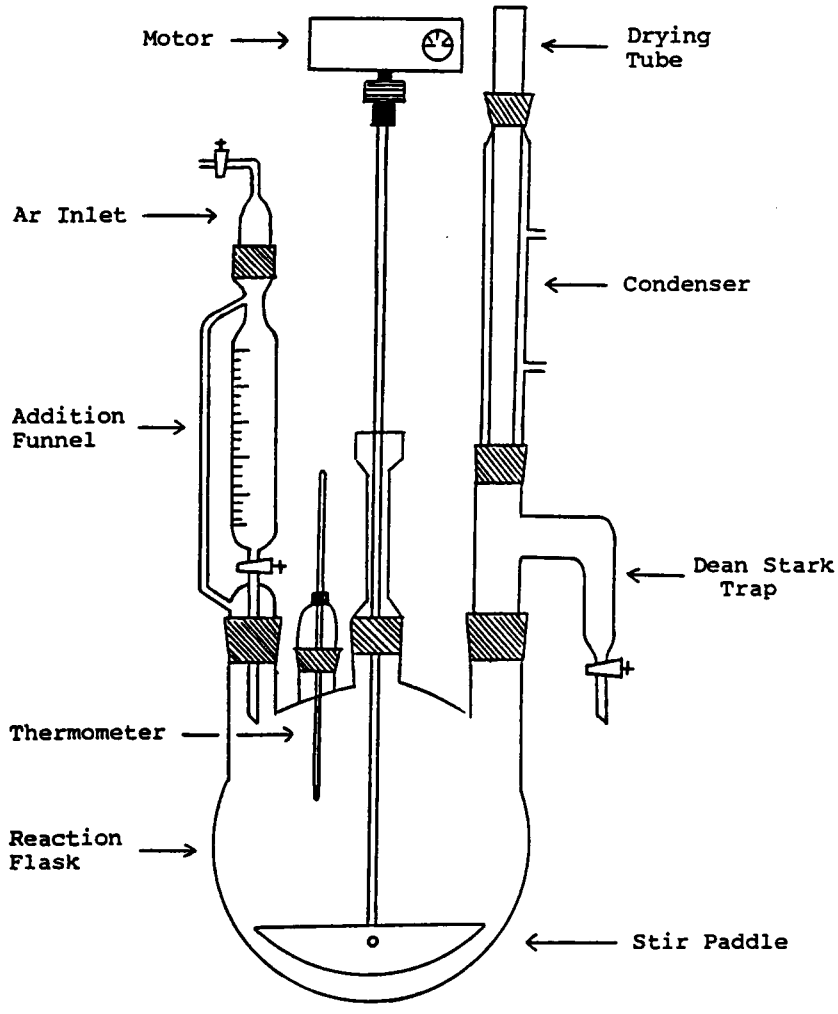

Figure 11: Apparatus used in the preparation of perfectly alternating block copolymers.

3.2.2.2 Perfectly Alternating Polyarylester-Polysiloxane Block Terpolymers

The perfectly alternating block terpolymers were also synthesized in solution using the silylamine-hydroxyl condensation reaction. The reactions were carried out in a one liter, five-necked round bottom flask equipped with a mechanical stirrer, Dean Stark trap, condenser, drying tube, thermometer, inert gas inlet and two addition funnels. In a typical reaction to produce a high molecular weight polyarylester-polysiloxane block terpolymers, 12.00g (0.0024 mole) of a 5,000g/mole hydroxyl terminated polyarylester was placed in the reaction flask with 340ml of distilled chlorobenzene and the temperature was raised to chlorobenzene reflux (132°C). To dehydrate the system, approximately 80ml of solvent was removed through the trap. Then, 6.00g (0.0012 mole) of a 5,000g/mole silylamine terminated poly(dimethyl)siloxane was placed in one of the addition funnels and 7.68g (0.0012 mole) of a 6,400g/mole silylamine terminated poly(trifluoropropylmethyl)siloxane was placed in the second addition funnel. Both polysiloxanes were added dropwise to the polyarylester solution over a period of 2 hours. A noticeable increase in the viscosity of the reaction mixture was observed as the stoichiometric point was approached. As in the previously described block copolymer synthesis, the reaction was allowed to run until the amine

by-product was no longer observed (as detected by pH paper). The reaction mixture was cooled and the product was precipitated in excess methanol/isopropanol. The fibrous, white product was filtered, then dried under vacuum at 80°C overnight. The recovered yield was 86 percent.

3.2.2.3 Segmented Polyarylester-Polysiloxane Block Copolymers

The segmented (or "random") polyarylester-polysiloxane block copolymers were synthesized interfacially in a laboratory Waring blender [98,99]. In a typical reaction to produce a 20 weight percent polysiloxane-containing copolymer, 20.00g (0.0877 mole) of bisphenol-A was added to a solution of 100ml of distilled water with 0.1757 mole of sodium hydroxide (45.5ml of a 3.86M aqueous solution). The bisphenol-A was converted to the bisphenate upon reaction with the sodium hydroxide. The solution was placed in the blender along with 200ml of distilled water and 6.00g (0.0362 mole) of tetraethylammonium chloride, the phase-transfer catalyst. Next, 8.00g (0.0020 mole) of a 4,100g/mole aminopropyl terminated polysiloxane dissolved in 250ml of methylene chloride was added to the stirring blender, followed by addition of a solution containing 9.10g (0.0448 mole) of terephthaloyl chloride and 9.10g (0.0448 mole) of isophthaloyl chloride in 250ml of methylene chloride. The reaction mixture

was stirred at high speed for 30 minutes. A thick, white emulsion generally formed within five minutes. When the blender was stopped, the immiscible solvent layers were allowed to separate. The upper water layer was discarded and the denser organic layer was coagulated in excess methanol/isopropanol. If the layers did not readily separate, the entire reaction mixture was coagulated. After filtering and drying overnight under vacuum at 80°C, the white, fibrous product was dissolved in chloroform and extracted several times with distilled water to remove residual salt by-products. The final product was coagulated in excess methanol/isopropanol, filtered, and dried at 80°C under vacuum overnight to afford a yield of 85 percent. It is important to note that in this type of synthetic procedure only the difunctional siloxane oligomer is synthesized prior to copolymerization; the polyarylester blocks are formed during the copolymerization reaction. Calculations for segmented block copolymer formation are presented in Appendix C.

3.3 CHARACTERIZATION OF OLIGOMERS AND POLYMERS

3.3.1 Structure Analysis

3.3.1.1 Fourier Transform Infrared Spectroscopy (FTIR)

The chemical structure of the oligomers and polymers were confirmed by FTIR. The spectra were recorded using a

Nicolet MX-1 spectrophotometer. Spectra of the siloxane oligomers (viscous liquids) were obtained by placing a drop of sample between two salt plates. Thin films of the polyarylester oligomers and the polymers were cast from chloroform on salt plates, then dried in a vacuum oven at low heat for 30 minutes before FTIR spectra were run.

Diffuse reflectance FTIR was used to study the effect of atomic oxygen on the surface of various solution cast polymer films. Spectra were obtained using a Nicolet MX-1 spectrophotometer fitted with a diffuse reflectance attachment (Barnes Analytical, Spectra-Tech, Inc.).

3.3.1.2 Nuclear Magnetic Resonance Spectroscopy (NMR)

Proton NMR was used routinely for structure analysis of monomers, oligomers, and polymers. Spectra were obtained using a Varian EM-390 90 MHz spectrometer on 10% (weight to volume) solutions of sample in deuterated chloroform. Tetramethylsilane (TMS) was used as the lock reference for the polyarylester oligomers. However, due to the presence of silicon methyl groups in the siloxane oligomers and the polymers, TMS obviously could not be used. Therefore, methylene chloride (5.37ppm from TMS) was used as the lock reference for the siloxane-containing samples.

The percent siloxane incorporated into the co- and terpolymers was calculated from the proton NMR spectra. The integration of the silicon methyl peak of the siloxane backbone at 0.3ppm was compared to the isopropylidene peak of the polyarylester backbone at 1.8ppm.

High resolution silicon-29 FT-NMR proved to be a powerful tool in the structural elucidation of the siloxane oligomers. The spectra were obtained at 53.67 MHz using a Bruker WP-270SY spectrometer. The samples were dissolved in deuterated chloroform (20 percent, weight to volume) and TMS was used as the internal reference. A small amount (0.02M) of a shiftless relaxation agent such as chromium acetylacetonate was added to reduce the long T_1 times associated with silicon-29. Typically, about 500 free induction decays (FIDs) were recorded with a flip angle of 40°. The spectra were also broadband decoupled at the proton frequency; the nuclear Overhauser effect (NOE) was not measured.

3.3.2 Molecular Weight Determination

3.3.2.1 Titration of Functional Oligomers

The $\bar{M}n$ of the amine terminated siloxane oligomers and the hydroxyl terminated polyarylester oligomers were determined by titration of the functional end-groups using a Fisher Titrimeter II automatic titration system. A standard

calomel electrode was used with a double junction reference. The siloxane oligomers were dissolved in isopropanol and titrated with a 0.1N solution of hydrochloric acid in isopropanol. The polyarylester oligomers were dissolved in freshly distilled tetrahydrofuran and titrated with a 0.2N solution of tetramethylammonium hydroxide in methanol.

In general, the oligomer to be titrated was weighed directly into a beaker, solvent was added, and the solution was stirred until the oligomer was completely dissolved. The solution was then transferred to the titration stand, the electrodes were lowered into the solution and the titration was begun while operating in the automatic endpoint seeking (AEP) mode. When the endpoint was reached, the final potential (mV) was noted and the endpoint volume was recorded by the computer. The electrodes were rinsed with the titration solvent, then with water, and placed in a pH 4.0 buffer solution for storage.

The blank titration was accomplished similarly by titrating the exact volume of pure solvent with the titrant until the sample endpoint potential was reached. The number-average molecular weight, $\bar{M}n$, was calculated from the following relation:

$$\bar{M}n = \frac{W \times N}{C \times (V - V_B)}$$

where W is the weight of the sample titrated in grams, N is the number of end-groups per molecule, C is the concentration of the titrant in moles/ml, V is the volume (in ml) of titrant used to reach the sample endpoint, and V_B is the volume (in ml) of titrant used to titrate the blank solvent.

3.3.2.2 Nuclear Magnetic Resonance (NMR)

Proton NMR was used to calculate the $\bar{M}n$ of the capped polyarylester oligomers by integrating and comparing the trimethylsiloxy end-group peak at 0.3ppm to the isopropylidene peak of the oligomer backbone at 1.8ppm. Spectra were obtained using a Varian EM-390 90 MHz spectrometer on 10 percent (weight to volume) solutions of sample in deuterated chloroform. Methylene chloride was used as the lock reference. With high resolution FT-NMR it may be possible to detect the hydroxyl end-groups of relatively low molecular weight polyarylester oligomers without capping. However, at the time of this work such capabilities were not available and capping was, therefore, necessary.

3.3.2.3 Intrinsic Viscosity Measurements

The intrinsic viscosity, $[\eta]$, of the oligomers and polymers were determined by a Cannon-Ubbelhodhe dilution viscometer. All measurements were made at 25°C with methy-

lene chloride as the solvent. Four concentrations of each sample solution were used for the measurements.

3.3.2.4 Size Exclusion Chromatography (SEC)

SEC was used as a qualitative check on the nature of the molecular weight distribution of the polyarylester oligomers and the polymers. SEC data was obtained with tetrahydrofuran solutions using a Waters instrument with 500, 10^3, 10^4, and 10^6 angstrom microstyrogel columns. Both differential refractive index and UV detectors were employed. The flow rate was 1.0 ml per minute.

3.3.3 Thermal Analysis

3.3.3.1 Differential Scanning Calorimetry (DSC)

A Perkin-Elmer Model DSC-2 was used to determine the glass transition (Tg), crystallization temperature (Tc), and melting temperature (Tm) of the oligomers and polymers. The scans were run at 10 degrees per minute with a sensitivity of 5 mcal per second. The baseline was checked for flatness at each heating rate and sensitivity used. Depending on the temperature range used, high purity solvents or metal standards were used for temperature calibration. High purity solvents such as cyclopentane, chloroform, tetrahydrofuran, and ethylene glycol were used for subambient temperature

calibration. High purity metal standards such as indium and tin were used for ambient temperature calibration. For subambient measurements, liquid nitrogen was used to cool the system and the sample chamber was constantly purged with helium. Ambient scans were done either by using the refrigeration unit or by immersing the cold finger in water. Glass transition temperatures were taken as the midpoint of the change in slope of the baseline obtained from the second run. Crystallization and melting temperatures were taken as the base of the exotherm peak and the apex of the endotherm peak, respectively.

3.3.3.2 Thermomechanical Analysis (TMA)

A Perkin-Elmer TMA-2, in the penetration mode, was used along with a System 4 Microprocessor temperature controller to generate psuedo modulus versus temperature curves of the oligomers and polymers. Measurements were taken at a heating rate of 10 degrees per minute. Temperature calibration was accomplished by the System 4 itself, while a sapphire disk was used according to the manufacturer's instructions for probe displacement calibration.

3.3.3.3 Thermogravimetric Analysis (TGA)

The relative thermal stabilities of the oligomers and polymers were assessed by thermogravimetry in a nitrogen atmosphere. A Perkin-Elmer TGS-2 along with a System 4 Microprocessor was used. The sample was placed in a platinum pan suspended from an electronic microbalance which monitored weight loss as a function of temperature. In all cases, the heating rate was 10 degrees per minute. Balance calibration was accomplished using standard weights according to the manufacturer's instructions, while temperature calibration was accomplished by the System 4.

3.3.4 Mechanical Property Determinations

3.3.4.1 Stress-Strain Measurements

Tensile property determinations were made using an Instron table model tensile tester. Dogbone shaped samples were cut from solution cast or compression molded polymer films using a die. The sample (0.11 in. x 0.28 in.) was clamped between pneumatic clamps and elongated at a rate of 10mm per minute. Tensile strength, tensile strain, yield strength and yield strain were calculated from the load extension plot. The modulus was determined by drawing a tangent to the initial slope of the load extension curve. The results reported were an average of four or five runs

per sample. Before running samples the load cell was calibrated using a standard two kilogram weight.

3.3.4.2 Dynamic Mechanical Thermal Analysis (DMTA)

The dynamic mechanical behavior is of great utility in studying the multiphase nature of the siloxane-ester block co- and terpolymers over a range of frequencies and temperatures. Dynamic mechanical spectra of compression molded polymer films were obtained using a Polymer Laboratories Dynamic Mechanical Thermal Analyzer operating at 1 and/or 30 Hz. Samples were run in single cantilever mode with a 1mm free length. The heating rate was 5 degrees per minute.

3.3.5 Surface and Bulk Analysis

3.3.5.1 Contact Angle Measurements

It has been shown that in siloxane-containing copolymers and blends, the siloxane can dominate the surface of the material even when only a small percentage of siloxane is present in the bulk [64,133-135]. For this reason, it was of interest to evaluate the surface of several of the block co- and terpolymers.

A contact angle measurement instrument from Rame'-Hart, Inc. was used to determine the contact angle of water on the surface of the siloxane-ester polymer films. A one inch

square sample was placed in the instrument and a 20µl drop of distilled water was placed on the polymer film surface using a microsyringe. The angle made between the drop and the polymer was measured. This type of measurement was performed on each side of a polymer film sample. Since contact angle is a relative technique, homopolyester films were also run and used as controls. XPS was utilized to obtain more quantitative results.

3.3.5.2 X-Ray Photoelectron Spectroscopy (XPS)

XPS was used to study the surface properties of solution cast films of the siloxane-ester block co- and terpolymers. Spectra were obtained on a KRATOS XSAM-800 x-ray spectrometer equipped with a dual anode x-ray source (Mg) and a hemispherical electron energy analyzer. A DEC RT-11 computer system with a software package interfaced to the spectrometer enabled automatic aquisition and simultaneous manipulation of data. Angle dependent-depth profiling was accomplished by the variation in the electron take-off angle between the analyzer and the sample surface [134].

3.3.5.3 Electron Microscopy

Scanning electron microscopy (SEM) and transmission electron microscopy (TEM) were used to observe the surface

and bulk characteristics of the siloxane-ester block co- and terpolymers, respectively. The SEM and TEM micrographs were obtained using a Philips 420T scanning transmission electron microscope.

SEM was used to study the effect of atomic oxygen on the surface of various solution cast polymer films. SEM micrographs of unexposed films were used as controls in determining the effect of atomic oxygen degradation. A Denton Vacuum DV-515 was used to coat the polymer films with platinum-palladium (about 75Å) prior to running SEM.

The nature of the bulk microphase separation of the siloxane-ester block polymers was directly observed by TEM. Due to the great degree of electron density difference between the siloxane and ester, staining of one of the phases was unnecessary. The films for TEM were made by casting a five percent chloroform solution of the polymer on distilled water and then transferring the thin film directly to a 150 mesh copper TEM grid.

3.3.6 Polymer Degradation Studies

A Plasma-Prep II Model 11005 (SPI Supplies, Division of Structure Probe, Inc.) operating at a reduced pressure of 200 millitorr and an oxygen flow rate of 3.5cc/min was used to determine the durability of the polysiloxane modified

polyarylester block polymers in an atomic oxygen environment. Each sample (2.5 inch diameter, solution cast film) was exposed to atomic oxygen for 30 minutes. Only the air-polymer surface of each film was exposed since it is generally more siloxane-rich relative to the polymer-glass surface.

3.3.7 Polymer Film Preparation

3.3.7.1 Solution Casting

A Millipore syringe filter was used to filter dust particles and other impurities from 15 percent (weight to volume) solutions of polymer in chloroform. The filtered solutions were cast either on clean glass plates using a doctor blade or in a clean glass petri dish. The films were allowed to air dry for 24 hours and then vacuum dried at 80°C for 24 hours. The films were removed from the glass surfaces, with water if needed, and again dried under vacuum and heat overnight. To avoid moisture, the films were stored in a desiccator.

3.3.7.2 Compression Molding

Polymer films were compression molded between clean ferrotype plates in a hot, hydraulic press (Pasadina Hydraulics, Inc.). The plates were treated with MS-136, a hot

molds release agent by Miller Stephenson, prior to use. A stainless steel spacer of the appropriate thickness was used to mold the samples to the desired dimensions. Each film was compression molded at approximately 50°C above their Tg value and at 1,000 to 1,200 psi pressure for 2.5 minutes. The films were stored in a desiccator to avoid moisture contamination.

Chapter IV

RESULTS AND DISCUSSION

4.1 SYNTHESIS AND CHARACTERIZATION OF FUNCTIONAL OLIGOMERS

4.1.1 Amine-terminated Siloxane Oligomers

4.1.1.1 Poly(dimethyl)siloxane Oligomer Synthesis

The reaction scheme for the synthesis of difunctional, amine-terminated poly(dimethyl)siloxane oligomers is illustrated in Scheme 20. The reaction involves the redistribution (or equilibration) of the cyclic dimethylsiloxane tetramer (D_4) with an amine-functional siloxane endblocker in the presence of a quaternary ammonium siloxanolate catalyst. The oligomer molecular weight is controlled by the endblocker/D_4 ratio (see Appendix A). Complete equilibration was ensured by allowing the reactions to run for 48 hours, even though recent studies show that the linear/cyclic equilibrium is reached at shorter times [35]. Raising the temperature to 150°C for 3 hours was sufficient to decompose the transient catalyst into inert, volatile by-products such as methanol, trimethylamine, and methoxysiloxane [22]. The levels of equilibrium cyclics have typically been found to be very low (<10%, removed by vacuum distillation), with the predominate species being D_4 [35].

Scheme 20

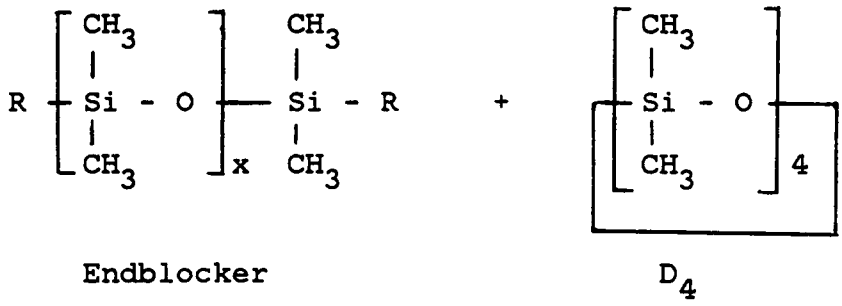

Endblocker D_4

80°C, 48 hrs.

Argon

N-Catalyst

Oligomer + Cyclics + Catalyst

Oligomer

150°C, 3 hrs.

Oligomer + Cyclics

Vacuum Distill

100°C, 0.5 torr

Oligomer

Silylamine : R = $N(CH_3)_2$, x ≈ 10

Aminopropyl : R = $(CH_2)_3NH_2$, x = 1

As discussed in the literature review, the polymerization of cyclic siloxanes in the presence of an endblocker and under base catalysis generally proceeds through a transient viscosity maximum after which the slower reacting endblocker equilibrates into the siloxane chain and begins to control the molecular weight [7,24]. In these systems, the reaction mixtures are transparent throughout the equilibration and a transient viscosity maximum is observed. The viscosity of the final product was observed to be greater than that of the original reaction mixture and it was also dependent upon molecular weight; a higher molecular weight oligomer has a higher viscosity.

Infrared spectroscopy is one of the best techniques available for structure analysis of silicone products. The infrared spectrum is a fingerprint which identifies the polymer as a silicone, and at the same time can provide a great deal of information about chemical structure and purity [6,138]. A typical FTIR spectrum of a poly(dimethyl)siloxane oligomer is shown in Figure 12; corresponding bands are listed in Table 6.

The chemical structure of polysiloxanes can also be determined by their characteristic proton NMR spectra. A typical spectrum of an amine-functional poly(dimethyl)siloxane oligomer, with corresponding peak assignments, is

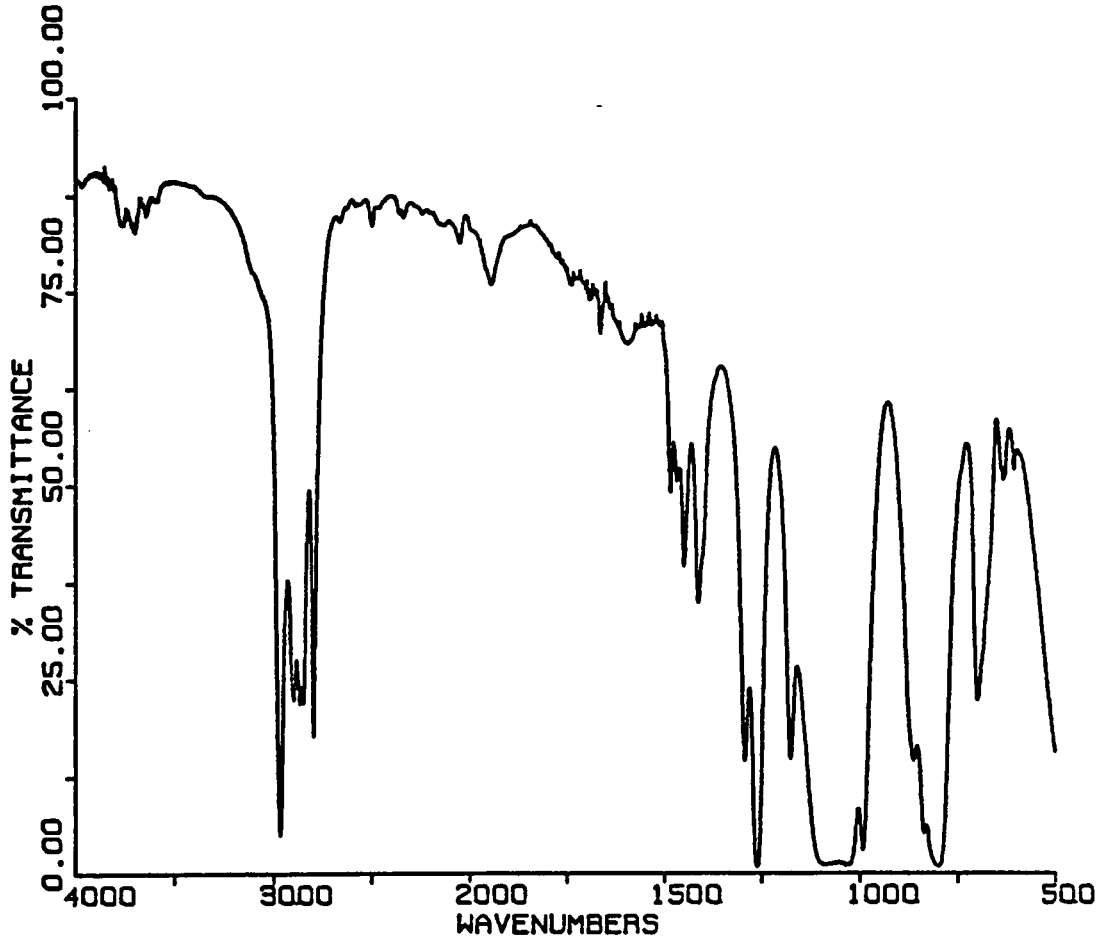

Figure 12: An FTIR spectrum of a silylamine-terminated poly(dimethyl)siloxane oligomer.

TABLE 6

Poly(dimethyl)siloxane FTIR Band Assignments

Frequency (cm^{-1})	Assignment
3000	C-H stretch of CH_3
1410	$Si(CH_3)_2O$ asymmetric deformation
1260	$Si(CH_3)_2O$ symmetric deformation
1130-1000	Si-O-Si stretch vibration
800	$Si(CH_3)_2O$ stretch; CH_3 rock
715	$Si(CH_3)_2O$ stretch
510	Si-O-Si bend vibration
1090-1080	Cyclic tetramers
1080-1050	Cyclics larger than tetramers
1070-1040	Disiloxanes
1020-1010	Cyclic trimers

shown in Figure 13. The characteristic Si-CH_3 resonance at 0.3 ppm is often used to determine the presence and amount of silicones in various materials. Structure analysis of siloxanes is aided by the fact that the Si-CH_3 resonance is generally a sharp singlet so that nonequivalencies are more easily detected. If the endgroups are observable, the oligomer molecular weight may be determined. However, the oligomer molecular weights used in this study were often too high to observe the few endgroup protons using the readily available 90 MHz NMR spectrometer. The less available 270 MHz instrument was more promising. In general, number average molecular weights of the amine-terminated siloxane oligomers were determined by potentiometric titration with alcoholic HCl.

High resolution ^{29}Si NMR has recently proved to be a powerful tool in the structural elucidation of organosilicones. The high sensitivity of silicon to changes in chemical environment, coupled with its wide range of chemical shifts, makes it possible to obtain detailed information about the microstructure and purity of complex molecules such as polyorganosiloxanes [139]. Since this analytical technique is much less common than FTIR and proton NMR, it will be discussed in detail in a subsequent section of this chapter.

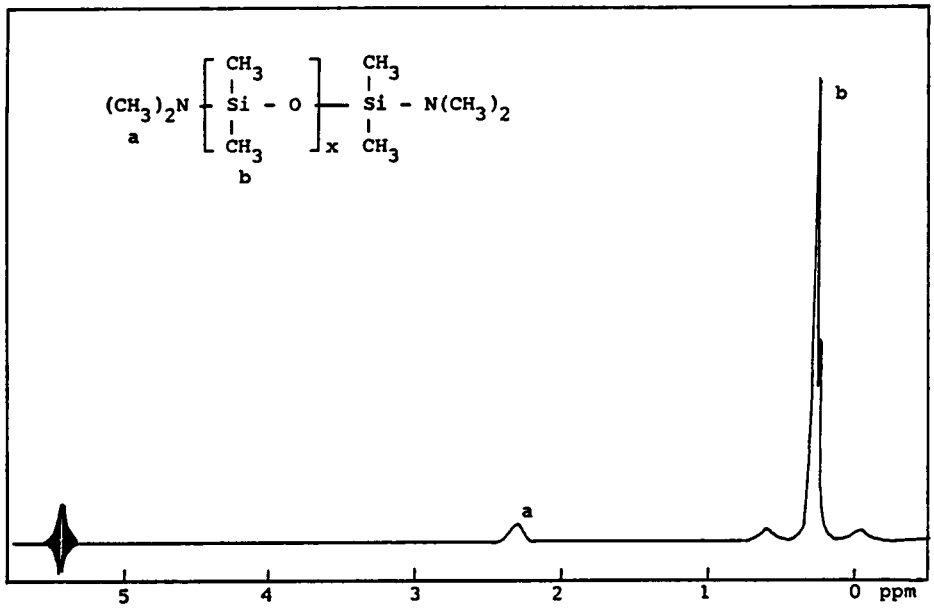

Figure 13: A proton NMR spectrum of a silylamine-terminated poly(dimethyl)siloxane oligomer.

4.1.1.2 Poly(dimethyl-co-diphenyl)siloxane Oligomer Synthesis

In order to increase the Tg, the solubility parameter and, therefore, the miscibility of the siloxane phase with the organic phase in a block copolymer system, co-oligomers of dimethylsiloxane and diphenylsiloxane were prepared. The synthesis of these co-oligomers, with amine functionality, is illustrated in Scheme 21. An amine-functional endblocker is equilibrated with a mixture of the cyclic dimethylsiloxane tetramer (D_4) and the cyclic diphenylsiloxane tetramer (D_4") in the presence of a quaternary ammonium siloxanolate catalyst for 48 hours at 80°C. The transient catalyst was decomposed at 150°C for 3 hours. The composition and molecular weight of the co-oligomers may be varied by controlling the ratio of the two cyclics to each other and to the endblocker, respectively (see Appendix A). The initial reaction mixture is heterogeneous since the D_4" is a crystalline solid that is not soluble in the other two components of the bulk reaction mixture. As a function of time and the D_4" content, the reaction mixture becomes homogeneous and transparent. This is apparently due to the fact that the D_4" is soluble in the low molecular weight oligomers formed from the equilibration of D_4 with the endblocker. The rate at which the reaction mixture becomes homogeneous and the level of cyclics at equilibrium are

Scheme 21

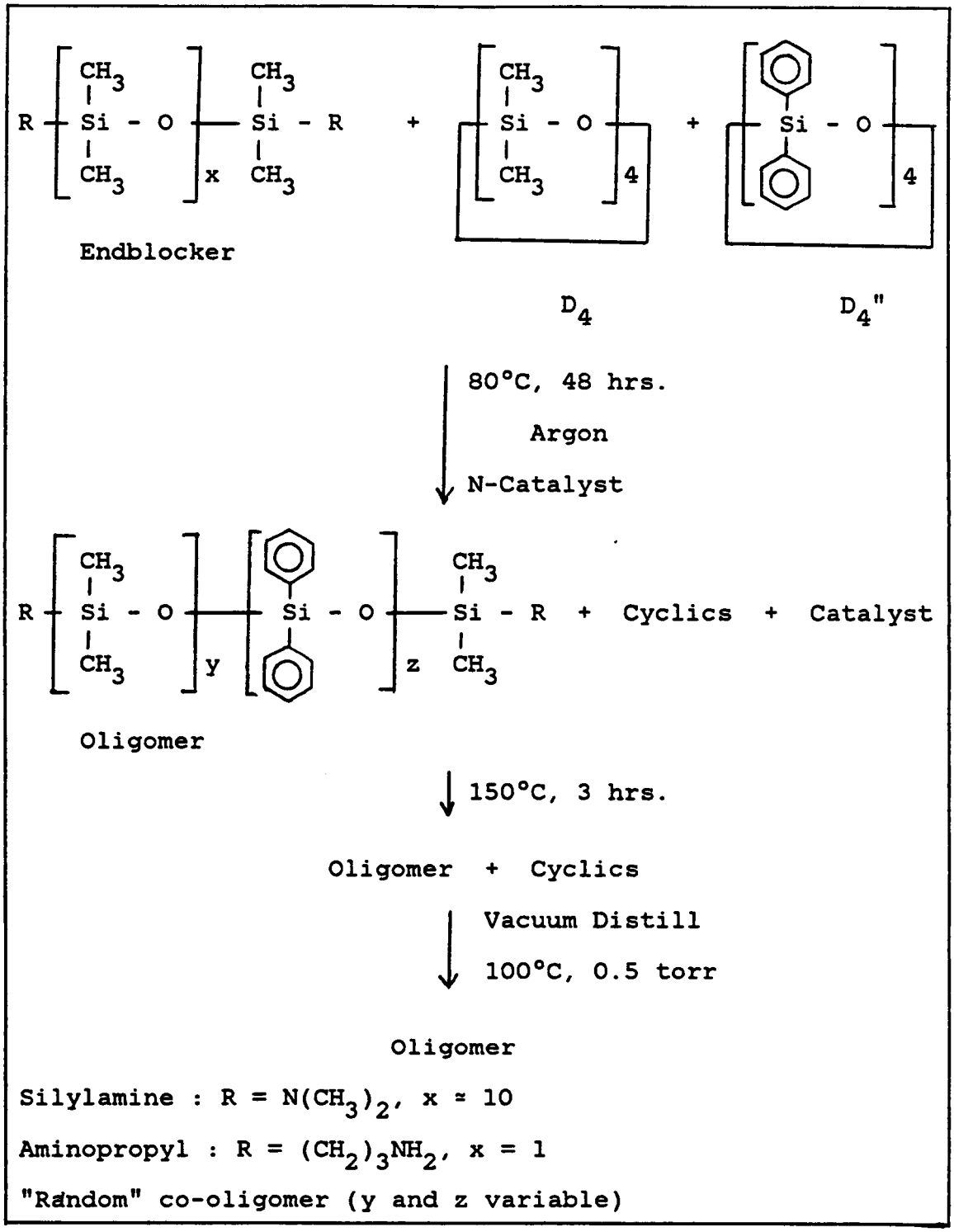
Endblocker
D4
D4"
80°C, 48 hrs.
Argon
N-Catalyst
Cyclics
Catalyst
Oligomer
150°C, 3 hrs.
Oligomer + Cyclics
Vacuum Distill
100°C, 0.5 torr
Oligomer
Silylamine : R = N(CH3)2, x ≈ 10
Aminopropyl : R = (CH2)3NH2, x = 1
"Random" co-oligomer (y and z variable)

dependent upon the diphenylsiloxane content. As the weight percent of diphenylsiloxane increases, the rate at which the reaction becomes homogeneous decreases and the level of equilibrium cyclics increases (approximately 17% cyclics for 75 weight % diphenylsiloxane charged). The equilibrium diphenyl and diphenyl-dimethyl cyclics are not easily removed by vacuum distillation since they are high boiling in comparison to dimethylsiloxane cyclics. Removal by selective extraction is not possible in the case of silylamine-terminated siloxane oligomers since the Si-N bond is very labile and would not survive such a procedure.

The viscosity of the dimethyl-diphenyl siloxane co-oligomers was observed to increase not only with molecular weight, but also with diphenyl content. This is due to the reduced flexibility of the polymer chains as bulky diphenyl units are incorporated.

Typical FTIR and proton NMR spectra of dimethyl-diphenyl siloxane oligomers are shown in Figures 14 and 15, respectively. The FTIR band frequencies are listed in Table 7. The IR bands and the proton NMR peak assignments agreed with the expected molecular structure. ^{29}Si NMR was used to study co-oligomer microstructure and will be discussed in a subsequent section of this chapter.

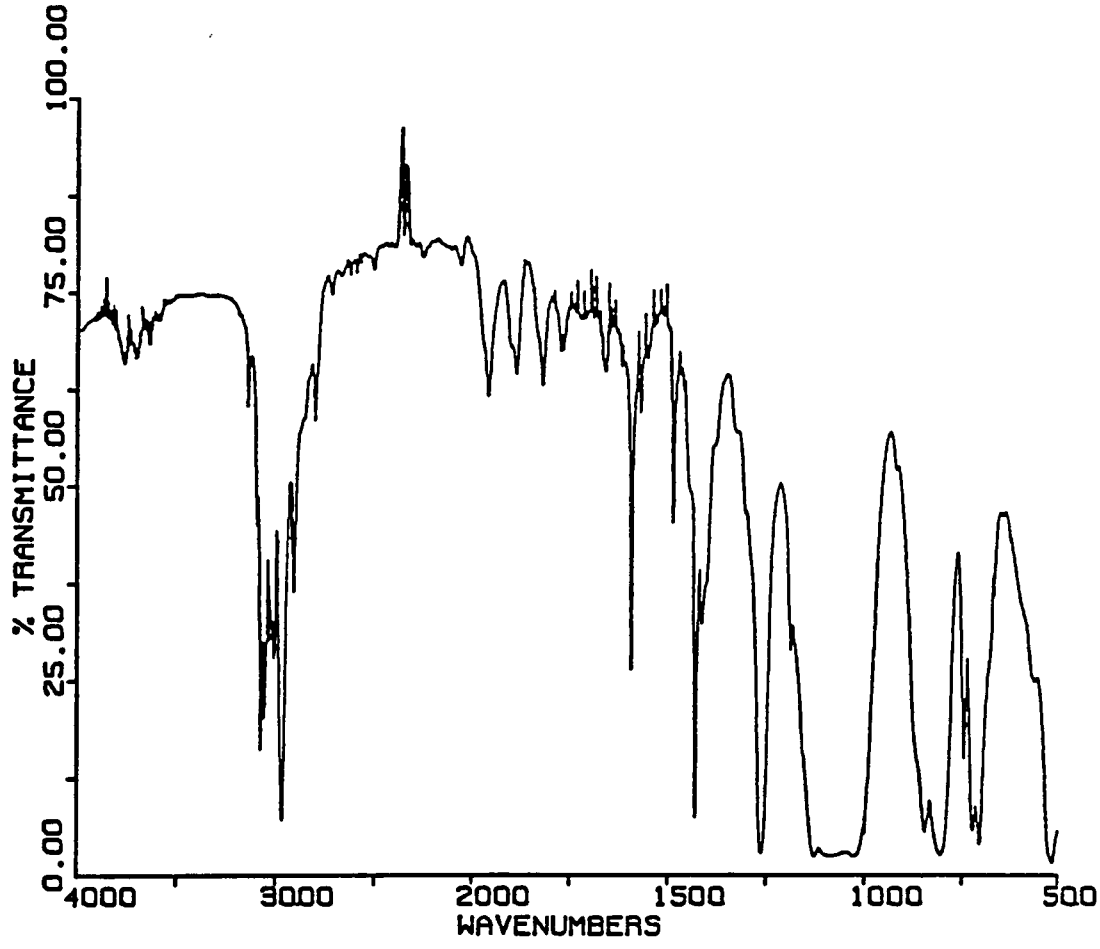

Figure 14: A typical (dimethyl-diphenyl)siloxane co-oligomer FTIR spectrum (50 CH_3/50 Ø in wt. %).

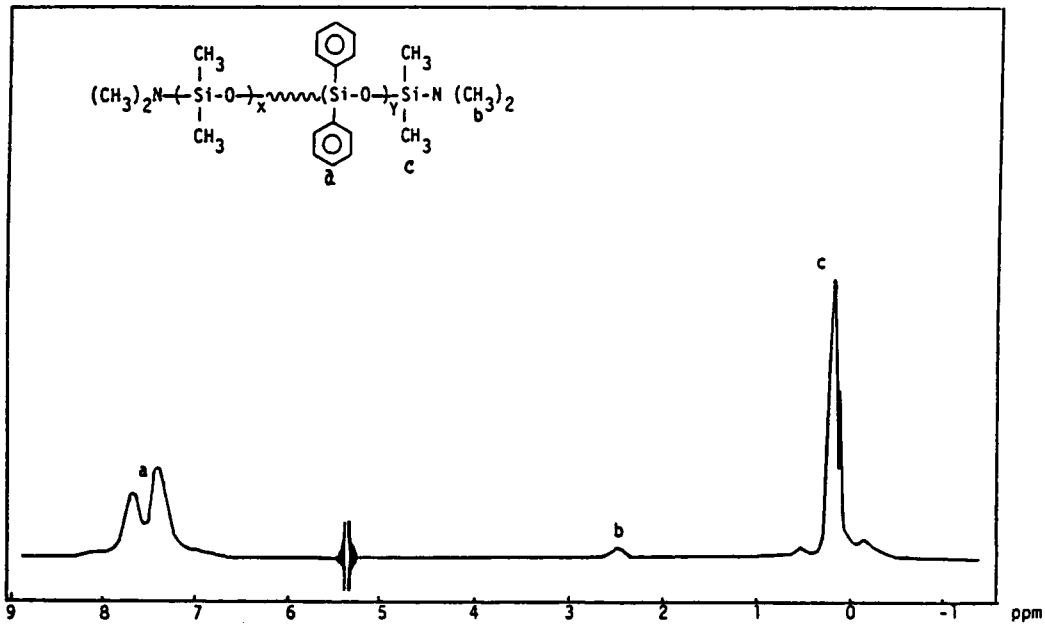

Figure 15: A typical proton NMR spectrum of a (dimethyl-diphenyl)siloxane co-oligomer (50 CH_3/50 Ø in wt. %).

TABLE 7

Poly(dimethyl-co-diphenyl)siloxane FTIR Band Assignments

Frequency (cm^{-1})	Assignment
3000	C-H stretch of CH_3
1600,1500	C-C aromatic stretch
1410	$Si(CH_3)_2O$ asymmetric deformation
1260	$Si(CH_3)_2O$ symmetric deformation
1130-1000	Si-O-Si stretch vibration
800	$Si(CH_3)_2O$ stretch; CH_3 rock
760-690	$Si(\emptyset)_2O$ stretch
715	$Si(CH_3)_2O$ stretch
510	Si-O-Si bend vibration
1090-1080	Cyclic tetramers
1080-1050	Cyclics larger than tetramers
1070-1040	Disiloxanes
1020-1010	Cyclic trimers

4.1.1.3 Poly(dimethyl-co-trifluoropropylmethyl)siloxane Oligomer Synthesis

The co-equilibration of the cyclic dimethylsiloxane tetramer (D_4) and the cyclic trifluoropropylmethylsiloxane trimer (F_3) with an amine-functional endblocker in the presence of a quaternary ammonium siloxanolate catalyst affords a co-oligomer with an increased solubility parameter relative to poly(dimethyl)siloxane. The preparation of these co-oligomers is illustrated in Scheme 22. Again, the co-oligomer composition and molecular weight may be varied by controlling the ratio of the cyclic monomers to each other and to the endblocker, respectively. The initial reaction mixture is transparent, but heterogeneous. This is due to the fact that the solid F_3 monomer is above its melting point at the reaction temperature, but it is nevertheless not initially miscible with the other two components of the bulk reaction mixture. As the F_3 begins to equilibrate, the reaction mixture becomes homogeneous. As with the previously discussed phenyl-containing co-oligomers, the rate at which the reaction mixture becomes homogeneous decreases with an increase in trifluoropropylmethyl units. The amount of equilibrium cyclics increases slightly with an increase in trifluoropropylmethyl siloxane units. It was difficult to remove the high boiling trifluoropropylmethyl and trifluoropropylmethyl-dimethyl siloxane cyclics. Due to the

Scheme 22

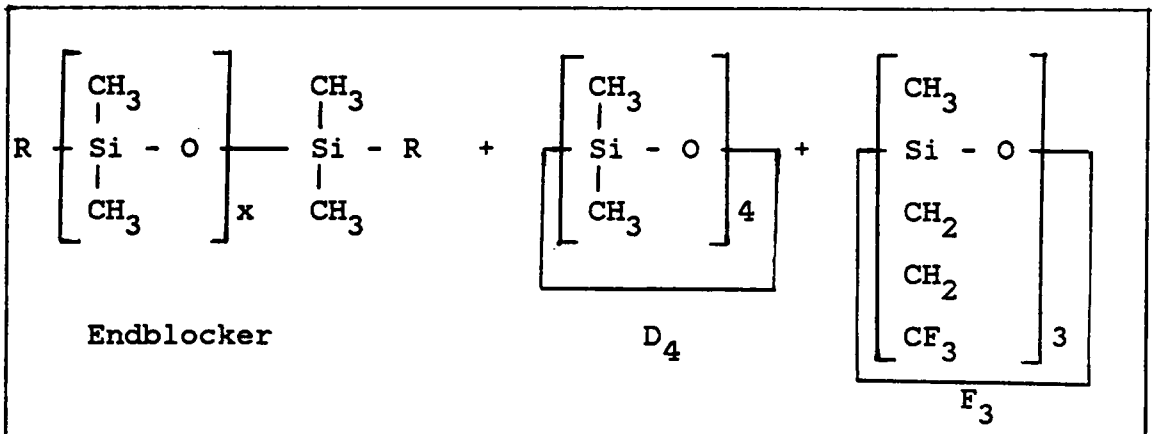

80°C, 48 hrs.

Argon

N-Catalyst

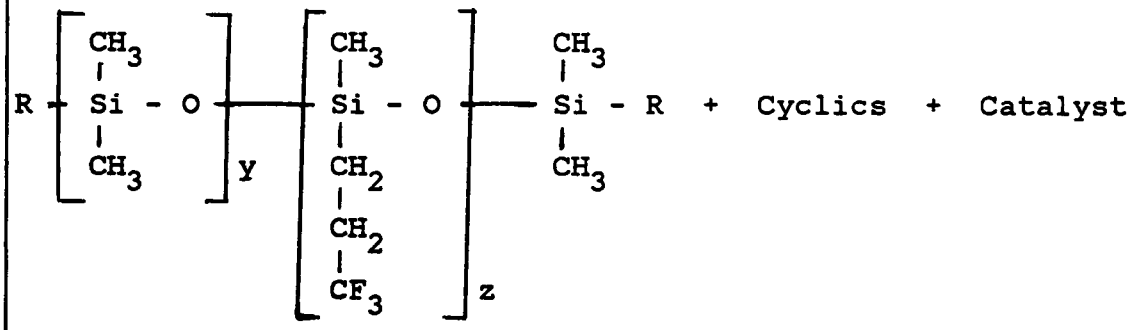

150°C, 3 hrs.

Oligomer + Cyclics

Vacuum Distill

100°C, 0.5 torr

Oligomer

Silylamine : R = $N(CH_3)_2$, x ≈ 10

Aminopropyl : R = $(CH_2)_3NH_2$, x = 1

"Random" Co-oligomer (y and z variable)

reactive nature of the silylamine endgroups, solvent extraction was not used at this stage.

The viscosity of these systems increased with both molecular weight and trifluoropropylmethyl content. However, the observed increase was not as dramatic as the previously discussed diphenylsiloxane case.

Structure analysis was again accomplished by FTIR and proton NMR, the spectra of which are shown in Figures 16 and 17, respectively. Band assignments for the FTIR spectrum are given in Table 8. ^{29}Si NMR did not prove to be useful in the structural characterization of dimethyl-trifluoropropylmethyl siloxane co-oligomers since the silicon atoms of both unit types have similar chemical environments and, therefore, their resonances not well resolved.

4.1.1.4 ^{29}Si NMR of Functional Siloxane Oligomers

In the early 1960's the promise of ^{29}Si NMR spectroscopy as a structural probe in organosilicon chemistry was demonstrated by Lauterbur [142]. Initially, little attention was given to the characterization of silicone polymers by this technique because the direct observation of the ^{29}Si nucleus was experimentally difficult. The tremendous growth of ^{29}Si NMR papers [143-163] in recent years has largely been due to the development and application of the pulsed Fourier transform (FT) method [164].

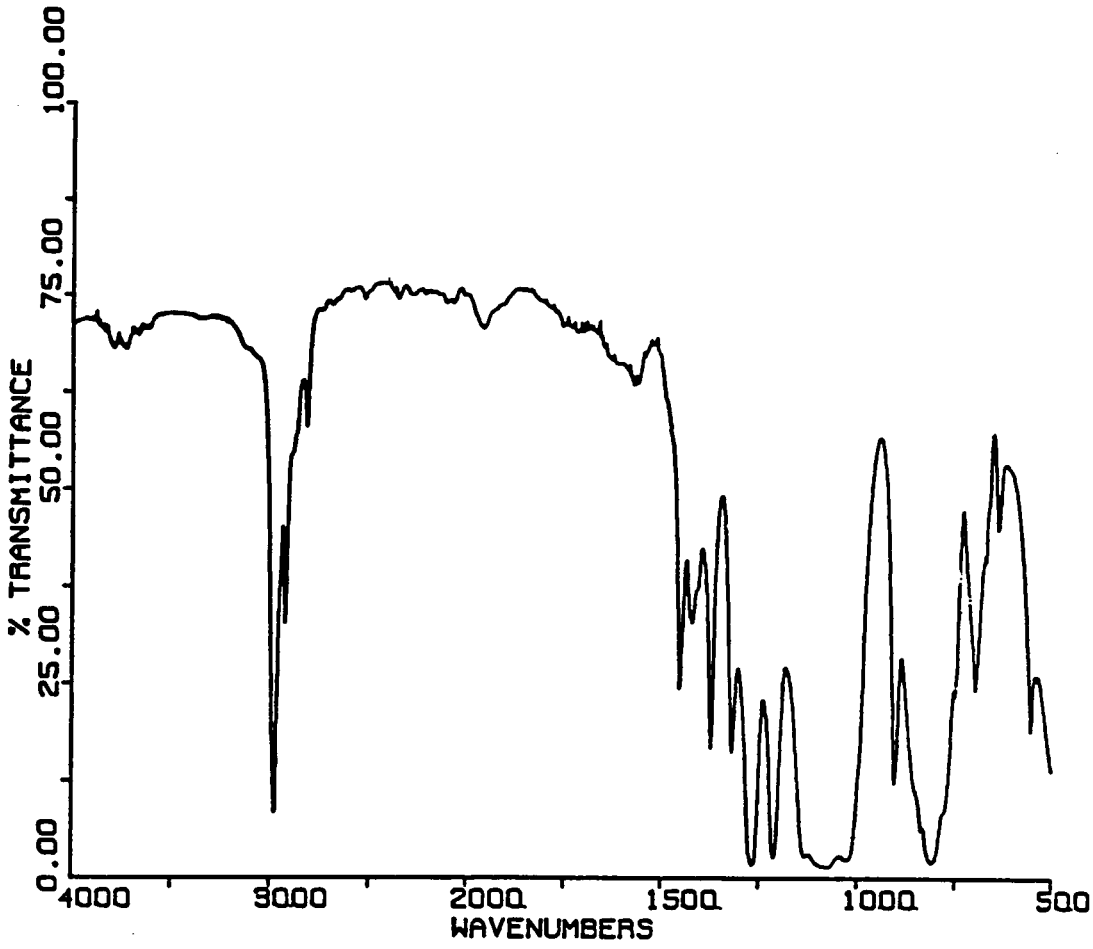

Figure 16: FTIR spectrum of a (trifluoropropylmethyl-dimethyl) siloxane co-oligomer (50 CH_3/50 F in wt. %).

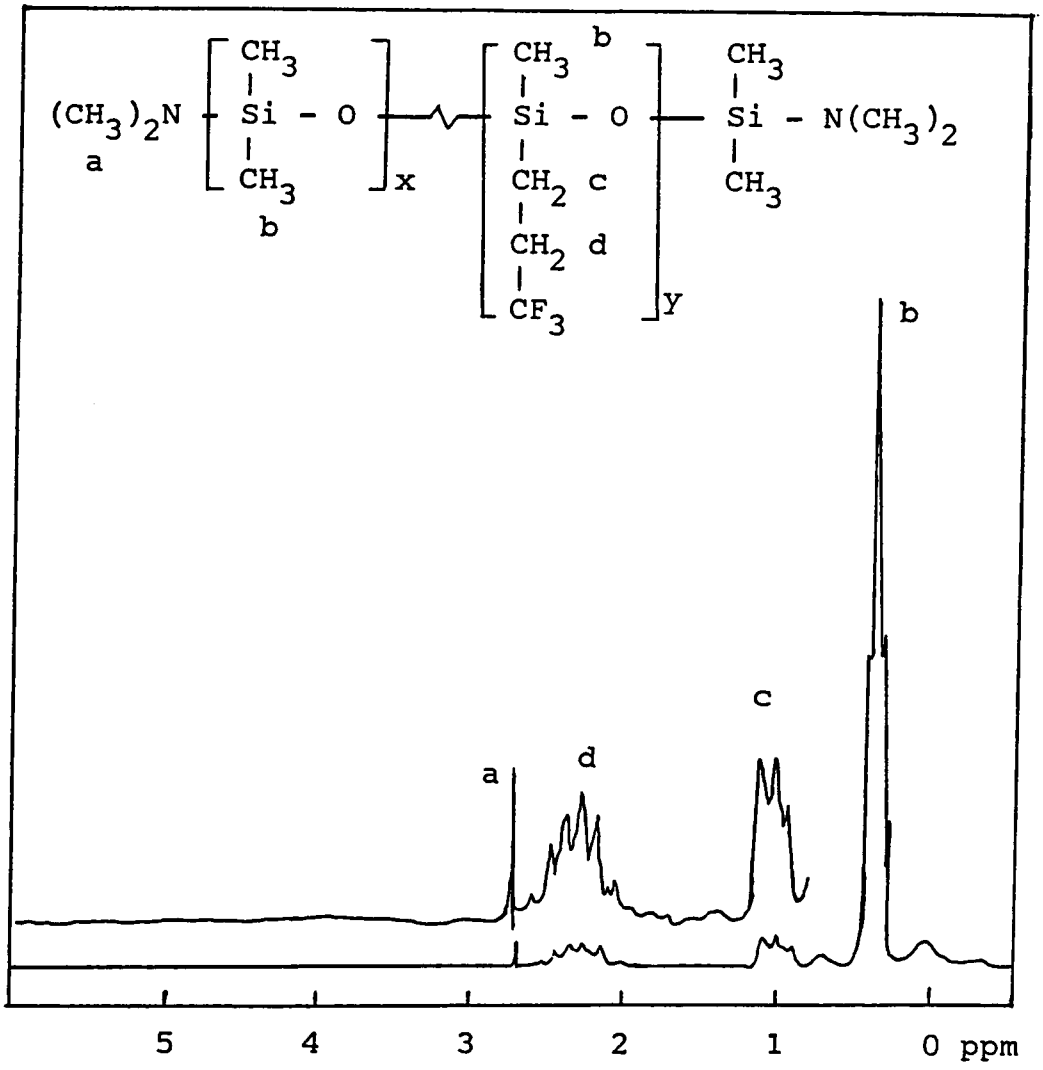

Figure 17: Proton NMR spectrum of a (dimethyl-trifluoropropylmethyl)siloxane co-oligomer (50 CH_3/50 F in wt. %).

TABLE 8

Poly(dimethyl-co-trifluoropropylmethyl)siloxane FTIR Band Assignments

Frequency (cm^{-1})	Assignment
3000	C-H stretch of CH_2 and CH_3
1410	$Si(CH_3)_2O$ asymmetric deformation
1350	$Si-CH_2$ scissoring
1260	$Si(CH_3)_2O$ symmetric deformation
1240	$Si-CH_2$ wagging
1130-1000	Si-O-Si stretch vibration
800	Si-C stretch
715	$Si(CH_3)_2O$ stretch
510	Si-O-Si bend vibration
1090-1080	Cyclic tetramers
1080-1050	Cyclics larger than tetramers
1070-1040	Disiloxanes
1020-1010	Cyclic trimers

Naturally occurring silicon consists of three isotopes: 92.21% ^{28}Si, 4.70% ^{29}Si, and 3.09% ^{30}Si; of these only ^{29}Si has a spin (I = 1/2). The characteristics of the ^{29}Si nucleus are listed in Table 9. The low natural abundance and low NMR sensitivity at constant field relative to ^{1}H places it with ^{13}C in the group of "rare" spin nuclei. Fortunately, the recent use of FT-NMR spectrometers eliminates the problem of low sensitivity. Difficulties also arise from the long spin-lattice relaxation times (T_1) frequently associated with ^{29}Si and its negative magnetogyric ratio (γ). The latter indicates that under proton decoupling conditions the Nuclear Overhauser Effect (NOE) is negative. This can result in greatly reduced signal intensities, signals nulled into the baseline, or negative peaks.

A further complication is that T_1 values for most ^{29}Si nuclei are greater than 20 seconds, which makes time average experiments very time consuming. Both of these problems can be overcome with the addition of a small amount (0.01-0.03M) of a paramagnetic relaxation reagent [157-159] such as the acetylacetonate of Cr III. The shiftless relaxation reagents are effective in reducing the T_1 values to a few seconds by replacing all the relaxation mechanisms with a much more efficient electron-nuclear dipole-dipole interaction which dominates the spin-lattice relaxation. Since the

TABLE 9

^{29}Si Characteristics

Spin = 1/2

Abundance = 4.7%

Relative Sensitivity = 7.84×10^{-3} [a]

Magnetic Momentum = -0.961 nuclear magnetions

Magnetogyric Ratio = -5.3×10^{-7} rad T^{-1} sec^{-1}

Chemical Shift Range > 550 ppm

Spin-Lattice Relaxation > 20 seconds

Negative NOE with ^{1}H decoupling

---

[a] At constant field relative to ^{1}H (1.0).

proton-nuclear dipole-dipole relaxation mechanism becomes unimportant, under proton decoupling conditions the NOE is eliminated. Short T_1 values and the absence of any NOE produces an absorption spectrum obtained with the same relative ease as a ^{13}C spectrum. For cases in which it is undesirable to add a relaxation reagent, pulse-modulated decoupling ("gated-decoupling") [165] may be used to eliminate the NOE. However, this technique does not eliminate the problem of long T_1 values and long recovery times may be needed in an FT experiment.

The range of the ^{29}Si NMR chemical shifts spans some 400 ppm. However, most organosilicones are clustered in a considerably narrower range of about 120 ppm. Figure 18 [155] summarizes ^{29}Si chemical shifts for various organosilicon compounds. Highly shielded ^{29}Si nuclei generally have multiple oxygen substitution, whereas substitution by aliphatic groups results in deshielding. It is interesting to note that the broad resonance given by the glass of the NMR tube may overlap sample signals in the region of -80 to -130 ppm. In such circumstances it may be desirable to use NMR tubes made of teflon or to use difference spectroscopy, i.e., subtracting the free induction decay (FID) of a blank run from the sample of interest.

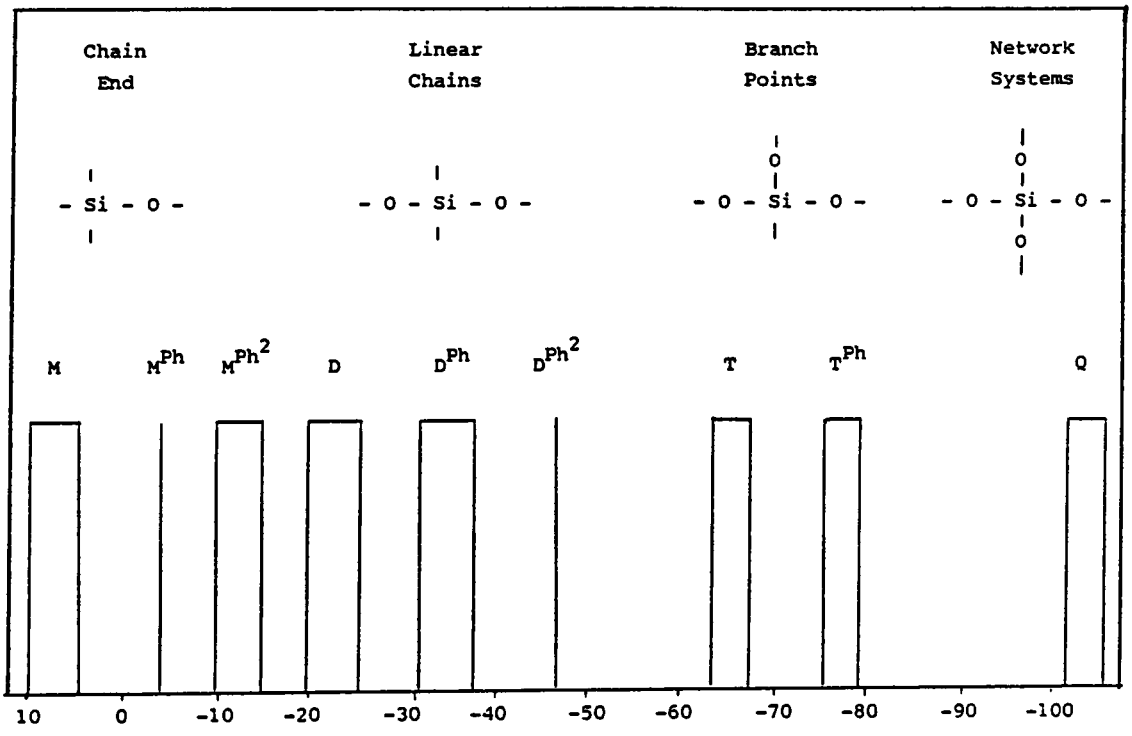

Figure 18: ^{29}Si chemical shifts of methyl, methyl-phenyl, and phenyl substituted siloxanes

Although the chemical shift range for ^{29}Si resonances is smaller than that observed in ^{13}C NMR, the spectral dispersion for many organosilicon compounds may be considerably greater in the ^{29}Si spectra. For comparative purposes, the characteristics and the NMR spectra of a siloxane oligomer for ^{1}H, ^{13}C, and ^{29}Si nuclei are shown in Table 10 and Figure 19 [144], respectively. The ^{13}C and ^{1}H spectra of the siloxane oligomer provide much less structural information than the ^{29}Si spectrum in which not only are the endgroups (M) and backbone (D) units separated by 28 ppm, but both types of D units show unique resonances. It has been reported that polysiloxanes show individual resonances for each unique silicon atom up to a 10-unit oligomer [151,163]. Data for a series of linear and cyclic polydimethylsiloxanes are collected in Table 11 [163]. Cyclic siloxanes were noted to have signals which are at higher frequencies than the linear siloxanes. However, siloxanes in a large ring are subjected to the same environment as those in a long chain and, therefore, have similar resonances [154].

The use of high resolution ^{29}Si NMR has proven useful in the purity and structural analysis of the functional siloxane oligomers prepared and used in our studies [139]. The high sensitivity of silicon to changes in chemical environment, coupled with its wide range of chemical shifts,

TABLE 10

Nuclei Comparison

	^{1}H	^{13}C	^{29}Si
Spin	1/2	1/2	1/2
% Abundance	100	1.1	4.7
Magnetic Momentum[a]	2.79	1.22	-0.96
Relative Sensitivity[b]	1.00	$1x10^{-2}$	$7.84x10^{-3}$

[a]Nuclear magnetons.

[b]For equal number of nuclei at constant field strength.

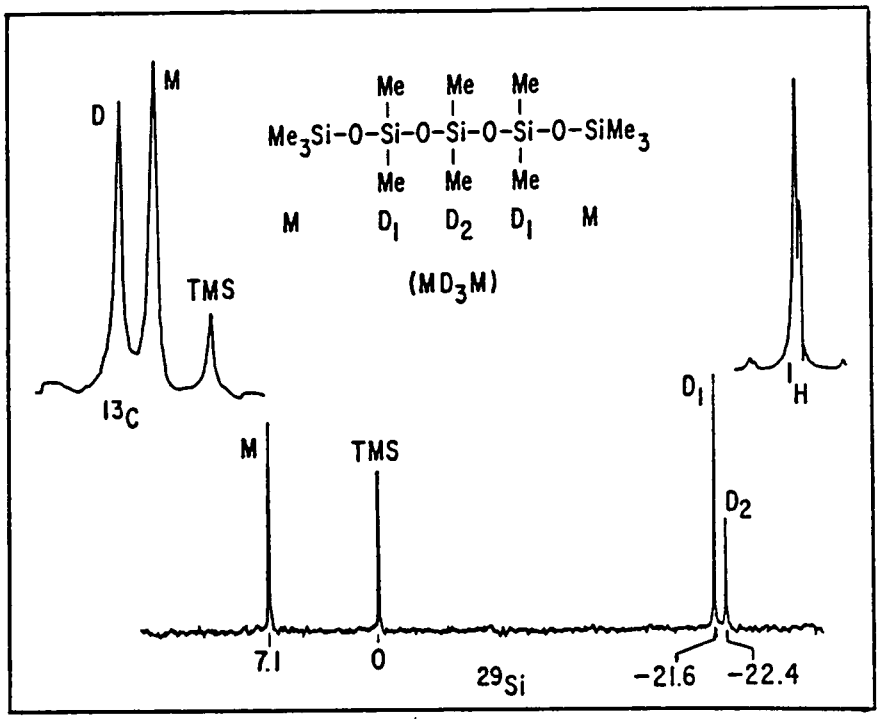

Figure 19: Comparison of ^1H, ^{13}C, and ^{29}Si NMR spectra of a siloxane oligomer [144].

TABLE 11

^{29}Si Chemical Shifts for Siloxane Oligomers [163]

	δ_{Si} [a]				
Compound	M	D^1	D^2	D^3	D^4
MM	6.79				
MDM	6.70	-21.50			
MD_2M	6.80	-22.00			
MD_3M	6.90	-21.80	-22.60		
MD_4M	7.00	-21.80	-23.40		
MD_5M	7.00	-21.80	-22.40	-22.30	
MD_6M	7.00	-21.80	-22.30	-22.20	
MD_7M	7.00	-21.89	-22.49	-22.33	-22.29
MD_8M	6.93	-21.86	-22.45	-22.30	-22.20
D_3 cyclic		-9.12			
D_4 cyclic		-19.51			
D_5 cyclic		-21.93			
D_6 cyclic		-22.48			

a: In ppm relative to internal Me_4Si (TMS).

M = $(CH_3)_3SiO_{0.5}$ and D = $(CH_3)_2Si(O_{0.5})_2$

makes it possible to obtain detailed information on the microstructure of the siloxane co-oligomers.

Prior to analyzing the synthesized functional siloxane oligomers and co-oligomers by ^{29}Si NMR, it was desirable to obtain the ^{29}Si spectra of several commercially available model compounds, some of which are starting materials for siloxane equilibrations used in our studies. Figure 20 illustrates the ^{29}Si NMR spectrum of a mixture of organosilicon model compounds. It is interesting to note that the aminopropyl disiloxane (DSX) is the only material to the left of $(Me)_4Si$ (TMS). This is due to the fact that the silicon atoms of the disiloxane are bonded to only one oxygen atom which produces a deshielding effect. The silicon atoms of the cyclic siloxanes, on the other hand, are shielded since they are bonded to two oxygen atoms and have negative resonance signals (right of TMS). It is also interesting to note that both ring size and substituent type influence the observed resonances.

A typical ^{29}Si NMR spectrum of an equilibrated aminopropyl-terminated polydimethylsiloxane (5,000 $\bar{M}n$) is shown in Figure 21a. The endgroup signal is observed at 7.5 ppm relative to TMS at 0 ppm. Residual equilibrium cyclics are noted at -19 ppm while the linear species are at -22 ppm. Due to the relatively high molecular weight, only two types

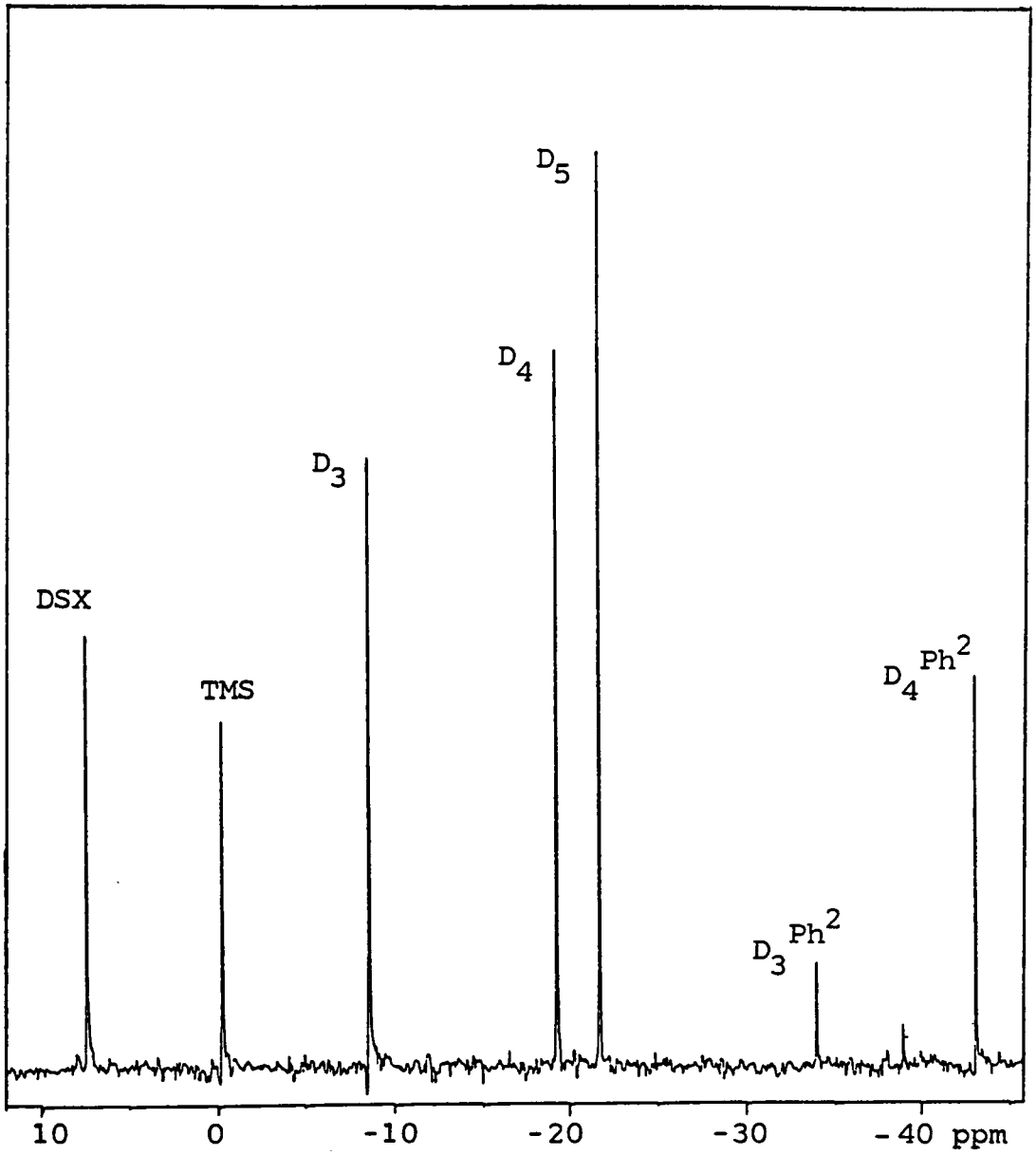

Figure 20: ^{29}Si NMR spectrum of silicon-containing model compounds.

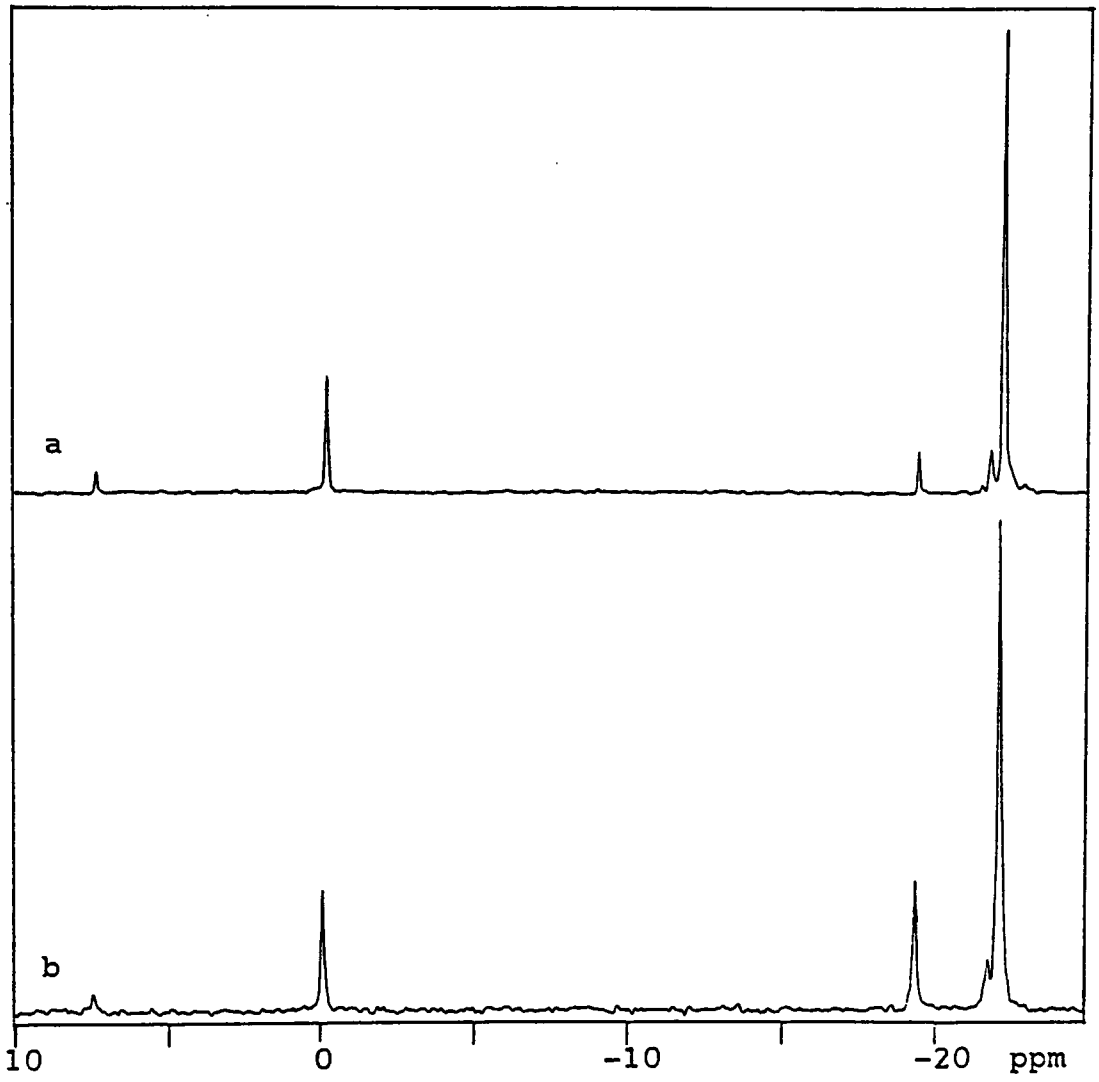

Figure 21: ^{29}Si NMR spectra: (a) aminopropyl-terminated dimethylsiloxane oligomer, (b) oligomer spiked with D_4.

of silicon atoms in the backbone are observable; a small signal at -21.5 ppm due to silicon atoms near the amine end-groups and at -22 ppm, a larger signal due to the linear backbone. Figure 21b illustrates the ^{29}Si NMR spectrum obtained from the same siloxane oligomer shown in Figure 21a except that it has been spiked with D_4, the cyclic dimethyl-siloxane tetramer. The signal at -19 ppm increased in intensity and, therefore, indicates that D_4 is the predominant cyclic species remaining at equilibrium.

High resolution ^{29}Si NMR was also useful in studying the microstructure of organosilicon co-oligomers consisting of two different types of silicon atoms. The chemical shift of a given silicon atom is affected by its immediate neighboring groups and the triad structure of the copolymer chain can be recognized by characteristic triplet splittings in the ^{29}Si NMR spectrum. Moreover, the influence of the second neighboring groups can cause a further triplet splitting of each triad line, i.e., pentad structures are represented in spectra by a triplet of triplets. This is shown schematically in Figure 22 [150] under the assumption of equal amounts and random distribution of A and B silicon units in the copolymer chain. Engelhardt et al. have shown by using model compounds that increasing numbers of diphenyl siloxane units in the neighborhood of a given dimethyl or diphenyl

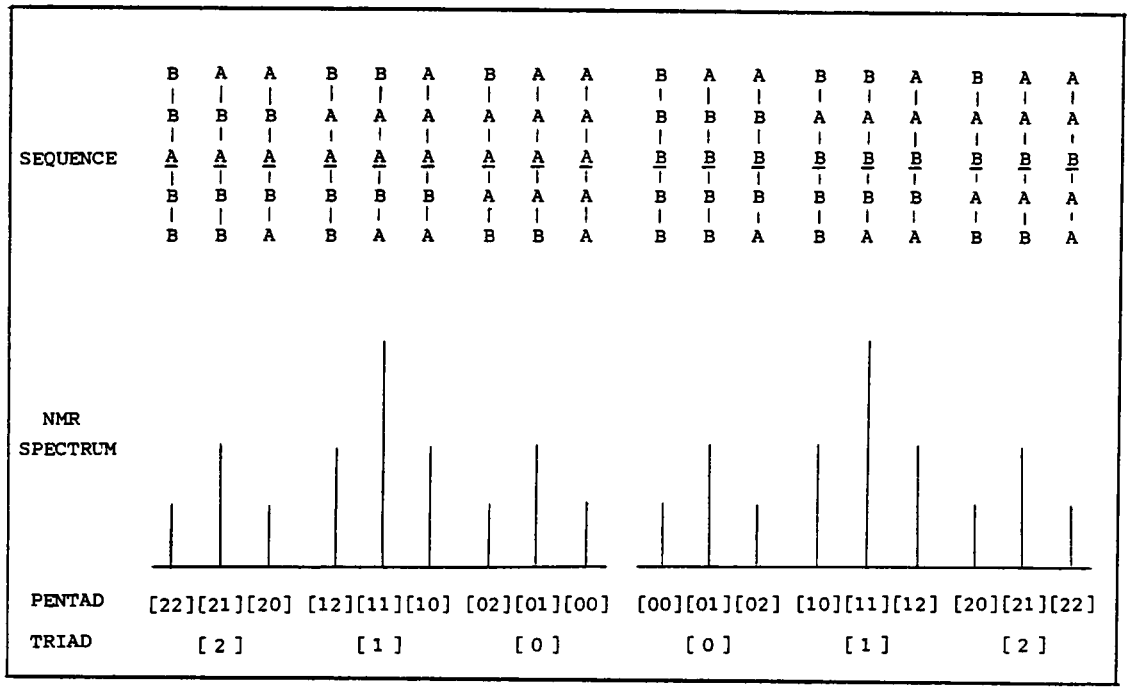

Figure 22: Signal assignment for pentad sequences of a random A-B copolymer with equal amounts of A and B units [150].

unit leads to low-field shifts of its ^{29}Si NMR signal [155]. As an example, the 39.75 MHz ^{29}Si NMR spectrum of the dimethyl-methylphenyl silicone oil OV-7 (Applied Science Lab., Inc.) is shown in Figure 23 [150]. The spectrum exhibits three groups of well resolved signals corresponding to endgroups, dimethyl silicon units (D), and methylphenyl silicon units (D^{Ph}) present in the copolymer chain. The M groups give rise to four signals according to the four different arrangements of the two neighboring silicon atoms near the chain ends. The D and D^{Ph} signals show the expected splitting for the nine different pentad sequences given in Figure 23. The pentad labels correspond to those given in Figure 22 for the theoretical spectrum of a random copolymer. The D^{Ph} triad (BBB) signal at -33.3 ppm shows line broadening effects probably due to different steric orientations of the closely adjacent phenyl groups.

A typical ^{29}Si NMR spectrum of an equilibrated aminopropyl-terminated dimethyl-diphenyl siloxane co-oligomer (5,000 Mn) containing 50 weight percent of each unit is shown in Figure 24. The spectrum exhibits three groups of well resolved signals corresponding to the endgroups at 7 ppm, the dimethyl siloxane units (D) centered at -21 ppm, and the diphenyl siloxane units (D^{Ph}) centered at -47 ppm. The signals show the expected splitting pattern for the nine

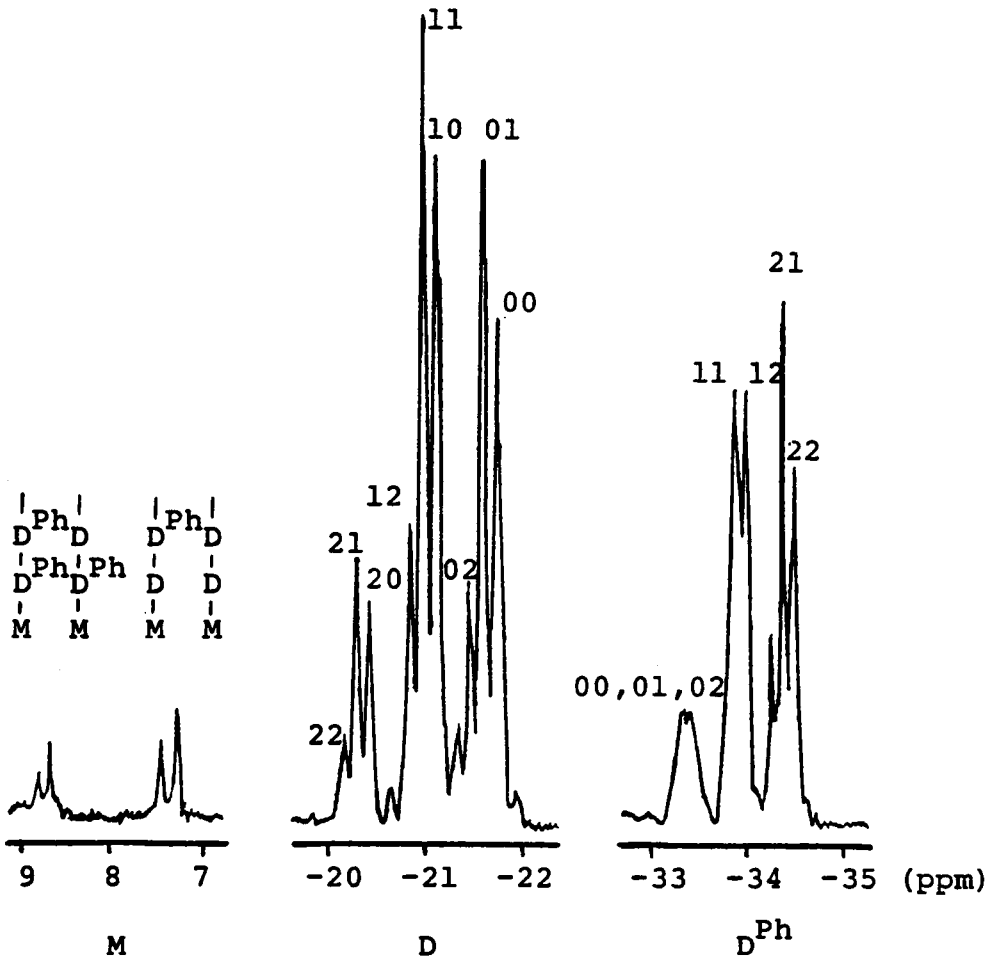

Figure 23: ^{29}Si NMR spectrum of dimethyl-methylphenyl silicone oil, OV-7 [150].

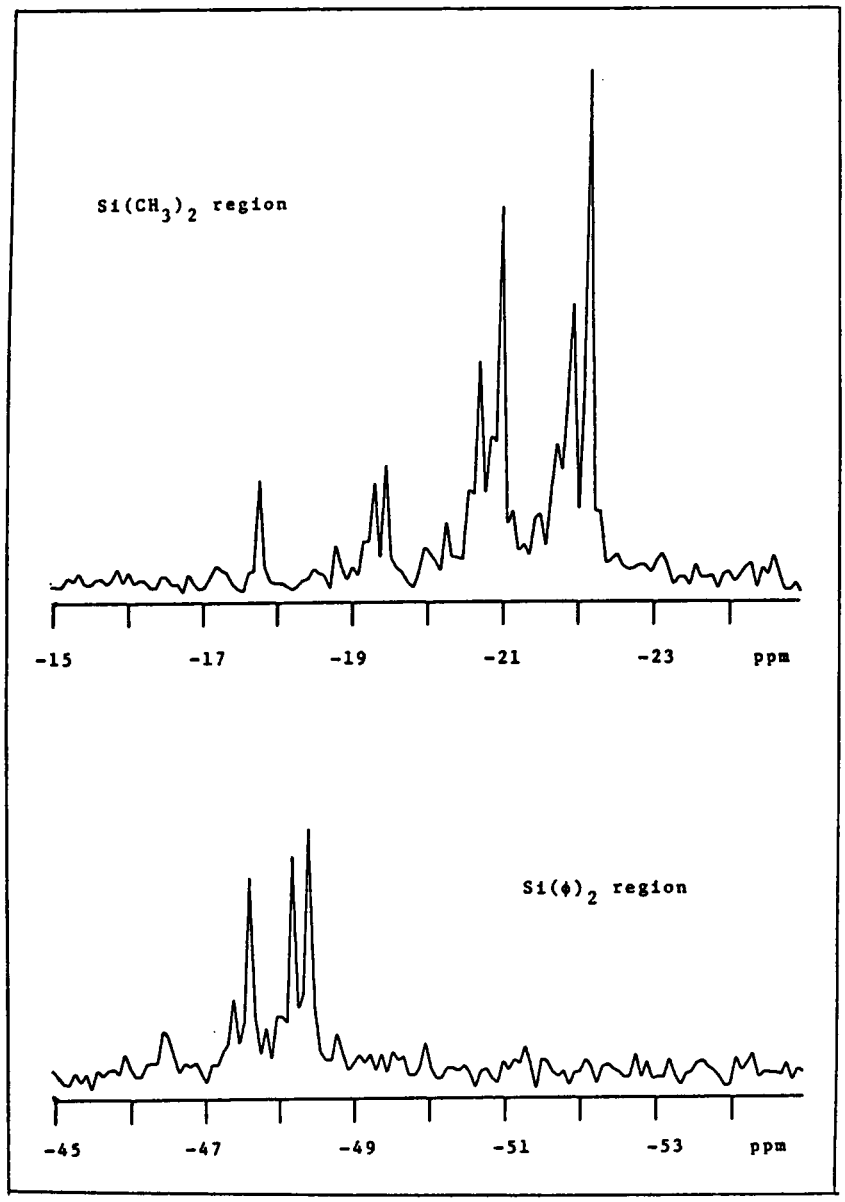

Figure 24: ^{29}Si NMR spectrum of an aminopropyl-terminated dimethyl-diphenyl siloxane co-oligomer. (CH_3/ϕ ratio 50/50 by weight or 73/27 by mole %).

different pentad sequences given in Figure 22. Due to the adjacent phenyl groups, the BBB triad peak at -46.5 ppm shows line broadening.

The signal intensities of the pentad or triad signals can be used to calculate the quantitative parameters describing the microstructure of the copolymer chain: mole fraction of the monomer units (A_M and B_M), number average sequence lengths ($\bar{\ell}_A$ and $\bar{\ell}_B$), and departure from random statistics (x). The parameter, x, is defined as:

$$x = \frac{P_2(AB)}{P_1(A)P_1(B)}$$

Since for a completely random process

$$P_2(AB) = P_1(B)P_1(A),$$

it follows that [166]:

x Value	Characteristic Feature
1	random or statistical
>1	alternating tendency
<1	blocky character
2	highly alternating
0	long blocky sequences

The microstructure parameters for two dimethyl-diphenyl co-oligomers are listed in Table 12. The calculations used to determine these values are shown in Appendix D [166].

Once the spectrum of a fully equilibrated siloxane has been assigned, it becomes feasible to study the effect of reaction conditions (catalyst concentration, reaction time, etc.) on sequence distribution and physical properties by obtaining spectra of samples extracted from reaction mixtures at different intervals of time [167].

4.1.1.5 Thermal Properties of Siloxane Oligomers and Co-Oligomers

The glass transition temperatures of the siloxane oligomers and co-oligomers were determined by Differential Scanning Calorimetry (DSC). The influence of diphenyl and trifluoropropylmethyl siloxane content on the glass transition temperatures of the co-oligomers are illustrated in Tables 13 and 14, respectively. The increase in the glass transition temperature with increasing diphenyl or trifluoropropylmethyl content was expected due to the incorporation of the more polar and bulky units which restrict molecular motions. Typical DSC traces for siloxane oligomers and co-oligomers are shown in Figures 25 and 26. Note, a T_c and T_m are not observed for the co-oligomers. The effect of composition on Tg is illustrated in Figure 27.

TABLE 12

^{29}Si NMR Microstructure Parameters for Dimethyl-Diphenyl Siloxane Co-oligomers

Mole % Theory	Mole % Exptl.	$\bar{\ell}_{CH_3}$	$\bar{\ell}_O$	x
47 CH_3	48 CH_3			
53 Ø	52 Ø	2.02	1.80	1.05[b]
73 CH_3	72 CH_3			
27 Ø	28 Ø	3.59	1.24	1.08[b]

[a]Samples co-equilibrated at 80°C for 48 hours.

[b]Indicates statistically random co-oligomer x ≈ 1.

TABLE 13

Poly(dimethyl-co-diphenyl)siloxane Oligomer Characteristics

Sample Number	Weight % Diphenyl	$\bar{M}n$ Theory	$\bar{M}n$ Titrated[a]	DSC Tg (°C)
1	0	5,000	6,000	-123
2	0	10,000	10,000	-124
3	25	5,000	5,400	-102
4	25	10,000	12,800	-104
5	50	5,000	5,400	-74
6	50	10,000	11,800	-71
7	75	5,000	5,000	--
8	75	10,000	11,500	--

[a]Amine endgroups were titrated with 0.1 N alcoholic HCl.

Note: -- indicates samples not run.

TABLE 14

Poly(dimethyl-co-trifluoropropylmethyl)siloxane Oligomer Characteristics

Sample Number	Weight % TFPM	$\bar{M}n$ Theory	$\bar{M}n$ Titrated[a]	DSC Tg(°C)
1	0	5,000	6,000	-123
2	0	10,000	10,000	-124
3	25	5,000	5,700	-117
4	25	10,000	10,200	-116
5	50	5,000	5,000	-105
6	50	10,000	11,900	-101
7	75	5,000	6,000	-93
8	75	10,000	13,000	-91
9	100	5,000	6,000	--
10	100	10,000	11,000	--

[a]Amine endgroups were titrated with 0.1 N alcoholic HCl.

Note: -- indicates samples not run.

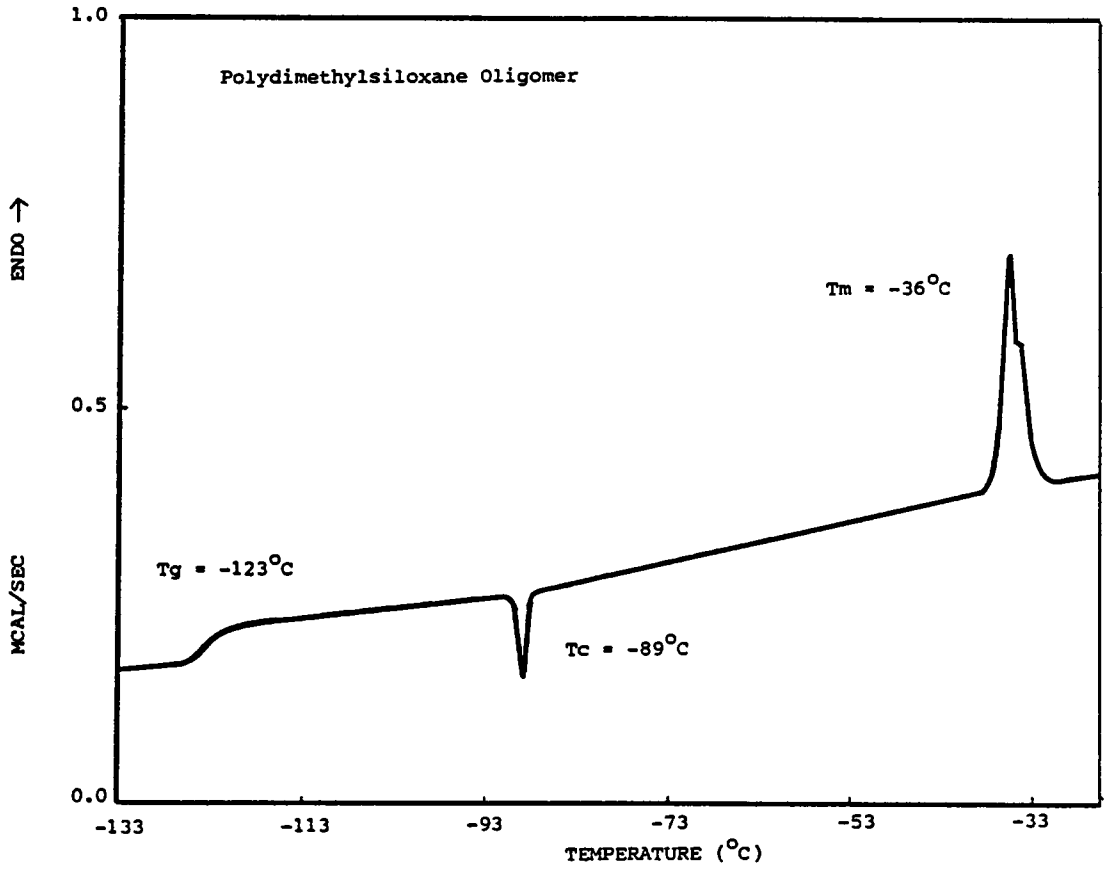

Figure 25: DSC trace of a polydimethylsiloxane oligomer.

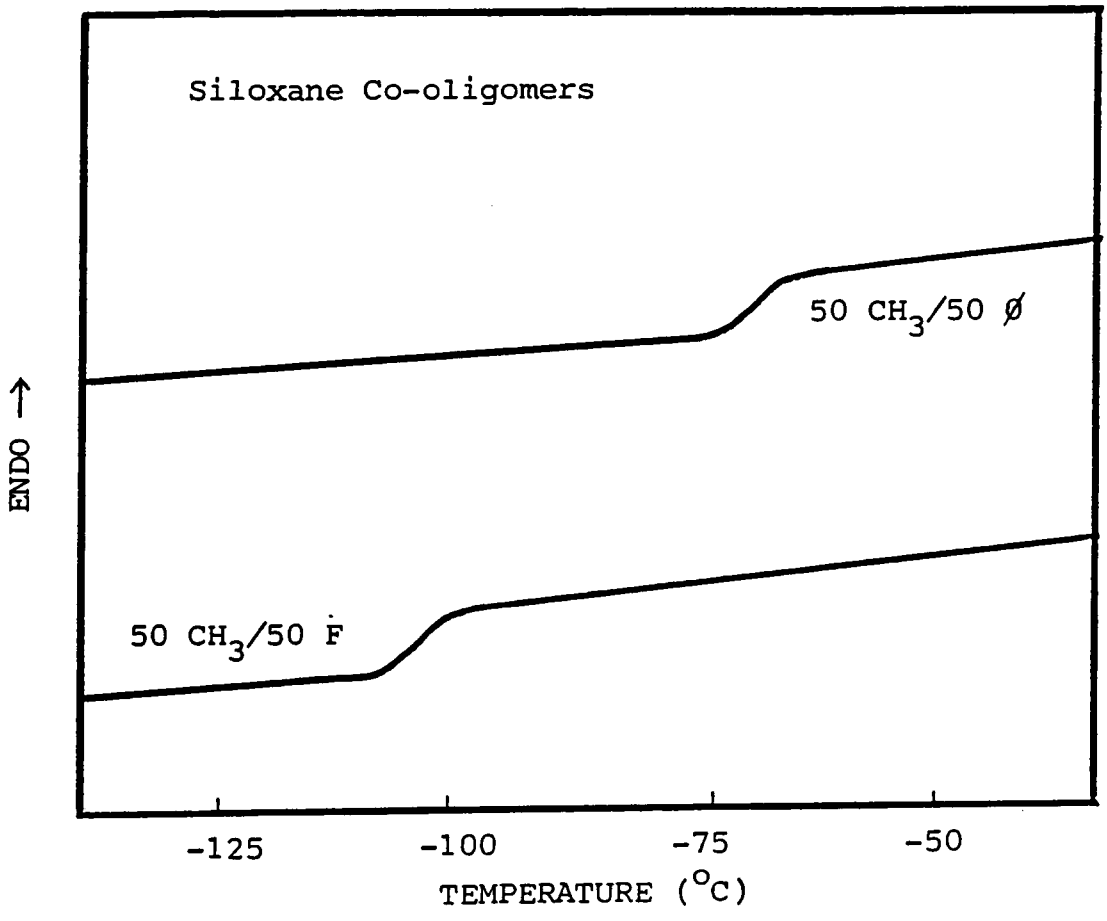

Figure 26: DSC traces of siloxane co-oligomers, compositions in weight %.

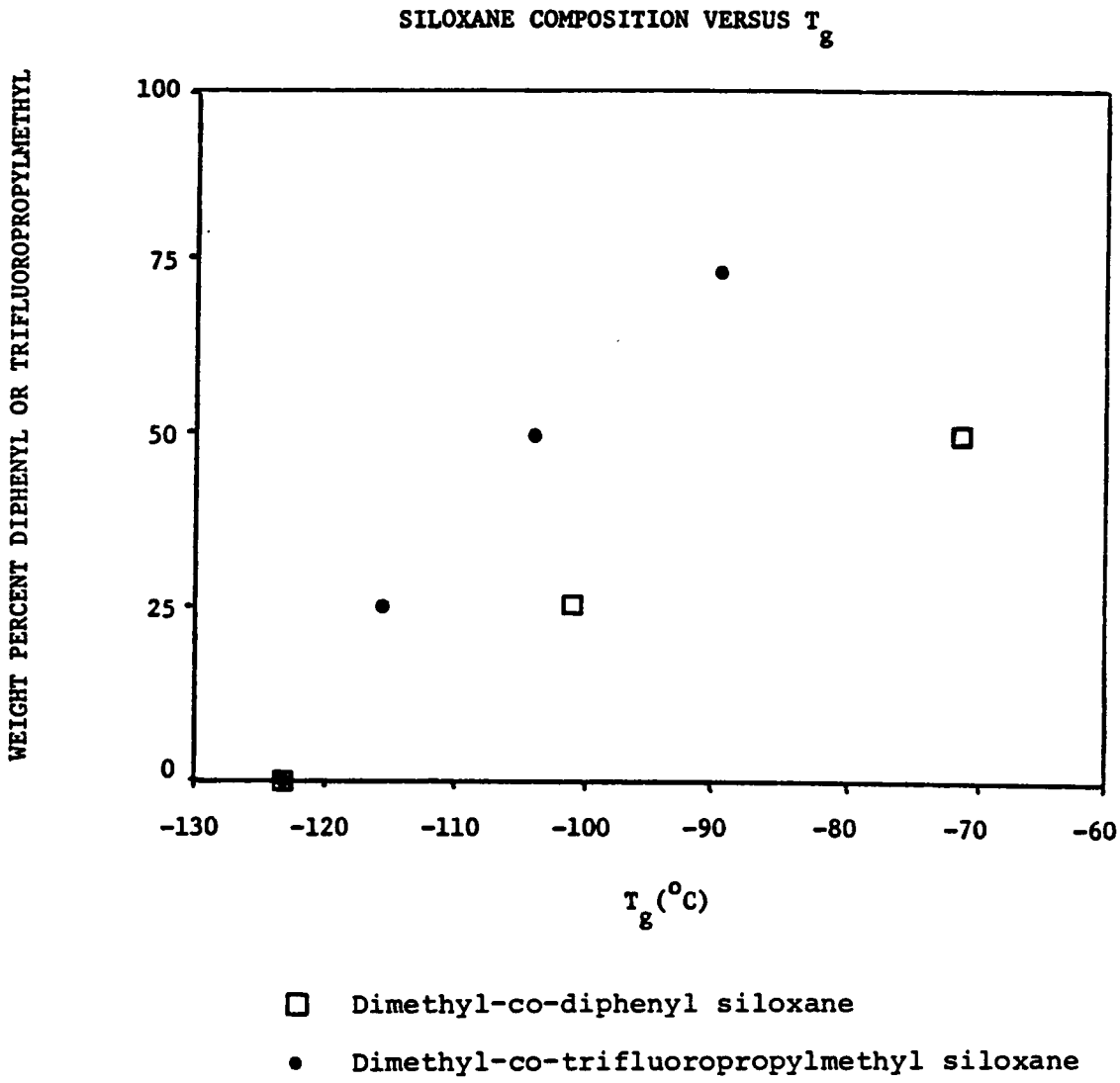

Figure 27: The effect of siloxane composition on glass transition temperature.

4.1.2 Hydroxyl-Terminated Polyarylester Oligomers

4.1.2.1 Synthesis and Structural Analysis

Several techniques are available for polyester synthesis as previously discussed in the literature review. Polyesters synthesized from bisphenols and acid chlorides have generally been prepared via interfacial routes which are facile and provide high molecular weight polymers in relatively short reaction times [54,56]. However, it is difficult to reproducibly prepare difunctional oligomers of controlled molecular weight by this technique for use in subsequent copolymerization reactions. Therefore, a solution technique was developed and involved the reaction of excess bisphenol-A with acid chlorides in the presence of triethylamine which served as an acid acceptor and catalyst. The synthetic route is illustrated in Scheme 23.

The desired molecular weight and functionality were obtained through the use of a stoichiometric imbalance of reactants according to Carother's equation [9] (see Appendix B). The calculated excess of bisphenol-A provides molecular weight control and hydroxyl functionality. Amorphous polyesters were ensured by incorporating equal amounts of terephthaloyl and isophthaloyl chlorides [54,55].

Structure analysis was determined by FTIR and proton NMR as shown in Figure 28 and 29, respectively. The

Scheme 23

Hydroxyl-Terminated Polyarylester Oligomer Synthesis

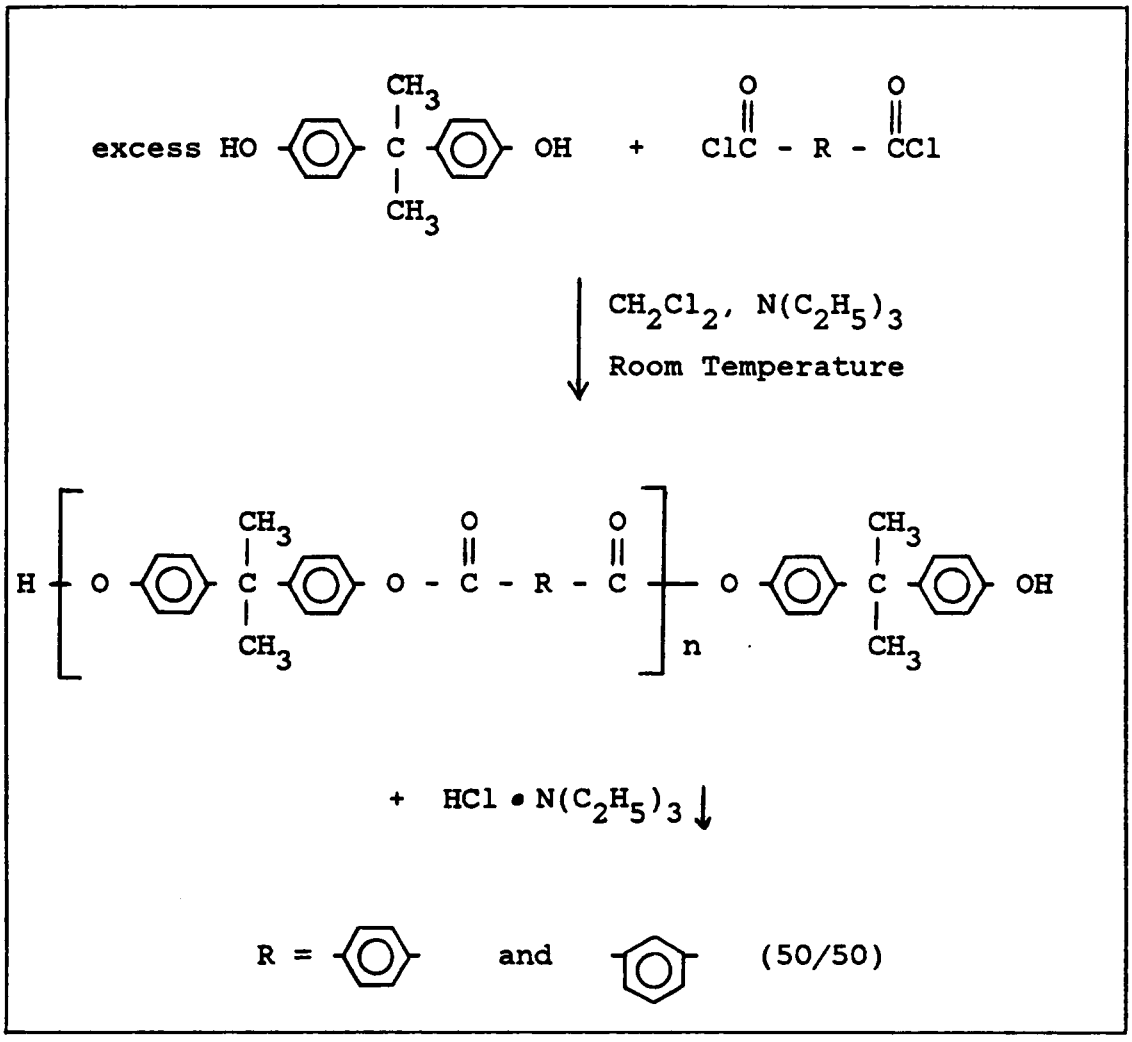

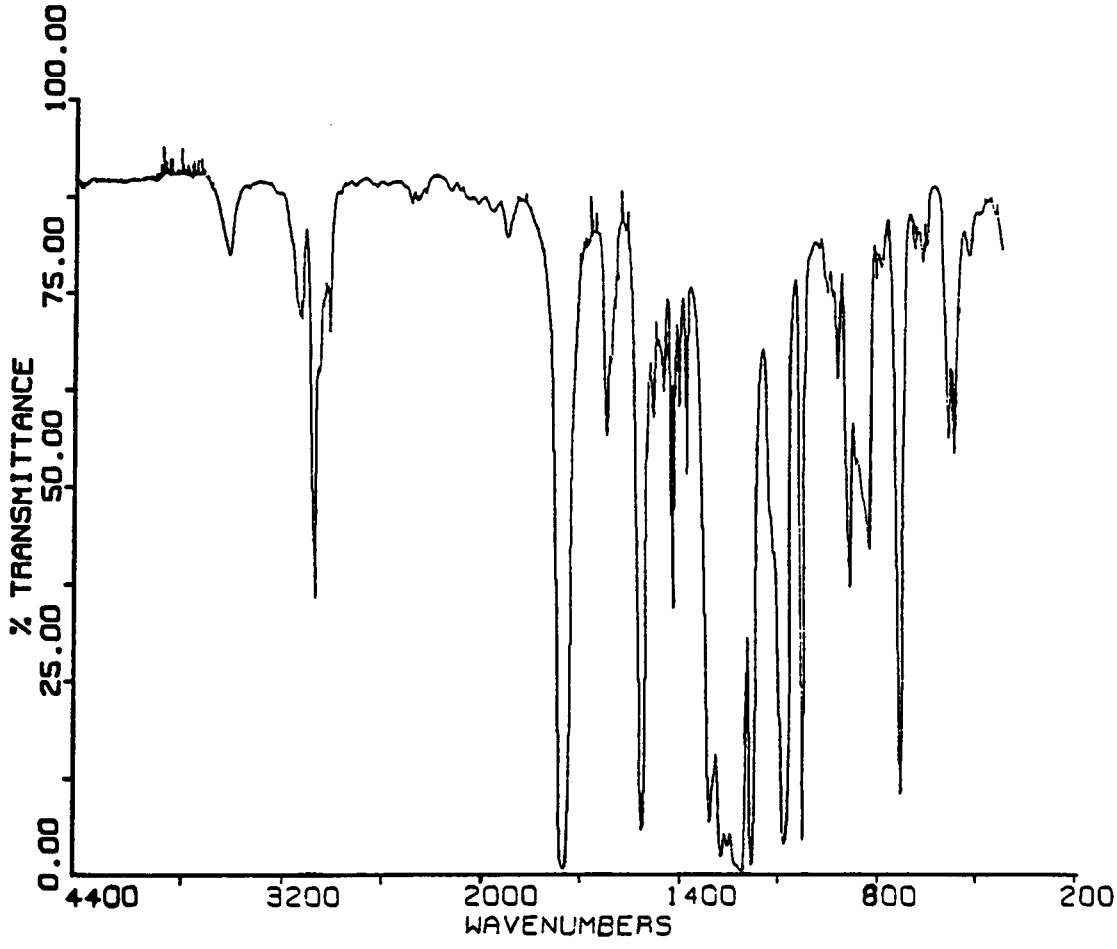

Figure 28: An FTIR spectrum of an hydroxyl-terminated polyarylester oligomer.

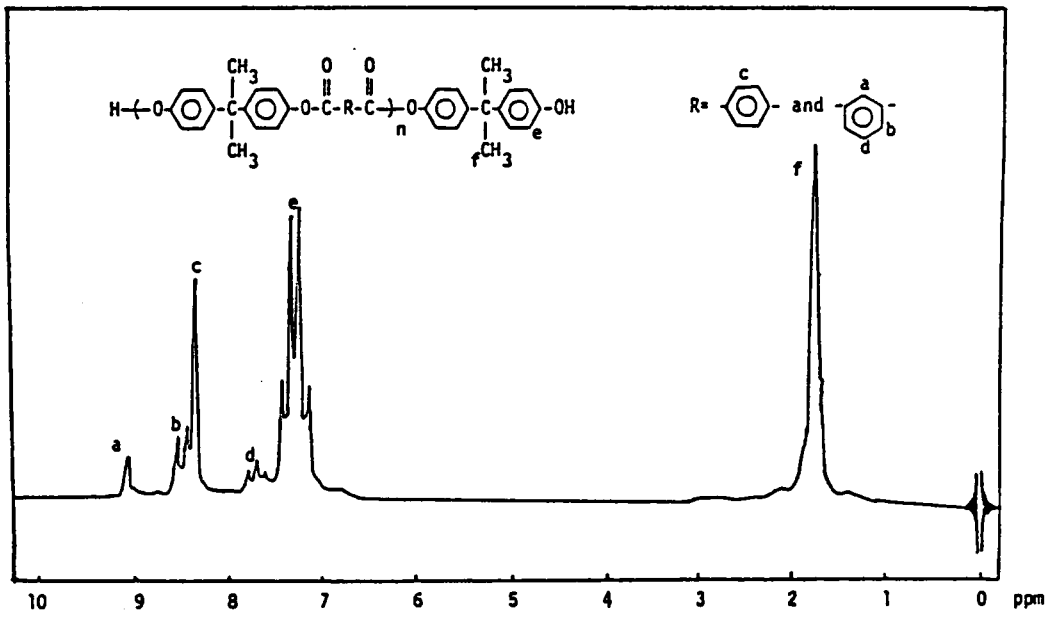

Figure 29: A proton NMR spectrum of an hydroxyl-terminated polyarylester oligomer.

observed FTIR bands and their assignments are listed in Table 15. The strong ester and hydroxyl bands indicate that an hydroxyl-terminated polyarylester was indeed prepared.

The proton NMR peak positions and splitting patterns listed in Table 16 are expected for the polyarylester structure. For low molecular weight oligomers, a small peak at about 4.5 ppm due to the OH endgroups may be observed. However, for high molecular weight samples, no peak due to the few hydroxyl group hydrogens can easily be detected.

4.1.2.2 Characterization

One requirement for preparation of high molecular weight polymers by condensation (or step growth) polymerization is exact stoichiometry. Therefore, the $\bar{M}n$ of each difunctional oligomer must be accurately determined. Endgroup analysis by titration was not accomplished as easily for the hydroxyl functionality as was the previously discussed amine functional siloxane oligomers. One difficulty encountered is that of obtaining a sharp endpoint in these non-aqueous titrations. A major source of the problem is water contaminated solvent which leads to large solvent blanks as well as "swamped out" endpoints. Therefore, it was important to use freshly distilled solvent [131].

TABLE 15

FTIR Band Assignments for Hydroxyl-Terminated Polyarylester Oligomers

Frequency (cm^{-1})	Assignment
3500	O-H stretch
3050	C-H stretch, aromatic
2950	C-H stretch, aliphatic
1750	Ester carbonyl stretch
1600,1500	C-C stretch, aromatic
1400-1200	Ø-O
1270-1170	Strong ester bands
1150	C-O

TABLE 16

Proton NMR Peak Positions and Assignments for Hydroxyl-Terminated Polyarylester Oligomers

Peak (ppm)	Assignment
0.0, singlet	TMS reference and lock
1.7, singlet	Isopropyledene hydrogens derived from bisphenol-A
7.3, AA'BB' multiplet	Aromatic hydrogens derived from bisphenol-A
7.5, triplet	Aromatic hydrogen derived from isophthaloyl cloride
8.2, singlet	Aromatic hydrogens derived from terephthaloyl chloride
8.3, doublet	Aromatic hydrogens derived from isophthaloyl chloride
8.8, singlet	Aromatic hydrogen derived from isophthaloyl chloride

To verify the sometimes questionable $\bar{M}n$ values obtained from endgroup titration, proton NMR was used. The few endgroup hydrogens were not easily detected, therefore, the hydroxyl endgroups were capped with trimethylsilicon groups to enhance the proton NMR endgroup signal. The capping reaction involves the use of hexamethyldisilazane and is illustrated in Scheme 24. The reaction was allowed to run until the hydroxyl band in the FTIR spectrum was no longer observable. The proton NMR of the hydroxyl-terminated polyarylester is compared to that of the capped oligomer in Figure 30. The Mn values calculated from the integration ratio of the trimethylsiloxy group at 0.3 ppm to the bisphenol-A isopropylidene group at 1.6 ppm agreed well with titrated values. For example, hydroxyl-terminated oligomers titrated to 5,100 and 10,000 g/mole had $\bar{M}n$ values from proton NMR of 5,200 and 9,900 g/mole, respectively. Before and after capping, no change in intrinsic viscosity was noted.

Differential scanning calorimetry (DSC) was used to evaluate the thermal properties of the polyarylester oligomers. A typical DSC trace is shown in Figure 31. Due to their highly aromatic character, relatively high glass transitions were observed. The thermal characteristics, along with other properties of the polyarylester oligomers, are listed in Table 17. The low intrinsic viscosity values

Scheme 24

Capping Hydroxyl Terminated Polyarylesters

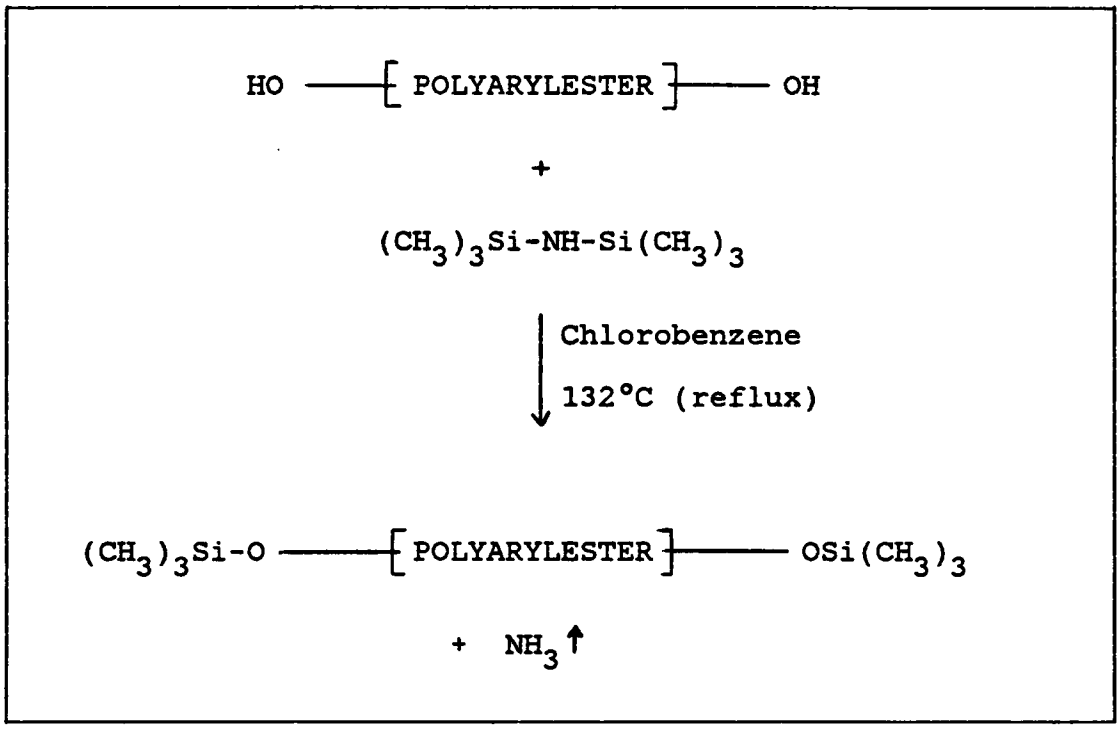

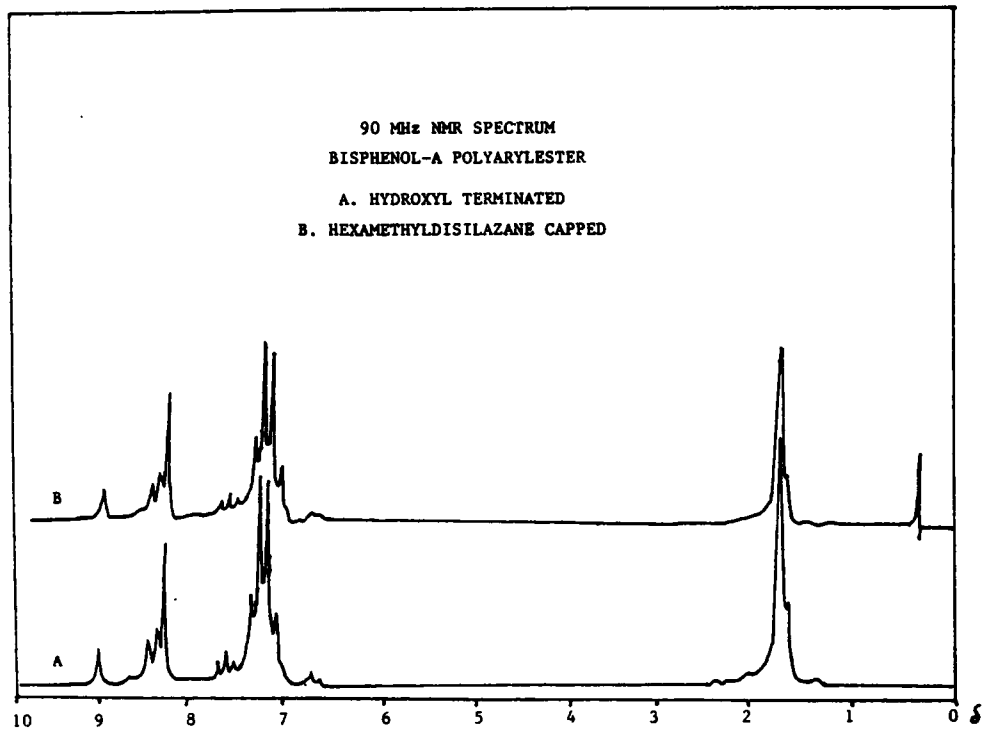

Figure 30: Proton NMR spectra of a polyarylester oligomer before and after capping.

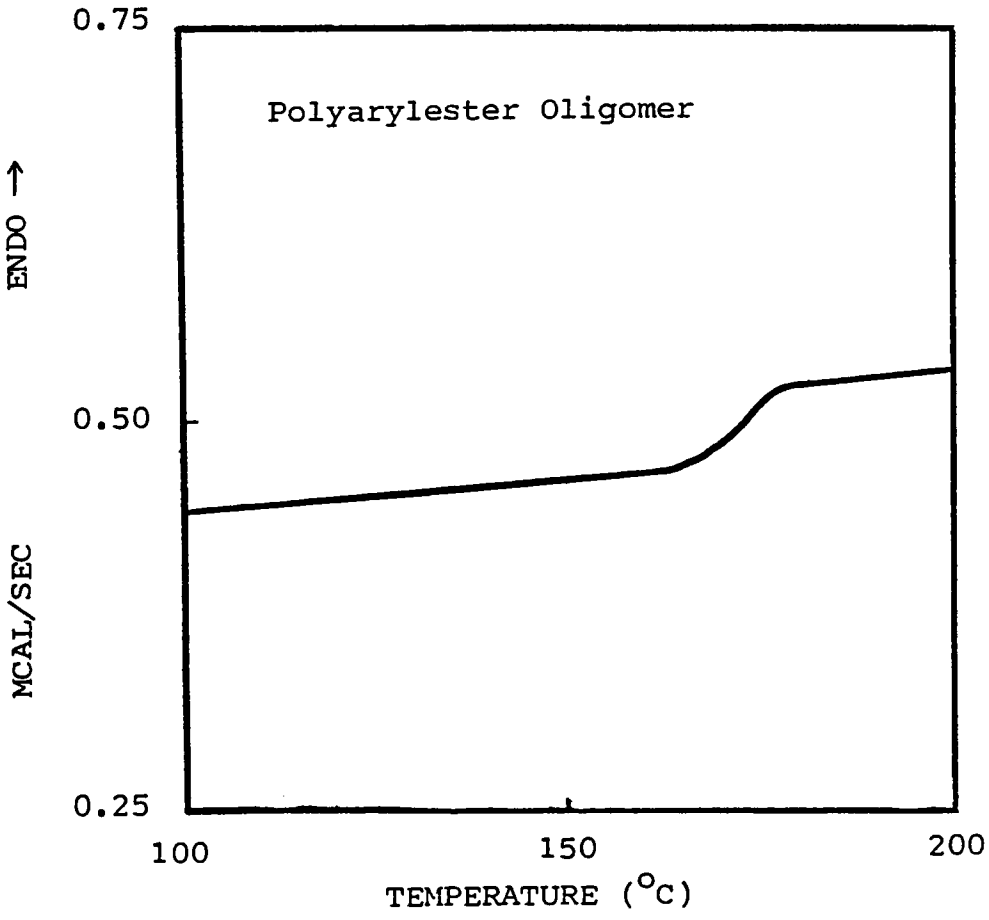

Figure 31: A DSC trace of a 10,000 $\overline{Mn}$ polyarylester oligomer.

TABLE 17

Polyarylester Oligomer Characteristics

Sample Number	$\bar{M}n$ Theory	$\bar{M}n$ Titrated	$[\eta]_{CH_2Cl_2}^{25°C}$	% Yield	DSC Tg(°C)
1	5,000	5,100	0.27	75	171
2	5,000	5,100	0.27	75	171
3	10,000	9,900	0.39	77	174
4	10,000	10,000	0.37	75	178

reflect the low molecular weights of the oligomers. It was difficult to isolate such low molecular weight materials because they are fine powders. Therefore, the relatively low reaction yields are attributed to mechanical losses during work-up.

4.2 SYNTHESIS AND CHARACTERIZATION OF HIGH MOLECULAR WEIGHT BLOCK POLYMERS

4.2.1 Perfectly Alternating Block Co- and Terpolymers

4.2.1.1 Synthesis and Structural Analysis

The well-known reaction of silylamines with hydroxyl compounds proceeds as follows:

$$\equiv Si\text{-}N= + HOR \rightarrow \equiv Si\text{-}OR + H\text{-}N=$$

In the early 1970's, Noshay and coworkers [96,97] employed the reaction of well-characterized hydroxyl-terminated aromatic polyethers (i.e., polysulfone), poly(bisphenol-A terephthalate), poly(bisphenol-A isophthalate), and poly(2,2,4,4-tetramethyl-1,3-cyclobutylene carbonate) with silylamine-terminated polydimethylsiloxanes in chloroaromatic solvents to produce perfectly alternating $(A\text{-}B)_n$ block copolymers. These structures are well-defined and strictly controlled, since the organic and siloxane oligomers can interact with each other but not with themselves. As a

result, the structure of the blocks in the copolymers is identical with that of the oligomers. The reactions were observed to proceed at high rates in those cases where aromatic hydroxyls were the terminal group. The rate of block copolymer formation was considerably slower with the less acidic and more sterically hindered cycloaliphatic hydroxyl functions.

The properties of organosiloxane block copolymers are very interesting due to their two-phase morphological behavior, which is a result of the microincompatibility of the dissimilar blocks. The morphology of these block copolymers is dependent upon molecular weight [132]. The critical block molecular weight ($\bar{M}n$) level is about 2,000 to 5,000. Below this level, single-phase systems are obtained with the properties characteristic of random copolymers. Above this level, two-phase morphological systems are obtained which display properties characteristic of both homopolymers. As expected with two-phase systems, two glass transitions are observable.

To produce siloxane-ester block copolymers potentially suitable for passive damping applications in the space environment, the silylamine-hydroxyl condensation reaction was used. To enhance damping characteristics, yet retain a two-phase morphology, silylamine-terminated siloxane co-oli-

gomers were copolymerized with hydroxyl-terminated polyaryl-ester oligomers. The two co-oligomer compositions used in this work were (1) dimethyl-diphenyl siloxanes and (2) dimethyl-trifluoropropylmethyl siloxanes. The miscibility of the siloxane phase with the organic phase is influenced by siloxane composition and block molecular weight [188,189]. The defined system variables and the systematic series of siloxane-ester block co- and terpolymers studied in this research are listed in Tables 18 and 19, respectively. The generalized reaction scheme for the preparation of the samples listed in Table 19 is illustrated in Scheme 25.

Structure analysis of the siloxane-ester block co- and terpolymers was accomplished by FTIR and proton NMR; typical spectra are shown in Figures 32 and 33, respectively. From FTIR it can be seen that the copolymer spectrum is a combination of the siloxane (Figure 12) and ester (Figure 28) oligomer spectra. As anticipated, the band from the hydroxyl endgroups of the ester oligomer is no longer observable in the copolymer spectrum. The copolymer band assignments are listed in Table 20.

The proton NMR spectra of the copolymers are simply a combination of the component oligomers. The peak assignments and splitting patterns of a typical siloxane-ester

TABLE 18

System Variables

Degree of phase mixing dependent upon:

1. Block molecular weights ($\bar{M}n$)

   5,000 and 10,000 g/mole

2. Block solubility parameter (δ)$(cal/cm^3)^{1/2}$

$Si(CH_3)_2O$	7.5
$Si(\emptyset)_2O$	9.5
$Si(CH_3)(CH_2CH_2CF_3)O$	9.6
Polyarylester[a]	11.0

[a]Calculated from VanKrevelen [175], siloxane δ from literature [7].

TABLE 19

Perfectly Alternating Block Copolymer Compositions

	Siloxane Composition[a]
COPOLYMERS	
Polyarylester	100% CH_3
	75% CH_3 with 25% Ø
	75% CH_3 with 25% F
	50% CH_3 with 50% Ø
	50% CH_3 with 50% F
	25% CH_3 with 75% Ø
	25% CH_3 with 75% F
TERPOLYMERS	
Polyarylester-PDMS[b]	25% CH_3 with 75% Ø
	25% CH_3 with 75% F
	100% F

[a]Composition in weight percent; CH_3 = dimethyl, Ø = diphenyl, and F = trifluoropropylmethyl.

[b]Polydimethylsiloxane.

[c]Ester and siloxane block lengths 5,000 and/or 10,000 $\bar{M}n$.

Scheme 25

Perfectly Alternating Block Polymer Synthesis

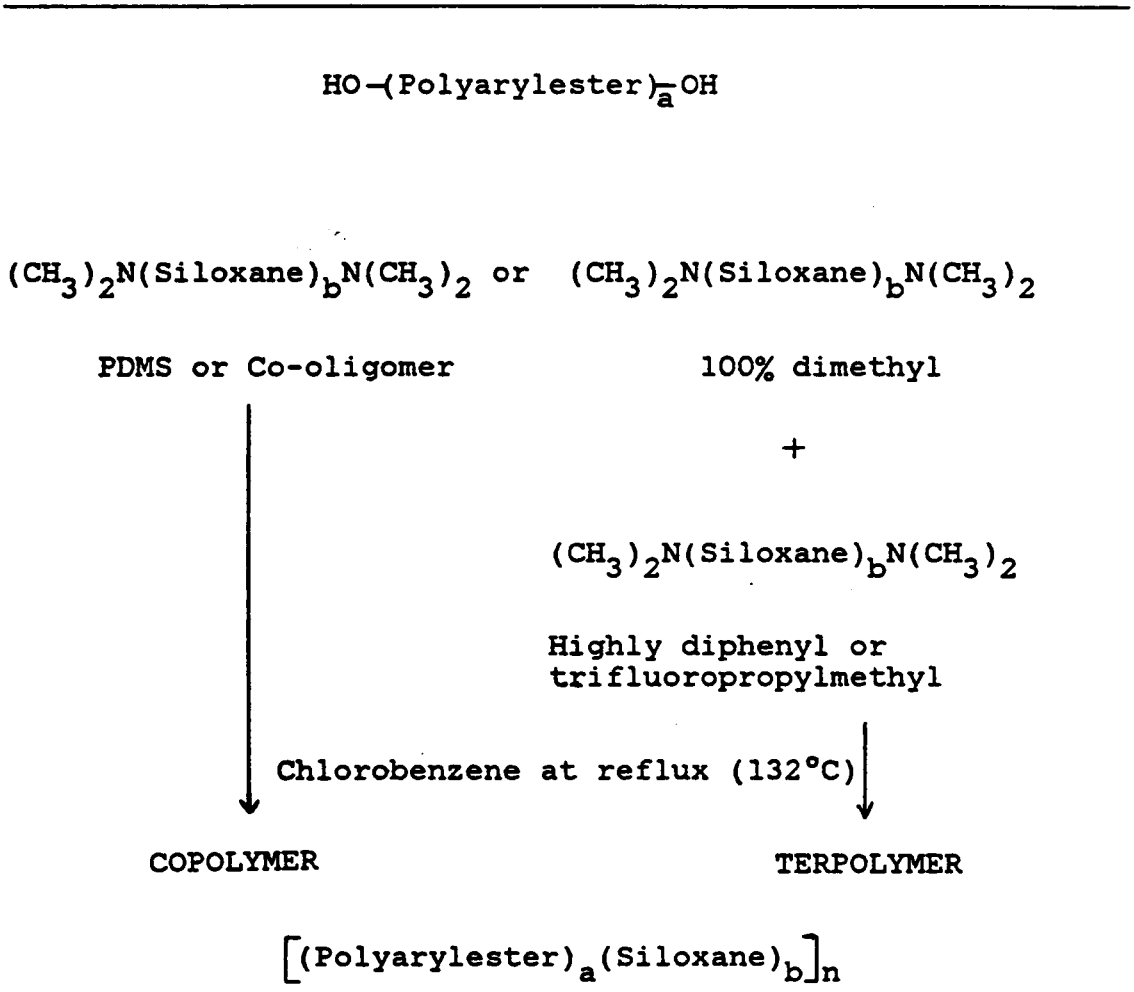

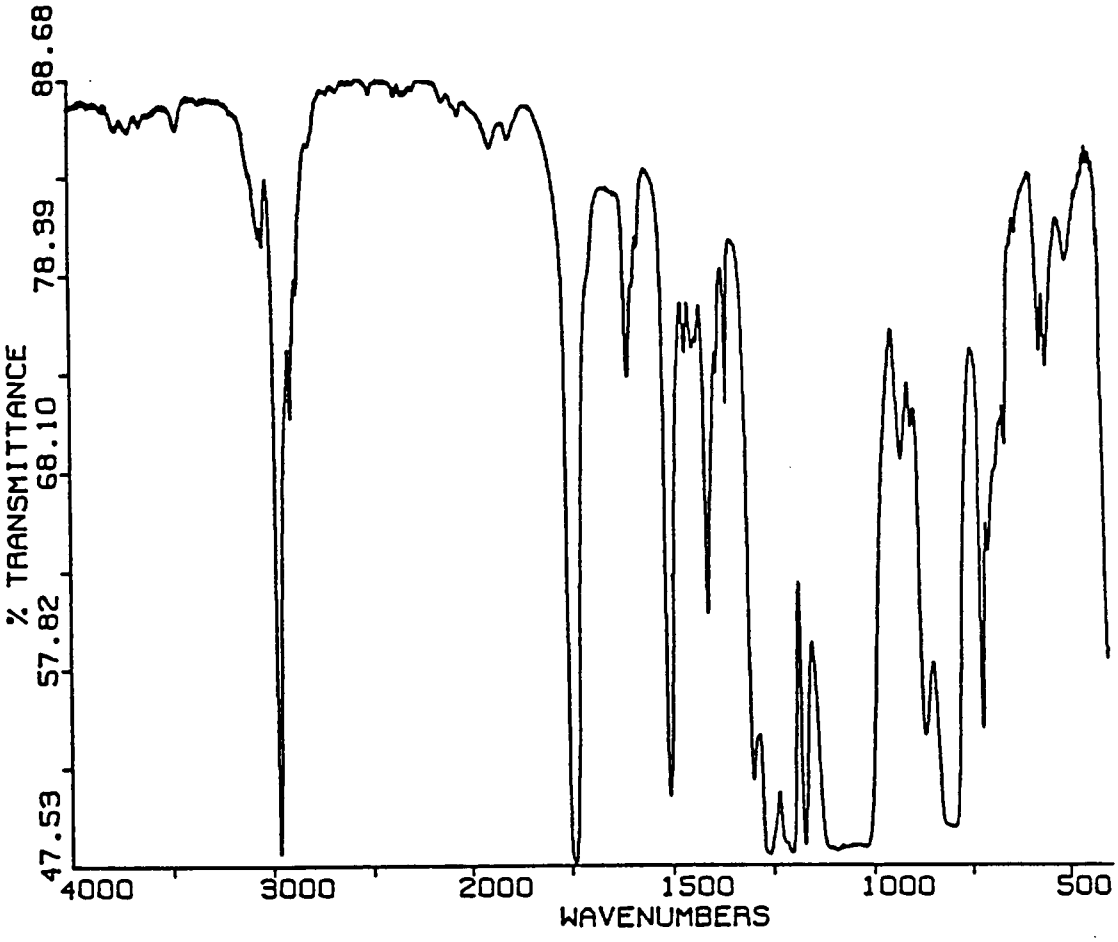

Figure 32: The FTIR spectrum of a perfectly alternating polydimethylsiloxane-ester block copolymer.

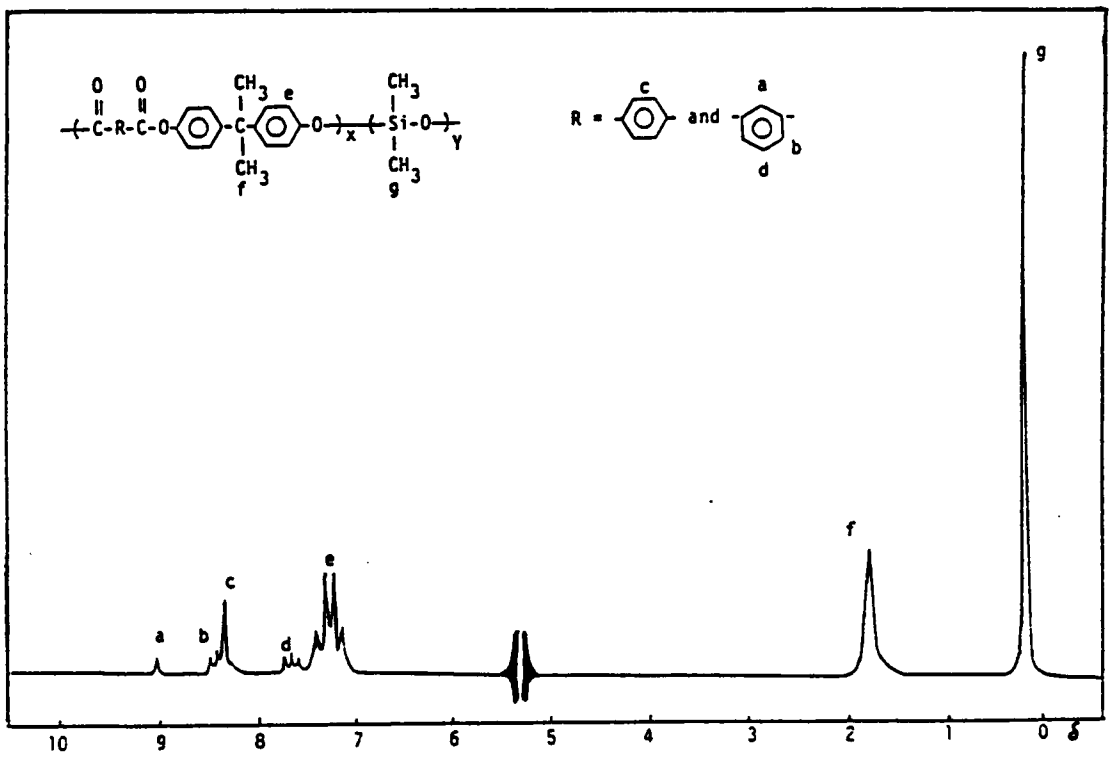

Figure 33: The proton NMR spectrum of a perfectly alternating polydimethylsiloxane-ester block copolymer. Block lengths 5,000 $\bar{M}n$.

TABLE 20

Perfectly Alternating Polydimethylsiloxane-Ester Block Copolymer FTIR Band Assignments

Frequency (cm^{-1})	Assignment
3050	C-H stretch, aromatic
2950	C-H stretch, aliphatic
1750	Ester carbonyl stretch
1600,1500	C-C stretch, aromatic
1410	CH_3 asymmetric deformation
1275	CH_3 symmetric deformation
1270-1170	Strong ester bands
1100-1000	Si-O-Si stretch vibration

copolymer are listed in Table 21. From the integration ratio of the $Si(CH_3)_2O$ peak at 0.3 ppm to the isopropylidene peak of the polyarylester at 1.7 ppm, the percent siloxane incorporated can be calculated. In general, the percent siloxane incorporation was quantitative.

4.2.1.2 Molecular Weight Determination

Analysis of molecular weight utilized intrinsic viscosity measurements, η, and size exclusion chromatography, SEC (or gel permeation chromatography, GPC). Intrinsic viscosities were used to quickly obtain an idea of the co- and terpolymer's relative molecular weights and SEC was used to obtain qualitative information concerning molecular weight distributions.

Viscometry

Viscometry is one of the oldest, and most popular, experiments to quickly determine relative molecular weights of macromolecules. The basis of this experiment is derived from the ability of macromolecules to increase the viscosity of a solvent when they are placed in a dilute solution. The intrinsic viscosities, $[\eta]$, of the co- and terpolymers are relatively high and each sample formed a tough, solvent cast transparent film. Both these factors indicate that the

TABLE 21

Perfectly Alternating Polydimethylsiloxane-Ester Block Copolymer Proton NMR Results

Peak (ppm)	Assignment
0.3, singlet	Dimethylsiloxane hydrogens
1.7, singlet	Isopropyledene hydrogens derived from bisphenol-A
5.3, lock	CH_2Cl_2 reference and lock
7.3, AA'BB' multiplet	Aromatic hydrogens derived from bisphenol-A
7.5, triplet	Aromatic hydrogens derived from isophthaloyl chloride
8.2, singlet	Aromatic hydrogens derived from terephthaloyl chloride
8.3, doublet	Aromatic hydrogens derived from isophthaloyl chloride
8.8, singlet	Aromatic hydrogens derived from isophthaloyl chloride

polymers are of sufficient molecular weight to be useful. The quantitative results from viscosity measurements, along with reaction yields, are presented in Tables 22 through 25.

Size Exclusion Chromatography

SEC was used as a qualitative check on the nature of molecular weight and molecular weight distribution. SEC fractionation occurs from exposure of a pressurized polymer solution to a distribution of micropores in a packed column. The diffusional volume accessible to smaller molecules is greater than that for larger molecules. Consequently, larger molecules elute from the column first. Such behavior was observed in this work; representative SEC curves are shown in Figure 34. The two siloxane-ester block copolymer SEC traces are observed at low elution volumes, indicating higher molecular weights than the polyarylester oligomer observed at a higher elution volume. Both the polyarylester oligomer and the block copolymers display broad, unimodal distributions of molecular weight typical of step-growth or condensation polymers. However, it should be noted that the SEC curves in Figure 34 will not represent molecular weight distributions until the elution volume scale is converted to a molecular weight scale. Unfortunately, a calibration problem arises since suitable standards are largely unavail-

TABLE 22

Intrinsic Viscosities of Dimethylsiloxane-Ester Block Copolymers

Sample Number	$\bar{M}n$ PSX/PE	$[\eta]$ 25°C CH_2Cl_2	% Yield
1	6,000/5,100	2.34	91
2	10,500/5,100	0.73	90
3	6,000/9,900	0.52	97
4	10,500/10,100	0.52	90

TABLE 23

Intrinsic Viscosities of (Dimethyl-Diphenyl)siloxane-Ester Block Copolymers

Sample Number	PSX Comp.[a]	$\bar{M}n$ PSX/PE Segments	25°C $[\eta]_{CH_2Cl_2}$	% Yield
1	25 Ø	6,300/4,800	0.34	86
2	25 Ø	15,000/4,800	0.45	84
3	25 Ø	6,300/10,100	0.57	87
4	25 Ø	15,000/10,900	0.51	84
5	50 Ø	5,400/5,000	0.51	86
6	50 Ø	11,800/5,000	0.68	82
7	50 Ø	5,400/10,000	0.47	84
8	50 Ø	11,800/10,000	0.43	88
9	75 Ø	5,000/5,000	0.39	80
10	75 Ø	11,500/5,000	0.28	60
11	75 Ø	5,000/10,000	0.20	80
12	75 Ø	11,500/10,000	0.32	75

[a]Siloxane composition in weight percent; Ø = diphenyl siloxane, remaining percentages are dimethyl siloxane units.

TABLE 24

Intrinsic Viscosities of (Dimethyl-Trifluoropropylmethyl) siloxane-Ester Block Copolymers

Sample Number	PSX Comp.[a]	$\bar{M}n$ PSX/PE Segments	25°C $[\eta]_{CH_2Cl_2}$	% Yield
1	25 F	7,800/4,800	0.32	62
2	25 F	14,200/4,800	0.41	85
3	25 F	7,800/10,100	0.34	86
4	25 F	14,200/10,100	0.56	88
5	50 F	5,700/5,100	0.71	81
6	50 F	11,500/5,100	0.62	83
7	50 F	5,700/10,900	0.40	82
8	50 F	11,500/10,900	0.43	73
9	75 F	6,000/5,000	0.30	71
10	75 F	13,000/5,000	0.38	76
11	75 F	6,000/10,000	0.26	86
12	75 F	13,000/10,000	0.58	92

[a]Siloxane composition in weight percent; F = trifluoropropylmethyl siloxane, remaining percentages are dimethyl siloxane units.

TABLE 25

Intrinsic Viscosities of Siloxane-Ester Block Terpolymers

Sample Number	PSX Comp.[a]	$\bar{M}n$ PSX/PDMS[b]/PE	25°C $[\eta]_{CH_2Cl_2}$	% Yield
1	75 Ø	5,000/5,000/5,000	0.41	76
2	75 Ø	10,000/10,000/5,000	0.37	73
3	75 Ø	5,000/5,000/10,000	0.24	78
4	75 Ø	10,000/10,000/10,000	0.28	79
5	75 F	6,000/5,000/5,000	0.30	82
6	75 F	13,800/11,400/5,000	0.36	85
7	75 F	6,000/5,000/10,000	0.44	83
8	75 F	13,800/11,400/10,000	0.36	83
9	100 F	5,000/5,000/5,000	0.25	74
10	100 F	13,000/10,000/5,000	0.29	73
11	100 F	5,000/5,000/10,000	0.20	80
12	100 F	13,000/10,000/10,000	0.41	75

[a]Siloxane composition in weight percent; Ø = diphenyl siloxane, F = trifluoropropylmethyl siloxane, and remaining percentages are dimethyl siloxane units.

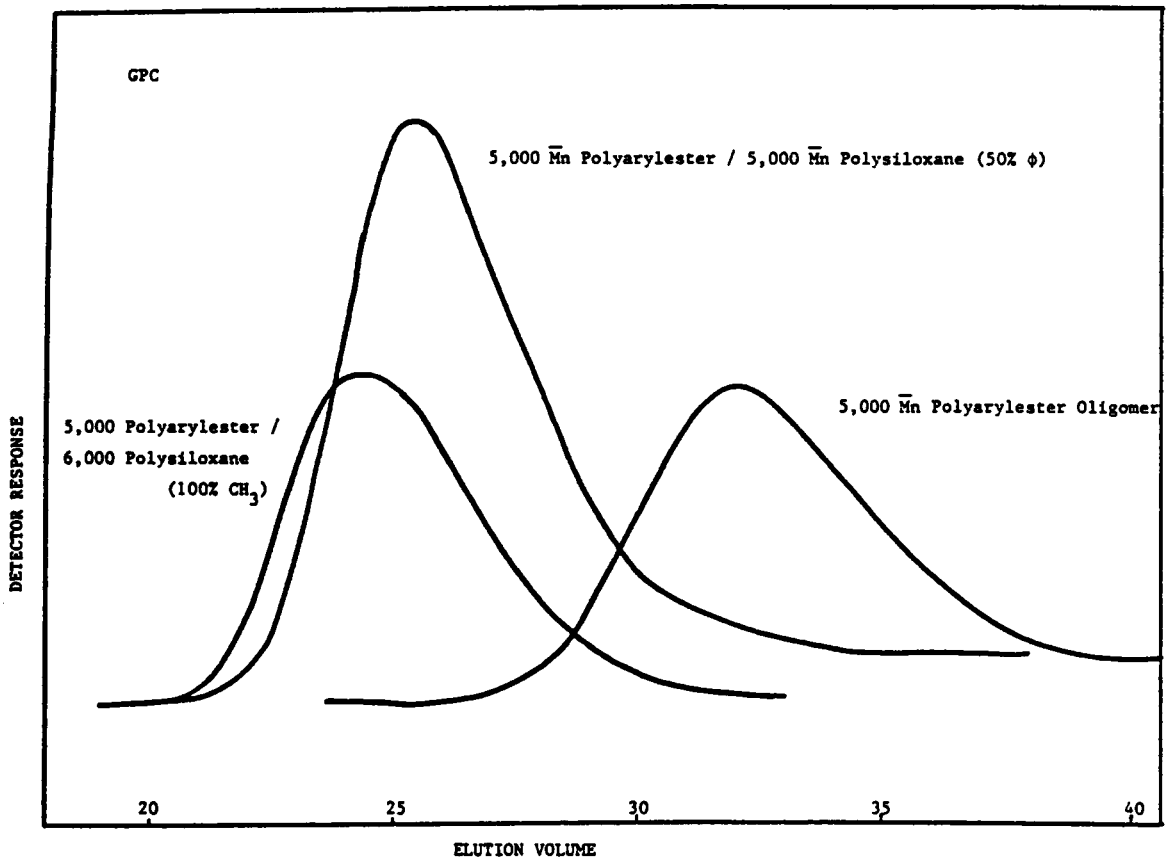

Figure 34: SEC curves of a polyarylester oligomer and two siloxane-ester block copolymers.

able for new polymers, copolymers, or branched polymers [176].

4.2.1.3 Thermal Analysis

Thermal properties are important in determining polymer performance and applications. Several techniques are available to measure thermal properties; the four utilized in this work include: (1) differential scanning calorimetry (DSC), (2) thermomechanical analysis (TMA), (3) thermogravimetric analysis (TGA), and (4) dynamic mechanical thermal analysis (DMTA). A discussion of DMTA will be included in a subsequent section concerned with mechanical properties.

Differential Scanning Calorimetry

DSC is a thermal analysis technique that measures the quantity of energy absorbed or evolved by a sample, in calories, as its temperature is changed. This is accomplished by heating a sample and an inert reference and measuring the difference in energy required to heat the two at a programmed rate. At a transition point (glass transition (Tg), crystallization, (Tc) or melting (Tm)), the sample requires either more or less energy than the reference, depending on whether the change is endothermic or exothermic.

The siloxane-ester block co- and terpolymer DSC results are presented in Tables 26 through 29. Microphase separation of the component blocks is indicated by the fact that two Tg values are observed for each sample. The low temperature transitions are attributed to the "soft" siloxane phases and in most cases they agree with the Tg values of the siloxane oligomers, suggesting a low or negligible degree of mixing of the ester phase into the siloxane phase. It is interesting to note that in addition to a glass transition, crystallization and melting transitions are displayed by copolymers containing a siloxane phase composed of dimethyl siloxane units only. This type of thermal behavior is expected since long dimethyl siloxane sequences are symmetrical and, therefore, crystallizable. This observation was also noted for the previously discussed functional polydimethylsiloxane oligomers. No crystallization or melting transitions were displayed by siloxane phases containing dimethyl units and trifluoropropylmethyl units or moderate amounts of diphenyl units which disrupt the symmetry of dimethyl siloxane sequences. For comparative purposes, experimental DSC traces for the low temperature transition of three different siloxane-ester block copolymers are shown in Figure 35 and 36.

TABLE 26

Thermal Properties of Dimethylsiloxane-Ester Block Copolymers

Sample Number	Siloxane Block $\bar{M}n$	Siloxane Block Tg(°C)[a]	Ester Block $\bar{M}n$	Ester Block Tg(°C)	Copolymer[b] Tg(°C)
1	6,000	-123	5,100	171	-123, 135
2	10,500	-123	5,100	171	-126, 158
3	6,000	-123	9,900	174	-123, 168
4	10,500	-123	10,500	175	-125, 173

[a]Dimethyl siloxanes also display Tc and Tm at -96 and -62°C, respectively.

[b]Copolymers containing dimethylsiloxane segments display Tc and Tm at -85 and -45°C, respectively.

TABLE 27

Thermal Properties of (Dimethyl-Diphenyl)siloxane-Ester Block Copolymers

Sample	Siloxane Block			Ester Block		Copolymer
Number	Comp.[a]	$\bar{M}n$	Tg(°C)	$\bar{M}n$	Tg(°C)	Tg(°C)
1	25 Ø	6,300	-102	4,800	144	-98, 141
2	25 Ø	15,000	-104	4,800	144	-102, b
3	25 Ø	6,300	-102	10,100	178	-105, 178
4	25 Ø	15,000	-104	10,860	180	-105, 176
5	50 Ø	5,400	-74	5,000	171	-61, 156
6	50 Ø	11,800	-71	5,000	171	-64, 156
7	50 Ø	5,400	-74	10,000	174	-72, 175
8	50 Ø	11,800	-71	10,000	174	-69, 176
9	75 Ø	5,000	--	5,000	155	--, 147
10	75 Ø	11,500	--	5,000	155	--, 148
11	75 Ø	5,000	--	10,000	157	--, 142
12	75 Ø	11,500	--	10,000	170	--, 164

[a]Siloxane composition in weight percent; Ø = diphenyl siloxane, remaining percentages are dimethyl siloxane units.

[b]Transition too weak to be detected by DSC.

Note: -- indicates sample not run.

TABLE 28

Thermal Properties of
(Dimethyl-Trifluoropropylmethyl)siloxane Block Copolymers

Sample Number	Siloxane Block Comp.[a]	$\bar{M}n$	Tg(°C)	Ester Block $\bar{M}n$	Tg(°C)	Copolymer Tg(°C)
1	25 F	7,800	-109	4,800	144	-108, 120
2	25 F	14,200	-116	4,800	144	-115, 157
3	25 F	7,800	-109	10,100	178	-107, 123
4	25 F	14,200	-116	10,100	178	-119, 177
5	50 F	5,700	-105	5,100	171	-102, 138
6	50 F	11,500	-101	5,100	171	- 96, 144
7	50 F	5,700	-105	10,900	180	-104, 174
8	50 F	11,500	-101	10,900	180	- 95, 175
9	75 F	6,000	-93	5,000	155	--, 148
10	75 F	13,000	-91	5,000	155	--, 156
11	75 F	6,000	-93	10,000	170	--, 177
12	75 F	13,000	-91	10,000	170	--, 174

[a]Siloxane composition in weight percent; F = trifluoropropoylmethyl siloxane, remaining percentages are dimethyl siloxane units.

Note: -- indicates sample not run.

TABLE 29

Thermal Properties of Siloxane-Ester Block Terpolymers

Sample Number	Siloxane Block Comp.[a]	$\bar{M}n$	Tg(°C)	PDMS[b] Block $\bar{M}n$	PDMS[b] Block Tg(°C)	Ester Block $\bar{M}n$	Ester Block Tg(°C)
1	75 Ø	5,000	--	5,000	-124	5,000	171
2	75 Ø	10,000	--	10,000	-123	5,000	171
3	75 Ø	5,000	--	5,000	-124	10,000	174
4	75 Ø	10,000	--	10,000	-123	10,000	174
5	75 F	6,000	-93	5,000	-124	5,000	171
6	75 F	13,800	-91	11,400	-123	5,000	171
7	75 F	6,000	-93	5,000	-124	10,000	174
8	75 F	13,800	-91	11,400	-123	10,000	174
9	100 F	5,000	--	5,000	-124	5,000	171
10	100 F	13,000	--	10,000	-123	5,000	171
11	100 F	5,000	--	5,000	-124	10,000	174
12	100 F	13,000	--	10,000	-123	10,000	174

[a]Siloxane composition in weight percent; Ø = diphenyl siloxane, F = trifluoropropylmethyl siloxane, remaining percentages are dimethyl siloxane units.

[b]Polydimethylsiloxane.

Note: -- indicates sample not run.

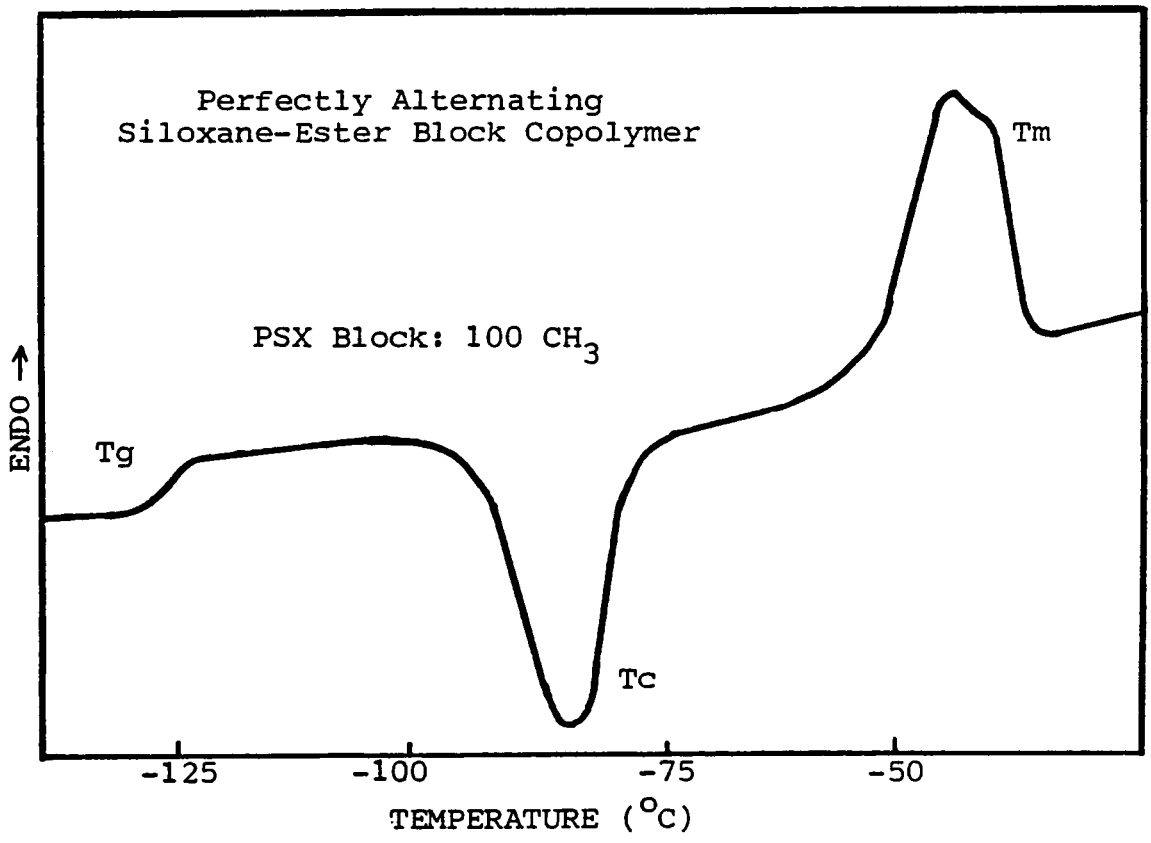

Figure 35: Experimental low temperature DSC curve of a siloxane-ester block copolymer.

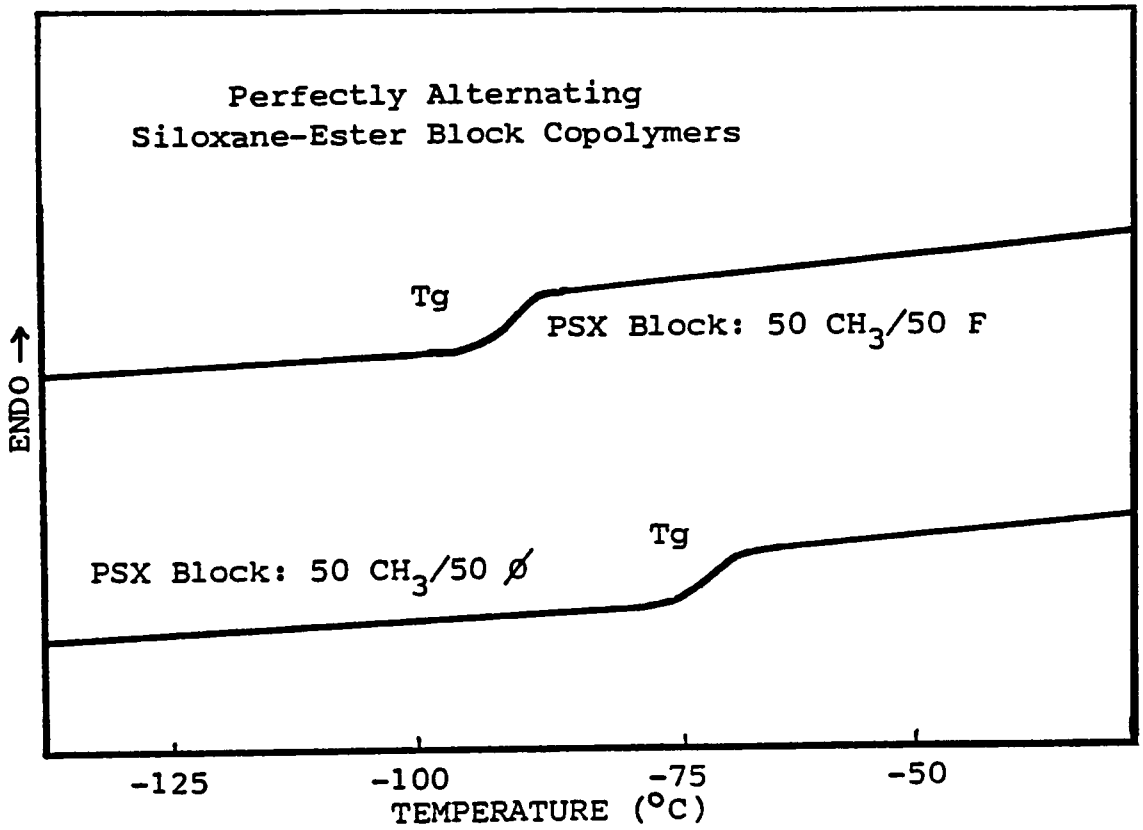

Figure 36: Experimental low temperature DSC cuves of siloxane-ester block copolymers.

The high temperature transition of each block co- and terpolymer is attributed to the "hard" polyarylester phase. From the data presented in Tables 26 through 29, it is readily apparent that the block polymer high temperature transitions are generally lower than those of the polyarylester homopolymers. It is probable that there is some degree of mixing of the siloxane phase into the ester phase. This would plasticize the ester phase, thereby lowering its glass transition temperature. However, this would not necessarily be accompanied by an increase of the siloxane phase glass transition temperature if the only mixing taking place was of the siloxane into the ester phase.

The degree of phase mixing appears to be dependent upon block molecular weight and siloxane composition, as one would expect. As previously mentioned, block copolymers consisting of low molecular weight blocks (≤5,000 $\bar{M}n$) have a tendency to undergo phase mixing more readily than block copolymers containing higher molecular weight blocks. In contrast to 5,000 $\bar{M}n$ ester segments, the Tg values of the 10,000 $\bar{M}n$ ester blocks were not observed to change significantly after copolymerization. Thus, block copolymers with 10,000 $\bar{M}n$ segments do not phase mix as readily as block copolymers with 5,000 $\bar{M}n$ segments.

Phase mixing was also influenced by siloxane composition. As the dimethyl content of a siloxane oligomer is decreased by incorporation of diphenyl or trifluoropropylmethyl siloxane units, the ability of the siloxane phase to mix with the organic phase is increased. Phase mixing is observed by an increase in the low temperature transition of the block copolymer relative to the siloxane co-oligomer Tg prior to copolymerization. No such change in Tg was noted for a dimethylsiloxane oligomer copolymerized with a polyarylester oligomer.

Thermomechanical Analysis

TMA, in the penetration mode, was used to study the modulus of the block copolymers as a function of temperature. It should be noted that TMA is not an absolute analytical technique, but it is useful for comparative purposes. Figure 37 illustrates typical TMA curves for two siloxane co-oligomers and two perfectly alternating siloxane-ester block copolymers. Unfortunately, the polyarylester oligomers used to synthesize the block copolymers were of too low a molecular weight to prepare films suitable for TMA.

As in the DSC studies, each block copolymer displayed two transitions, one for each component of the microphase

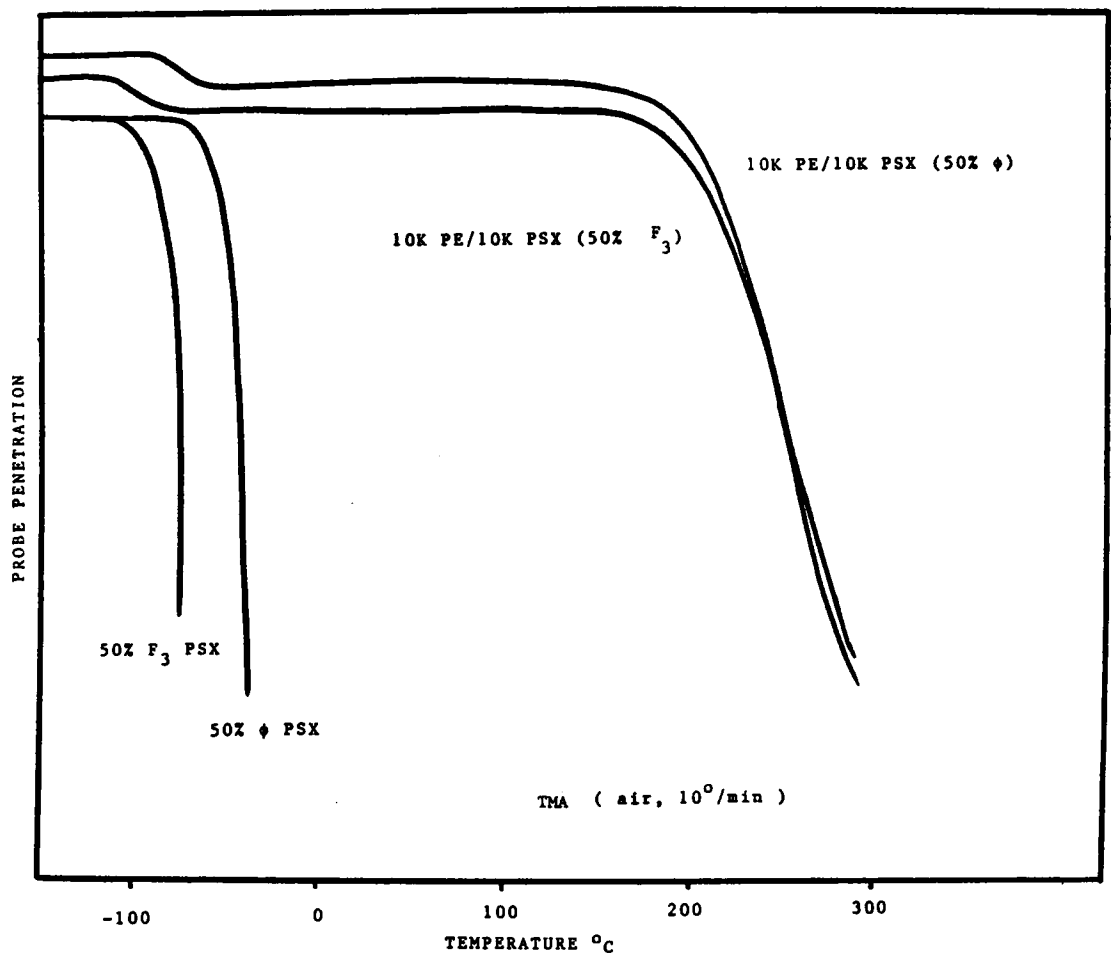

Figure 37: TMA curves for siloxane-ester block copolymers and corresponding oligomers.

separated block copolymer system. Above the low temperature transition of the siloxane phase, material integrity is maintained (broad plateau) until the high temperature transition of the ester phase is surpassed.

Thermogravimetric Analysis

TGA involves the continuous monitoring of sample weight as temperature is increased at a constant rate. Components of a polymer volatilize or decompose at various temperatures and are quantitatively measured in terms of percent weight loss. Typical TGA curves are shown in Figure 38.

4.2.1.4 Mechanical Properties

Stress-Strain Behavior

Along with thermal properties, mechanical properties are among the most important properties in determining end-use applications of polymeric materials. In this work, stress-strain behavior and dynamic mechanical thermal analysis (DMTA) were utilized to evaluate the mechanical properties of the siloxane modified polyarylester block copolymers.

Tensile property determinations were made using an Instron table model tensile tester. Dogbone shaped samples were cut from solution cast or compression molded polymer films using a die. Each sample was subjected to tensile

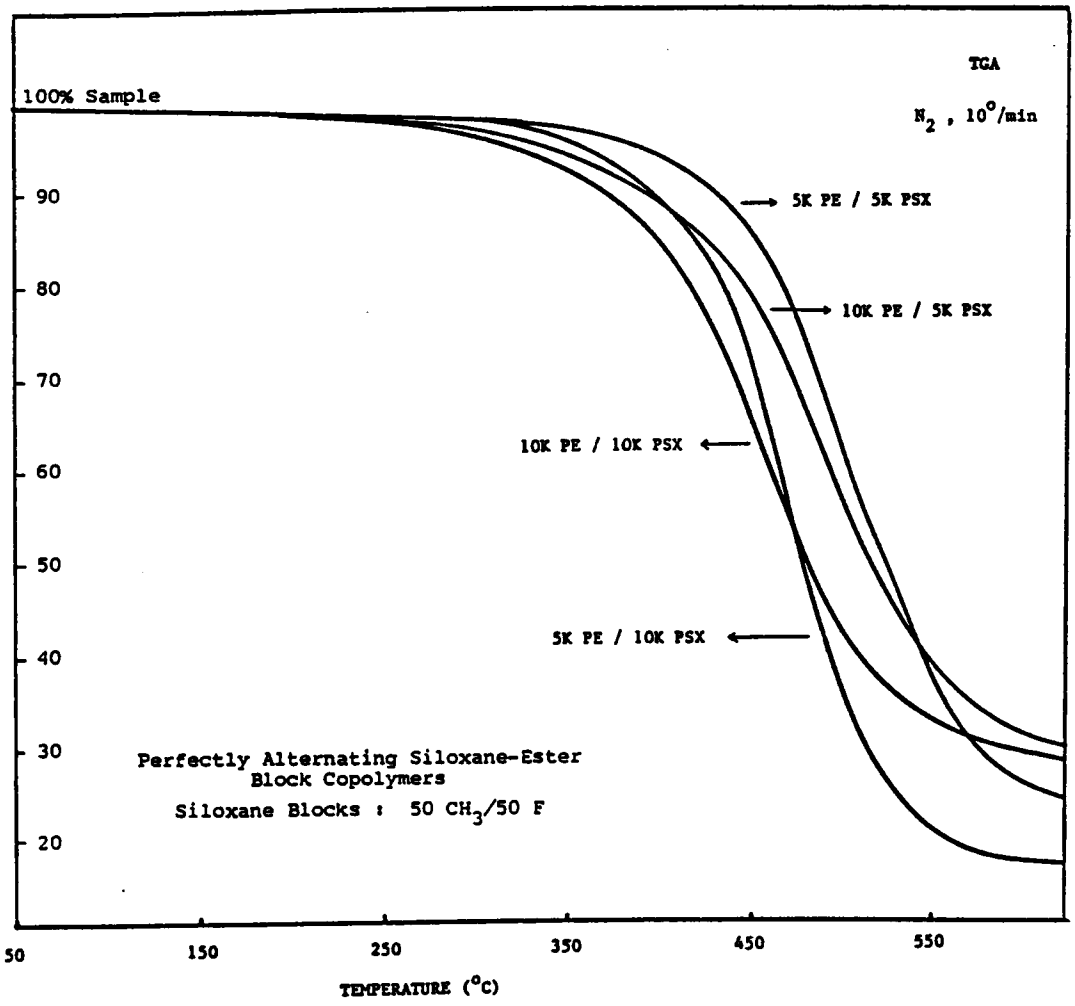

Figure 38: TGA curves of siloxane-ester block copolymers.

forces at the rate of 10 mm/minute under ambient conditions. Modulus, tensile stress, and percent elongation at break were determined from the load extension plot.

The stress-strain diagram illustrated in Figure 39 [177] is typical of that obtained in tension for a constant rate of loading. The initial portion of the stress-strain curve between points A and C is linear and it follows Hooke's Law which states that for an elastic material the stress is proportional to the strain. From the initial, linear portion of this curve the modulus (measure of material stiffness) may be determined from the ratio of stress to corresponding strain. The behavior of the plastic material in the linear region is essentially elastic in nature and, therefore, the deformations are recoverable. However, extensions that occur beyond the yield point or the elastic limit of the material are not recoverable. These deformations occur due to the actual displacement of the molecules with respect to each other and permanent set occurs.

Typical experimental stress-strain data and curves are illustrated in Table 30 and Figures 40 and 41. The results are dependent upon block molecular weights and siloxane composition. In general, samples with high siloxane content show superior elongations at break, but low modulus values.

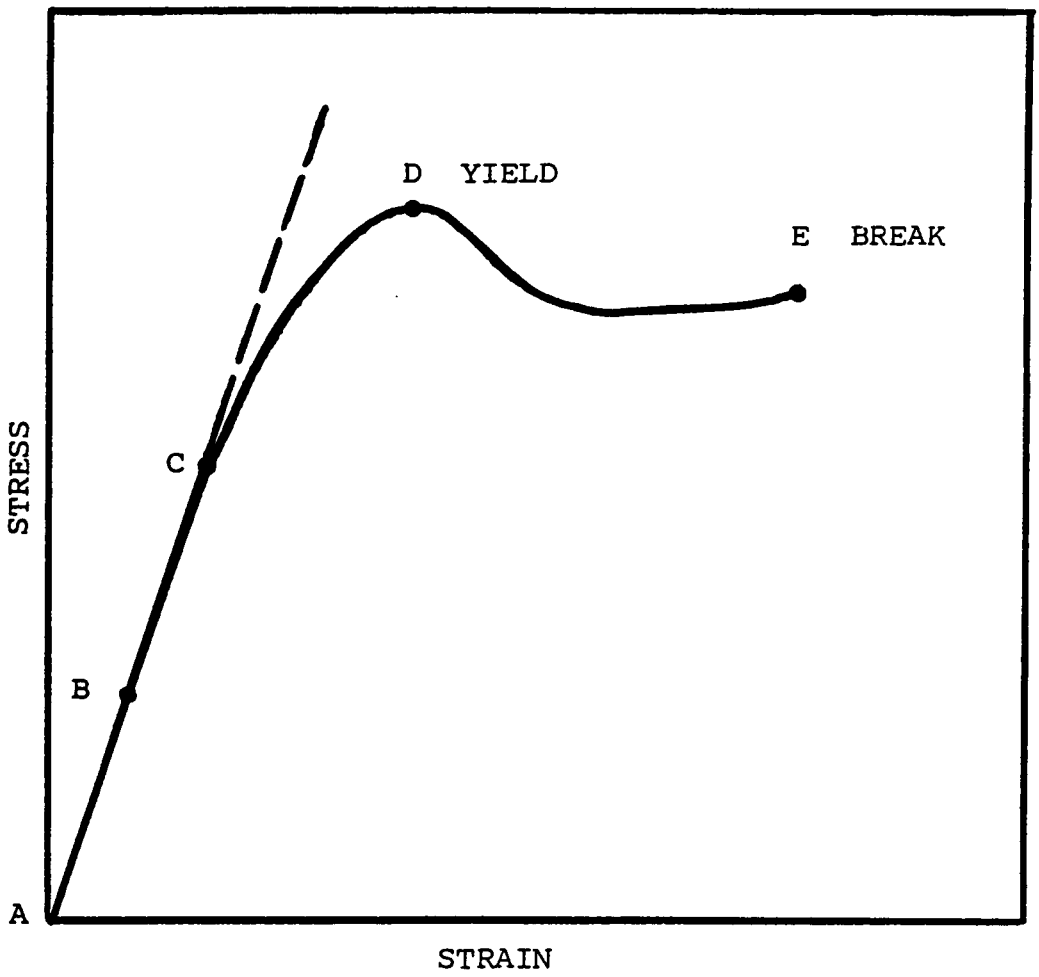

Figure 39: A typical stress-strain curve [177].

TABLE 30

Mechanical Properties of Films Cast from CH_2Cl_2 Solutions of Siloxane-Ester Block Copolymers

Sample Composition	Modulus psi	Modulus MPa	Tensile Stress psi	Tensile Stress MPa	% Elongation at Break
1. 5K PE/5K PSX(CH_3)	12,500	86	2,300	16	146
2. 5K PE/10K PSX(CH_3)	1,400	9	1,400	10	202
3. 10K PE/5K PSX(CH_3)	29,000	200	4,400	31	34
4. 10K PE/10K PSX(CH_3)	9,700	67	1,500	10	47
5. 10K PE/5K PSX(25Ø)	51,000	354	6,100	42	58
6. 10K PE/5K PSX(50Ø)	68,000	470	4,400	31	58
7. 10K PE/5K PSX(25F)	32,000	218	1,300	9	16
8. 10K PE/5K PSX(50F)	39,000	270	3,900	27	30

[a]Tested as 8-10 mm films at 10 mm/minute.

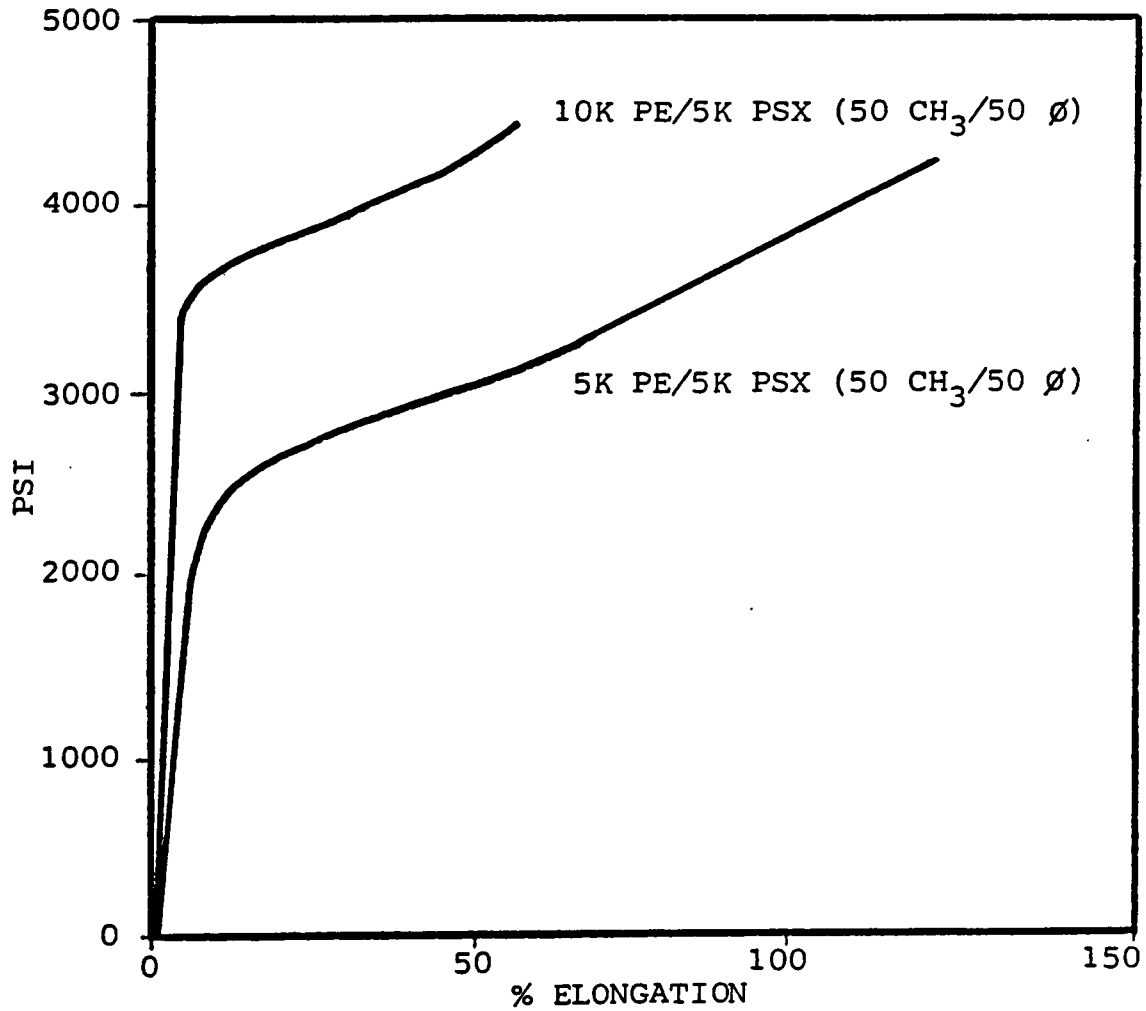

Figure 40: The effect of block molecular weight on tensile properties of siloxane-ester block copolymers.

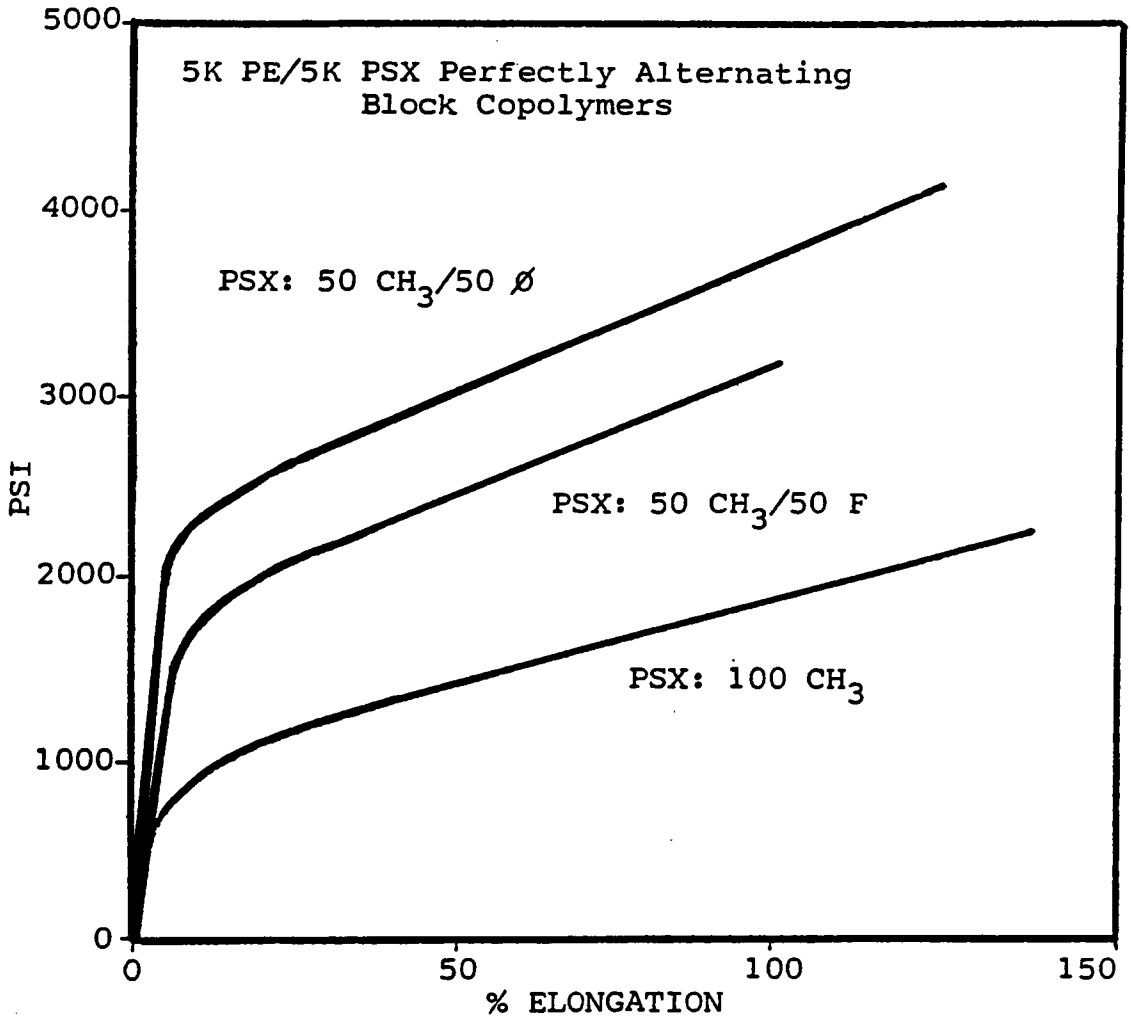

Figure 41: The effect of siloxane composition on tensile properties of siloxane-ester block copolymers.

However, samples with a high concentration of aromatic ester display low elongations at break and high modulus values. For example, when comparing samples 2 and 3 in Table 30, it is evident that the high soft segment content of sample 2 is responsible for the low modulus and the high elongation at break. On the other hand, sample 3 contains a high hard segment content and consequently displays a higher modulus and a lower percent elongation at break relative to sample 2. The effect of ester block length in diphenylsiloxane-ester block copolymers is illustrated in Figure 40.

The effect of siloxane block composition is illustrated in Table 30 and Figure 41. The flexible nature of dimethylsiloxane units provides a soft segment with a low glass transition temperature of -123°C. Therefore, block copolymers containing such siloxane units display a low modulus, low tensile stress, and high elongation when compared to block copolymers containing the more rigid diphenyl and trifluoropropylmethyl siloxane units. The presence of aromatic units in the soft segment of a block copolymer influences the mechanical properties by providing strength which is displayed as high modulus, high tensile stress, and high elongations. On the other hand, trifluoropropylmethyl siloxane units provide an intermediate modulus, tensile stress, and elongation when compared to block copolymers containing dimethyl or diphenyl siloxane units.

Dynamic Mechanical Thermal Analysis

DMTA was used to study the modulus-temperature behavior and the damping characteristics of the siloxane-ester block co- and terpolymers. The following parameters may be determined from DMTA studies: storage modulus (E'), loss modulus (E''), and loss tangent (tan δ = E''/E'). The subsequent discussion briefly defines these parameters.

When the stress is decomposed into its two components, the ratio of the in-phase stress to the strain amplitude is called the storage modulus. This parameter is associated with the periodic storage and complete release of energy in the sinusoidal deformation process of the dynamic experiment. The ratio of the out-of-phase stress to the strain amplitude is the loss modulus and reflects the nonrecoverable use of applied mechanical energy to cause flow in the specimen. Tan δ measures the ratio of the work dissipated as heat to the maximum energy stored in the specimen during one cycle of a periodic deformation. The conversion of applied work to thermal energy in the sample is called damping; it occurs because of flow of macromolecular segments past each other in the sample. Consequently, damping is at a maximum at Tg [178,179]. DMTA was, therefore, a useful technique in determining if the siloxane-ester block polymers would be potentially useful as passive damping materials.

To serve as a control for the following discussion of block polymer DMTA, the log E' and tan δ versus temperature curves for Ardel, a commercial bisphenol-A polyarylester, are shown in Figure 42. DMTA shows one major transition at 200°C, the glass transition temperature. A broad secondary peak centered at -70°C is also observed. Secondary transitions arise from the motions of side groups or segments of the main chain that are smaller than those involved in the displacements associated with glass transitions. It should be noted that the glass transition is relatively sharp, spanning a narrow temperature range. The tan δ values at temperatures other than Tg are very close to zero, indicating negligible damping.

Representative block polymer DMTA curves are shown in Figures 43-48. Microphase separation was indicated by the fact that two glass transitions were observed for each block copolymer. In some cases, three glass transitions were observed for the block terpolymers. In general, the transitions cover a broader temperature range than that observed in Figure 42 for the polyarylester homopolymer. Also, the damping (tan δ) of the block polymers remains relatively high at temperatures intermediate to the low siloxane transition and the high ester transition. Broader transitions and higher damping suggests phase mixing.

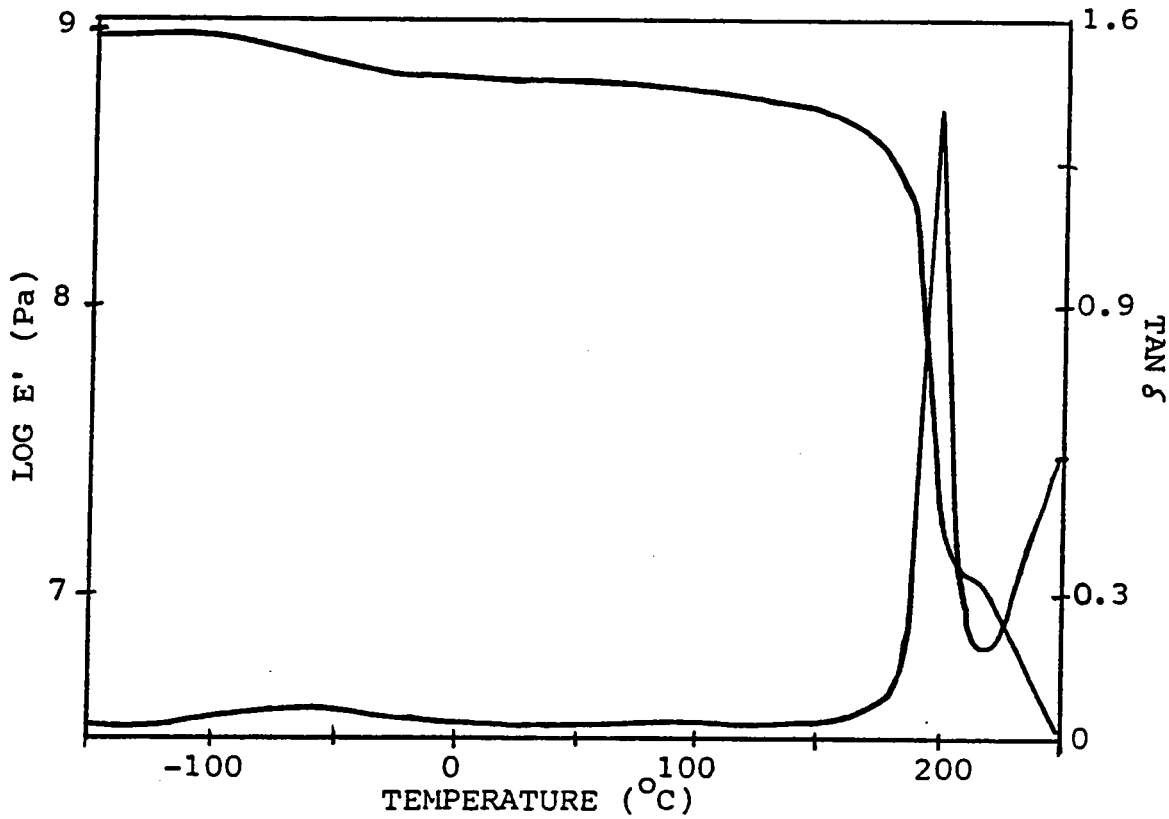

Figure 42: DMTA of Ardel at 1 Hz and 5°C/minute.

Figure 43 illustrates the log E' and tan δ versus temperature curves for a perfectly alternating polydimethylsiloxane-ester block copolymer. As expected, two transitions are observable; one for each component of the copolymer. Both transitions are broad relative to Ardel. The broad secondary transition of the ester phase is noted at -55°C. At temperatures intermediate to the transition temperatures, the tan δ values are higher than those observed in Figure 42 for Ardel.

Figures 44 and 45 illustrate the DMTA results for perfectly alternating siloxane-ester block copolymers where the siloxane blocks contain equal weight percents of dimethyl and diphenyl units. In both cases, the tan δ peaks are broad, and at temperatures intermediate to the two transitions, damping remains relatively high. These facts indicate phase mixing which is anticipated since the phenyl-containing siloxane phase is more miscible with the organic phase than is an all dimethyl siloxane phase. As previously discussed, this is due to the change in solubility parameter upon incorporation of diphenyl units into a polydimethylsiloxane chain.

When comparing the samples shown in Figures 44 and 45, the only difference is siloxane block molecular weights. In Figure 44, both the siloxane and ester blocks are approxi-

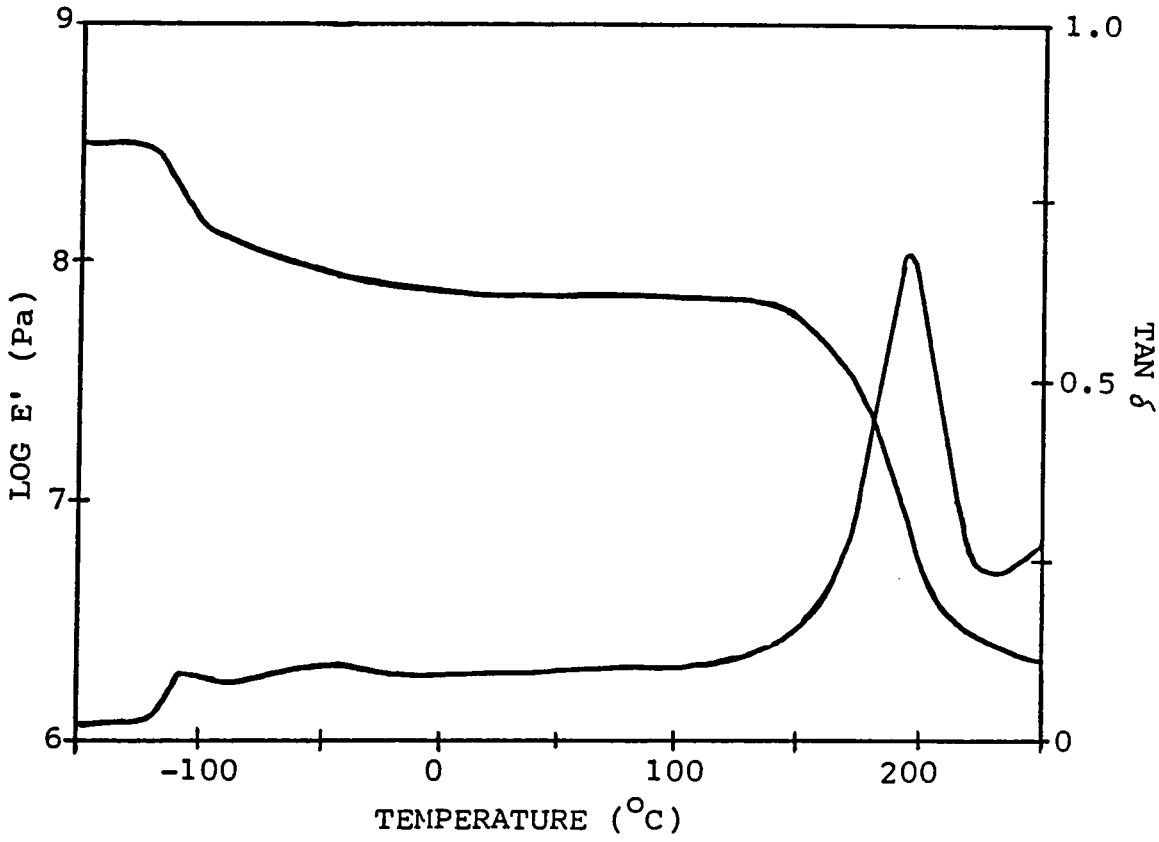

Figure 43: DMTA of a 7,000 $\overline{Mn}$ dimethylsiloxane-9,900 $\overline{Mn}$ ester block copolymer (30Hz, 3°C/min).

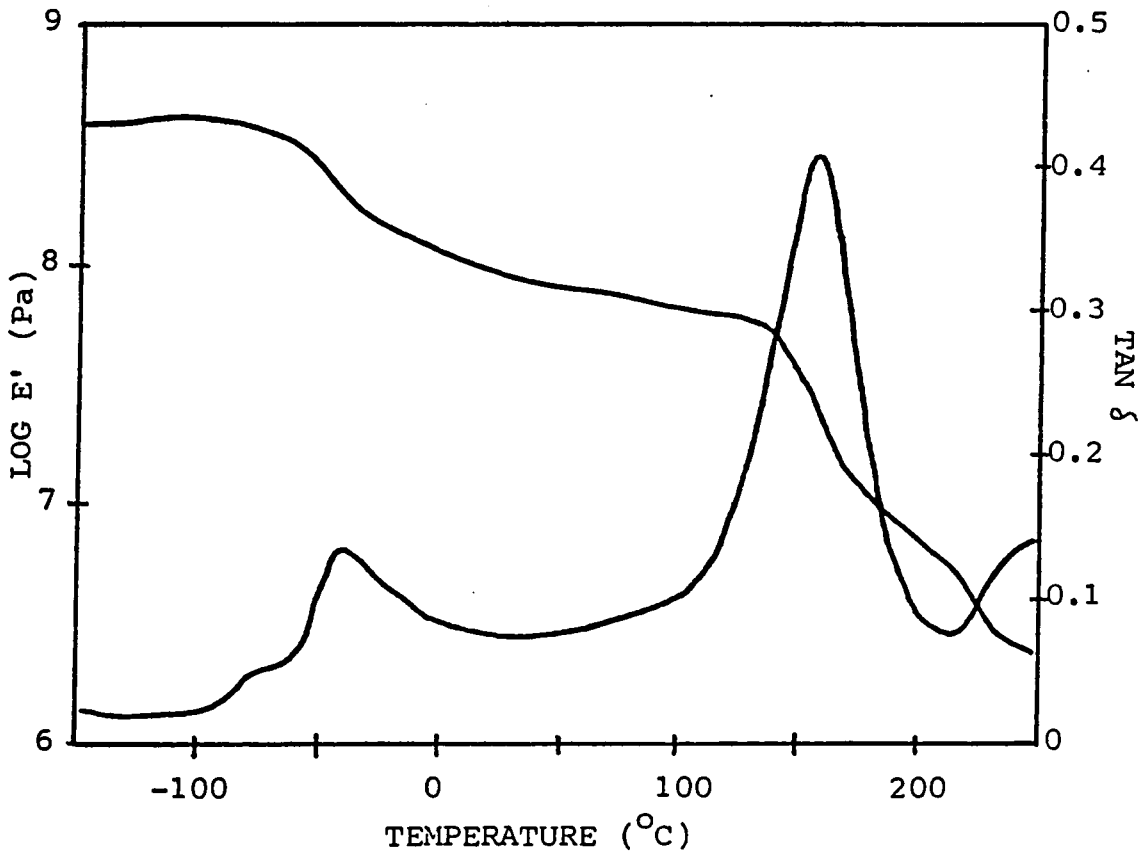

Figure 44: DMTA of a 5,400 $\overline{Mn}$ siloxane (50 CH_3/50 Ø) - 5,100 $\overline{Mn}$ ester block copolymer (30 Hz, 5°C/min).

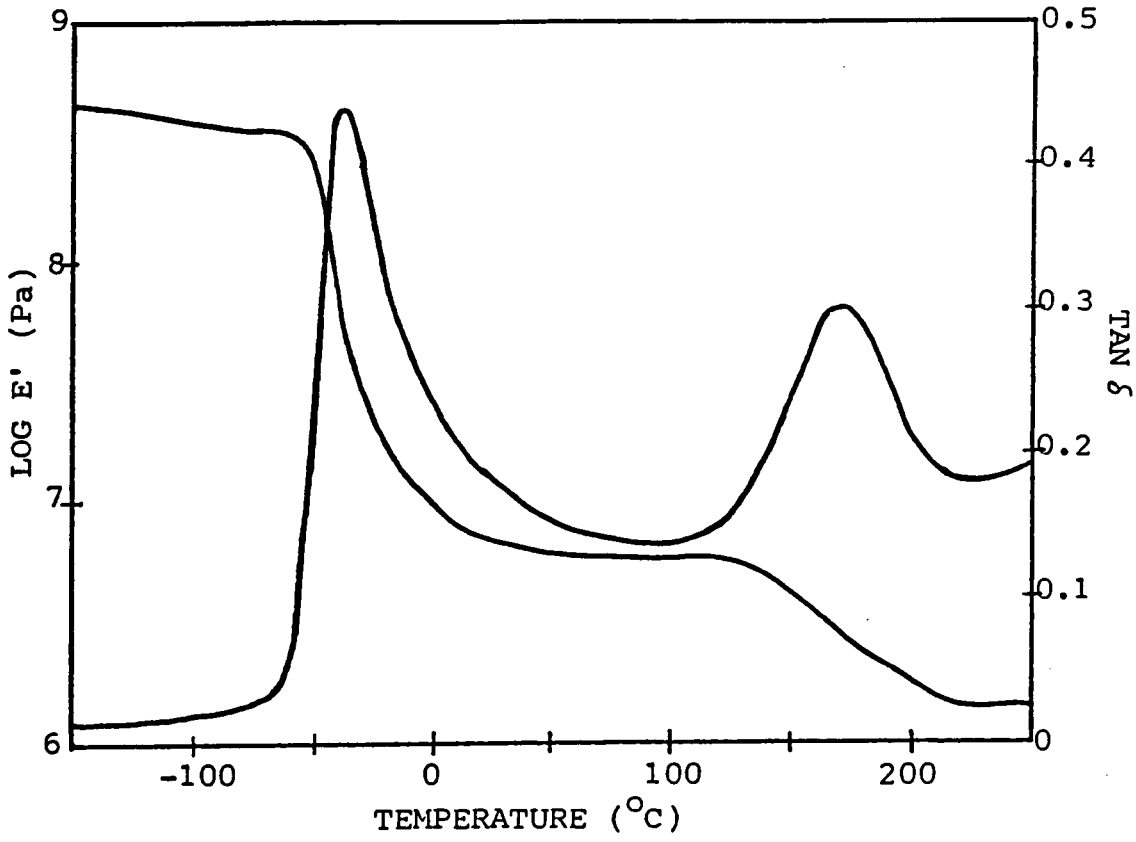

Figure 45: DMTA of a 11,800 $\overline{Mn}$ siloxane (50 CH_3/50 Ø) - 5,100 $\overline{Mn}$ ester block copolymer (30 Hz, 5°C/min).

mately 5,000 $\bar{M}n$. A small change in log E' (0.5 Pa) is observed at the siloxane transition temperature of -55°C. This sample also displays a broad peak at -80°C which is likely a secondary transition of the ester phase. In Figure 45, the sample contains a higher percentage of soft segments since the siloxane block length is 11,800 $\bar{M}n$ and the ester block length is about 5,000 $\bar{M}n$. At the siloxane transition temperature, a log E' decrease of almost 2 Pa is observed and is due to the high siloxane content. Similar results, shown in Figures 46 and 47, were displayed by trifluoropropylmethyl-containing siloxane-ester block copolymers.

A representative siloxane-ester block terpolymer is shown in Figure 48. The terpolymer consists of: (1) a 5,000 $\bar{M}n$ ester block, (2) a 5,000 $\bar{M}n$ dimethylsiloxane block, and (3) a 5,000 $\bar{M}n$ trifluoropropylmethylsiloxane block. Each component displays a tan δ peak, and a relatively high degree of damping is observed between transitions.

Table 31 illustrates the effect of siloxane composition on tan δ and modulus of siloxane-ester block copolymers with 5,000 $\bar{M}n$ block lengths. As expected, copolymers containing flexible dimethylsiloxane segments show the lowest transition temperatures. As diphenyl or trifluoropropylmethyl units are incorporated into dimethylsiloxane segments, the low temperature transitions increase due to decreasing chain

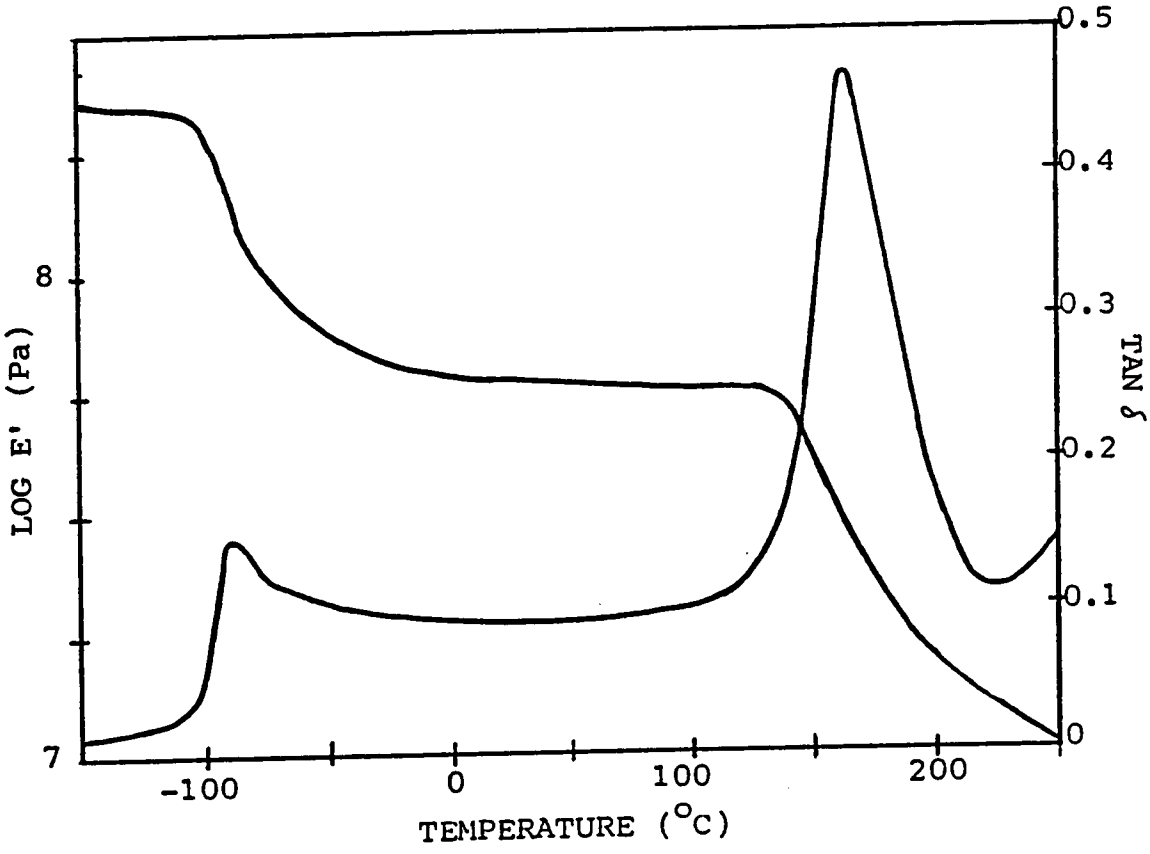

Figure 46: DMTA of a 5,100 Mn siloxane (50 CH_3/50 F) - 5,100 Mn ester block copolymer (30 Hz, 3°C/min).

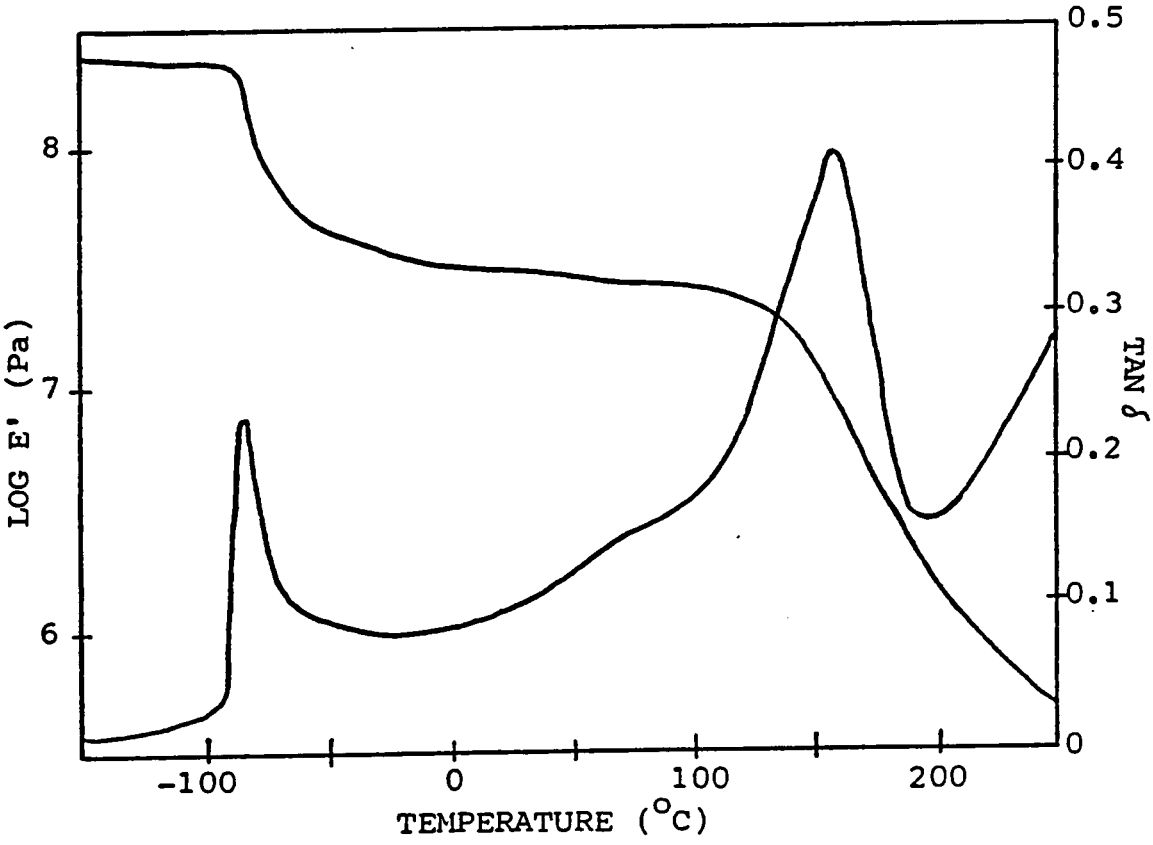

Figure 47: DMTA of a 11,900 $\bar{M}n$ siloxane (50 CH_3/50 F) - 5,000 $\bar{M}n$ ester block copolymer (1 Hz, 5°C/min).

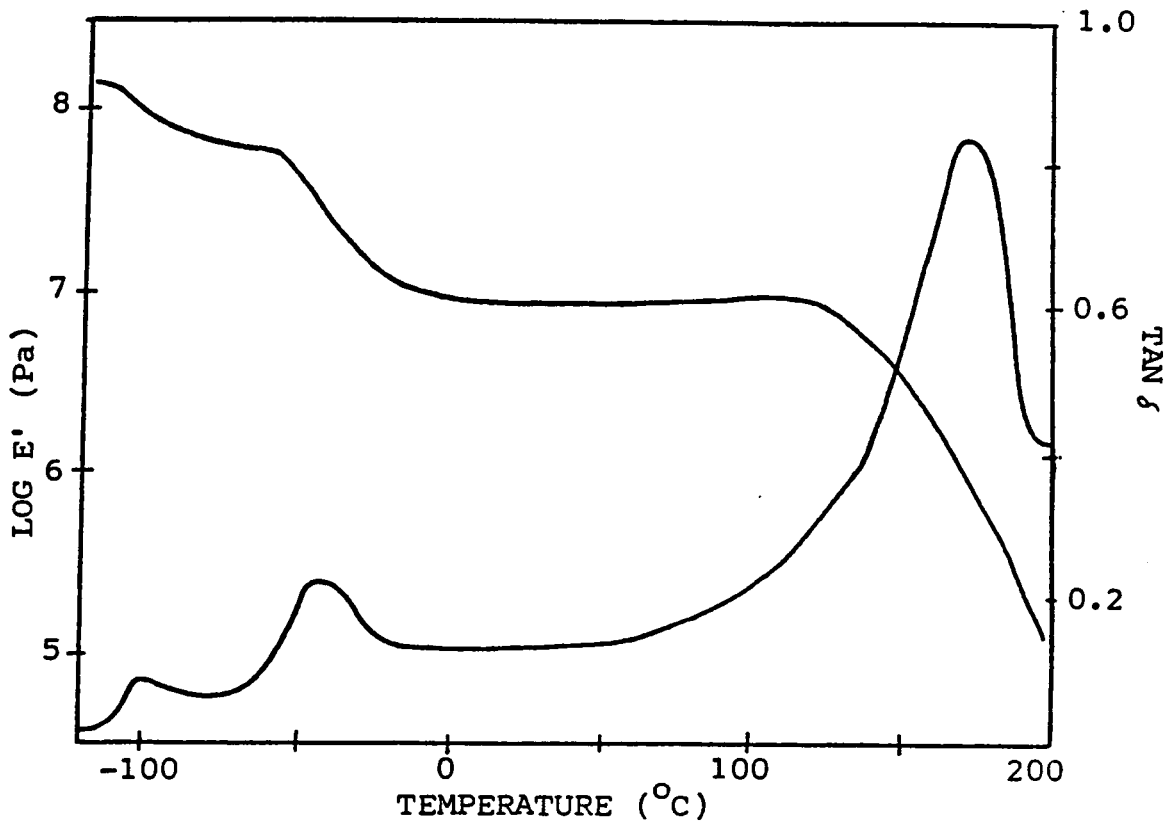

Figure 48: DMTA of a (trifluoropropylmethyl-co-dimethyl)siloxane-ester block terpolymer with 5,000 $\bar{M}n$ blocks (1 Hz, 5 C/min).

TABLE 31

The Effect of Siloxane Composition on DMTA and DSC Transitions

Siloxane Composition[b]	Copolymer Transitions (°C) DMTA[c]	DSC
100 CH_3	-110	-123
75 CH_3/25 Ø	-65	-98
50 CH_3/50 Ø	-40	-61
25 CH_3/75 Ø	0	--
75 CH_3/25 F	-95	-108
50 CH_3/50 F	-90	-102
25 CH_3/75 F	-60	--

[a]Siloxane-ester copolymer block lengths, 5,000 $\bar{M}n$.

[b]Composition in weight percent.

[c]Center of tan δ peak.

Note: -- indicates sample not run.

flexibility of the soft segment. The rigid diphenyl groups show a more dramatic change than the trifluoropropylmethyl groups. This trend was also observed in the previously discussed DSC studies. It was interesting to note that DSC transition values correspond to the onset of the DMTA tan δ peaks. The DMTA values listed in Table 31 are the center of the broad tan δ peaks.

In addition to siloxane composition, block molecular weight also affects phase mixing, and consequently, influences tan δ. Figure 49 illustrates this effect. Both samples are perfectly alternating (dimethyl-diphenyl)siloxane-ester block copolymers where the siloxane segments contain 50 weight percent of each type of unit. One copolymer sample has 5,000 $\bar{M}n$ blocks and displays broad tan δ peaks. The second sample has 10,000 $\bar{M}n$ blocks and exhibits much sharper tan δ peaks, indicating better phase separation than the copolymer with lower block molecular weights. The effect of block molecular weight on dynamic mechanical properties of siloxane-containing block copolymers has been reported by other investigators [96,173].

4.2.1.5 Surface and Bulk Analysis

The surface properties of block copolymers originate from the difference in the surface free energies of the com-

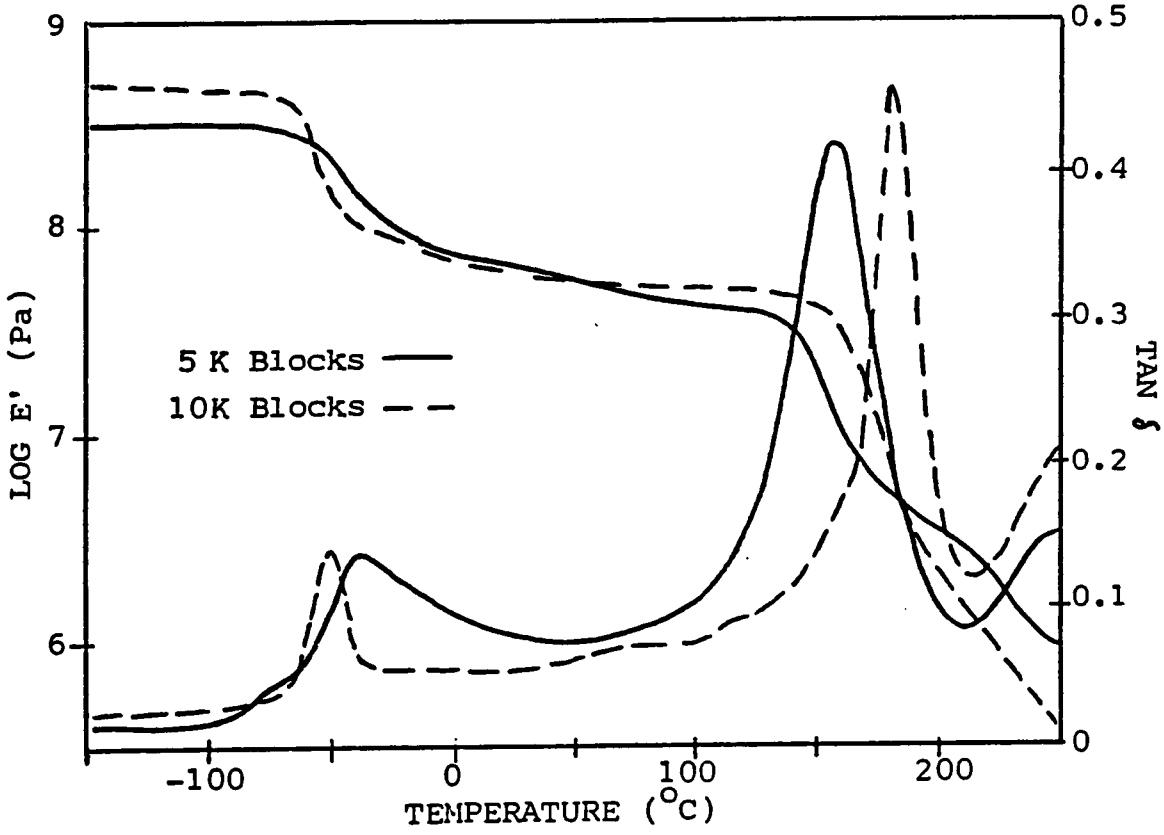

Figure 49: The effect of block molecular weight on tan δ.

ponents involved. Gibbs [183] showed that any component that has a lower surface free energy would tend to enrich the surface of a condensed phase. Thus, in a block copolymer, the component of lower surface free energy would preferentially segregate to the surface, and the surface may differ in character than the bulk. In siloxane-containing blends and copolymer systems, the siloxane is generally the component of lower surface free energy, and therefore, dominates the surface of a polymer film [64,133-135]. For this reason, it was of interest to evaluate the surface and bulk characteristics of the siloxane-ester block co- and terpolymers. Contact angle measurements, x-ray photoelectron spectroscopy (XPS), and electron microscopy were used for surface and bulk analysis.

Contact Angle Measurements

Data from contact angle measurements of representative block polymer samples is presented in Table 32. A 20 μℓ drop of water was placed on the surface of a one inch square polymer film and the angle made between the drop and the film surface was measured as shown in Figure 50. Since this is a relative technique, a polyarylester homopolymer was used as a control. Due to the hydrophobic nature of siloxanes, the contact angle of a surface dominated by siloxane

TABLE 32

Contact Angle Measurements

Sample	Contact Angle[a]
Ardel-polyester control	77°
Copolymers	
5K PE/5K PSX(100 CH_3)	98°
5K PE/10K PSX(100 CH_3)	105°
10K PE/5K PSX(100 CH_3)	99°
10K PE/10K PSX(100 CH_3)	105°
5K PE/5K PSX(25 Ø)	99°
5K PE/5K PSX(50 Ø)	97°
5K PE/5K PSX(75 Ø)	102°
5K PE/5K PSX(25 F)	103°
5K PE/5K PSX(50 F)	96°
5K PE/5K PSX(75 F)	104°
Terpolymers	
5K PE/5K PDMS/5K PSX(75 Ø)	102°
5K PE/5K PDMS/5K PSX(75 F)	100°
5K PE/5K PDMS/5K PSX(100 F)	98°

[a]20 µℓ water drops.

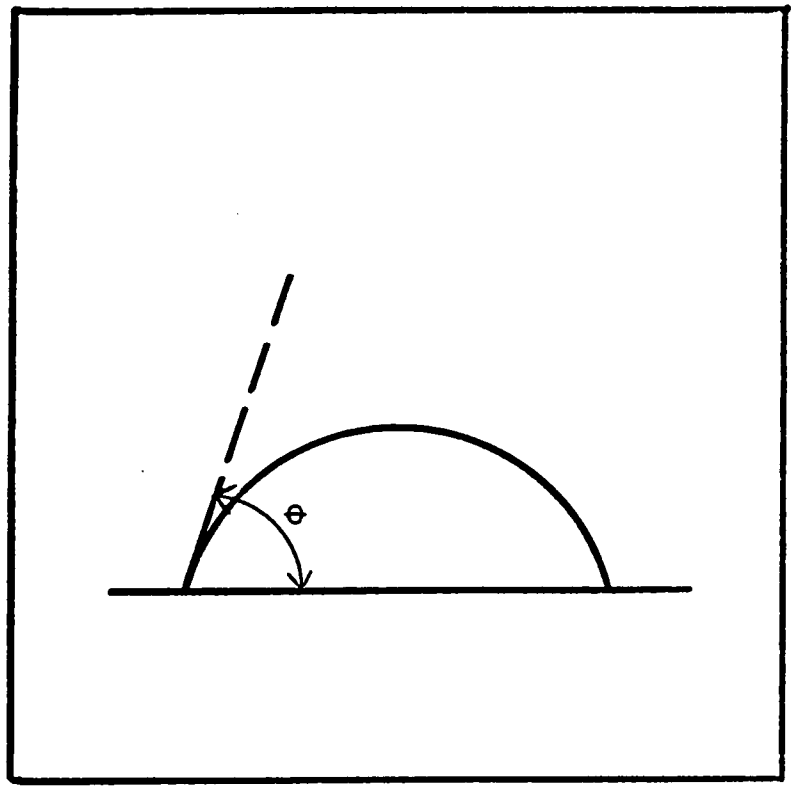

Figure 50: Contact angle measurements.

would be expected to have a larger contact angle than a control without siloxane. Such a trend was noted in this study. As seen from the data presented in Table 32, the contact angles of siloxane-containing block polymers were significantly larger than the polyarylester control. Qualitatively, it may be concluded from these results that the surface of the block polymer films are dominated by siloxane, the lower surface free energy component of these polymer systems.

X-Ray Photoelectron Spectroscopy

XPS (or Electron Spectroscopy for Chemical Analysis, ESCA) has recently proven to be an excellent spectroscopic tool for studying, in considerable detail, aspects of structure and bonding in the surface region (< 75 Å) of polymers. The information available from this technique, and the principal features observed in XPS spectra, are listed in Table 33 [180]. The advantages of XPS include: (1) a non-destructive nature, (2) the capability of detecting all elements except hydrogen, (3) the ability to analyze any solid that can withstand the bombardment of x-rays and vacuum, (4) small sample size requirements, and (5) small sampling depth [181].

TABLE 33

Principal Features in the XPS Spectra of Polymers [180]

Spectral Feature	Information
Main peak position	Atom identification
Chemical shift	Oxidation state
Peak-area ratios	Stoichiometry
Shake-up satellites	$\pi \rightarrow \pi^*$ transitions

The XPS experiment involves the measurement of binding energies of electrons ejected by interactions of a molecule with a monoenergetic beam of soft x-rays. The fundamental processes involved in XPS are illustrated in Figure 51 [182]. The incident x-ray energy (eV) exceeds the binding energy (BE) of the core electrons, thus ejecting the core electrons from the sample. The kinetic energy (KE) of the ejected electrons are given as the difference between the incident x-ray energy and the binding energy:

$$KE = eV - BE$$

The removal of a core electron is accompanied by substantial reorganization of the valence electrons in response to the effective increase in nuclear charge. This perturbation gives rise to a finite probability for photoionization to be accompanied by simultaneous excitation of a valence electron from an occupied to an unoccupied level (shake-up) or ionization of a valence electron (shake-off). These processes, giving rise to satellites to the low kinetic energy side of the main photoionization peak, are measurable parameters and broaden the scope of this technique [182].

A greater surface sensitivity can be achieved by angular dependent XPS studies. This type of experiment varys the angle θ between the sample surface and the analyzer as

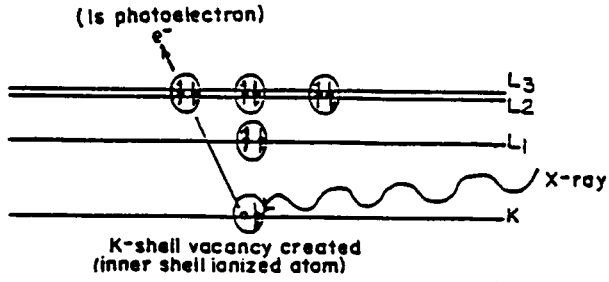

(a) The basic process.

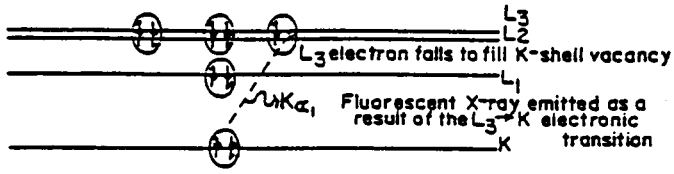

(b) Relaxation by x-ray flourescence.

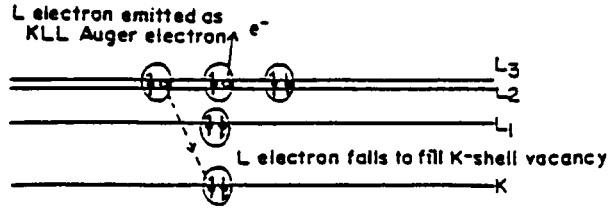

(c) Relaxation by the Auger process.

Figure 51: Fundamental processes involved in XPS [182].

shown in Figure 52 [184]. With decreasing take-off angle, the effective sampling depth decreases and thus a composition profile from the first 75 Å of the surface can be determined.

The following discussion briefly summarizes the results obtained from XPS of siloxane-ester block copolymers. A more detailed discussion of surface analysis by XPS will be presented in the subsequent section which deals with polymer degradation; XPS proved to be a valuable technique for evaluating the change in surface composition before and after exposure to atomic oxygen.

Figure 53 depicts the angular dependence of the O_{1s} peak from a representative perfectly alternating dimethylsiloxane (6,700 $\bar{M}n$)-ester(5,000 $\bar{M}n$) block copolymer. Dimethylsiloxane homopolymer and homopolyarylester O_{1s} peaks are also shown and are useful as controls. The insert of Figure 53 shows the O_{1s} peak of the homopolyester is made up of two equal size component peaks; one at 532.2 eV due to C-O-C and the other at 533.9 eV due to C=O. In contrast, the siloxane homopolymer displays a single O_{1s} peak at 532.4 eV due to the Si-O-Si backbone. The O_{1s} peak of a siloxane-ester block copolymer at 3 different take-off angles is similar to the single peak observed for the siloxane homopolymer. This suggests that the surface of the copolymer film is dominated

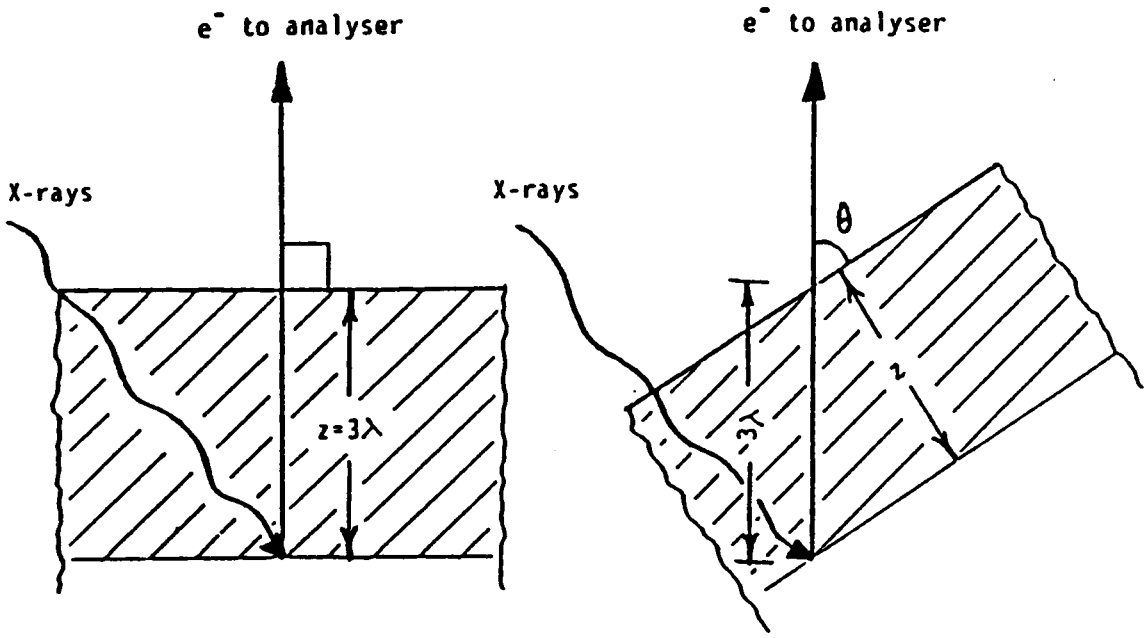

Figure 52: Angular dependent XPS.

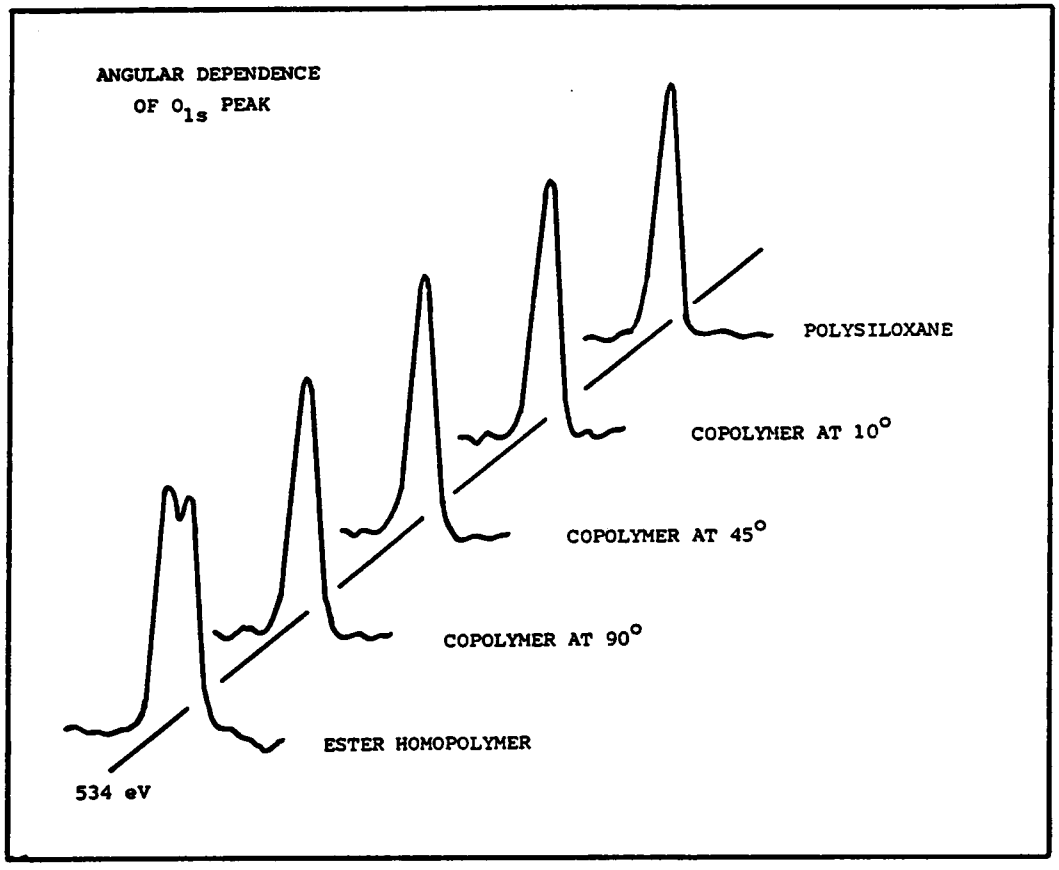

Figure 53: The XPS angular-dependent behavior of a dimethylsiloxane (6,700 $\overline{Mn}$)-ester (5,000 $\overline{Mn}$) block copolymer.

by siloxane, the low surface free energy component of the copolymer system. At $\theta = 90°$ (deepest profile), a small shoulder to the left of the major O_{1s} peak indicates the presence of some ester. However, this shoulder vanishes as θ is decreased (i.e., a smaller depth is analyzed). In summary, Figure 53 demonstrates that the top few angstroms of a solution cast siloxane-ester block copolymer film is dominated by siloxane [134].

Transmission Electron Microscopy

Recently, much attention has been given to the study of microphase separation behavior of block copolymers since it is one of the most important factors imparting the physical and mechanical properties unique to these systems. Depending on the (1) chemical nature of the blocks, (2) architecture of the copolymer, (3) lengths of the blocks individually and in relation to one another, and (4) processing conditions, a number of morphological configurations are possible for microphase separation which, in turn, give rise to a variety of properties [64,81,141].

To directly observe the nature of the bulk microphase separation of the siloxane-ester block copolymers, TEM was performed on thin solution cast films. Staining of one of the phases was unnecessary since there is a great degree of

electron density difference between the siloxane and ester phases. Representative TEM micrographs are shown in Figures 54 through 58. In all cases, microphase separation with spherical domains of ester (light areas) and siloxane (dark areas) is clearly observed.

The effect of copolymer block molecular weight is shown in Figures 54/55 and 56/57. As expected, the copolymers with lower block lengths have smaller domains than the copolymers with higher block lengths. Figures 54, 56, and 58 illustrate the effect of siloxane composition at constant block molecular weight. As previously discussed, the ability of the siloxane phase to mix with the organic phase is enhanced by incorporation of diphenyl units or trifluoropropylmethyl units into dimethylsiloxane segments. Therefore, the sharpness of the phase boundaries is decreased with an increase in phase mixing. A representative TEM micrograph of a siloxane-ester terpolymer is shown in Figure 59.

4.2.1.6 Atomic Oxygen Degradation Studies

Long-term stability within the space environment is a major materials concern. It is estimated that large space structures must be able to exist in the low earth orbit (LEO) atmosphere for at least 20 years to be monetarily feasible. As discussed in the literature review, atomic oxygen

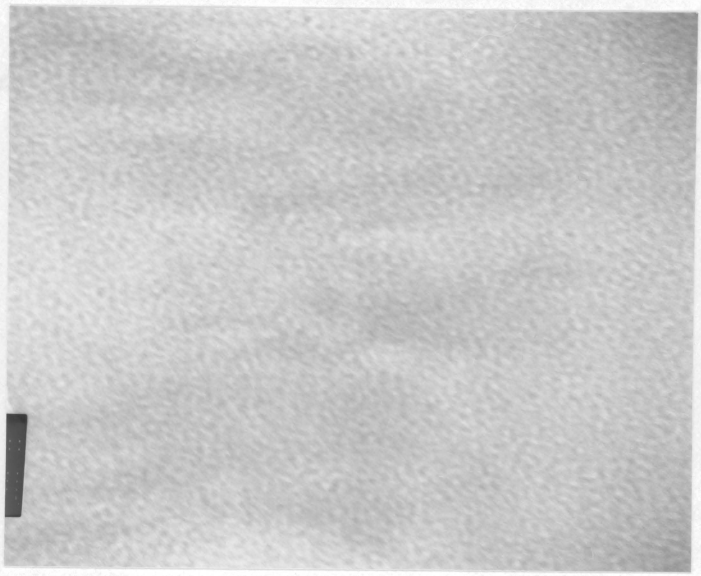

Figure 54: TEM of a dimethylsiloxane (6,000 $\bar{M}n$)-ester (5,100 $\bar{M}n$) block copolymer, magnification 105,000X.

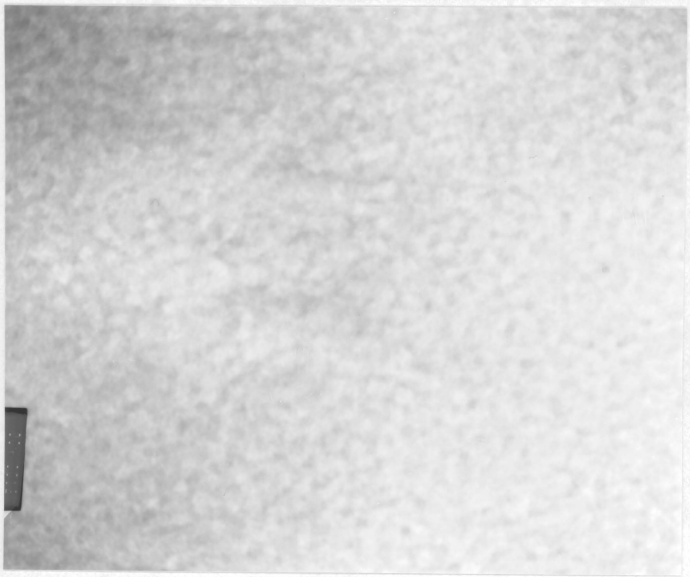

Figure 55: TEM of a dimethylsiloxane (10,500 $\bar{M}n$)-ester (10,000 $\bar{M}n$) block copolymer, magnification 105,000X.

Figure 56: TEM of a 5Ø CH_3/50 Ø siloxane (5K $\bar{M}n$)-ester (5K $\bar{M}n$) block copolymer, magnification 105,000X.

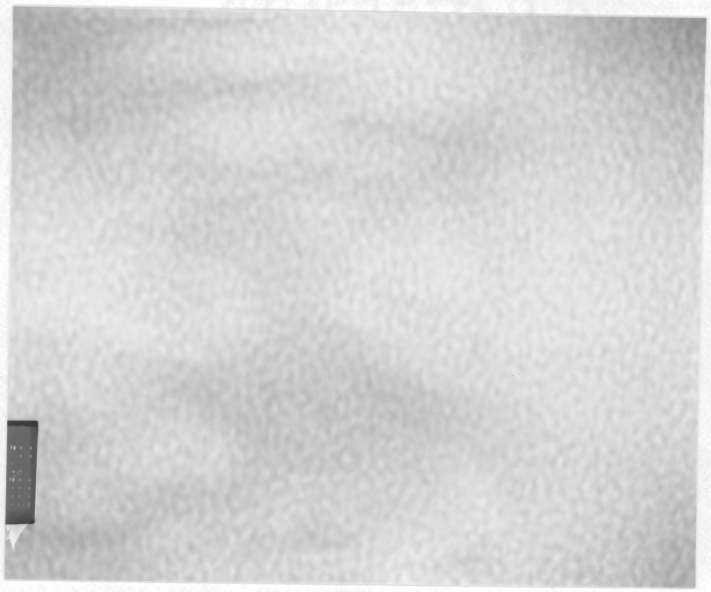

Figure 57: TEM of a 50 CH_3/50 Ø siloxane (5K $\bar{M}n$)-ester (10K $\bar{M}n$) block copolymer, magnification 105,000X.

Figure 58: TEM of a 50 CH_3/50 F siloxane (5K $\bar{M}n$)-ester (5K $\bar{M}n$) block copolymer, magnification 105,000X.

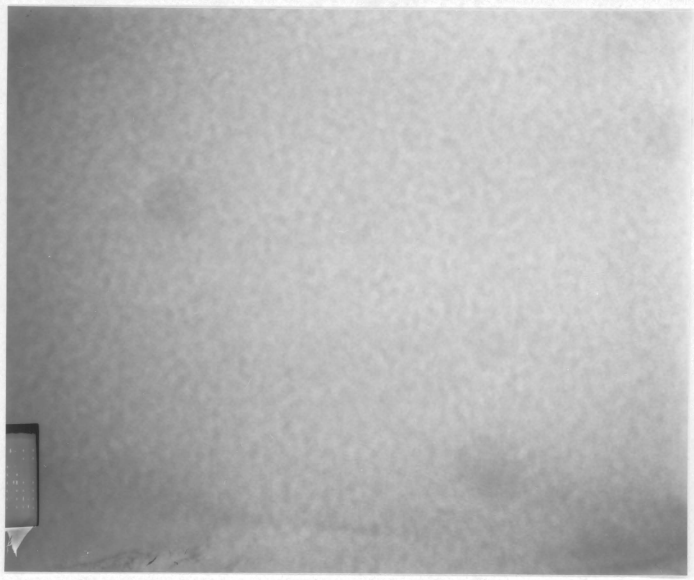

Figure 59: TEM of a 5K PE/5K PDMS/6K PSX(75 F) block terpolymer, magnification 105,000X.

(AO) is the predominant species a spacecraft is bombarded by in LEO. Therefore, it was of interest to evaluate the stability of the siloxane-ester block polymers in a simulated atomic oxygen environment. After exposure to atomic oxygen, each sample was evaluated for weight loss. Contact angle measurements, diffuse reflectance infrared (DR-IR), x-ray photoelectron spectroscopy (XPS), and scanning electron microscopy (SEM) were used to determine surface properties of each sample before and after exposure.

Contact Angle and Weight Loss Measurements

Ardel was used as a control for this study. Table 34 lists the contact angle and weight loss results for various exposure times of Ardel. The experiment was continuous time, i.e., five separate samples were exposed for different times. The data shows a significant change in both weight and contact angle.

The effects of exposure to atomic oxygen for 30 minutes are presented in Table 35 for a polyarylester control and various siloxane-ester block co- and terpolymers. In copolymer samples 2 through 4, block molecular weight is constant while siloxane block composition is varied. Samples 5 through 8 vary block molecular weight while retaining the same siloxane block composition, 50 weight percent each of

TABLE 34

Atomic Oxygen Degradation of Ardel

Exposure Time (min.)	% Weight Loss	Contact Angle
0	--	77°
12	0.18	30°
24	3.11	25°
36	2.51	23°
48	2.41	23°
60	2.30	25°

TABLE 35

Atomic Oxygen Degradation of Siloxane-Ester Block Polymers

Composition[a]	Contact Angle[b] Unexposed	Contact Angle[b] Exposed[c]	% Weight Loss
1. Polyarylester-control	79°	40°	3.46
2. 5K PE/5K PSX(100 CH_3)	100°	98°	0.71
3. 5K PE/5K PSX(50 Ø)	98°	95°	0.36
4. 5K PE/5K PSX (50 F)	98°	94°	1.12
5. 5K PE/5K PSX(50 Ø)	98°	95°	0.36
6. 5K PE/10K PSX(50 Ø)	103°	97°	0.21
7. 10K PE/5K PSX(50 Ø)	98°	90°	2.62
8. 10K PE/10K PSX(50 Ø)	101°	98°	1.92
9. 5K PE/5K PDMS/5K PSX(75 Ø)	102°	97°	1.02
10. 5K PE/5K PDMS/5K PSX(75 F)	100°	92°	1.05

[a]Solution cast polymer films.

[b]20 µℓ water drops.

[c]30 min. exposure to atomic oxygen.

dimethyl and diphenyl units. Samples 9 and 10 are block terpolymers containing blocks of a 5,000 $\bar{M}n$ polyarylester, a 5,000 $\bar{M}n$ polydimethylsiloxane, and a 5,000 $\bar{M}n$ siloxane co-oligomer (either highly diphenyl or trifluoropropylmethyl).

The most significant weight loss and change in contact angle after exposure to atomic oxygen for 30 minutes was displayed by the polyarylester control, sample 1. Siloxane incorporation was observed to reduce both weight loss and change in contact angle. NASA obtained similar results with a novel polyimide-polydimethylsiloxane block copolymer [110,133]. The oxidation reaction efficiency was approximately an order of magnitude lower than the currently used polyimide (Kapton) thermal blanket materials. These findings are attributed to the fact the siloxanes that dominate the surface of copolymer systems are more resistant to oxidative degradation by atomic oxygen since their physical structures can be converted to largely inorganic silicates which are much more resistant to atomic oxygen than any organic material. The data from Table 35 also suggests that weight loss is influenced by the composition of the siloxane segments. High diphenyl incorporation, sample 6 for example, showed negligible weight loss compared to other samples.

Diffuse Reflectance Infrared

DR-IR was used for chemical characterization of the polymer films before and after exposure to atomic oxygen. However, this technique did not prove as useful as anticipated. DR-IR showed no change in chemical composition after exposure to atomic oxygen (see Figure 60). This is likely due to the fact that DR-IR analyzes the top 1,000 Å of a surface and atomic oxygen apparently affects only the top few angstroms. Theoretical and quantitative aspects of this technique were not investigated; they are discussed in several cited references [185-187].

X-Ray Photoelectron Spectroscopy

XPS proved to be much more useful than DR-IR in the analysis of surfaces etched by oxygen plasma. As previously discussed, angle dependent XPS is an excellent spectroscopic technique for studying aspects of structure and bonding in the first 75Å of a polymer surface. After exposure to atomic oxygen, XPS detected changes in oxidation state of atoms (shift of photopeak) and changes in the ratio of atom types to one another.

The wide scan XPS spectra (θ=90°) of a polyarylester control before and after exposure to atomic oxygen are shown in Figures 61 and 62, respectively. The quantitative inter-

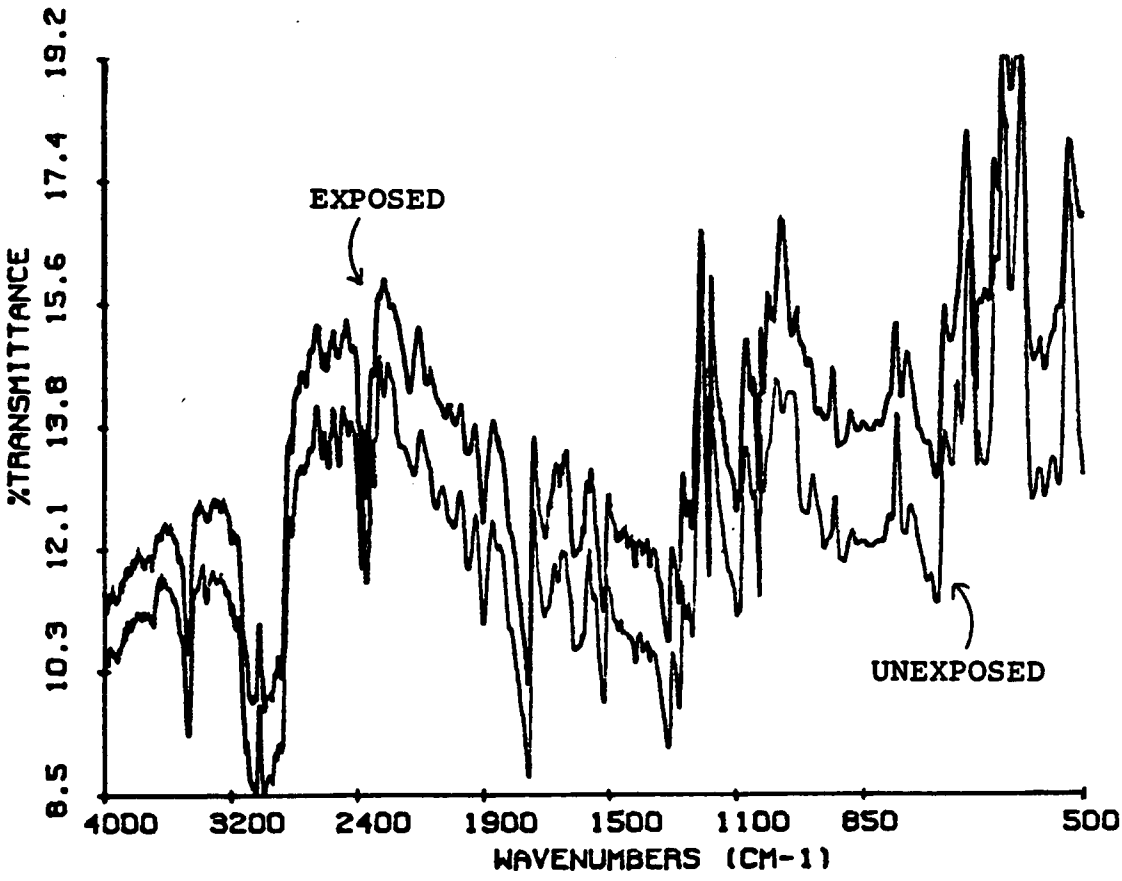

Figure 60: DR-IR of a polyarylester homopolymer before and after exposure to atomic oxygen.

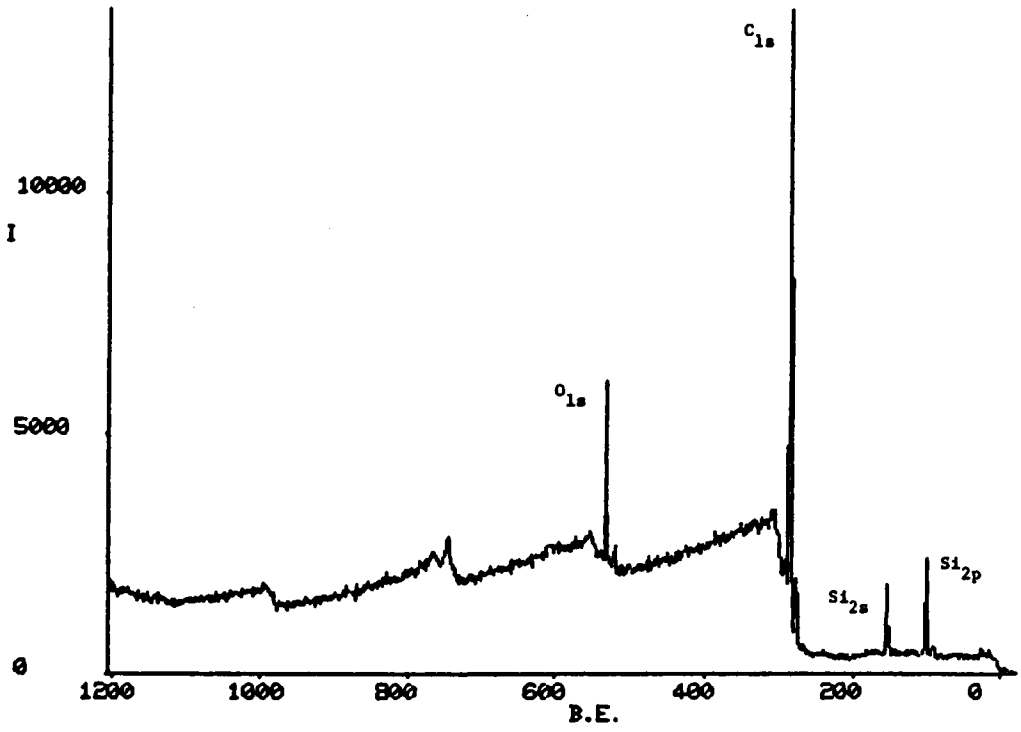

Figure 61: A wide scan XPS spectrum of an unexposed polyarylester control.

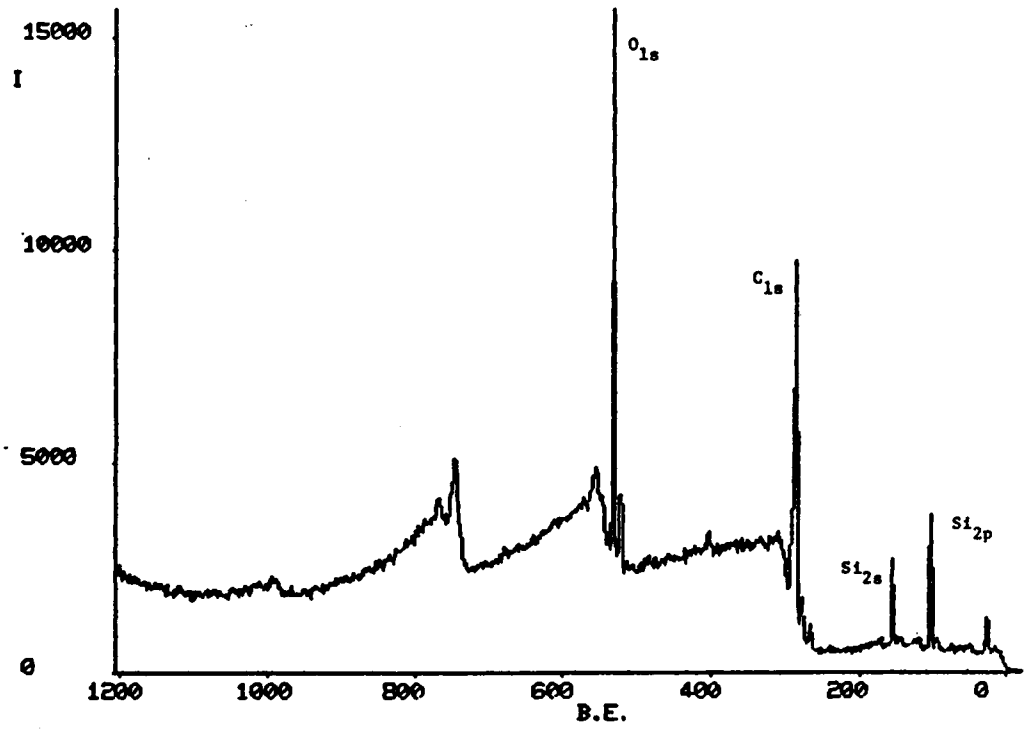

Figure 62: A wide scan XPS spectrum of a polyarylester control exposed to atomic oxygen for 30 minutes.

pretations of these figures are presented in Table 36. The percent of each atom present at the polymer surface, atom binding energies (BE), and the full width at half height (FWHH) of each peak are given for two different exit angles, θ=10° and 90° (normal). As anticipated, the amount of oxygen detected on the surface increased after exposure to atomic oxygen. Unfortunately, silicon was observed to be a surface contaminant. The amount of silicon on the surface significantly decreased after oxidation, suggesting that it was, indeed, merely a surface contaminant.

Figures 63 and 64 illustrate the wide scan XPS spectra at θ=90° for a dimethylsiloxane (5,000 $\bar{M}n$)-ester (5,000 $\bar{M}n$) block copolymer before and after exposure to atomic oxygen. Quantitative results for θ=10° and 90° are tabulated in Table 37. As with the control, the oxygen-carbon ratio at the surface increased significantly after oxidation. The Si_{2p} peak showed a binding energy shift and an increased width at half height, indicating a possible change in oxidation state due to atomic oxygen exposure. It is thought that dimethylsiloxanes on the surface of a copolymer or blend undergo oxidation (oxygen insertion) as shown in Scheme 26 [124]. The resulting ceramic-like structure would provide a protective coating to the bulk material.

TABLE 36

Polyarylester XPS Results

	C_{1s}(10°)	(90°)	O_{1s}(10°)	(90°)	Si_{2p}(10°)	(90°)
Unexposed						
%	58.9	72.0	20.6	21.2	21.5	15.2
BE[a]	285.0	285.0	532.5	532.4	102.1	102.0
FWHH[b]	1.7	2.1	1.6	1.6	1.8	2.2
Exposed						
%	49.1	52.5	37.4	36.6	12.4	10.9
BE[a]	285.0	285.0	533.2	533.1	103.6	103.4
FWHH[b]	2.4	2.6	2.2	2.5	2.0	2.4

[a]Binding energy.

[b]Full width at half height.

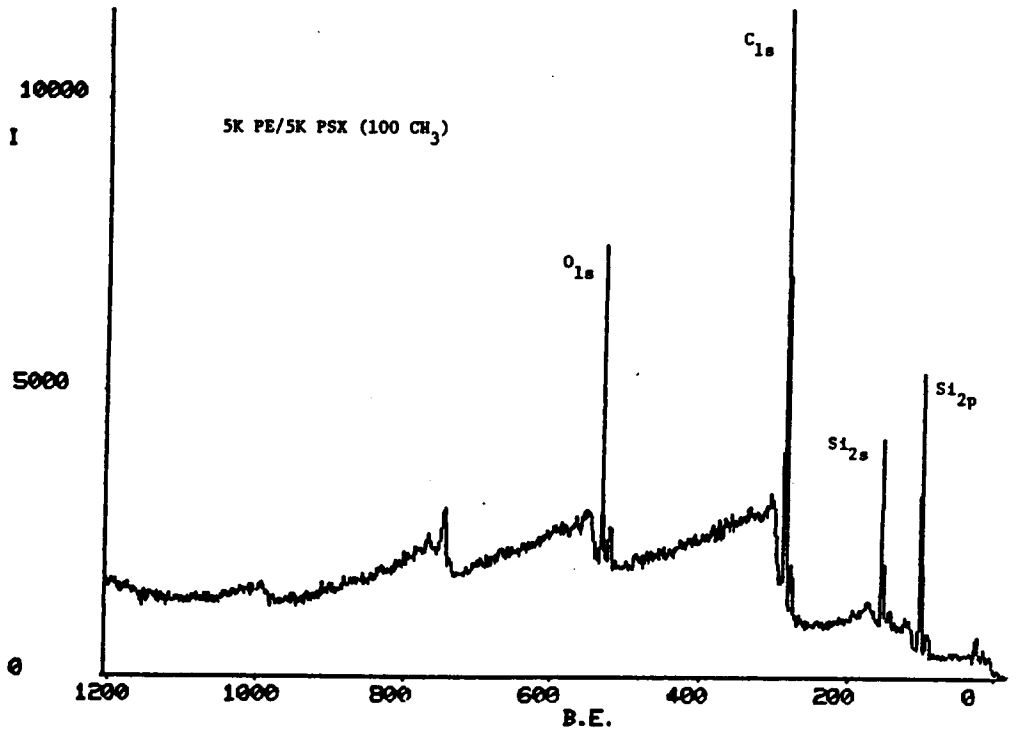

Figure 63: A wide scan XPS spectrum of a dimethylsiloxane-ester block copolymer.

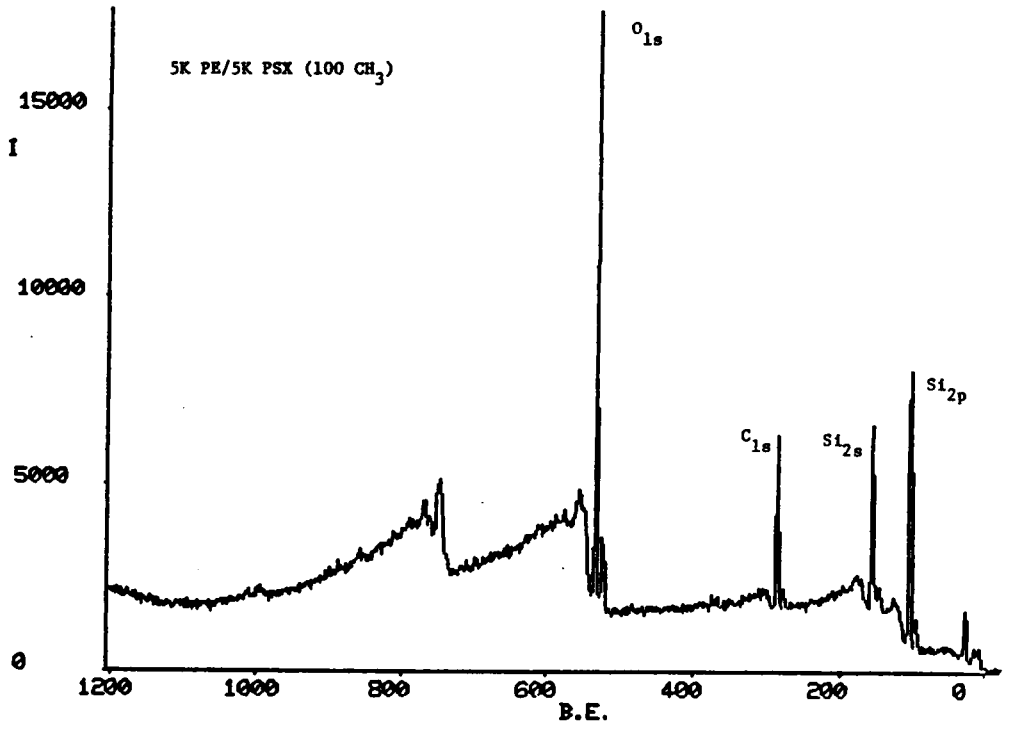

Figure 64: A wide scan XPS spectrum of a dimethylsiloxane-ester block copolymer after exposure to atomic oxygen for 30 minutes.

TABLE 37

Dimethylsiloxane-Ester Block Copolymer XPS Results

	C_{1s}(10°)	(90°)	O_{1s}(10°)	(90°)	Si_{2p}(10°)	(90°)
Unexposed						
%	53.3	57.0	21.5	21.4	25.2	21.6
BE[a]	285.0	285.0	532.6	532.6	102.2	102.3
FWHH[b]	1.6	2.1	1.6	2.0	2.2	2.2
Exposed						
%	42.4	23.0	29.3	42.3	28.3	34.6
BE[a]	285.0	285.0	533.0	533.2	103.5	103.6
FWHH[b]	1.8	2.2	1.9	2.2	2.6	2.7

[a]Binding energy.

[b]Full width at half height.

Scheme 26

The Reaction of Polydimethylsiloxane with Atomic Oxygen

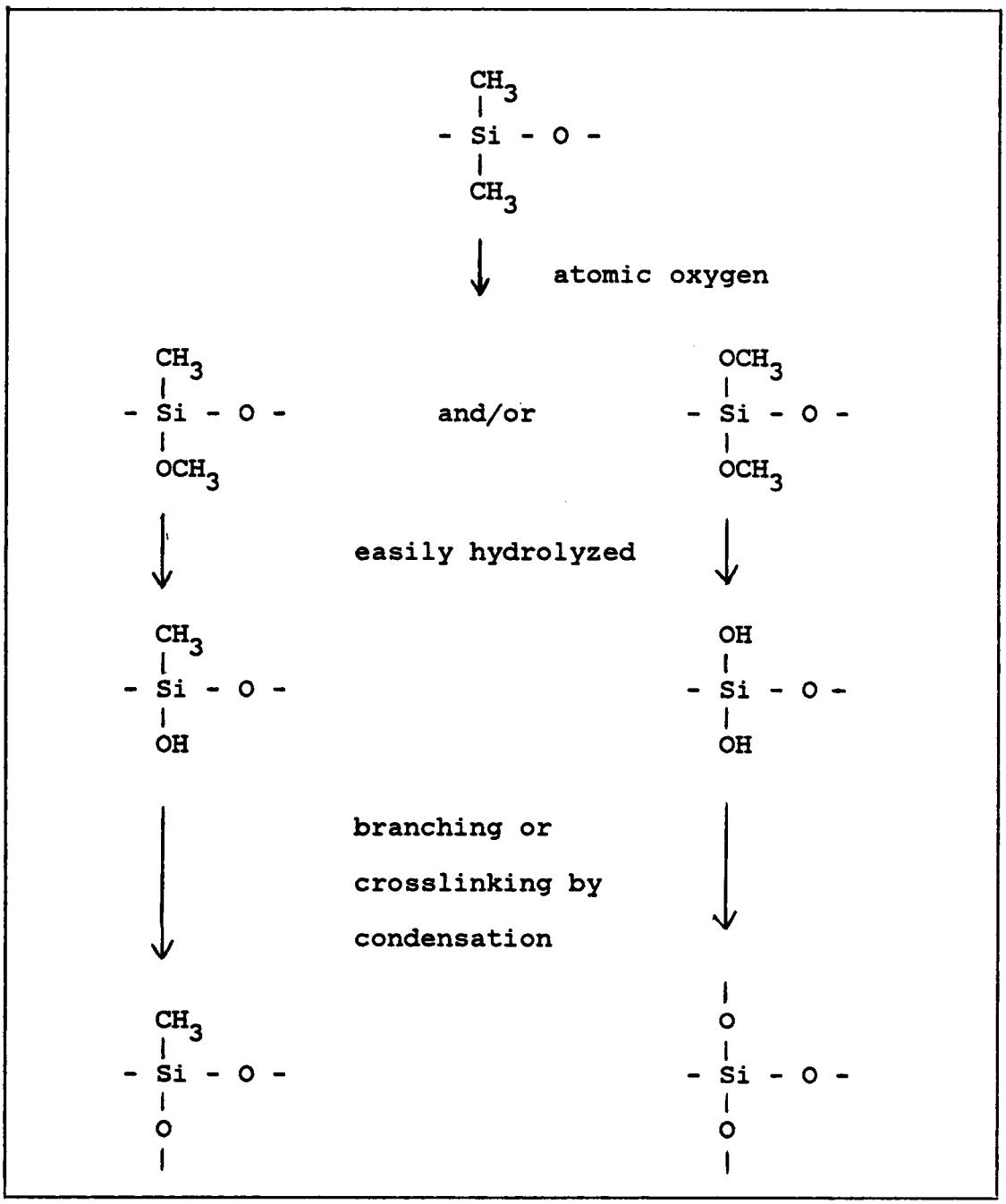

Similar results were found for block copolymers with siloxane blocks that contained diphenyl or trifluoropropylmethyl units. The Si_{2p} peaks shifted by approximately 1 eV to a higher binding energy, the full width at half height of each peak increased, and the amount of oxygen on the surface significantly increased. In addition to the above observations, it was interesting to note that in the case of diphenyl siloxanes, the shake-up satellite due to π-π^* transitions of the aromatic rings (292 eV) was no longer observable at θ=90° after exposure to atomic oxygen (see Figure 65). For (trifluoropropylmethyl)siloxane-containing block copolymers, the amount of fluorine on the surface decreased, but the F_{1s} binding energy remained the same (688 eV).

In summary, angle-dependent XPS showed that (1) etched film surfaces exhibit increased oxygen coverage and reduced carbon signal while the silicon signal intensity remains more or less constant, (2) the carbon, oxygen, and fluorine binding energies were unchanged, however, the full width at half height of each peak increased, and (3) the silicon binding energy and the full width at half height increased after exposure, suggesting an increased number of oxygen atoms bonded to the silicon atoms.

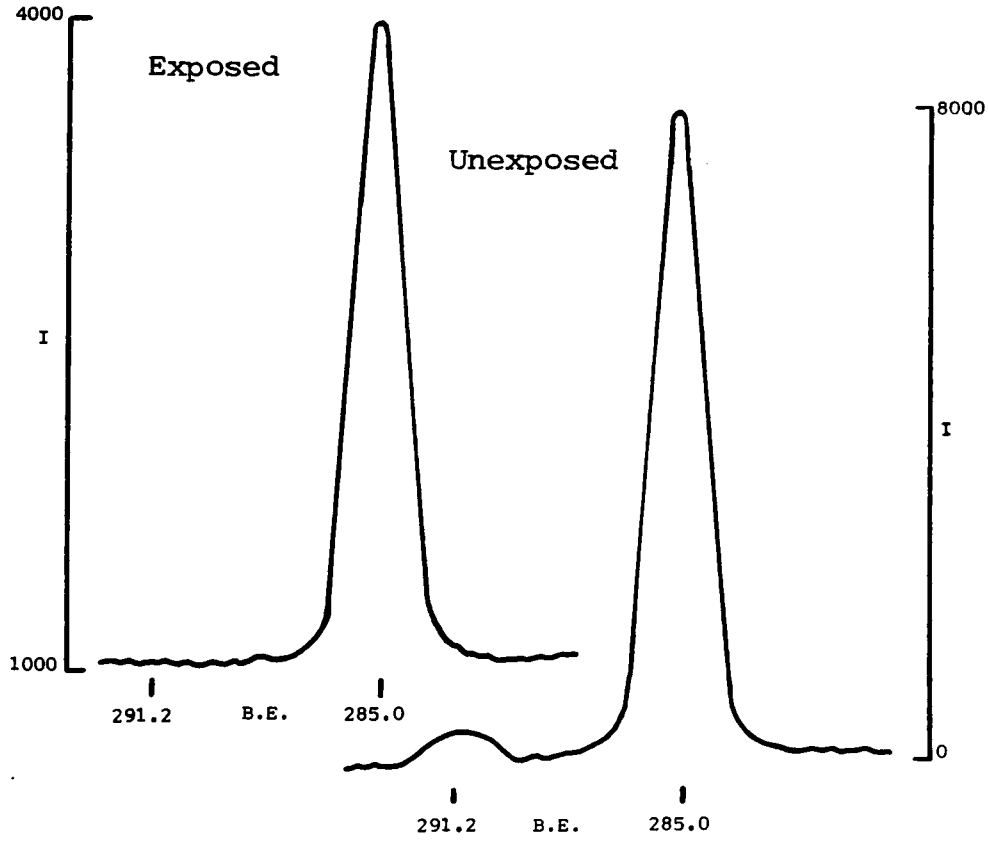

Figure 65: The shake-up satellite peak of a siloxane (50 CH_3/50 Ø)-ester block copolymer.

Scanning Electron Microscopy

SEM was used to study surface morphology. Several representative micrographs are shown in Figures 66 through 70. The surface morphology of a polyarylester control before and after oxygen plasma etching is shown in Figures 66 and 67, respectively. The unexposed surface was smooth, but the exposed surface displayed evidence of induced texturing due to oxidative degradation. As previously discussed, the ester homopolymer control displayed significant changes in weight (loss), contact angle, and surface oxygen coverage (XPS), but no change in composition around 1,000 Å (DR-IR).

In general, the surface characteristics of the etched siloxane-ester block copolymers displayed evidence of micro-cracks with no texturing. Representative SEM micrographs are shown in Figures 68 through 70. Similar results were observed by Knopf and co-workers [111] with homo polydimethyl siloxane coated Kapton films. It was proposed that oxygen diffused through the permeable siloxane coating and due to the bulk property changes, surface cracking and crazing took place. Although the siloxane-ester block copolymers also displayed micro-cracks, there was no evidence of bulk property changes. This may be due to the fact that block copolymers (with siloxane in the bulk, as well as on the surface) behave differently than a siloxane coated substrate.

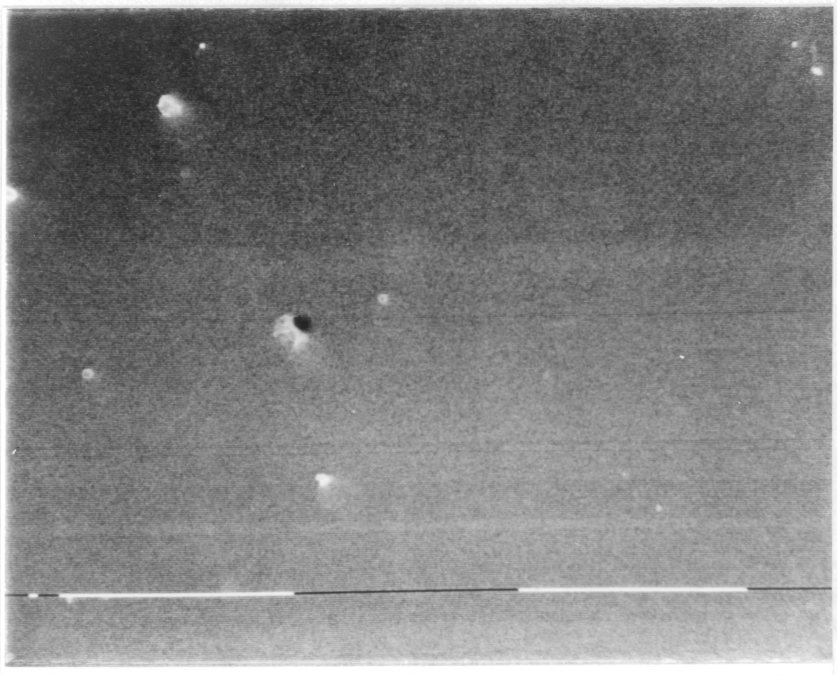

Figure 66: SEM of a homopolyarylester control, magnification 6400X, bars represent 5 μ.

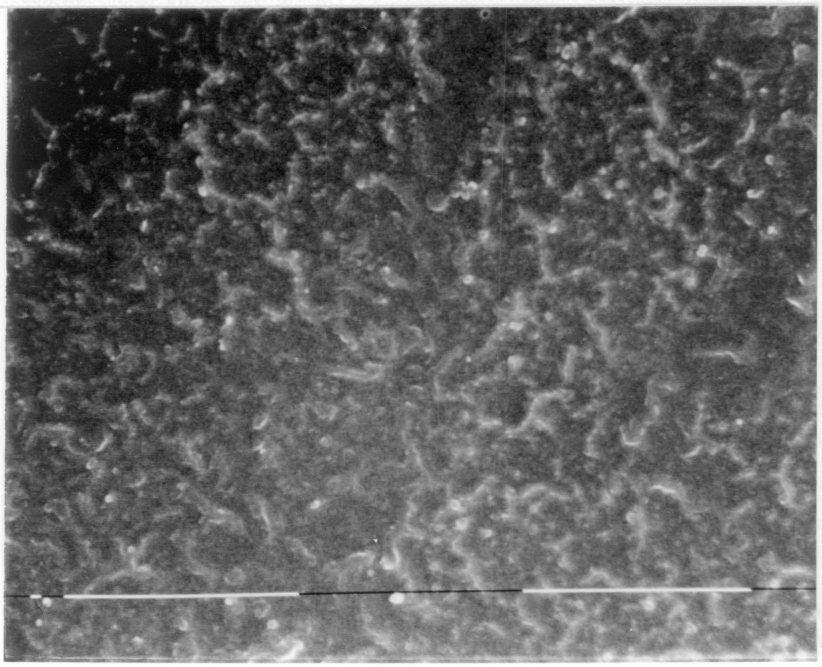

Figure 67: SEM of the ester control exposed to AO for 30 min., magnification 6400X, bars represent 5µ.

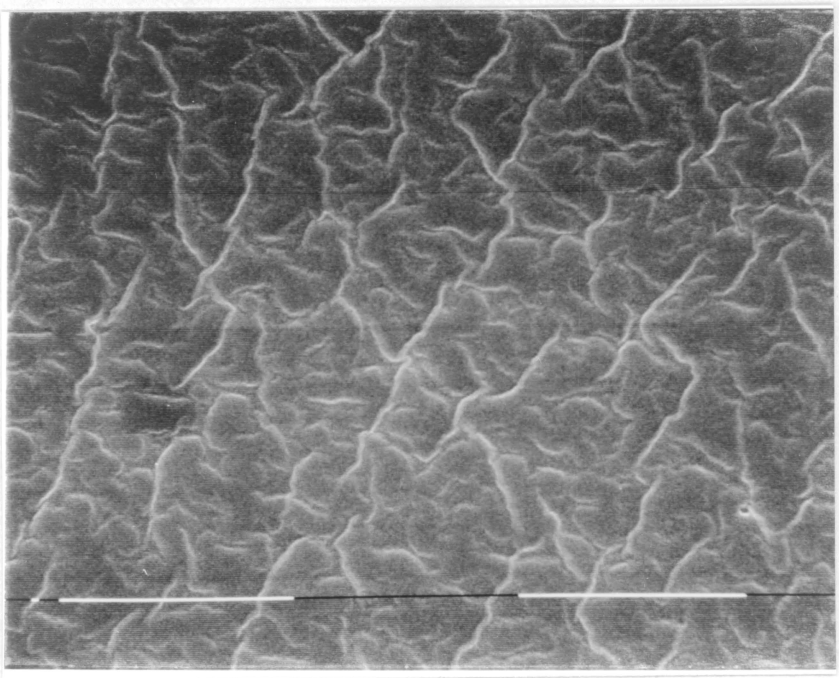

Figure 68: SEM of a dimethylsiloxane-ester block copolymer, magnification 6400X, bars represent 5μ. Block lengths 5,000 $\overline{Mn}$.

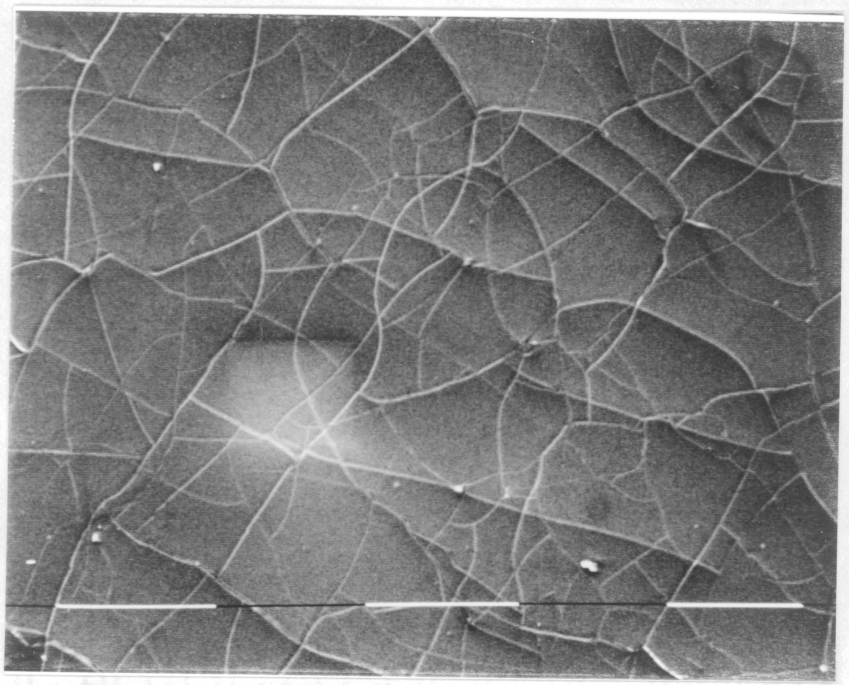

Figure 69: SEM of a dimethylsiloxane-ester block copolymer exposed to AO for 30 min, magnification 400X, bars represent 50 μ. Block lengths 5,000 $\bar{M}n$.

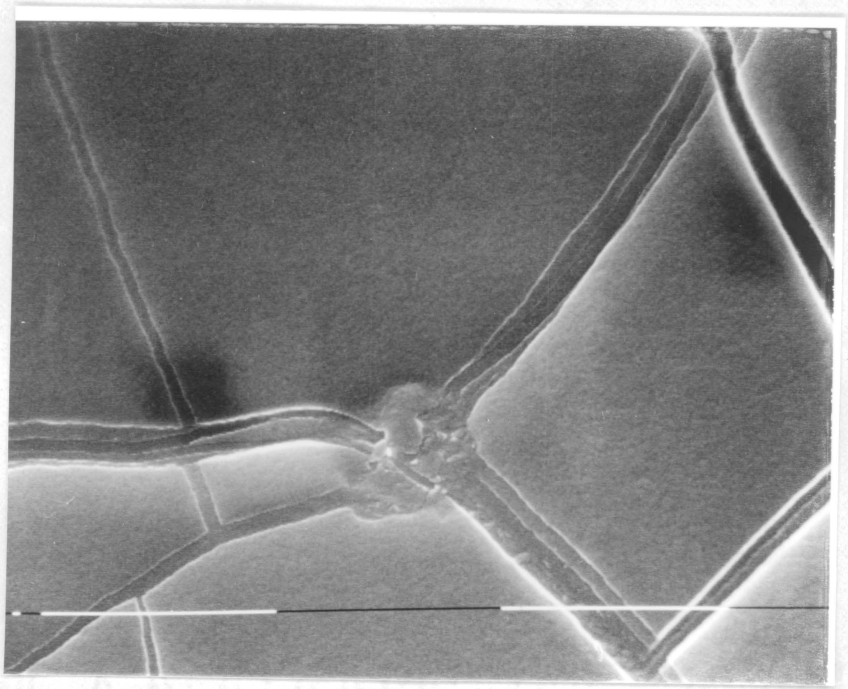

Figure 70: SEM of a dimethylsiloxane-ester block copolymer exposed to AO for 30 min., magnification 6400X, bars represent 5μ. Block lengths 5,000 $\bar{M}n$.

In summary, weight loss determinations, contact angle measurements, DR-IR, XPS, and SEM suggest that siloxane-containing block copolymers resist surface degradation by atomic oxygen relative to homopolymer controls.

4.2.2 Segmented Block Copolymers

4.2.2.1 Synthesis and Structural Analysis

The siloxane-ester block copolymers discussed thus far were prepared by the silylamine-hydroxyl condensation reaction [96,97]. Although well-defined, perfectly alternating block copolymers are prepared by this technique, Si-O-C linkages between the blocks are formed. This type of link is known to be less hydrolytically stable than the Si-C bond [1,2]. Some may view the necessity of synthesizing each block, then copolymerizing them into the final block copolymer as a disadvantage. Thus, a synthetic approach which required the synthesis of only one block prior to copolymerization was investigated. The synthetic route employed was similar to the interfacial synthesis of high molecular weight polyarylesters discussed in the literature review, however, the procedure was extended to include the aminopropyl-terminated siloxane oligomer which was placed in the organic phase with the acid chlorides (Scheme 27). The reaction of the amine-functional siloxane oligomer with an

Scheme 27

Segmented Block Copolymer Synthesis

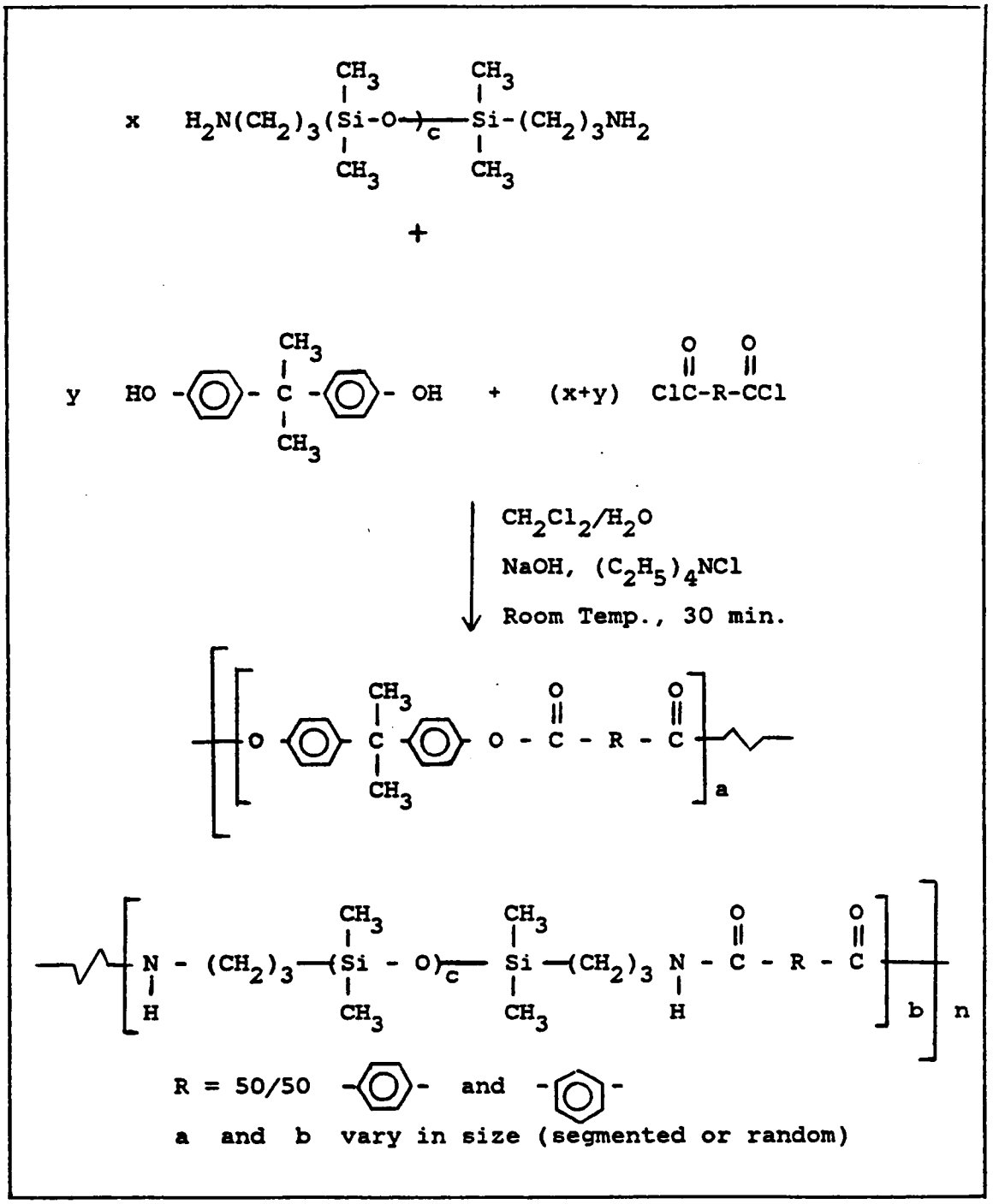

acid chloride produces an amide bond which links the siloxane and ester blocks, while repeated reactions of the bisphenol with the acid chlorides produces the ester blocks of various (random) lengths. The chain architecture for these copolymer systems is, therefore, less well-defined than those made by the coupled-oligomer approach. However, the interfacial technique produces block copolymers with Si-C bonds which are known to be more hydrolytically stable than Si-O-C bonds.

Structure analysis was accomplished by FTIR and proton NMR; representative spectra are shown in Figures 71 and 72, respectively. Corresponding IR band and NMR peak assignments are listed in Tables 38 and 39. These results are similar to those observed for the perfectly alternating siloxane-ester block copolymers previously discussed (Figures 32 and 33, Tables 20 and 21). The major difference in structure analysis between the alternating and segmented block copolymers is the amide I band that can be identified in the segmented block copolymer FTIR spectrum as the minor peak at lower wavenumbers relative to the ester carbonyl due to resonance effects.

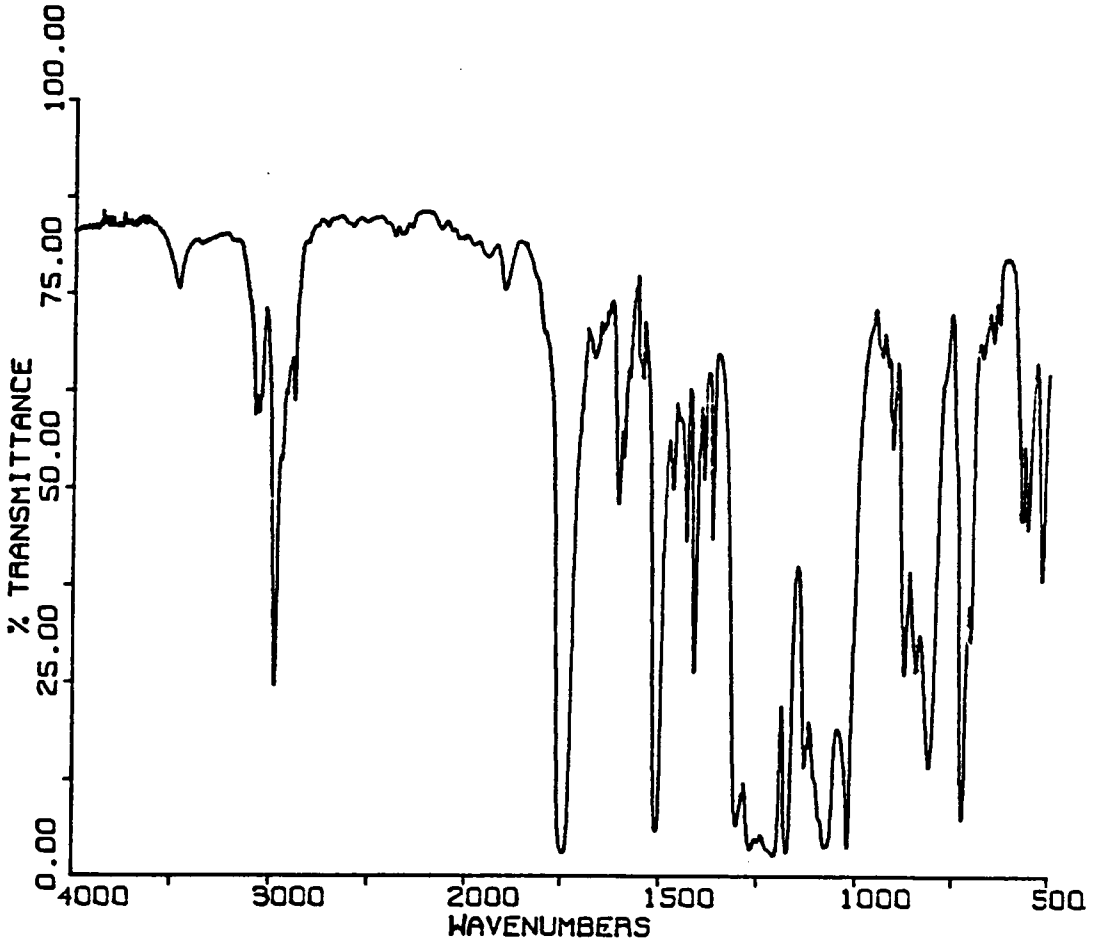

Figure 71: FTIR spectrum of a segmented dimethylsiloxane-ester block copolymer. (20 weight % of a 5,000 $\bar{M}n$ PDMS oligomer).

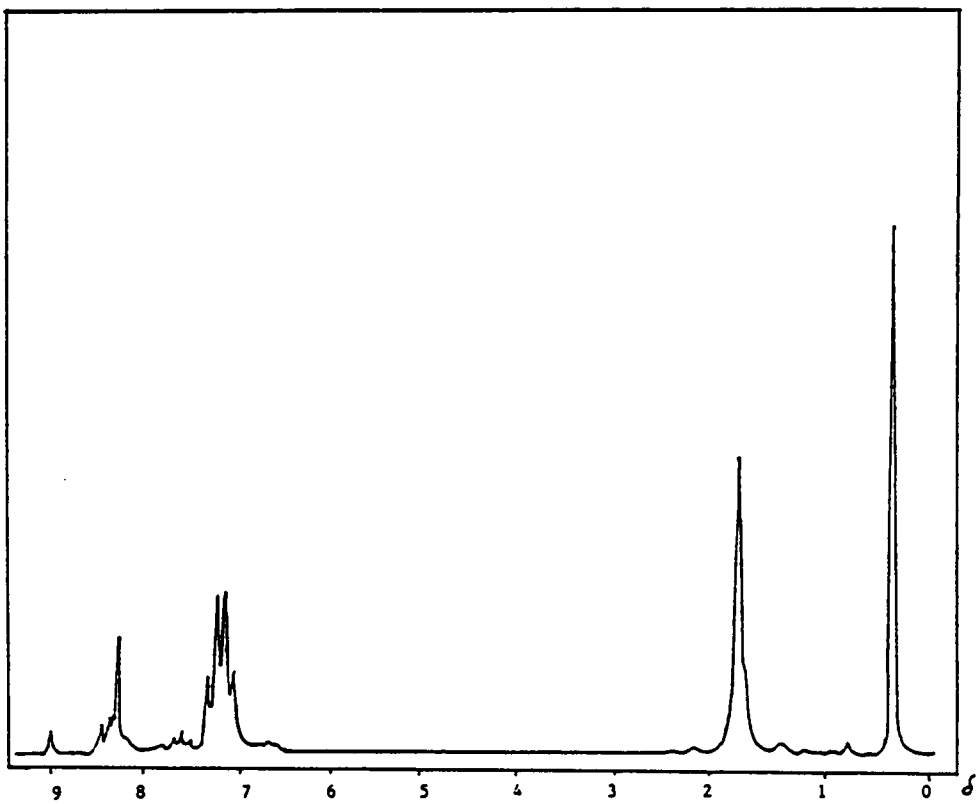

Figure 72: Proton NMR spectrum of a segmented dimethylsiloxane-ester block copolymer (90 MHz). (60 weight % of a 5,000 $\bar{M}n$ PDMS oligomer).

TABLE 38

Segmented Polydimethylsiloxane-Ester Block Copolymer FTIR Band Assignments

Frequency (cm^{-1})	Assignment
3050	C-H stretch, aromatic
2950	C-H stretch, aliphatic
1750	Ester carbonyl stretch
1640	Amide I - amide carbonyl
1600,1500	C-C stretch, aromatic
1570-1515	Amide II - N-H bending
1410	CH_3 asymmetric deformation
1400	C-N stretching
1275	CH_3 symmetric deformation
1270-1170	Strong ester bands
1100-1000	Si-O-Si stretch vibration
800	$Si(CH_3)_2O$ stretch; CH_3 rock
715	$Si(CH_3)_2O$ stretch
510	Si-O-Si bend vibration

TABLE 39

Segmented Polydimethylsiloxane-Ester Block Copolymer Proton NMR Results

Peak (ppm)	Assignment
0.3, singlet	Dimethylsiloxane hydrogens
1.7, singlet	Isopropyledene hydrogens derived from bisphenol-A
5.3, lock	CH_2Cl_2 reference and lock
7.3, AA'BB' multiplet	Aromatic hydrogens derived from bisphenol-A
7.5, triplet	Aromatic hydrogen derived from isophthaloyl chloride
8.2, singlet	Aromatic hydrogens derived from terephthaloyl chloride
8.3, doublet	Aromatic hydrogens derived from isophthaloyl chloride
8.8, singlet	Aromatic hydrogen derived from isophthaloyl chloride

4.2.2.2 Characterization

The series of segmented siloxane-ester block copolymers prepared is presented in Table 40 along with relevant characterizatioin data which illustrates the change in copolymer properties with siloxane composition and the weight percent siloxane incorporated into the copolymer.

The $\bar{M}n$ of the amine-functional siloxane oligomers was determined by potentiometric titration with alcoholic HCl as described earlier. As noted with the siloxane oligomers used to prepare the previously discussed perfectly alternating block copolymers, the effect of siloxane composition on Tg is apparent; as diphenyl or trifluoropropylmethyl units are incorporated into a dimethylsiloxane, the Tg increases.

The amount of siloxane incorporated into the segmented copolymer (in weight percent) was determined from proton NMR ($Si(CH_3)_2$ versus $C(CH_3)_2$). The values listed in Table 40 are theoretical weight percents; actual incorporation is considered quantitative (within experimental error of the EM-390 90 MHz spectrometer). The reaction yields listed are those obtained after work-up. Yields after the first coagulation were typically 90-95 percent, indicating that the losses are due to the work-up procedure which includes several washings with water to remove by-product salts.

TABLE 40

Characteristics of Segmented Siloxane-Ester Block Copolymers

Sample Number	Siloxane Block Comp.[a]	Wt.%[b]	$\bar{M}n$	Tg (°C)	25°C $[\eta]_{CH_2Cl_2}$	% Yield	Tg(°C)
1	100 CH_3	20	4,500	-123	0.33	85	-123, 174
2	100 CH_3	30	4,500	-123	0.49	84	-129, 176
3	25 F	20	5,000	-117	0.25	92	-116, 188
4	25 F	40	5,000	-117	0.45	82	-122, 187
5	25 F	60	5,000	-117	0.20	76	-115, 129
6	25 Ø	20	5,400	-102	0.37	80	-105, 178
7	25 Ø	40	5,400	-102	0.45	85	-106, 169
8	25 Ø	60	5,400	-102	0.39	65	-102, 147
9	50 F	20	5,000	-105	0.61	83	-105, 187
10	50 F	40	5,000	-105	0.74	74	-109, 187
11	50 F	60	5,000	-105	0.42	70	-102, 187
12	50 Ø	20	4,100	-72	0.46	88	-66, 175
13	50 Ø	40	4,100	-72	0.36	85	-69, 164
14	50 Ø	60	4,100	-72	0.53	84	-65, 161

[a]Composition in weight percent; remaining percents are dimethyl.

[b]Weight percent of siloxane charged to copolymer; remaining percents are ester.

The intrinsic viscosities and the fact that tough solution cast films are formed indicate that relatively high molecular weight block copolymers were prepared. It should be noted that extensive washing of each sample is necessary to obtain a transparent film. Otherwise, cloudiness is observed due to residual salt contamination. When comparing the perfectly alternating and segmented block copolymers, it is apparent that the former are not contaminated since the reaction by-product is gaseous and eliminated at the reaction temperature. Quantitative percent transmission measurements would probably also be influenced by the polyester sequence length, which increases with hard segment composition with this "in situ" procedure.

Thermal Properties

Microphase separation of the siloxane and ester phases of the segmented block copolymers is indicated by the fact that there are two glass transitions observed by DSC. The low temperature transitions are attributed to the siloxane phase and agree closely with the Tg of the siloxane oligomer prior to copolymerization. This indicates that there is a low or negligible degree of mixing of the hard ester phase

in the soft siloxane phase. However, the copolymer samples containing siloxane segments with 50 weight percent diphenyl and dimethyl units show an increase in the copolymer low temperature transition relative to the siloxane oligomer. This observation is likely due to the fact that the presence of diphenyl units increases the miscibility of the two phases.

The high temperature transitions are attributed to the polyarylester block of the copolymer. Since the ester block is synthesized during the copolymerization reaction there are no ester oligomer Tg values for comparative purposes as with the siloxanes. In general, the Tg values for the ester phase of the segmented block copolymers are higher than those observed for the perfectly alternating block copolymers. This is likely due to the fact that higher ester block lengths are possible with the interfacial technique. The ester block lengths were limited to 5,000 and 10,000 $\bar{M}n$ in the perfectly alternating block copolymers.

One trend noted is that the ester Tg value decreases as the amount of siloxane incorporated into the block copolymer increases. For example, samples 6 through 8 represent a series of segmented block copolymers containing 20, 40, and 60 weight percent siloxane (75/25 $CH_3/\emptyset$), respectively. As the amount of soft segment increases, the high Tg value due to the hard segment decreases from 178 to 147°C.

In addition to DSC, TMA in the penetration mode was also used to evaluate the thermal properties of the segmented siloxane-ester block copolymers. Typical pseudo-modulus curves are illustrated in Figure 73. Two transitions are displayed by each sample and they agree closely with those observed by DSC. The lower soft segment transition becomes more pronounced and the high temperature transition is lowered as the amount of siloxane incorporated into the copolymer system increases. As observed with the perfectly alternating block copolymers (Figure 37), a broad plateau region is displayed between the two transition temperatures. For comparative purposes, the siloxane oligomer used to prepare the segmented block copolymers is also shown in Figure 73.

Mechanical Properties

To evaluate the mechanical properties of the segmented siloxane-ester block copolymers, stress-strain measurements and DMTA were utilized. Tensile property determinations were made using an Instron table model tensile tester. Dog-bone shaped samples were cut from solution cast films using a die. Under ambient conditions, each sample was subjected to tensile forces at a rate of 10 mm/minute. The stress-strain behavior of a series of segmented block copolymers is

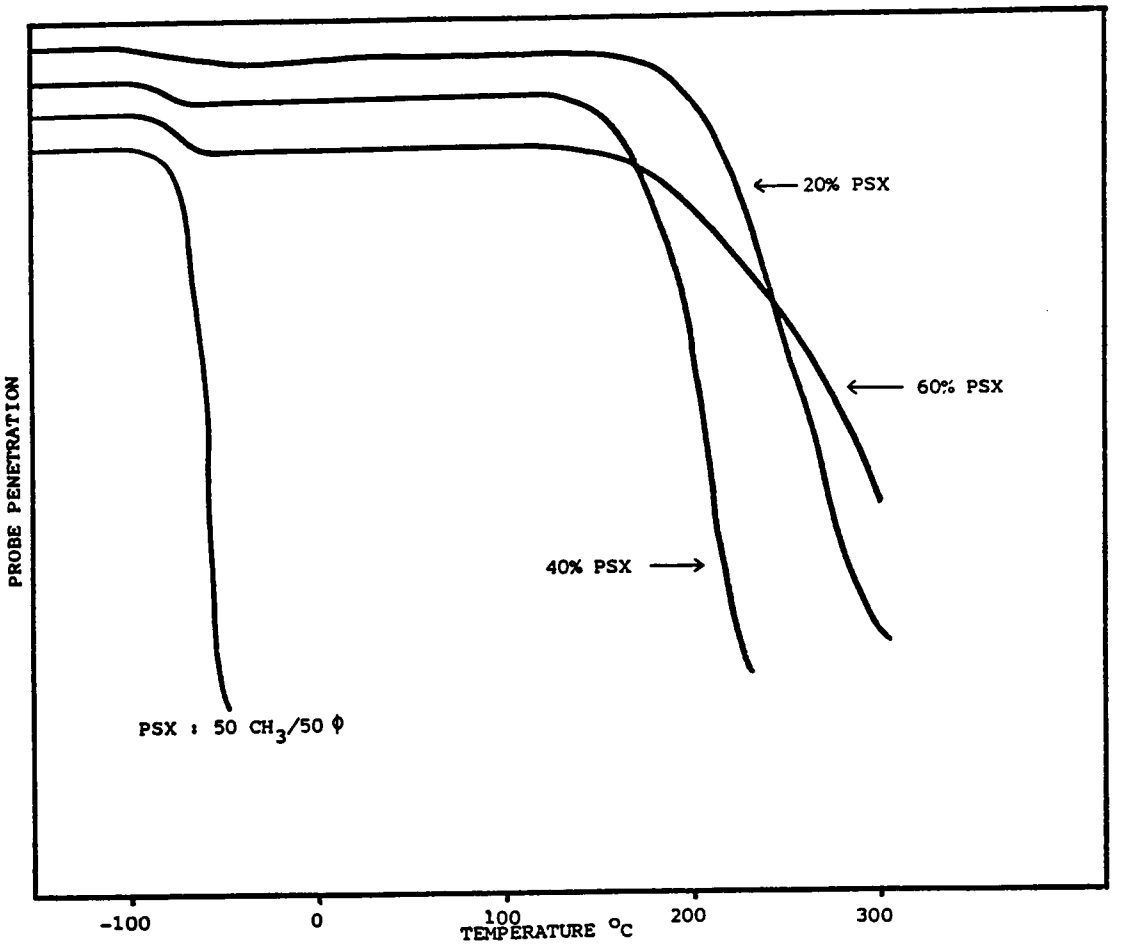

Figure 73: TMA of segmented siloxane (50/50 CH_3/Ø)-ester block copolymers.

presented in Figure 74; corresponding modulus, tensile stress, and percent elongation values are listed in Table 41. As anticipated, the tensile properties were dependent upon siloxane content. As the weight percent of siloxane incorporated into the copolymer system increased, modulus and tensile stress decreased, but percent elongation at break increased. Similar conclusions were drawn from the previously discussed perfectly alternating block copolymers (see Figures 40 and 41 and Table 30).

DMTA was used to study the modulus-temperature behavior and the damping characteristics of the segmented siloxane-ester block copolymers. The effect of siloxane content, 40 versus 60 weight percent, is shown in Figures 75 and 76, respectively. Microphase separation is indicated by the fact that two broad transitions are observed for each sample. At the siloxane and ester transition temperatures, a decrease in modulus (log E') is displayed. As expected, the sample containing a higher siloxane content showed a greater decrease in modulus at the siloxane transition. Also, damping (tan δ) increased with an increase in siloxane content.

Surface and Bulk Analysis

Contact angle measurements, x-ray photoelectron spectroscopy (XPS or ESCA), and transmission electron microscopy

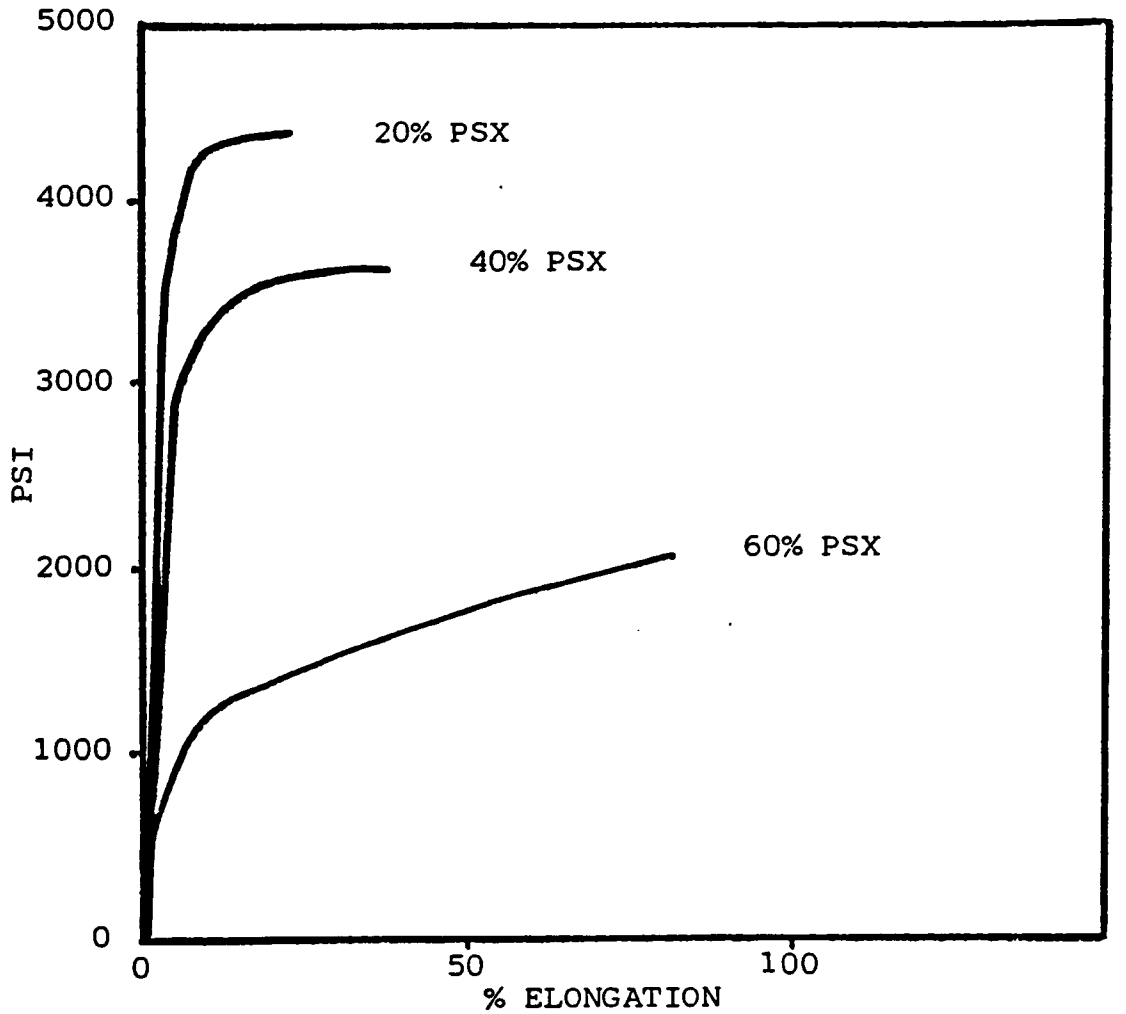

Figure 74: The stress-strain behavior of segmented siloxane (50/50 $CH_3/\emptyset$)-ester block copolymers.

TABLE 41

Mechanical Properties of Segmented Siloxane-Ester Block Copolymers Films Cast from CH_2Cl_2

Copolymer Weight % PSX[a]	Modulus[b] psi	Modulus[b] MPa	Tensile Stress[b] psi	Tensile Stress[b] MPa	% Elongation at Break[b]
20	98,000	674	4,600	32	23
40	69,000	477	3,600	25	38
60	20,000	136	2,300	16	81

[a]Polysiloxane: 4,100 $\bar{M}n$ and 50/50 $CH_3/\emptyset$.

[b]Tested at 10 mm/minute.

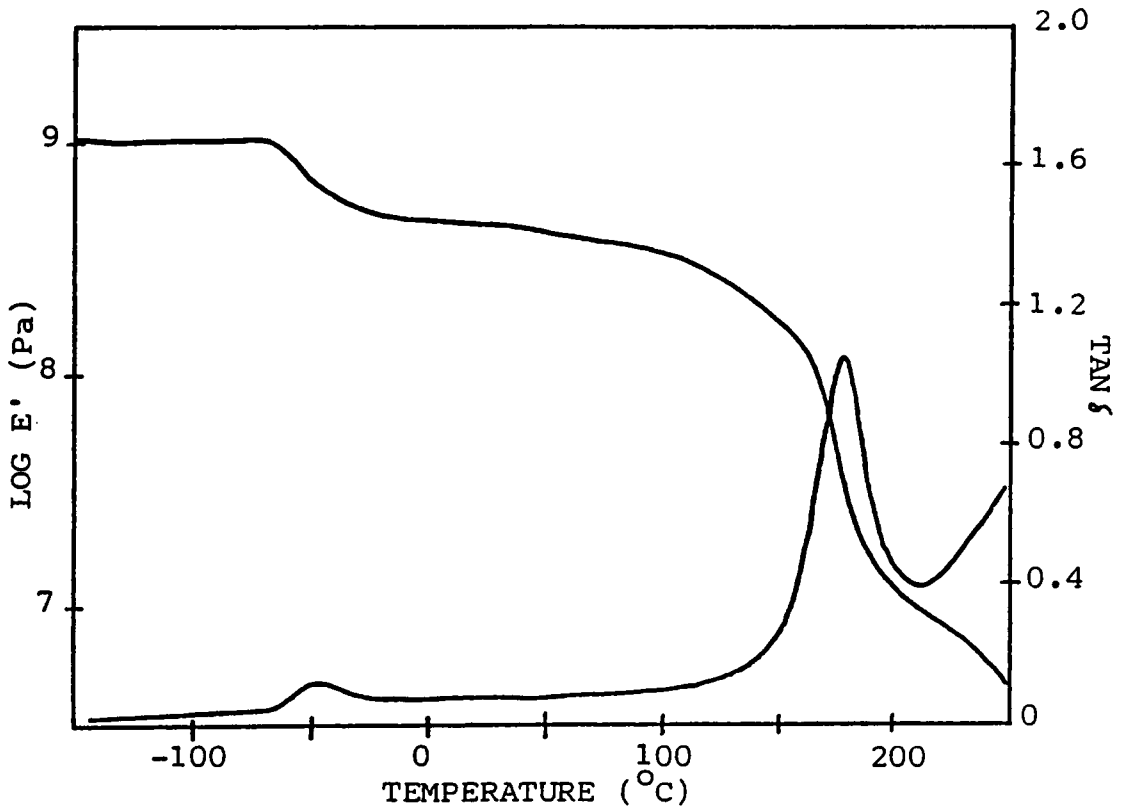

Figure 75: DMTA of a segmented siloxane (50 Ø)-ester block copolymer, 40 weight % PSX, 4100 $\bar{M}n$.

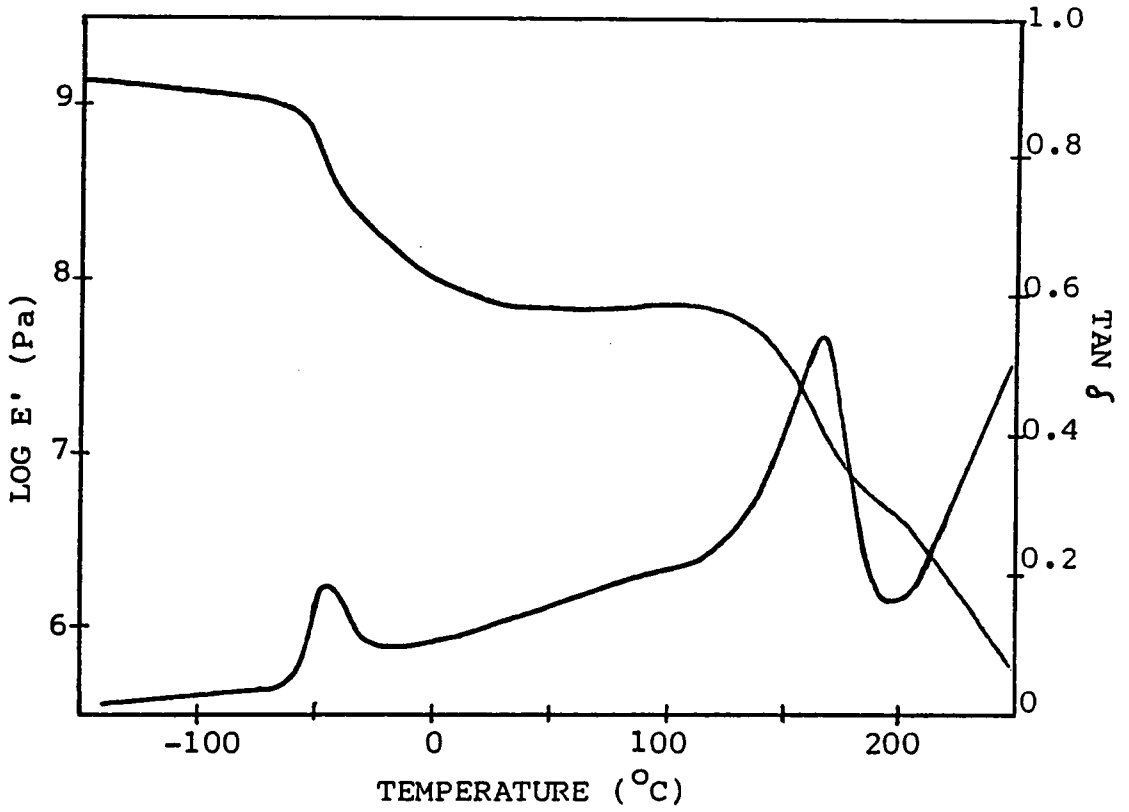

Figure 76: DMTA of a segmented siloxane (50 Ø)-ester block copolymer, 60 weight % PSX, 4100 $\bar{M}n$.

(TEM) were used to evaluate the surface and bulk properties of the segmented block copolymers.

Data from contact angle measurements of a series of segmented block copolymers is presented in Table 42. As was observed with the perfectly alternating block copolymers, the contact angle of a siloxane-ester copolymer is larger than that of an ester control due to the hydrophobic nature of a siloxane-dominated surface.

X-ray photoelectron spectroscopy was used to study the surface of representative segmented block copolymers. The results were similar to those obtained from the previously discussed perfectly alternating block copolymers. At 532.4 eV, a single O_{1s} was displayed by each copolymer sample and by the siloxane homopolymer standard. The Si-O-Si backbone gives rise to the XPS peak at this binding energy. The polyarylester displays a double peak, 532.2 eV and 533.9 eV, due to the two different types oxygen atoms in the ester link. Since a shoulder or double peak is not observed for the siloxane-ester block copolymers, it may be concluded that the surface region observed by XPS (top 75 Å) is dominated by siloxane. A more detailed discussion of XPS is included in the section concerning surface analysis of perfectly alternating block copolymers.

TABLE 42

Contact Angles of Segmented
(Dimethyl-diphenyl)siloxane-Ester Block Copolymers

Weight % PSX[a] in Copolymer	Contact Angle[b]
0 (Ester control)	77°
20	85°
40	90°
60	94°

[a]Polysiloxane: 50/50 $CH_3/\emptyset$ and 4100 $\bar{M}n$.

[b]20 µℓ water drops.

Transmission electron microscopy was used to study the bulk microphase separation of the segmented block copolymers. TEM was performed on thin solution cast films. Staining was unnecessary since there is a great degree of electron density difference between the siloxane and ester phases. A representative segmented block copolymer TEM micrograph is shown in Figure 77.

The copolymer sample contains 20 weight percent of a 5,000 $\bar{M}n$ dimethylsiloxane. Siloxane domains in an ester matrix are observed and confirm the microphase separation suggested by DSC, TMA, and DMTA studies. For comparative purposes, refer to Figures 54 and 59 which illustrate the smaller domain sizes of perfectly alternating block copolymers.

Figure 77: TEM of a segmented dimethylsiloxane-ester block copolymer, 20 weight % PSX, 5000 $\bar{M}n$, magnification 20,000X.

Chapter V

CONCLUSIONS

The major objectives of the research described in this dissertation were to synthesize and characterize ductile, multiphase, transparent block copolymers that would be suitable candidates for passive damping applications in large space structures.

Several series of relatively high molecular weight polysiloxane-polyarylester block copolymers were prepared by two different synthetic techniques. Well-defined, perfectly alternating block co- and terpolymers were synthesized in solution by coupling silylamine-terminated siloxane blocks with hydroxyl-terminated polyarylester blocks. An interfacial, phase-transfer technique was used to prepare segmented (or "random") block copolymers by reacting bisphenol-A and an equal amount of terephthaloyl chloride and isophthaloyl chloride with an aminopropyl-terminated siloxane oligomer. In this type of reaction, various polyarylester block lengths are formed during the copolymerization. Although the segmented block copolymer systems were more easily prepared, they ultimately were of less interest than the perfectly alternating block copolymers due to residual salt by-products that were difficult to remove.

Structure analysis by FTIR and proton NMR indicated that the desired oligomers and block copolymers were prepared. In addition to the above analytical techniques, high resolution ^{29}Si NMR proved useful in the structural analysis of the amine-functional siloxane oligomers. The high sensitivity of silicon to changes in chemical environment, coupled with its wide range of chemical shifts, made it possible to obtain detailed information on the purity and microstructure of the siloxane oligomers. In the case of siloxane co-oligomers, ^{29}Si NMR showed that "random" or statistical co-oligomers were produced via the equilibration process used in this work.

Due to the high degree of incompatibility of the "soft" siloxane phase and the "hard" ester phase in the block copolymers, a two-phase microstructure developed at relatively low block molecular weights as evidenced by thermal properties (DSC, TMA, DMTA) and electron microscopy (TEM). Hence, each block copolymer displayed two thermal transitions; the low temperature transition is attributed to the siloxane phase and the high temperature transition to the ester phase. To enhance damping, yet retain a two-phase morphology, the typically used dimethylsiloxane oligomers were modified to increase compatibility of the siloxane and ester phases. This was accomplished by preparing siloxane co-oligomers in

which diphenyl or trifluoropropylmethyl units were incorporated into a polydimethylsiloxane oligomer. DMTA of block copolymers containing siloxane co-oligomers suggested that several samples would be potential passive damping materials since tan δ (damping characteristic) remains relatively high at temperatures intermediate to the two transition temperatures.

The mechanical properties of the block copolymers showed a dependence on siloxane block composition and block molecular weight. Typically, high siloxane content (long block lengths relative to ester blocks) resulted in high elongations at break, but low modulus and tensile stress values. Due to the bulky, rigid nature of diphenyl or trifluoropropylmethyl siloxane units, block copolymers containing these siloxane types displayed higher modulus and tensile stress values relative to dimethylsiloxane-ester block copolymers.

Surface analysis by contact angle measurements and XPS indicated that the surface of the siloxane-ester block copolymers was dominated by siloxane, the lower surface free energy component of these copolymer systems. Surface analysis (SEM and XPS) was also useful in demonstrating that, in contrast to an ester homopolymer, the surface of a siloxane-ester block copolymer is resistant to degradation by atomic

oxygen, the major materials concern in the low earth orbit (LEO) atmosphere.

In summary, the research reported in this dissertation demonstrates that perfectly alternating polysiloxane-polyarylester block copolymers are potential materials for passive damping applications in the space environment.

Chapter VI

FUTURE STUDIES

At the conclusion of a successful scientific study, there are generally unanswered questions that outline the course for future studies. This chapter briefly discusses some recommended additional investigations that would be necessary, in order to use the siloxane-ester block copolymers in the space environment as a passive damping material.

The research in this dissertation described (1) the synthesis of several series of siloxane-ester block copolymers and (2) the general structure-property relationships. Particular emphasis was placed on synthetic procedures, damping characteristics, and atomic oxygen degradation. However, before these materials are considered for passive damping applications in large space structures, further detailed investigations are a necessity, i.e., more sophisticated atomic oxygen degradation studies are required. High level simulation (Lockheed) or actual LEO exposure (NASA Space Shuttle experiments) would determine the stability of the siloxane-ester block copolymers to the combined effects of atomic oxygen, ultraviolet radiation, and vacuum.

Although XPS was a useful analytical technique in the degradation studies, secondary ion mass spectroscopy (SIMS)

would provide complementary and perhaps more conclusive evidence of the surface changes that occur upon exposure to atomic oxygen.

Appendix A

SAMPLE CALCULATIONS

Functional Siloxane Oligomers

The number-average molecular weight, $\bar{M}n$, and the composition of the functional siloxane oligomers were controlled by varying the ratio of the cyclic monomers to each other and the difunctional end-blockers. Sample calculations are shown below for (1) a silylamine-terminated polydimethylsiloxane oligomer and (2) an aminopropyl-terminated poly(dimethyl-diphenyl)siloxane co-oligomer.

(1) Silylamine-terminated polydimethylsiloxane oligomer.

$\bar{M}n$ (Olig) = desired oligomer $\bar{M}n$

$\bar{M}n$ (EB) = end-blocker $\bar{M}n$

$\bar{M}n$ (Si) = siloxane backbone $\bar{M}n$

$= \bar{M}n\ (Olig) - \bar{M}n\ (EB)$

$$\text{grams } D_4 \text{ cyclic needed} = \bar{M}n\ (Si) \times \frac{\text{grams end-blocker}}{\bar{M}n\ (EB)}$$

For example:

$\bar{M}n$ (Olig) = 5,000g/mole

$\bar{M}n$ (EB) = 690g/mole (silylamine)

$\bar{M}n$ (Si) = 5,000 - 690 = 4,310g/mole

If one chooses to start with 6.00g of the silylamine end-blockers, then

$$\text{grams } D_4 \text{ cyclic needed} = 4{,}310\text{g/mole} \times \frac{6.00\text{g}}{690\text{g/mole}} = 37.48\text{g}$$

(2) Aminopropyl-terminated poly(dimethyl-diphenyl)siloxane co-oligomer.

$\bar{M}n$ (Olig) = desired oligomer $\bar{M}n$

$\bar{M}n$ (EB) = end-blocker $\bar{M}n$

Wt % Ø = desired weight % phenyl

$\bar{M}n$ (Ø) = diphenylsiloxane $\bar{M}n$

= $\bar{M}n$ (Olig) x Wt % Ø

$\bar{M}n$ (CH_3) = dimethylsiloxane $\bar{M}n$

= $\bar{M}n$ (Olig) - $\bar{M}n$ (EB) - $\bar{M}n$ (Ø)

$$\text{grams } D_4 \text{ cyclic needed} = \bar{M}n\ (CH_3) \times \frac{\text{grams end-blocker}}{\bar{M}n\ (EB)}$$

$$\text{grams } D_4'' \text{ cyclic needed} = \bar{M}n\ (Ø) \times \frac{\text{grams end-blocker}}{\bar{M}n\ (EB)}$$

For example:

$\bar{M}n$ (Olig) = 5,000g/mole

$\bar{M}n$ (EB) = 248.5g/mole (aminopropyl)

Wt % Ø = 0.50

$\bar{M}n$ (Ø) = 5,000 x 0.50 = 2,500g/mole

$\bar{M}n$ (CH_3) = 5,000 - 248.5 - 2,500 = 2,251.5g/mole

If one chooses to start with 6.00g of the (aminopropyl)disiloxane end-blocker, then

$$\text{grams } D_4 \text{ cyclic needed} = 2{,}251.5\text{g/mole} \times \frac{6.00\text{g}}{248.5\text{g/mole}} = 54.36\text{g}$$

$$\text{grams } D_4^{\text{n}} \text{ cyclic needed} = 2{,}500\text{g/mole} \times \frac{6.00\text{g}}{248.5\text{g/mole}} = 60.36\text{g}$$

The siloxane oligomers in this work were prepared by an equilibrium process. At equilibrium, approximately 10 to 15% cyclics are present. This would give a lower molecular weight than desired. Therefore, it is necessary to add an additional 10 to 15% of the cyclic starting materials along with the initial charge of reactants in order to obtain the targeted molecular weight.

Appendix B

SAMPLE CALCULATIONS

Hydroxyl Terminated Polyarylester Oligomers

In order to properly control the molecular weight and functionality of an oligomer, one must precisely adjust the stoichiometric imbalance of the bifunctional monomers. The calculations used to correctly determine the stoichiometric imbalance for the hydroxyl terminated polyarylester oligomers are presented below.

$\bar{M}n$ (Olig) = desired oligomer $\bar{M}n$

$\bar{M}n$ (RU) = oligomer repeat unit molecular weight

DP = degree of polymerization

r = stoichiometric imbalance ratio

For the polymerization of two bifunctional monomers,

$$DP = 2 \times \frac{\bar{M}n\ (Olig)}{\bar{M}n\ (RU)} \quad \text{and} \quad r = \frac{DP-1}{DP+1}$$

Note that the value of r is always less than one.

For example:

$\bar{M}n$ (Olig) = 5,000g/mole

$\bar{M}n$ (RU) = 358g/mole

$$DP = 2 \times \frac{5{,}000 g/mole}{358 g/mole} = 27.9330$$

$$r = \frac{DP-1}{DP+1} = \frac{27.9330-1}{27.9330+1} = 0.9309$$

For hydroxyl termination, an excess of bisphenol-A is needed. Therefore, if one chooses to start with 30g (0.1316 mole) of bisphenol-A, then

r x 0.1316 mole bis-A = 0.1225 mole acid chloride

(0.1225 mole acid chloride)(203g/mole) = 24.8648g acid chloride

24.864g/2 = 12.4324g of each acid chloride, terephthaloyl and isophthaloyl chloride

A 10 mole percent of the acid acceptor, triethylamine (MW = 101g/mole; density = 0.726g/ml), was used:

2(0.1316 mole)(101g/mole)(1ml/0.726g)(1.1 excess) = 40.28ml

Appendix C

SAMPLE CALCULATIONS

Segmented Polyarylester-Polysiloxane Block Copolymers

The segmented (or "random") polyarylester-polysiloxane block copolymers were synthesized interfacially. In this type of synthetic procedure only the siloxane blocks are prepared prior to copolymerization; the polyarylester blocks are formed during the copolymerization reaction. Siloxane incorporation involves reaction of the aminopropyl terminated siloxane oligomer with an acid chloride to produce an amide bond. Polyester formation is accomplished by reaction of bisphenol-A with an acid chloride. The calculations for preparation of a high molecular weight segmented polyarylester-polysiloxane block copolymer are shown below.

Define: Theoretical yield = 40.00g

Wt. % siloxane = 20

Grams of siloxane = (40g)(0.20) = 8.00g

Grams of bisphenol-A and acid chloride =

(40g - 8g) = 32g

Consider reaction 1 of siloxane incorporation:

If the oligomer $\bar{M}n$ = 4,100g/mole, then

moles of siloxane = (8g)/(4,100g/mole) = 0.0020 mole

grams of acid chloride = (0.0020)(203g/mole)

= 0.3961g

Consider reaction 2 of polyester formation:

Grams remaining for synthesis of

polyester = (32g - 0.3961g) = 31.6039g

To achieve high molecular weight polymer, 1:1 stoichiometry of the monomers is necessary. Therefore, an equal number of moles are needed for bisphenol-A and the acid chlorides. In the equation below, molecular weight contributions to the polyarylester repeat unit molecular weight (358g/mole) are given by 226g/mole and 132g/mole for bisphenol-A and the acid chlorides, respectively.

[(X moles)(226g/mole bis-A)] + [(X moles)(132g/mole acid chloride)] = 31.6039g

Solving for X, 0.0883 moles of bisphenol-A and the acid chlorides are needed. The grams of each are calculated below:

(0.0883 mole)(228g/mole bis-A) = 20.1324g bis-A

(0.0883 mole)(203g/mole acid chloride) = 17.9249g acid chloride

The total number of grams of acid chloride needed for the copolymerization reaction is (17.9249g + 0.3961g) =

18.3210g. For a 50:50 mixture of terephthaloyl and isophthaloyl chlorides, (18.3210g/2) = 9.1605g of each is needed.

The amount of NaOH necessary to convert the bisphenol to its more reactive bisphenate is simply (2 x moles bisphenol-A).

In summary, the materials needed to produce a high molecular weight segmented block copolymer containing 20 weight percent siloxane are listed below:

20.1324g (0.0883 mole) bisphenol-A
8.0000g (0.0020 mole) siloxane oligomer (4,100g/mole)
9.1605g (0.0451 mole) terephthaloyl chloride
9.1605g (0.0451 mole) isophthaloyl chloride
45.75ml (0.1766 mole) NaOH (3.86N aqueous solution)

Note, the moles of siloxane and bisphenol-A equal the total number of moles of acid chlorides.

Theoretical Yield:
(133/203 x 18.3210g acid chlorides) + (8g siloxanes) + (20.1324g bisphenol-A) = 40.14g

Percent siloxane = (8g siloxane)/(40.14g total)
= 19.93 ≈ 20 Wt. %

Appendix D

^{29}Si NMR MICROSTRUCTURE PARAMETERS

1. Define: P = Probability

F = Triad signal intensity

$\bar{\ell}$ = Number average sequence length

A = Dimethyl siloxane unit (6 hydrogens/unit)

B = Diphenyl siloxane unit (10 hydrogens/unit)

$$F(AAA) = \frac{P(AAA)}{P(A)} = [1-P(B/A)]^2$$

Solving for P(B/A):

$$P(B/A) = 1 - (F_{AAA})^{1/2}$$

$$\bar{\ell}_A = \frac{1}{P(B/A)} = \frac{1}{1-(F_{AAA})^{1/2}}$$

By similar derivation, $\bar{\ell}_B = \frac{1}{1-(F_{BBB})^{1/2}}$

2. Define: A_M = Mole fraction of dimethyl siloxane units

B_M = Mole fraction of diphenyl siloxane units

H = Number of hydrogens/siloxane unit

$F_{AAA} + F_{BAA} + F_{BAB} = F_A$ (total dimethyl signal intensities)

$F_{BBB} + F_{BBA} + F_{ABA} = F_B$ (total diphenyl signal intensities)

$$\frac{F_A}{6\ H's} = A \qquad \frac{F_B}{10\ H's} = B$$

Let C = A + B, then

$$A_m = \frac{A}{C} \quad \text{and} \quad B_M = \frac{B}{C}$$

3. Define: χ = a measure of departure from random statistics.

$$\chi = P(A/B) + P(B/A)$$

$$= [1-(F_{BBB})^{1/2}] + [1-(F_{AAA})^{1/2}]$$

$$= 2-(F_{BBB})^{1/2} - (F_{AAA})^{1/2}$$

Note: See reference [166] for details.

REFERENCES

1. W. Noll, "Chemistry and Technology of Silicones," Academic Press, New York, 1968.

2. M. G. Voronkov, V. P. Mileshkevich, Y. A. Yuzhelevskii, "The Siloxane Bond," Plenum Press, New York, 1978.

3. E. G. Rochow, "An Introduction to the Chemistry of the Silicones," 2nd Edition, Wiley, New York, 1951.

4. C. Eaborn, "Organosilicon Compounds," Butterworth Scientific Publications, London, 1960.

5. V. Bazant, V. Chvalovsky, J. Rathousky, "Organosilicon Compounds," Academic Press, New York, 1965.

6. A. L. Smith, "Analysis of Silicones," Wiley, New York, 1974.

7. F. O. Stark, J. R. Falender, A. P. Wright in "Comprehensive Organometallic Chemistry," Vol. 2, Pergamon Press, New York, 1982.

8. H. K. Lichtenwalner, M. N. Sprung in "Encyclopedia of Polymer Science and Technology," Vol. 12, p. 464, Wiley, New York, 1970.

9. B. B. Hardman, A. Torkelson in "Encyclopedia of Chemical Technology," Vol. 20, Wiley, New York, p. 922, 1978.

10. B. C. Arkles, W. R. Petersen, Jr. (eds.), "Silicon Compounds, Register and Review," Petrarch Systems, Inc., 1979.

11. K. E. Polmanteer, J. Elastoplastics, 2, 165 (1970).

12. K. B. Yerrick, H. N. Beck, Rubber Chem. Tech., 37, 261 (1964).

13. Y. K. Kim in "Encyclopedia of Chemical Technology," Vol. 11, Wiley, New York, p. 74, 1978.

14. O. R. Pierce, Y. K. Kim, J. Elastoplastics, 3, 82 (1971).

15. S. K. Novikov, Y. G. Kagan, A. N. Pravednikov, Polym. Sci. USSR, 8(6), 114 (1967).

16. E. G. Rochow, General Electric Co., U.S. Pat. 2,380,995, 26 Sept. 1941.

17. R. J. H. Voorhoeve, "Organohalosilanes: Precursors to Silicones," Elsevier, New York, 1967.

18. D. T. Hurd, E. G. Rochow, J. Amer. Chem. Soc., 67, 1057 (1945).

19. H. Jacobson, W. H. Stockmayer, J. Phys. Chem., 18, 1600 (1950).

20. J. E. McGrath, J. S. Riffle, A. K. Banthia, I. Yilgor, G. L. Wilkes in "Initiation of Polymerization," (F. E. Bailey, Jr., ed.), ACS Symposium Series 212, 1983.

21. J. S. Riffle, Ph.D. Dissertation, Virginia Polytechnic Institute and State University, December, 1980.

22. A. R. Gilbert, S. W. Kantor, J. Polym. Sci., 40, 35 (1959).

23. Z. Laita, P. Hlozek, B. Bucek, M. Jelinek, J. Polym. Sci. [C], 16, 669 (1967).

24. S. W. Kantor, W. T. Grubb, R. C. Osthoff, J. Amer. Chem. Soc., 76, 5190 (1954).

25. D. T. Hurd, R. C. Osthoff, M. L. Corrin, J. Amer. Chem. Soc., 76, 249 (1954).

26. P. V. Wright, J. A. Semlyen, Polymer, 11, 462 (1969).

27. K. Kojima, C. R. Gore, C. S. Marvel, J. Polym. Sci., A1, 4(9), 2325 (1966).

28. Z. Laita, M. Jelinek, Polym. Sci. USSR, 5, 342 (1964).

29. K. A. Andrianov, B. G. Zavin, G. F. Sablina, Polym. Sci. USSR, A14(5), 1294 (1972).

30. J. A. Yuzhelevskii, et al., Polym. Sci. USSR, B13, 95 (1971).

31. E. D. Brown, J. B. Carmichael, J. Poly. Sci., B3, 473 (1965).

32. K. J. Saunders, "Organic Polymer Chemistry," Chapman and Hall, Ltd., London, 1976.

33. B. Arkles, Chem. Tech., Sept., 542 (1983).

34. W. Lynch, "Handbook of Silicone Rubber Fabrication," D. VanNostrand Co., New York, 1978.

35. P. M. Sormani, R. J. Minton, J. E. McGrath in "Ring-Opening Polymerization," (J. E. McGrath, ed.), ACS Symposium Series 286, 1985.

36. I. Goodman, J. A. Rhys, "Polyesters: Saturated Polymers," Vol. 1, Iliffe Books, London, 1965.

37. I. Goodman in "Encyclopedia of Chemical Technology," Vol. 16 (2nd ed.), Wiley, New York, p. 159, 1968.

38. I. Goodman in "Encyclopedia of Polymer Science and Technology," Vol. 11, Wiley, New York, p. 62, 1969.

39. P. W. Morgan, "Condensation Polymers: By Interfacial and Solution Methods," Interscience Publishers, New York, 1965.

40. R. W. Lenz, "Organic Chemistry of Synthetic High Polymers," Interscience Publishers, New York, 1967.

41. R. J. Cella in "Encyclopedia of Polymer Science and Technology," Supplement Vol. 2, Wiley, New York, p. 485, 1977.

42. J. R. Caldwell, W. J. Jackson, Jr., T. F. Gray, Jr., in "Encyclopedia of Polymer Science and Technology," Supplement Vol. 1, Wiley, New York, 1977.

43. W. H. Carothers, J. Am. Chem. Soc., 51, 2548, 2560 (1929).

44. J. R. Winfield, Nature, 158, 930 (1946).

45. H. V. Boenig, "Unsaturated Polyesters: Structure and Properties," Elsevier, Amsterdam, 1964.

46. B. Parkyn, F. Lamb, B. V. Clitton, "Polyester: Unsaturated Polyesters and Polyester Plasticizers," Vol. 2, American Elsevier, New York, 1967.

47. R. D. Lundberg, E. F. Cox in "Ring-Opening Polymerization," Chapt. 6, (K. C. Frisch, S. L. Reegen, eds.), Marcel Dekker, New York, 1969.

48. R. H. Young, M. Matzner, L. A. Pilato in "Ring-Opening Polymerization," Chapt. 11, (T. Saegusa, E. Goethals, eds.), American Chemical Society, Washington, D.C., 1977.

49. R. E. Wilfong, J. Polym. Sci., 54, 385 (1961).

50. B. L. Dickinson, "Modern Plastics Encyclopedia," 56, 1981-82.

51. B. G. Ranby, "Photodegradation, Photo-oxidation and Photostabilization of Polymers," Wiley, New York, 1975.

52. S. B. Maerov, J. Polym. Sci., Part A, 3, 487 (1965).

53. S. M. Cohen, R. H. Young, A. H. Markhart, J. Polym. Sci., Part A-1, 9, 3263 (1971).

54. A. Conix, Ind. Eng. Chem., 51, 147 (1959).

55. W. M. Eareckson, J. Polym. Sci., 40, 339 (1959).

56. H. G. Weyland, C. A. M. Hoefs, K. Yntema, W. J. Mys, Europ. Polym. J., 6, 1339 (1970).

57. D. L. Love, Mod. Plast., March, 60 (1984).

58. G. Bier, Polymer, 15, 527 (1974).

59. M. P. Stevens, "Polymer Chemistry, An Introduction," Addison-Wesley, Massachusetts, 1975.

60. N. A. J. Platzer, ed., Adv. Chem. Ser., 99 (1971).

61. L. H. Sperling, ed., "Recent Advances in Polymer Blends, Grafts, and Blocks," Plenum, New York, 1974.

62. N. A. J. Platzer, Adv. Chem. Ser., 142 (1975).

63. D. Klempner, K. C. Frisch, eds., "Polymer Alloys: Blends, Blocks, Grafts and Interpenetrating Networks," Plenum, New York, 1977.

64. A. Noshay, J. E. McGrath, "Block Copolymers, Overview and Critical Survey," Academic Press, New York, 1977.

65. S. L. Cooper, G. M. Estes, eds., Adv. Chem. Ser., 176 (1978).

66. R. J. Ambrose, S. L. Aggarwal, eds., J. Polym. Sci., Polym. Symp., 60 (1977).

67. G. E. Molau in "Block Copolymers," (S. L. Aggarwal, ed.), Plenum, New York, 1970.

68. D. R. Paul, S. Newman, eds., "Polymer Blends," Academic Press, New York, 1978.

69. O. Olabisi, L. M. Robeson, M. T. Shaw, "Polymer-Polymer Miscibility," Academic Press, New York, 1979.

70. G. E. Ham in "Encyclopedia of Polymer Science and Technology," Vol. 4, Wiley, New York, 1966.

71. H. J. Harwood, Chairman, "Symposium on Alternating Copolymers," Polym. Prep., Vol. 14(1), 1973.

72. H. Battaerd, G. W. Tregear, "Graft Copolymers," Wiley, New York, 1967.

73. R. J. Ceresa, "Block and Graft Copolymers," Butterworth, London, 1962.

74. M. Morton, L. J. Fetters, Macromol. Rev., 2, 71 (1967).

75. L. J. Fetters, J. Polym. Sci., Part C, 26, 1 (1969).

76. R. H. Gobran in "Chemical Reactions of Polymers," (E. M. Fetters, ed.), Wiley, New York, p. 295, 1964.

77. A. S. Hoffman, R. Bacskai in "Copolymerization," (G. Ham, ed.), Wiley, New York, p. 335, 1964.

78. M. Szwarc, "Carbanions, Living Polymers and Electron Transfer Processes," Wiley, New York, 1968.

79. M. Matzner, L. M. Robeson, A. Noshay, J. E. McGrath in "Encyclopedia of Polymer Science and Technology," Supplement Vol. 2, Wiley, New York, p. 129, 1977.

80. R. J. Ceresa in "Encyclopedia of Polymer Science and Technology," Vol. 2, Wiley, New York, p. 485, 1965.

81. M. Matsuo in "Encyclopedia of Polymer Science and Technology," Supplement Vol. 2, Wiley, New York, p. 402, 1977.

82. D. J. Meier, ed., "Block Copolymers, Science and Technology," Harwood Academic (MMI Press), New York, 1983.

83. S. L. Aggarwal, Polymer, 17, 938 (1976).

84. D. J. Meier in "Block and Graft Copolymers," Syracuse University Press, 1973.

85. L. H. Sperling in "Advances in Preparation and Characterization of Multiphase Polymer Systems," (R. J. Ambrose, S. L. Aggarwal, eds.), Wiley, New York, 1977.

86. H. A. Vaughn, Jr., J. Polym. Sci., Part B, 7(8), 569 (1969).

87. M. Narkis, A. V. Tobolsky, J. Macromol. Sci., Phys., 4, 877 (1970).

88. R. P. Kambour in "Block Polymers," (S. L. Aggarwal, ed.), p. 263, 1970.

89. R. P. Kambour, J. Polym. Sci., B7(8), 573 (1969).

90. H. A. Vaughn, Jr., Am. Chem. Soc., Div. Org. Coat. Plast. Chem., 29(1), 133 (1969).

91. J. E. Lundstrom, U.S. Patent 3,767,737 (General Electric, Co.) (1973).

92. H. A. Vaughn, British Patent 989,379 (General Electric, Co.) (1965).

93. D. G. LeGrand, Trans. Soc. Rheol., 15(3), 541 (1971).

94. D. G. LeGrand, G. L. Gaines, Jr., Polym. Prepr., Am. Chem. Soc., Div. Polym. Chem, 11(2), 442 (1970).

95. M. Matzner, A. Noshay, J. E. McGrath, Polym. Prepr., Am. Chem. Soc., Div. Polym. Chem., 14(1), 68 (1973).

96. M. Matzner, A. Noshay, L. M. Robeson, C. N. Merriam, R. Barclay, Jr., J. E. McGrath, Appl. Polym. Symp., 22, 143 (1973).

97. A. Noshay, M. Matzner, T. C. Williams, Ind. Eng. Chem., Prod. Res. Dev., 12(4), 286 (1973).

98. D. C. Webster, Ph.D. Dissertation, Virginia Polytechnic Institute and State University, January 1984.

99. D. C. Webster, P. J. Andolino, J. S. Riffle, F. L. Keohan, J. E. McGrath, Polym. Prepr., 24(1), 161 (1983).

100. M. F. Hitchock, "A Review of Polymeric Satellite Thermal Control Material Considerations," SAMPE J., Sept./Oct., p. 15 (1984).

101. D. R. Tenney, S. S. Tompkins, G. F. Sykes, "NASA Space Materials Research," NASA Report No. N85-23831.

102. D. R. Tenney, W. S. Slemp, E. R. Long, Jr., G. F. Sykes, "Advanced Materials for Space," NASA Report No. N80-19172.

103. V. O. Hoehne, "AFWAL Space Control Technology Program," NASA Report No. N85-23839.

104. J. R. Sesak, "Control of Large Space Structures via Singular Perturbation Optimal Control," AIAA Conference on Large Space Platforms: Future Needs and Capabilities, Los Angeles, Calif., Sept. 27-29, 1978. (AIAA-78-1690).

105. J. Canavin, "Control Technology for Large Space Structures," AIAA Conference on Large Space Platforms: Future Needs and Capabilities, Los Angeles, Calif., Sept. 27-29, 1978. (AIAA-78-1691).

106. R. W. Trudell, R. C. Curley, L. C. Rogers, "Passive Damping in Large Precision Space Structures," AIAA/ASME/ASCE/AHS 21st Structures, Structural Dynamics and Materials Conference, Seattle, Washington, May 12-14, 1980. (AIAA-80-0677-CP).

107. M. F. Kluesener, "The Effects of the Space Environment on Damping Materials and Damping Designs on Flexible Structures," NASA Report No. N84-17217.

108. R. Plunkett, W. L. Garrard, B. S. Liebst, "Measurement of Damping in Structures in a Space Environment," NASA Report No. N84-17217.

109. M. McCargo, R. E. Dammann, J. C. Robinson, R. J. Milligan, "Effects of Combined Ultraviolet and Oxygen Plasma Environment on Spacecraft Thermal Control Materials," Environmental and Thermal Control Systems for Space Vehicles, International Symposium, Toulouse, France, Oct. 4-7, 1983.

110. W. S. Slemp, B. Santos-Mason, G. F. Sykes, Jr., W. G. Witte, Jr., "Effects of STS-8 Atomic Oxygen Exposure on Composites, Polymeric Films and Coatings," AIAA 23rd Aerospace Sciences Meeting, Reno, Nevada, Jan. 14-17, 1985. (AIAA-85-0421).

111. P. W. Knopf, R. J. Martin, R. E. Dammann, M. McCargo, "Correlation of Laboratory and Flight Data for the Effects of Atomic Oxygen on Polymeric Materials," AIAA 20th Thermophysics Conference, Williamsburg, Va., June 19-21, 1985. (AIAA-85-1066).

112. B. Singh, L. J. Amore, W. Saylor, G. Racette, "Laboratory Simulation of Low Earth Orbital Atomic Oxygen Interaction with Spacecraft Surfaces," AIAA 23rd Aerospace Sciences Meeting, Reno, Nevada, Jan. 14-17, 1985. (AIAA-85-0477).

113. G. S. Arnold, D. R. Peplinski, "Reactions of High Velocity Atomic Oxygen with Carbon," AIAA 22nd Aerospace Sciences Meeting, Reno, Nevada, Jan. 9-12, 1984. (AIAA-84-0549).

114. L. J. Leger, J. T. Visentine, J. A. Schliesing, "A Consideration of Atomic Oxygen Interactions with Space Station," AIAA 23rd Aerospace Sciences Meeting, Reno, Nevada, Jan. 14-17, 1985. (AIAA-85-0476).

115. A. F. Whitaker, S. A. Little, R. J. Harwell, D. B. Griner, R. F. DeHaye, "Orbital Atomic Oxygen Effects on Thermal Control and Optical Materials - STS-8 Results," AIAA 23rd Aerospace Sciences Meeting, Reno, Nevada, Jan. 14-17, 1985. (AIAA-85-0416).

116. G. S. Arnold, D. R. Peplinski, "Kinetics of Oxygen Interaction with Materials," AIAA 23rd Aerospace Sciences Meeting, Reno, Nevada, Jan. 14-17, 1985. (AIAA-85-0472).

117. L. J. Leger, J. T. Visentine, J. F. Kuminecz, "Low Earth Orbit Atomic Oxygen Effects on Surfaces," AIAA 22nd Aerospace Sciences Meeting, Reno, Nevada, Jan. 9-12, 1984. (AIAA-84-0548).

118. J. T. Visentine, L. J. Leger, J. F. Kuminecz, I. K. Spiker, "STS-8 Atomic Oxygen Effects Experiment," AIAA 23rd Aerospace Sciences Meeting, Reno, Nevada, Jan. 14-17, 1985. (AIAA-85-0415).

119. L. J. Leger, "Oxygen Atom Reaction with Shuttle Materials at Orbital Altitudes - Data and Experiment Status," AIAA 21st Aerospace Sciences Meeting, Reno, Nevada, Jan. 10-13, 1983. (AIAA-83-0073).

120. A. L. Lee, G. D. Rhoads, "Prediction of Thermal Control Surface Degradation Due to Atomic Oxygen Interaction," AIAA 20th Thermophysics Conference, Williamsburg, Va., June 19-21, 1985. (AIAA-85-1065).

121. L. J. Leger, "Oxygen Atom Reaction with Shuttle Materials at Orbital Altitudes," NASA Technical Memorandum 58246, May, 1982.

122. D. C. Ferguson, "The Energy Dependence and Surface Morphology of Kapton Degradation Under Atomic Oxygen Bombardment," NASA Report No. N84-34484.

123. B. A. Banks, M. J. Mirtich, S. K. Rutledge, D. M. Swec, "Sputtered Coatings for Protection of Spacecraft Polymers," NASA Technical Memorandum 83706.

124. N. J. Chou, C. H. Tang, J. Paraszczak, E. Babich, Appl. Phys. Lett., 46(1), 31 (1985).

125. R. H. Hansen, J. V. Pascale, T. DeBenedictis, P. M. Rentzepis, J. Polym. Sci., Part A, 3, 2205 (1965).

126. J. S. Riffle, I. Yilgor, A. K. Banthia, C. Tran, G. L. Wilkes, J. E. McGrath in "Epoxy Resin Chemistry II," (R. S. Bauer, ed.), ACS Symposium Series 221, 1983.

127. C. Tran, Ph.D. Dissertation, Virginia Polytechnic Institute and State University, October 1984.

128. J. E. McGrath in "Ring-Opening Polymerization" (J. E. McGrath, ed.), ACS Symposium Series 286, 1 (1985).

129. I. Yilgor, J. S. Riffle, J. E. McGrath in "Reactive Oligomers," (F. W. Harris, H. J. Spinelli, eds.), ACS Symposium Series 282, 1984.

130. G. Odian, "Principles of Polymerization," 2nd ed., Wiley, New York, 1981.

131. A. J. Wnuk, T. F. Davidson, J. E. McGrath, J. Appl. Polym. Sci., Appl. Symp. No. 39, 89-101 (1978).

132. A. Noshay, M. Matzner, C. N. Merriam, J. Polym. Sci., Part A-1, 9, 3147 (1971).

133. B. C. Johnson, Ph.D. Dissertation, Virginia Polytechnic Institute and State University, June 1984.

134. N. M. Patel, M. S. Thesis, Virginia Polytechnic Institute and State University, March 1984.

135. G. L. Gaines, Macromolecules, 14(6), 208 (1981).

136. D. T. Clark, Adv. Polym. Sci., 125 (1977).

137. J. E. McGrath, D. W. Dwight, J. S. Riffle, T. F. Davidson, D. C. Webster, R. Viswanathan, Polym. Prepr., 20(2), 528 (1979).

138. P. J. Launer in "Silicon Compounds, Register and Review," Petrarch Systems, Inc., p. 77, 1984.

139. P. J. Andolino Brandt, R. Subramanian, P. M. Sormani, T. C. Ward, J. E. McGrath, Polym. Prepr., 26(2), 213 (1985).

140. T. Hashimoto, M. Shibayama, M. Fujimura, H. Kawai in "Block Copolymers, Science and Technology," (D. J. Meier, ed.), Harwood Academic (MMI Press), New York, p. 74, 1983.

141. J. E. McGrath, M. Matzner, L. M. Robeson, R. Barclay, Jr. in "Advances in Preparation and Characterization of Multiphase Polymer Systems," (R. J. Ambrose, S. L. Aggarwal, eds.), J. Polym. Sci.: Polym. Symp. No. 60, Wiley, New York, p. 31, 1977.

142. P. C. Lauterbur in "Determination of Organic Structure by Physical Methods," Vol. 2, (F. C. Nachod, W. D. Phillips, eds.), Academic Press, New York, 1962.

143. J. Schraml, J. M. Bellama in "Determination of Organic Structure by Physical Methods," Vol. 6, (F. C. Nachod, J. J. Zuckerman, E. W. Randall, eds.), Academic Press, New York, 1976.

144. E. A. Williams in "Annual Reports on NMR Spectroscopy," Vol. 15, (G. A. Webb, ed.), Academic Press, London, 1983.

145. E. A. Williams, J. D. Cargioli, Ann. Rep. on NMR Spectros., 9, 221 (1979).

146. R. K. Harris, B. J. Kimber, Appl. Spec. Rev., 10(1), 117 (1975).

147. G. L. Marshall, Brit. Polym. J., 14(1), 19 (1982).

148. R. K. Harris, M. L. Robins, Polymer, 19, 1123 (1978).

149. R. K. Harris, B. J. Kimber, J. Organomet. Chem., 70, 43 (1974).

150. G. Engelhardt, H. Jancke, Polym. Bull., 5, 577 (1981).

151. G. Engelhardt, H. Jancke, M. Magi, T. Pehk, E. Lippmaa, J. Organomet. Chem, 28, 293 (1971).

152. H. Jancke, G. Engelhardt, H. Kriegsmann, F. Keller, Plaste und Kautschuk, 26, 612 (1979).

153. R. K. Harris, B. J. Kimber, M. D. Wood, A. Holt, J. Organomet. Chem., 116, 291 (1976).

154. D. J. Burton, R. K. Harris, K. Dodgson, C. J. Pellow, J. A. Semlyen, Polym. Comm., 24(9), 278 (1983).

155. G. Engelhardt, M. Magi, E. Lippmaa, J. Organomet. Chem., 54, 115 (1973).

156. H. G. Ham, H. C. Marsmann, Die Makromol. Chem., 162, 255 (1972).

157. G. C. Levy, J. D. Cargioli, J. Magn. Res., 10, 231 (1973).

158. G. C. Levy, J. D. Cargioli, P. C. Juliano, T. D. Mitchell, J. Magn. Res., 8, 399 (1972).

159. G. C. Levy, J. D. Cargioli, P. C. Juliano, T. D. Mitchell, J. Am. Chem. Soc., 95(11), 3445 (1973).

160. G. A. Morris, R. Freeman, J. Am. Chem. Soc., 101(3), 760 (1979).

161. H. Marsmann in "NMR - Basic Principles and Progress," Vol. 17 (P. Diehl, E. Fluck, R. Kosfeld, eds.), Springer-Verlag, Berlin, 1981.

162. R. K. Harris, F. J. Kennedy, W. McFarlane, "NMR and the Periodic Table," Academic Press, New York, 1978.

163. G. C. Levy, J. D. Cargioli in "Nuclear Magnetic Resonance Spectroscopy of Nuclei Other Than Protons," (T. Axenrod, G. A. Webb, eds.), Wiley, New York, 1974.

164. R. R. Ernst, W. A. Anderson, Rev. Sci. Inst., 37, 93 (1966).

165. R. Freeman, J. Chem. Phys., 53, 457 (1970).

166. J. L. Koenig, "Chemical Microstructure of Polymer Chains," Chapter 3, Wiley, New York, 1980.

167. P. M. Sormäni, Ph.D. Dissertation, Virginia Polytechnic Institute and State University, February 1986.

168. A. Noshay, M. Matzner, Die Angew. Makromol. Chem., 37, 215 (1974).

169. P. V. Wright in "Ring-Opening Polymerization," Vol. 2, (K. J. Ivin, T. Saegusa, eds.), Elsevier, New York, 1984.

170. J. Chojnowski, M. Scibiorek, Makromol. Chem., 177, 1413 (1976).

171. J. Chojnowski, M. Scibiorek, J. Kowalski, Makromol. Chem., 178, 1351 (1977).

172. S. H. Tang, E. A. Meinecke, J. S. Riffle, J. E. McGrath, Rubber Chem. Tech., 53, 1160 (1980).

173. S. H. Tang, E. A. Meinecke, J. S. Riffle, J. E. McGrath, Rubber Chem. Tech., 57, 184 (1984).

174. T. C. Ward, D. P. Sheehy, J. S. Riffle, J. E. McGrath, Macromolecules, 14, 1791 (1981).

175. D. W. Van Krevelen, "Properties of Polymers," Elsevier, 1976.

176. T. C. Ward, J. Chem. Ed., Nov. , p. 867 (1981).

177. V. Shah, "Handbook of Plastics Testing Technology," Wiley, New York, 1984.

178. A. Rudin, "The Elements of Polymer Science and Engineering," Academic Press, New York, 1982.

179. J. J. Aklonis, W. J. McKnight, M. Shen, "Introduction to Polymer Viscoelasticity," Wiley, New York, 1972.

180. D. W. Dwight, J. E. McGrath, J. P. Wightman, J. Appl. Polym. Sci.: Appl. Polym. Symp., 34, 35 (1978).

181. P. K. Ghosh, "Introduction to Photoelectron Spectroscopy," Wiley, New York, 1983.

182. D. T. Clark in "Polymer Surfaces," (D. T. Clark, W. Feast, eds.), Wiley, New York, 1978.

183. J. W. Gibbs, "The Scientific Papers of J. Willard Gibbs," Vol. 1, Dover, 1961.

184. S. Fadley in "Progress in Solid State Chemistry," Vol. 11 (G. Somorjai, J. McCaldin, eds.), Pergamon Press, Oxford, 1976.

185. M. P. Fuller, P. R. Griffins, Anal. Chem., 50, 1906 (1978).

186. M. P. Fuller, P. R. Griffins, Appl. Spectrosc., 34, 533 (1980).

187. H. Maulhardt, D. Kunath, Appl. Spectrosc., 34, 383 (1983).

188. P. J. Andolino Brandt, D. C. Webster, J. E. McGrath in "Advancing Technology in Materials and Processes," Vol. 30, 30th National SAMPE Symposium/Exhibition, p. 959, 1985.

189. P. J. Andolino Brandt, D. C. Webster, J. E. McGrath, Polym. Prepr., 25(2), 91 (1984).

190. P. M. Sormani, R. J. Minton, I. Yilgor, P. J. Andolino Brandt, J. S. Riffle, C. Tran, J. E. McGrath, Polym. Prepr., 25(1), 227 (1984).

The vita has been removed from the scanned document